UNIVERSITY OF HAWAII
LIBRARY

eochimica et Cosmochimica Acta

JOURNAL OF THE GEOCHEMICAL SOCIETY

ecutive
Editors
tors

C. W. CORRENS, *Göttingen.* E. INGERSON, *Austin, Texas.* L. R. WAGER, *Oxford.*

L. H. AHRENS, *Capetown.* S. R. NOCKOLDS, *Cambridge.* H. C. UREY, *La Jolla, Calif.*
JOHN VERHOOGEN, *Berkeley, Calif.* A. P. VINOGRADOV, *Moscow.*
W. A. WAHL, *Helsingfors.*

CONTENTS VOLUME 22, NOS. 2–4 MARCH 1961

FARRINGTON DANIELS: Kinetics and thermoluminescence in geochemistry . . 65
J. H. FETH, S. M. ROGERS and C. E. ROBERSON: Aqua de Ney, California, a spring of unique chemical character 75
IAN CARMICHAEL and ALISON MCDONALD: The colorimetric and polarographic determination of some trace elements in the standard rocks G–1 and W–1 . . . 87
L. O. NICOLAYSEN, A. J. BURGER, T. TATSUMI and L. H. AHRENS: Age measurements on pegmatites and a basic charnockite lens occurring near Lützow-Holm Bay, Antarctica 94
R. PARK and H. N. DUNNING: Stable carbon isotope studies of crude oils and their porphyrin aggregates 99
R. NEWTON and G. F. ROUND: The diffusion of helium through sedimentary rocks . 106
M. HONDA, J. P. SHEDLOVSKY and J. R. ARNOLD: Radioactive species produced by cosmic rays in iron meteorites 133
S. R. TAYLOR, MAUREEN SACHS and R. D. CHERRY: Studies of tektite composition—I. Inverse relationship between SiO_2 and the other major constituents . . . 155
R. D. CHERRY and S. R. TAYLOR: Studies of tektite composition—II. Derivation from a quartz–shale mixture 164
D. V. N. SARMA and T. MAYEDA: Meteorite analysis: the search for diamond . . 169
L. R. STIEFF and T. W. STERN: Graphic and algebraic solutions of the discordant lead–uranium age problem 176
J. N. WEBER and G. V. MIDDLETON: Geochemistry of the turbidites of the Normanskill and Charny formations—I. Effect of turbidity currents on the chemical differentiation of turbidites 200
J. N. WEBER and G. V. MIDDLETON: Geochemistry of the turbidites of the Normanskill and Charny formations—II. Distribution of trace elements 244
Geochemical Note:
A. C. COOK: The carbon isotopic compositions of certain marine invertebrates and coals from the Australian Permian 289
Book Reviews 291

PERGAMON PRESS OXFORD • LONDON • NEW YORK • PARIS

GEOCHIMICA ET COSMOCHIMICA ACTA

EXECUTIVE EDITORS

PROF. C. W. CORRENS (1959) *Sedimentpetrographisches Institut der Universität, Lotzestr.* 13, *Göttingen, Germany*
PROF. E. INGERSON (1959–1960) *Department of Geology, University of Texas, Austin* 12, *Texas, U.S.A.*
PROF. L. WAGER, F.R.S. (1959–1961) *Department of Geology and Mineralogy, The University Museum, Oxford, England*

EDITORS

PROF. L. H. AHRENS (1959–1960) *Department of Chemistry, University of Capetown, Rondebosch, Cape Province, South Africa*
Dr. S. R. NOCKOLDS *Department of Mineralogy and Petrology, The University, Cambridge, England*
PROF. H. C. UREY, For. Mem. R. S. (1959) *University of California, La Jolla, California, U.S.A.*
Dr. JOHN VERHOOGEN (1959–1961) *Department of Geology, University of California, Berkeley, California, U.S.A.*
PROF. A. P. VINOGRADOV (1959–1961) *Vernadsky Institute, Moscow, U.S.S.R.*
PROF. W. A. WAHL (1959–1961) *Observatoriegaten* 8, *Helsingfors, Finland*

EDITORIAL ADVISORY BOARD

EUROPE

T. F. W. BARTH, *Oslo*
L. CAPDECOMME, *Toulouse*
E. J. CONWAY, *Dublin*
P. ESKOLA, *Helsinki*
P. GALLITELLI, *Modena*
A. HADDING, *Lund*
O. HAHN, *Göttingen*
H. W. HARVEY, *Plymouth*
F. HEIDE, *Jena*
A. HOLMES, *Edinburgh*
W. Q. KENNEDY, *Leeds*
PH. H. KUENEN, *Gröningen*
S. LANDERGREN, *Stockholm*
F. MASHATSCHKI, *Vienna*
A. MUIR, *Harpenden*
J. ORCEL, *Paris*
E. RAGUIN, *Paris*
E. REINHARD, *Basle*
TH. G. SAHAMA, *Helsinki*
C. E. TILLEY, *Cambridge*
T. VOGT, *Trondheim*

AMERICAN CONTINENT

A. F. BUDDINGTON, *Princeton*
D. GUIMÃRAES, *Belo Horizonte*
G. E. HUTCHINSON, *New Haven*
B. H. MASON, *New York*
F. WHIPPLE, *Cambridge*
R. WILDT, *New Haven*
H. S. YODER, *Washington*

FAR EAST

T. WATANABE, *Tokyo*

AUSTRALIA

D. J. SWAINE, *Sydney*

Publishing Offices: Pergamon Press Ltd., Headington Hill Hall, Oxford

Four issues per volume, three volumes per year

Subscription *per annum* (including postage) (A) £21 (U.S.A. $60.00); (B) For individual subscribers who write directly to the publisher certifying that the Journal is for their private use, £7.7s. (U.S.A. $21.50). Members of the Geochemical Society, or non-members who occasionally publish papers in the Journal, £3. 11s. 6d. (U.S.A. $10.00) *per annum.*

Back numbers, £10 (U.S.A. $28.00) per volume

Single issues, £2. 10s. (U.S.A. $7.00) each

Copyright © 1961 Pergamon Press Ltd.

PERGAMON PRESS LTD.

HEADINGTON HILL HALL, OXFORD 122 EAST 55TH STREET, NEW YORK 22, N.Y.

PRINTED IN NORTHERN IRELAND AT THE UNIVERSITIES PRESS, BELFAST

Appearing in 1961

Adventures in Radiosotope Research

by GEORGE de HEVESY

This collection of the work of George de Hevesy, the world famous Swedish chemist, Nobel prize winner, and a winner of the second Atoms for Peace Award, will be warmly welcomed as a permanent record of the work of this outstanding scientist. The book includes de Hevesy's summation of his work in Activation Analysis; Tracers in the Search for Unknown Stable Elements; Permeability Studies; Labelling of Red Corpuscles; Studies in Radiation Biology; Botanical Studies.

Approx. £7 ($20.00)

Printing Inks and Color

Advances in Printing Science and Technology, Volume I

Edited by W. H. BANKS

This volume contains the proceedings of the Fifth International Conference of Printing Research Institutes held at Lehigh University, U.S.A. Its contents cover discussions on the influence of ink, paper and press on colour printing; some aspects of the chemistry and physics of lithographic printing; colour control and instrumentation for colour measurement; control of ink film thickness on the press; and studies of ink transfer in relation to the ink. It is invaluable for chemists and physicists working with paper or ink or in control of printing plant.

80s. net ($12.50)

Azeotropy and Polyazeotropy

by W. SWIETOSTAWSKI

Dr. Swietostawski's monograph differs in principle from all others published on azeotropy. It is based on quite a new approach to the physico-chemical nature of most of the organic raw materials. These findings will be of great value to chemists working on theoretical as well as experimental problems including the processes of azeotropic purification and dehydration of organic substances. For technologists dealing with various organic raw materials containing usually very complicated mixtures of binary, ternary and quarternary azeotropes, it will give new methods of treatment.

In preparation

The Behavior of Plasticizers

by IBERT MELLAN

This is a new approach to the subject. It covers recent advances in a way no other book has done, and is ideal for courses dealing with plastics, polymers and plasticizers. Some of the subjects covered are The Mechanism of Plasticizers Based on Strong Primary Valency Bonds; The Ratio of Tensile Strength to Melt Viscosity; The Thermodynamic Treatment of Solubility Based on the Second Law of Thermodynamics; The Relationship between the Position of Polar Groups in the Plasticizer and the Shape of the Molecule.

50s. net ($8.00)

The Chemistry and Technology of Edible Oils and Fats

Edited by J. DEVINE and P. N. WILLIAMS

This volume contains the important proceedings of a Conference sponsored by Unilever. It includes both the papers read and the authoritative discussions which followed them. This is a subject of increasing importance in certain fields of medical and industrial research. Topics under discussion included Fatty Foods and the Pattern of Their Consumption in the United Kingdom; The Determination of Linoleic Acid with Special Reference to the Isotopic Dilution Technique; The Analysis of Oils and Fats.

35s. net ($6.00)

Descriptive leaflets will be sent on request

PERGAMON PRESS

OXFORD LONDON NEW YORK PARIS

Headington Hill Hall, Oxford. *4 & 5 Fitzroy Square, London W.1.*

122 East 55th Street, New York 22, N.Y.

Appearing in 1961

International Series of Monographs on Pure and Applied Biology: Biochemistry Division

Physical Constants of Steroids

Edited by L. L. ENGEL

In this volume the diverse properties of steroid hormones and their metabolites which are useful in their isolation identification, and quantitative estimation are dealt with. Among the physical properties covered are fluorescence spectra, the chromogens formed upon treatment of steroids with sulphuric acid and correlation of the sulphuric acid chromogens with structure of the steroid. Laboratory workers in the field of steroid hormone metabolism and chemistry will find this an invaluable handbook.

Approx. £5 ($15.00)

Oxytocin

Proceedings of an International Symposium held in Montevideo

Edited by R. CALDEYRO-BARCIA and H. HELLER

This book represents the most comprehensive account of the physiology of oxytocin with special reference to its importance in human labour. The following recent advances and special aspects have been covered: extra-uterine effects of oxytocin; its actions as analysed by electrophysiological methods; its effect on the pregnant and parturient human uterus; the effects of synthetic analogues of oxytocin on uterine function; a comparison of oxytocin with other oxytocic drugs and the physiological (and possibly pathological) importance of oxytocinase, *i.e.* the oxytocin inactivating enzyme which appears in human blood during pregnancy.

Approx. 63s.

A Short Textbook of Colloid Chemistry

2nd Revised Edition

by B. JIRGENSONS and M. E. STRAUMANIS

This text is an introduction to colloids for those who are interested in the fundamentals of colloids and their applications in chemical industry, pharmacy, clinical medicine, biology and similar fields. All types of inorganic and organic colloids are treated, emphasizing the effects of particle size and shape on the properties of the systems. The experimental procedures are described in detail, stressing the methods that are now used in industrial and clinical laboratories.

Approx. 63s. ($10.00)

A TECHNICAL WRITING SERVICE FOR INDUSTRY

Do you need the services of professional technical writers, highly competent illustrators and compilers of modern, effective technical literature? A technical writing service is available to industrial companies and research organizations to prepare, illustrate, print and disseminate instruction manuals, parts lists, user handbooks, sales brochures, internal reports, etc.

The Technical Writing Division is staffed with experienced and highly qualified technical writers, engineers and illustrators and at their disposal are all the very extensive resources and connections of the Pergamon Press.

For further information please write to:

The Manager, Pergamon Press Technical Writing Division,
4 & 5 Fitzroy Square, London W.1.

PERGAMON PRESS

OXFORD LONDON NEW YORK PARIS

Headington Hill Hall, Oxford 4 & 5 *Fitzroy Square, London W.*1

122 *East 55th Street, New York* 22, *N.Y.*

Geochimica et Cosmochimica Acta, 1961, Vol. 22, pp. 65 to 74. Pergamon Press Ltd. Printed in Northern Ireland

Kinetics and thermoluminescence in geochemistry*

FARRINGTON DANIELS
Department of Chemistry, University of Wisconsin

I GREATLY appreciate this honor of addressing geochemists and geologists. I plan to survey with you a few selected branches of geochemistry and point out where physical chemistry has been or could be of help (DANIELS, 1956). Then I want to discuss in more detail two of the special research fields in which I have enjoyed working. One of these involves a theoretical principle,—chemical kinetics, with application to the calcite-aragonite problem; and the other, a laboratory technique, the thermoluminescence of crystals.

The ability to check geological theories with laboratory experiments is one reason for the rapid development of geochemistry. It is somewhat easier to measure a planned reaction between chemicals than to wait for the next glacial age,—and the variables are more easily controlled in a laboratory.

Let me say first that not only does physical chemistry help in solving geological problems, but geochemistry helps to solve chemical problems also. The earth is a wonderful experimental laboratory with its large-scale operations, its enormously high pressures, its high temperatures, its permanent records and its infinite time. Where else could a scientist find such extreme conditions, and work on experiments conveniently started for him millions of years ago?

The geochemical work in which I have been engaged for the past decade has been supported by the U.S. Atomic Energy Commission and I am pleased to take this opportunity to express my appreciation (DANIELS, AECU-3599). The Commission's interest in uranium has done much to advance our knowledge of geochemistry.

THERMODYNAMICS AND KINETICS

Some of the problems of geochemistry involve answers to the following questions. How are minerals deposited, how are they transported, how are they dated and how may they be recovered?

In applying physical chemistry to these problems we think first of thermodynamics which tells us just what chemical reactions and physical changes are theoretically possible and gives us quantitative numbers, in terms of calories of free energy, to predict just how far a chemical reaction will go before the reverse reaction catches up. It deals with solids, liquids and gases and solutions of solids in water. When the number of different chemical compounds become too great we resort to pictures and phase diagrams. An understanding of the crystallization of molten material to give igneous rocks involves at least ten different metallic oxides. Thermodynamics enables us to calculate the influence of temperature, pressure and concentration on systems at equilibrium. It tells us what precipitates

* Presidential address, The Geochemical Society, St. Louis, Mo., November 8, 1958.

will be formed in water solutions and predicts solubilities even in superheated water.

But thermodynamics has nothing to do with time—it is concerned only with the starting material and the final products. When time is a factor, we make use of kinetics. In many sciences it is necessary to realize the importance of kinetics. Organic chemistry would be in great difficulties if it relied on thermodynamics alone without considering kinetics. For example, two chemical materials can react in different ways to give many different products, all possible by thermodynamics and all giving a decrease in free energy. That product which predominates is the one which goes by the fastest chemical reaction and uses up the reacting material first. The petroleum companies spend a great deal of effort in finding just the right catalyst to produce the preferred type of gasoline by increasing the rate of the desired reaction.

In geology, too, we should explore the importance of kinetics. The minerals which are deposited may sometimes be influenced, more by the reaction rates that produce them, than by the thermodynamic relations involved with equilibrium. There are examples in geochemistry. Precipitations, changes in crystal form, the formation of dolomite, the devitrification of obsidian glasses, the weathering of rocks and volcanic ashes are all areas where applications of chemical kinetics might be helpful. Other kinetics processes involve mixing rates, sedimentation rates, escape of gases from the atmosphere and photochemical reactions.

Chemical reactions between different solids in contact with each other are extremely slow unless the solids are close to their melting points or unless they are in contact with water which permits them to dissolve and react in solution. Reactions between dry solids are usually limited by the rates of diffusion in the solid, which are extremely slow. They would be still slower if it were not for the imperfections in the crystals caused by chemical impurities and physical defects. Reactions in the gas phase and in solution are much faster because the molecules and ions are free to move.

Electrochemistry

The chemical reactivity of an element depends to a large extent on the relative ease with which electrons are removed from, or added to, the outer electron shell of its atoms. This tendency for oxidation or reduction is measured by the voltage of the element in a solution of its ions. The chemical free energy changes and the concentrations of reactants and products can be predicted quantitatively with the help of electrode potentials in the electromotive force series.

One of the most important factors in many chemical reactions is the effective concentration of hydrogen ions—the pH of the solution. We can determine the pH electrochemically with a hydrogen electrode or its equivalent, a glass electrode.

Garrels (1960) and others have shown that a knowledge of the pH of a solution and the oxidation-reduction potentials enable one to predict the conditions under which a given mineral such as iron oxide or lead sulfide will be precipitated.

Adsorption

Ions are readily adsorbed on colloidal particles, which have extremely large surface areas. This adsorption has several applications in geochemistry.

With the help of OCKERMAN we conducted a survey (OCKERMAN and DANIELS, 1954), of the alpha ray activity of many geological materials including clays which had adsorbed uranium or thorium or their radioactive disintegration products. The following table gives the number of alpha particles emitted per sq. cm. per hour by an infinitely thick layer of powder.

Table 1. Alpha radioactivity

36 samples of bentonite ranged from 1·0 to 10·3 with an average of 4·1
25 miscellaneous samples of tile and brick ranged from 1·5 to 3·4 with an average of 2·4
40 samples of granites ranged from 0·2 to 9·6 with an average of 3·2
82 samples of limestones ranged from 0·05 to 1·7 with an average of 0·4
33 samples of soil below plant litter in Wisconsin ranged from 1 to 6·8 with an average of 2·2

It is evident that uranium and radioactive elements are readily adsorbed on solid particles and that the alpha ray activity of clays is sometimes greater than that of granites. Perhaps more uranium goes down the rivers to the ocean attached to clay particles than goes down as dissolved uranium in solution.

An excellent example of the adsorption of uranium was discovered by DENSON (MILLER and GILL, 1954). In western North and South Dakota, lignite beds are overlain with volcanic ash containing one or two parts per million of uranium. The uranium is leached out by rain water which flows down through the lignite in extremely dilute solution. The upper part of the lignite deposits is high in uranium, and the lower parts of the deposit are low in uranium. It is a clear cut case of selective or chromatographic adsorption or chemical reduction by the porous lignite.

Some shales are uraniferous. The uranium in the shallow seas in which the shale was formed may have been leached out of granites, but in some areas at least, it seems more likely that it came from volcanic ash dropped into the sea.

Different growing organisms having varying abilities to take up and concentrate the elements that are present in their environment. For example, some plants concentrate selenium. After the Bikini tests, the hulls of some of the ships became radioactive weeks after the atomic explosion because the barnacles growing on them took up selectively some of the greatly diluted radioactive fission-product elements.

Another application of adsorption lies in the possible recovery of metals from low-grade ores. Organic exchange resins can be prepared which take up selectively the different ions, such as uranium, copper, cobalt, nickel and tungsten. Another hope lies in developing plastic membranes which are selectively permeable to different ions. When these chemical elements become sufficiently rare, it may be possible to extract several of them at once from a single mining and grinding operation of granite or other low-grade material followed by acid leaching and selective adsorption, even when the cost of recovering one of the elements alone would be prohibitive.

ISOTOPES

The use of isotopes in geochemistry is so well known that I will recall only two or three examples. THODE *et al.* (1953) found that S^{34} is enriched in a fractionating process under oxidizing conditions which give sulfates and that it is depleted under reducing conditions which give sulfides. Native sulfur is in a reduced state and it is depleted in S^{34}. The history of oxidation of a mineral or petroleum deposit may be studied with the help of this ratio. Evidence may be obtained also for the time in the geological past when the atmosphere acquired its oxygen.

The ratio of O^{18} to O^{16} is affected by chemical reactions and photosynthesis and the geological implications of this oxygen isotope fractionation in air and water have been studied. The ratio has been used as a geological thermometer to determine the temperature at which rocks were deposited from the sea.

The geological dating of rocks through the use of radio-isotopes is one of the striking successes of modern geochemistry. It includes the uranium–lead ratio, the argon-potassium ratio and others. Remarkable progress has been made in using tritium for time-spans of decades, carbon^{14} for thousands of years and beryllium^{10} for hundreds of thousands of years.

I want to throw out a suggestion for dating with gadolinium. The precision of mass spectrometers has not been high enough as yet, but it is hoped that a new mass spectrometer may make this method possible. One difficulty with radioactive dating is the possible loss of radioactive elements. If one radioactive product escapes as a gas or is leached out more than the parent, the ratio does not give an accurate date. An isotope of gadolinium, Gd^{158}, is formed from gadolinium^{157} by neutron bombardment, and since both isotopes have the same chemical properties and the same chances of loss by weathering, a determination of the isotopic ratio, the neutron flux of the mineral, and the neutron absorptions would give the age without errors due to weathering. A suitable mineral for this determination would be one with a high neutron flux which contains gadolinium. Minerals with uranium and thorium give some neutrons from spontaneous fission and some from α, n reactions with light elements.

RADIATION DAMAGE

The metamict crystals are excellent examples of drastic change produced in a crystal by exposure to alpha-ray activity. The random displacement of atoms is so complete that the minerals do not give a diffraction pattern with X-rays but when heated the normal crystal lattice is restored and heat is evolved. We have found up to 130 calories of heat released per gram (KURATH, 1957). TNT evolves only 1000 calories per gram. Most highly radioactive minerals do not contain this stored energy because the atomic displacements are annealed out at earth temperatures. To be metamict, the lattice must be quite complicated so that displaced atoms do not readily find their place in the normal lattice. Furthermore, the radioactivity must be high and the mineral old.

It can be calculated that if all the energy of the alpha particles went into permanent atomic displacements, rocks containing only a moderate amount of uranium and thorium and an age of only a few million years could store enough energy to melt the rock when triggered off by eventual radioactive heating

(Daniels, 1954). It now seems unlikely that such a process can account for intermittent geological heating, unless the efficiency of atomic displacement by alpha particles and the permanence of atomic displacement are greatly increased at high geological pressures.

New Physical Chemical Tools

X-ray diffraction patterns are invaluable for identifying crystals. Shadow photographs with soft X-rays can be used to analyze for the concentration and location of elements of differing atomic weight. Neutron activation in nuclear reactors is an extremely sensitive and accurate method for determining traces of elements. After removal from the reactor, the induced radioactivity and its decay rate are measured. The element is identified by its half-life and its abundance is determined by the intensity of radioactivity.

Solar furnaces are useful for studies on highly refractory materials. An old army searchlight concentrated sunlight from a 5-foot diameter to an area $\frac{1}{2}$ inch in diameter and easily melted granites and other high melting materials at the point of focus. Lower temperatures are obtained by moving the sample slightly out of focus. The de-focussing can be done slowly so as to get any desired rate of cooling. A melted pool is made right in the surface of the specimen and there is no problem of contamination by a containing vessel.

DTA, differential thermal analysis, is an excellent new tool for determining at what temperatures exothermic or endothermic chemical reactions, or crystalline transitions take place.

Another tool which could find more use in geochemistry is infrared absorption spectroscopy. Every large organic chemistry research laboratory now leans heavily on automatically recorded curves giving the intensity at different wave lengths throughout the infrared. Each minimum corresponds to a definite chemical group or structural feature. Rocks and minerals should also give valleys in the spectrogram corresponding to definite chemical compounds present. A finely powdered sample is thoroughly mixed with potassium bromide and subjected to pressures of about 50 tons per sq. inch. The potassium bromide flows together around the particles and is transparent throughout the infrared. It is easily possible to distinguish aragonite from calcite by this method and it should be possible to distinguish between the various crystalline ingredients of a rock. The operations are simple, automatic and rapid.

Calcite-Aragonite

Calcite is the stable form of calcium carbonate at ordinary temperatures and pressures and yet, under certain circumstances, the aragonite is formed. The aragonite usually has a higher content of strontium than calcite under comparable conditions, and the strontium ion has a larger diameter than the calcium ion.

The classical view is that the unstable form, aragonite crystallizes out first and that its crystal unit, with more oxygen atoms contacting the cation takes into its lattice more readily the larger strontium ion.

Although I do not want to encourage a fruitless controversy on cause and

effect, let me suggest a different hypothesis. It seems to be borne out by laboratory experiments, which should be submitted to still further tests:

Calcite and aragonite are both formed from calcium and carbonate ions with a decrease in free energy. The one which is formed under a given set of conditions is the one which is formed by the more rapid reaction. The presence of strontium with its larger diameter, tends to cause the formation of the aragonite. it is suggested that this crystal form grows faster under the specified conditions than calcite,—that strontium accelerates the growth of crystalline aragonite.

Both aragonite and calcite are found in geological deposits. According to this hypothesis the aragonite was deposited when the ratio of aragonite to calcite was high. Both calcite and aragonite are found in shells and it is suggested that the organisms concentrate strontium in their shells and that a high concentration of strontium leads to the formation of aragonite. If the aragonite is out of contact with water or if it is surrounded with strontium-containing sea water, it will remain as aragonite for long periods of time, in spite of its thermodynamical tendency to go to calcite. If it is in contact with fresh water, low in strontium, the more soluble aragonite will dissolve and recrystallize as calcite.

Some single shells show adjacent areas of calcite and aragonite in contact with each other. SIEGEL (1960) showed some at this meeting. We have some fossil shells with the same differentiation. The sea water and the calcium concentration must have been the same in contact with both areas. The aragonite portions are higher in strontium. The difference in the two areas is probably due to a difference in the ability of the organism to concentrate strontium. Again, some different organisms tend to give aragonite and others calcite. I believe that it will be found that the difference lies in the relative uptake of strontium by the different organisms. Barium or lead have larger ions, too, which can function in the same way as the strontium.

The occurrence of aragonite and calcite in stalactites should be investigated with reference to the strontium content. The temperatures of the cave and the conditions of stalactite formation are about the same. In some years the water run-off may be such that areas containing strontium-bearing rocks are contributing more strontium to the dripping ground-water thus leading to the formation of aragonite.

Now let me review some laboratory experiments on calcite and aragonite (ZELLER, WRAY, and DANIELS, 1955, 1956, 1957). Using calcium nitrate and sodium carbonate in 0·1 to 1 molar solutions, it is easily possible to get either aragonite or calcite, depending on the conditions of precipitation. The calcium nitrate used for the experiments contained 30 to 60 parts per million of strontium. These solutions are, of course, much more concentrated than those in nature from which calcite and aragonite are precipitated and the conditions are quite different.

The pH of the solution changes as the carbonate is used up. The character of this precipitation is very sensitive to conditions of pH and temperature. As sodium carbonate is added to calcium nitrate, the iron and manganese and magnesium precipitate. When they come down as hydroxides they are not incorporated in the calcium carbonate lattice and have no effect. As more carbonate is added,

the pH increases and strontium and barium carbonates co-precipitate with the calcium carbonate.

In the rapid precipitation of calcium carbonate under these conditions, there are three stages in the crystallization process: (1) an aggregation in which the ions are brought together and precipitated in a colloidal or amorphous state; (2) an orientation in which the material crystallizes; and (3) a recrystallization. The first is extremely rapid, the second stage is complete in a few seconds but the recrystallization requires a longer time,—minutes, hours or days, depending on the conditions.

At low pH's strontium does not come down and calcite is formed. At high pH, strontium is precipitated as carbonate and aragonite is formed. The surrounding solution, however, has been depleted in strontium by the precipitation and the strontium ions diffuse out later from the recrystallizing precipitate. In the presence of the lower strontium ion concentration, the product of recrystallization is more likely to be calcite. Factors, such as lower temperatures, which tend to lengthen this time for the escape of strontium ions before recrystallization is completed, tend to produce calcite. When extra strontium is added to the solution surrounding the precipitates there is no conversion from aragonite into calcite, even on long standing.

The calcite-aragonite ratio is very sensitive to temperature as explained. Under the conditions described, precipitation below 40°C gives calcite and precipitation above 50° gives aragonite, 25 per cent of which changes to calcite on standing for 18 hours. At 45° a mixture of 70 per cent aragonite is produced which changes to pure calcite after standing for 10 hours.

Thermoluminescence of Crystals

When crystals are exposed to X-rays or radioactivity, some electrons are re-released from the atoms in the crystal and as they fall back into lower energy levels, they emit light. Some of the electrons become trapped in imperfections in the crystal lattice and remain there. Later when the crystal is heated, these electrons are released by the increased kinetic energy and in falling to a lower energy level, they emit light. This phenomenon is called thermoluminescence. The low energy traps are emptied at low temperatures, and those in the high-energy traps are released later when the temperature is increased sufficiently. Heating a crystal with trapped electrons, from room temperature to red heat, gives a succession of bursts of light of varying intensity. When light intensity, measured with a photomultiplier cell, is plotted against temperature (or time of heating,) a "glow-curve" is produced with peaks and valleys of varying intensity coming in at definite temperatures. These glow curves are reproducible and they give a means of characterizing a given sample of material. The shapes of the curve depend on the chemical impurities and on the state of the crystal and its previous history.

We have studied the thermoluminescence glow curves for many thousands of laboratory-prepared crystals, rocks and minerals (Daniels, Boyd and Saunders, 1953).

Early in the program we found from the literature and from experience in our own laboratory that many rocks exhibit natural thermoluminescence without

exposure to X-rays. This was mysterious. We found that it is caused by traces of uranium or other radioactive elements. For example, although limestones contain only about 1 part per million of uranium, the accumulated effect over millions of years is sufficient to produce marked thermoluminescence. About a third of the specimens in a small commercial mineral collection will exhibit some thermoluminescence.

Limestones, dolomites, fluorites, granites and several other rocks and minerals give natural thermoluminescence and many others exhibit it after previous exposure to X-rays or gamma rays. Our first experiments were carried out with a heating rate of 50° per minute, but now we use a nichrome heating ribbon with a rate of 50° per second and get a considerably greater sensitivity.

Mechanism

The most common type of electron trap is a lattice vacancy caused by a missing anion. The trapped electron gives color to the irradiated crystal and this color is bleached out when the electron is driven from its trap by heating.

Chemical impurities in the lattice give distortions which produce electron traps. A sodium chloride crystal gives much greater thermoluminescence when silver chloride is incorporated into it.

When a crystal is exposed to excessive high energy radiation, new electron traps and new peaks in the glow curve are produced.

Annealing a crystal at high temperature commonly alters the electron traps and affects the glow curves.

It was a surprise to find that the grinding of a crystal can produce thermoluminescence. Apparently the small total pressure of grinding can be transferred to extremely small areas in the crystal to give an energy equivalent to the several electron volts which is necessary to release an electron in the crystal lattice. Triboluminescence, the light generated at the time of grinding of crushing a crystal, has long been known. Recent experiments (Johnson and Daniels, 1961) show that the grinding produces distortions in the crystal structure. When the crystal is later heated the movement of the atoms in the annealing process produces energy locally which is sufficient to drive out electrons and exhibit thermoluminescence.

Applications

We have endeavored to apply thermoluminescence to chemical and geological problems. Among the laboratory uses are radiation dosimetry, and studies of the properties of pure and impure crystals. In stratigraphy, it is possible to follow sedimentary beds of limestone over long distances by the characteristic glow curves.

The sequence of glow curve patterns in a vertical column gives a unique identification of a sedimentary deposit. The time of intrusion of hot molten rock into a crack in limestone has been studied through measurements of the decrease in thermoluminescence of the limestone adjacent to the intrusion.

Houtermans *et al.* (1957) has made an interesting application of thermoluminescence. He found that the outer shell of a stone meteorite gave glow curves in which the low-temperature peaks were missing. But the inside of the meteorite gave the low temperature peaks. These experiments show that in its passage through the

atmospheric air only the outer shell of the meteorite was heated enough to anneal out the thermoluminescence which had been induced by the uranium content or by cosmic rays. The time of heating was too short to heat up the interior.

Age Determination

The total amount of thermoluminescence light emitted by a rock depends on three things:

(i), the intensity of radioactivity to which it has been exposed. The radioactivity can be determined by counting alpha particles emitted with a scintillometer,—only a few per hour per sq. cm.

(ii), the length of time since the last crystallization or heating.

(iii), the thermoluminescence sensitivity of the rock to radioactivity. An estimate of this sensitivity can be approximated by determining how much gamma-ray activity is required to reproduce the natural thermoluminescence after the rock sample has been heated. Laboratory measurements of the total thermoluminescence combined with the rate of alpha-ray emission and the sensitivity to thermoluminescence leave only the age to be calculated. A considerable effort has been devoted to the determination of age by this method and some success has been obtained. Zeller (1957) is exploring vigorously these possibilities for age determination. He has estimated the ages of many limestones in this way and checked them with their known geological ages. There are difficulties and further work is necessary. He (1961) has been able to estimate the age of the Antartica ice cap over the limestone.

The low temperature thermoluminescence peaks are annealed out on long standing and so it is necessary to use only the high temperature peaks. Sometimes the crystallization-induced thermoluminescence is appreciable and gives to the younger limestones an older age than that based on alpha-particle induced thermoluminescence alone. In the older limestones the error introduced by the initial crystallization thermoluminescence is smaller in proportion to total age. It is hoped that it may be possible to distinguish crystallization-induced thermoluminescence from radiation-induced thermoluminescence. Kennedy (1960) is studying the dating of lavas. No work has been done yet on the dating of fluorites and other minerals.

There is hope that thermoluminescence measurements combined with alpha-ray activity can be applied also to archaeology. All clays contain some uranium and when pottery is fired, all the trapped electrons are released. We have found that pottery 4000 years old has accumulated enough trapped electrons, since the time of its firing, to give an easily measurable thermoluminescence. Kennedy (1959) has reported important results in archeological dating.

Thermoluminescence is one of the many tools which deserve further attention in geochemistry.

Conclusion

In conclusion, I congratulate the geochemists on the large number of interesting problems which they are expected to solve and I hope that physical chemistry will prove to be an ever increasing help. I hope particularly that the young and vigorous

Geochemical Society will be effective in bringing about the necessary close cooperation between chemists and geologists.

References

Daniels F., Final Report, "Uranium Geochemistry, Thermoluminescence and Related Studies", Contract AT(11–1)–178 with the Atomic Energy Commission, Department of Chemistry, University of Wisconsin. AECU-3599 Technical Information Service Extension, Oak Ridge, Tenn.

Daniels F. (1954) *Radiation Damage and Energy Storage*, Chapter 6, pp. 188–194, Nuclear Geology, Edited by H. Faul, John Wiley, New York.

Daniels F. (1956) Physical Chemistry in Geochemistry *J. Phys. Chem.*, **60,** 705–707.

Daniels F., Boyd C. A. and Saunders D. F. (1953) Thermoluminescence as a Research Tool, *Science* **117,** 343–349.

Garrels R. M. (1960) *Mineral equilibria at low temperature and pressure*, p. 254 Harper, New York.

Houtermans F. G., Jager E., Schon M. and Stauffer H. (1957) *Ann. Physik*, (6) **20,** 283.

Johnson N. M. and Daniels F. (1961) Luminescence from annealing and phase change of crystals. *J. Chem. Phys.* (in press).

Johnson N. M. and Daniels F. (1961 Luminescence from annealing and phase change of crystals. *J. Chem. Phys.* (in press)

Kennedy G. E. (1959) *Sci. Newsletter*. 79, 10, 148.

Kennedy G. E. (1960) Private communication.

Kurath S. F. (1957) Storage of Energy in Metamict Minerals, *Amer. Mineral.* **42,** 91–99.

Miller R. L. and Gill J. R. (1954) Uranium from Coal, *Scientific American*, **191,** 36–39.

Ockerman J. B. and Daniels F. (1954) Alpha-Radioactivity of Some Rocks and Common Materials, *J. Phys. Chem.* **58,** 926–927.

Siegel F. R. (1960) The effect of strontium on the aragonite-calcite ratios of Pleistocene corals. *J. Sed. Pet.* **30** (2), 297–304.

Thode H. G., Macnamara J. and Flemming N. H. (1953) Sulfür isotope fractionation in Nature and geological and biological time scales. Geochim. et Cosmochim. Acta **3,** 235.

Wray J. L. and Daniels F. (1957) Precipitation of Calcite and Aragonite, *J. Am. Chem. Soc.*, **79,** 2031–2034.

Zeller E. J. and Wray J. L. (1956) Factors Influencing Precipitation of Calcium Carbonate. *Bull. Amer. Assoc. Petrol. Geol.*, **40,** 140–152.

Zeller E. J., Wray J. L. and Daniels F. (1955) Thermoluminescence Induced by Pressure and Crystallization. *J. Chem. Phys.* **23,** 2187.

Zeller E. J., Wray J. L. and Daniels F. (1957) Factors in age determination of carbonate sediments by thermoluminescence. *Bull. Amer. Assoc. Petrol. Geol.* **41,** 121–129

Zeller E. J. (1961) Forthcoming communication.

Geochimica et Cosmochimica Acta, 1961, Vol. 22, pp. 75 to 86. Pergamon Press Ltd. Printed in Northern Ireland

Aqua de Ney, California, a spring of unique chemical character*

J. H. Feth† S. M. Rogers‡ and C. E. Roberson‡
U.S. Geological Survey, Menlo Park, California

(*Received* 18 *November* 1960)

Abstract—The chemistry of water of Aqua de Ney, a cold spring of unusual character located in Siskiyou County, Calif., has been re-examined as part of a study of the relation of water chemistry to rock environment. The water has a pH of 11·6 and a silica content of 4000 parts per million (p.p.m.), the highest values known to occur in natural ground waters.

The rocks exposed nearby consist of two volcanic sequences, one predominantly basaltic in composition, the other highly siliceous. Neither these rocks nor the sedimentary and igneous rocks presumed to underlie the area at depth seem to offer explanation of the unusual mineralization which includes 240 p.p.m. of boron, 1000 p.p.m. of sulphide (as H_2S), and 148 p.p.m. of ammonia nitrogen (as NH_4) in a water that is predominantly sodium chloride and sodium carbonate in character.

By analogy, it is assumed that water from Aqua de Ney is the product of an initial mixture of connate sea water with a calcium magnesium sulphate water. It is postulated that ion exchange has increased the content of sodium and reduced that of calcium and magnesium, and that sulphate reduction has brought about the high alkalinity, high pH, and high content of sulphide. The large silica value is explained as the result of solution of silica by water having the high pH observed.

Introduction

The exceptional chemical character of the water from Aqua de Ney, a cold (54°F) mineral spring located in Siskiyou County, California, near the town of Mount Shasta, has been known (Waring, 1915, pp. 264–265) since the latter of part the nineteenth century. The present report results from a re-examination of the water chemistry and a geologic reconnaissance of the area immediately adjacent to the spring by personnel of the U.S. Geological Survey. This discussion of Aqua de Ney is incidental to a broader study of the chemistry of natural waters as related to the rock environment.

Chemical analyses (Table 1) of samples collected from Aqua de Ney, and from other water sources in the vicinity, show that the water at the maximum concentration determined contained about 4000 p.p.m. of silica, 148 p.p.m. of ammonium ion, and several hundred parts per million of boron, and had a pH of 11·6. These values for silica and pH are the highest that occur in natural ground waters, so far as the writers know. The analyses indicate that the principal constituents are sodium chloride and sodium carbonate. The maximum concentration of dissolved solids as residue on evaporation at 180°C was 30,400 p.p.m.

The springs, of which Aqua de Ney is the most highly mineralized, are near the $S\frac{1}{4}$ corner sec. 32, T. 40 N, R. 4 W, in a small canyon occupied by Ney Springs Creek, which is a tributary in the headwaters of the Sacramento River. The spring area is reached by a forest road, and is 5 miles south-west of the town of Mount Shasta. At the time of Waring's visit in 1908 (Waring, 1915, pp. 264–265), there was a small resort or spa at Ney Springs, but the present ruined condition of the

* Publication authorized by the Director, U.S. Geological Survey.
† Geologist.
‡ Chemist.

buildings suggests that the last occupancy must have been 20 or 30 years ago. The canyon was logged in the winter of 1957–1958, but otherwise the area has been visited in recent years only occasionally, by picnickers or by hunters in deer season.

Waring has remarked (D. E. White, 1959, oral communication) that the chemistry of the spring water appeared so strange, when the analytical report was returned to him, that he suspected the water had been artificially altered by the (then) owner, who secretly added some undetermined substance or substances to it. The work reported here, however, shows that the chemical nature of the water is a natural phenomenon.

In October 1957, water samples were taken from Aqua de Ney and from a spring of low mineralization that discharges immediately west of the former hotel. The results (Table 1, spring N-1, 1957) of analysis of the water from Aqua de Ney were so unusual that a sample was sent to the Geological Survey Quality of Water laboratory in Denver, where several determinations were made (J. D. Hem, 1957, written communication). These confirmed the exceptional character of the water, especially with respect to silica, pH, and total carbonate species by evolution of carbon dioxide.

In September 1958, the senior writer made a measurement of discharge in Ney Springs Creek, prepared a reconnaissance geologic map (Fig. 1) of a small area including the springs, and collected water samples not only from the sources sampled earlier but also from other springs (Table 1, nos. N–3 to N–8) that emerge along Ney Springs Creek directly across the canyon from the former Ney Springs resort.

The 1958 water samples were taken in bottles to which were added zinc acetate, to fix the hydrogen sulphide in the water, and formaldehyde, to stabilize the nitrogen-containing components. Comparison of the results obtained in 1957 and those obtained in 1958, shows that the fixatives were effective in retaining a larger proportion of the unstable constituents in the water than remained in solution without fixation in the 1957 samples.

The other differences between the two analyses may be attributed to direct dilution of the spring water by rain prior to collection of the 1957 samples and by the resulting interchange of creek water and spring water which occurs at high creek stages. The 1958 sample was collected after a dry summer, when there was little opportunity for dilution. Further, the samples collected in 1958 were analysed within a few days after their return to the laboratory, whereas the samples taken in 1957 remained in storage for a number of weeks prior to analysis. From this standpoint, the 1958 data are considered to represent more accurately the chemical character of the discharge of Aqua de Ney Spring.

Another visit to the spring site was made by project personnel on 5 May, 1959, for the purpose of obtaining samples and determining whether or not the chemical character of the water might have been altered by materials composing the masonry wall of the spring pool or by other non-natural agencies. The undisturbed well contents were sampled and then removed and disposed into the flowing stream in such a manner as to prevent return of the water in the cistern. The inflowing spring water was then sampled at the source beneath the masonry structure. This sample is believed to represent the spring water in its natural state out of contact

Table 1. Chemical analyses of water sampled in Ney Springs Canyon (Values in parts unless otherwise stated.)

Source	Date of collection	Temperature (°F)	Silica (SiO_2)	Aluminium (Al)	Iron (Fe)	Manganese (Mn)	Chromium (Cr)	Copper (Cu)	Lead (Pb)	Zinc (Zn)	Arsenic (As)	Calcium (Ca)	Magnesium (Mg)	Strontium (Sr)	Barium (Ba)	Sodium (Na)	Potassium (K)	Lithium (Li)	Ammonia nitrogen as NH_4	Bicarbonate (HCO_3)	Carbonate (CO_3)	Hydroxide (OH)	Sulphite (SO_3)	Sulphate (SO_4)	Chloride (Cl)	Fluoride (F)	Bromide (Br)	Iodide (I)	Nitrite (NO_2)	Nitrate (NO_3)	Orthophosphate (PO_4)	Boron (B)	Dissolved solids: Calculated	Dissolved solids: Residue on evap. at 180°C	Hardness as $CaCO_3$	Noncarbonate hardness as $CaCO_3$	Specific Conductance (micromhos at 25°C)	pH	Density at 20°C	Sulphides as H_2S
Spring N–1 Aqua de Ney (Fig. 1, no. 1)	1958	54	3970*	1·8	0·00	0·00					0·00	7·3	2·6		0·0	10,900	135	3·2	148	0	5560†	1430†	295	267	7180	3·0	11	5·7	0·00	0	4·3	242*	31,200	30,400	29	0	36,800	11·6	1·024	1000*
Spring N–1 Aqua de Ney (Fig. 1, no. 1)	1957	50	3400*	0·90	0·00	n.d.					n.d.	2·5	0·9			8710	116	1·5	122	0	4790†	948†	139	172	5950	2·0	9·2	5·4	0·00	10	0·00	200*	24,800	24,800	10	0	29,700	10·9	1·018	400*
Spring N–1 Aqua de Ney (Waring, 1915)	1910	–	420	Trace	Trace	n.d.					n.d.	Trace	7·2			11,090	72	n.d.	152	—	4872	1720	—	272	7310	n.d.	n.d.	n.d.	n.d.	n.d.	Trace	Trace	26,179				—	—		264‡
Spring N 4 "Sulfur Spring" (Fig. 1, no. 4)	1958	47	87	0·14	0·00	0·10					0·00	18	4·9			139	19	0·0	1·3	143	69	-	5·8	14	88	0·4	0·1	0·0	0·03	0·1	0·07	2·4	520	486	65	0	758	9·2		4·9
Spring N–5 "Sweet Spring" (Fig. 1, no. 5)	1958	47	52	0·17	0·00	?					0·00	18	6·1			25	2·5	0·0	0·0	134	0	—	4·6	2·5	13	0·3	0·0	0·0	0·00	0·2	0·08	0·32	188	—	71	0	259	7·4		n.d.
Spring N–6 "Stagnant Spring" (Fig. 1, no. 6)	1958	54	941	0·16	0·00	0·00					0·00	2·5	2·4			3160	29	0·0	29	—	2030†	169‡	12	191	2280	2·5	3·5	0·0	0·06	0·0	1·2	73	9070	8950	16	0	12,300	10·4	1·004	144
Ney Springs Creek above spring area (Fig. 1, no. 7) Discharge 315 g.p.m. measured	1958	53	20	0·00	0·00	0·00					0·00	3·6	10			6·9	0·6	0·0	0·3	72	0	—	-	0·2	6·2	0·1	0·0	0·0	0·00	0·0	0·00	0·08	83	—	52	0	139	7·8		n.d.
Ney Springs Creek below spring area (Fig. 1, no. 8) Discharge estimated 316 g.p.m.	1958	58	23	0·00	0·00	0·00					0·00	3·2	11			27	0·0	0·0	0·0	94	0	—	-	4·6	20	0·1	0·0	0·0	0·00	0·7	0·02	0·53	136	—	53	0	220	8·0		n.d.
Spring N–2 at west end of former lodge (Fig. 1, no. 2)	1957	50	31	-		-						7·2	6·3			4·8	0·5	—	- -	62	0	—	—	—	1	—	—	-	—	0·2	—	0·00	—	—	44	0	102	7·9		—

* Probably present in dissociated form
† Based on conventional alkalinity titration; includes effects of other ions.
‡ Sulphide as S.
n.d., not determined.

with man's artifacts. Field and subsequent laboratory tests showed the composition of the inflowing spring water to be the same in chemical character as the water earlier removed from the masonry cistern.

A few problems in the analysis of this unusual natural water remain unsolved and many matters relating to its genesis can only be surmised. However, the water deserves to be reported as a geochemical phenomenon, and the related studies of the geologic environment and the analytical data are believed to be a worthwhile contribution to the field of geochemistry of natural waters.

Geology

The geology of the south-central Klamath Mountains, which include the Ney Springs area, is incompletely known. Rocks exposed in the vicinity of the canyon are chiefly lavas, which are assumed to be comparable to those from the southern Klamath Mountains, several miles south of the Ney Springs area, described by

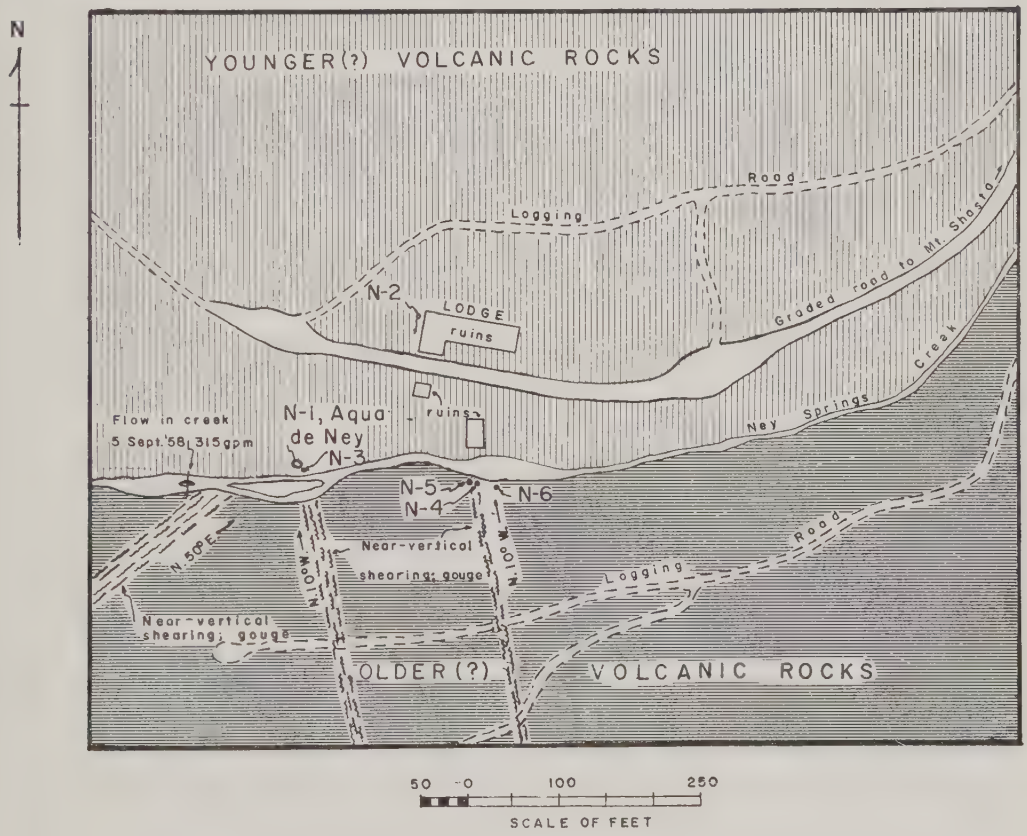

MAP OF NEY SPRINGS AREA, SISKIYOU COUNTY, CALIF., SHOWING INFERRED GEOLOGY AND LOCATIONS OF SPRINGS

Fig. 1.

Hinds (1935) and deposits of fluvioglacial gravels that are preserved as discontinous terraces along the sides of Ney Springs Canyon. The gravels are surface deposits, however, and are thought to have no relation to the mineralization of the water from the springs. Paleozoic sedimentary rocks and the volcanic rocks overlying them, together with igneous intrusions and the resulting metamorphism (Hinds, 1940), have resulted in a geochemical environment that causes the peculiar chemical character of the water from Auqa de Ney, although the interrelations that bring about so unusual an environment can only be guessed at. Some possible conditions are postulated later in the present discussion.

Geologic information on the immediate area of Aqua de Ney springs has been obtained by geologists of the Southern Pacific Company, whose preliminary reports have been made available through the courtesy of George A. Kiersch, and have been published in an abstract (Bonham and Sharp, 1958). It appears that the Ney Springs area may be underlain by a series of greenstones of early Paleozoic age and limestones and shales of a later time; that these rocks are overlain by volcanic rocks of probable Eocene to Miocene age, principally andesitic in composition; and that even later volcanic rocks may have been deposited in at least part of the area adjacent to Ney Springs Canyon. The relation, if any, of these events to the formation of the two groups of volcanic rocks exposed (Fig. 1) in the canyon is not known. The authors cited above ascribed the last period of intrusive igneous activity to the Jurassic, at which time ultrabasic rocks were emplaced in parts of the area, serpentine was formed in veins and dikes, and locally a diorite porphyry was intruded into all pre-existing rocks.

The field work of the present study was restricted to an area in Ney Springs Canyon, the geologic results of which are shown on a reconnaissance map (Fig. 1). It is not possible from the information available to correlate precisely the rocks found near Ney Springs with the regional geologic section. It is apparent, however, that the two sides of the canyon consist of volcanic-rock suites of quite different character and possibly of different geologic age.

The designations "older(?) volcanic rocks" and "younger(?) volcanic rocks" (Fig. 1) are based on the observation that the rocks on the south side, inferred to be the older, are more deeply weathered and the mineral grains are more altered than is true of the rocks on the north side of the canyon. The rocks on the south side of the canyon, the older(?) volcanic rocks (Fig. 1), are highly siliceous. Four samples observed in thin section were all albitized and considerably altered, having abundant micaceous and clay minerals. These rocks probably can best be named quartz keratophyres. In contrast, the rocks that make up the north wall of Ney Springs Canyon are uniformly dark, mostly very fine grained, show highly developed flow structures, and all are of a composition close to basaltic andesite. Under the microscope, the specimens examined have labradorite as the dominant feldspar, small amounts of pyroxenes, and some iron oxides. One specimen, representing a small outcrop low on the canyon wall, consisted entirely of serpentine.

According to Waring (1915, p. 264), a small area of rock immediately adjacent to Aqua de Ney consisted of dark schistose material. The area has been covered to some extent by masonry and by the collapse of wooden boardwalk structures that were part of the equipment of the one-time spring resort. The brief examination

made in 1958 did not suffice to distinguish whether the rocks in question are part of the old greenstone series of the Klamath Mountains that is considered to be of early Paleozoic age, or whether, as the present writers consider more probable, they consist of partly altered volcanic rocks. Also, according to WARING, the water of Aqua de Ney appeared to rise from a seam of clay-like decayed serpentine, a few inches wide, in the dark schistose rock mentioned. Subsequent construction at the spring site has apparently completely concealed this band of altered material.

On the geologic map (Fig. 1) the contact between the two suites of volcanic rocks is shown to coincide with the bed of Ney Springs Creek. The nature of that contact is not known. The contact may be either a fault or an overlap of younger volcanic rocks upon older ones. In addition to the terrace gravels mentioned, thick growths of shrubs and trees screen parts of the rock walls of the canyon, and since the logging operations of 1957–1958 heaps of logging debris and slash effectively conceal outcrops in large parts of the canyon. It is possible, however, to see what may be the most important geologic features related to the occurrence of the springs. These are shear zones oriented approximately at right angles to the bed of Ney Springs Creek. Two shear zones (Fig. 1) trend toward Aqua de Ney and a third strikes toward the mineral springs N–4, N–5, and N–6 (Table 1) that discharge from the south wall of the canyon a little east of Aqua de Ney. These zones of fracture may be the conduits by which water rises from depth. The high degree of comminution of rock particles characteristic of shear zones may be important in the geochemistry of the water by exposing large surface areas of rock for solution.

The geochemically important rocks that underlie the volcanic suites described remain unknown except by inference. It is thought that a thick sedimentary section underlies the volcanic rocks.

Chemistry of the Waters

The unique chemical nature of water from Aqua de Ney relative to other natural waters can most readily be appreciated by comparison with waters that have a salinity in the same general range.

It is possible that the high content of silica and of sodium in the spring water is genetically related to the chemical composition of the quartz–albite rocks composing the south wall of the canyon. As the rocks are relatively old, however, and the spring is non-thermal, it seems more reasonable to seek an explanation of mineralization other than one related to volcanism.

A survey of many mineral waters, including oil-field brines and thermal waters (WHITE, 1957, Table 4, p. 1666), suggests certain concentration ranges for significant dissolved constituents and ratios between selected constituents by which tentative separation of waters can be made according to origin. A comparison with the suggested characteristics should show the individuality of water from Aqua de Ney and make clear the points on which this uniqueness is based. Parts of WHITE's data are reproduced below (Table 2) and additional columns have been added showing comparable values for Aqua de Ney and the interpretations as to origin suggested by these comparisons.

The tabulated data show that Aqua de Ney has many characteristics in common with WHITES's oil-field brines and a few with his volcanic hot springs. The water

from Aqua de Ney is most strongly characterized, however, by three differences. These are the low value for the (Ca + Mg)/(Na + K) ratio, the high silica content, and the high pH. The pH (11·6) exceeds that of any other ground water so far described in the literature, or, in fact, of the vast majority of natural waters (White, 1957, pp. 1664, 1665, 1676; Hem, 1959, p. 54; and unpublished analyses, U.S. Geological Survey, Menlo Park). An extensive search of the literature on "mineral" waters by Waring and White has not revealed any other comparable ground water (White, 1959, written communication).

Table 2. Comparsion of analytical data for Aqua de Ney with data for oil-field brines and volcanic hot springs, according to White (1957, Table 2)

Ratios by weight	Oil-field brines	Volcanic hot springs	Aqua de Ney 1958	Aqua de Ney resembles
HCO_3/Cl	0·0001–1	0·01–3	0·483	Either
SO_4/Cl	0·00000–1	0·01–0·5	0·037	Either
F/Cl	0·00001–0·001	0·0005–0·1	0·00041	Brine
Br/Cl	0·0001–0·01	0·0001–0·001	0·0015	Brine
I/Cl	0·00003–0·02	0·00001–0·0005	0·0079	Brine
B/Cl	0·00001–0·02	0·01–0·1	0·0337	Volcanic
K/Na	0·001–0·03	0·03–0·3	0·0124	Brine
Li/Na	0·0001–0·003	0·003–0·03	0·00029	Brine
Ca + Mg/Na + K	0·01–5	0·001–0·2	0·00089	Neither
Concentrations (p.p.m.)				
SiO_2	10–100	100–700	3970	Neither
Ca	10–20,000	1–100	7·3	Volcanic
Mg	1–10,000	0·1–10	2·6	Either
Sr	1–3000	0·1–10	Not determined	
Ba	None–5000	0–1	0·0	Either
NH_4	0–500	None ?	148	Brine
NO_3	None–100	None ?	0·00	Either
As	?	0·1–10	0·00	Brines(?)
Sb	?	0·0–1	Not determined	
H_2S	0–3000	0–10	1000	Brine
CH_4	Large	None	Not determined	
Water soluble organic	large	None	Trace	Either

The unusual composition of this water raises many questions as to its origin. The most unusual aspect of this water is the high pH. If this can be explained, then an approach may be made to understanding the other unusual characteristics of Aqua de Ney.

Several approaches to an understanding of the problem have been suggested by interested persons. These are presented in brief, after which the writers' reconstruction of a sequence of events that may have occurred, is indicated.

Hydrolysis of silicate minerals in dilute high-temperature waters in contact with reactive rocks can account for pH's up to 9 and 10. The upper Basin in Yellowstone National Park and alkaline waters in the Tertiary basalts of Iceland provide instances (White, 1959, written communication).

Solution of sodium carbonate and sodium bicarbonate from evaporites by a normal connate water in contact with them could raise the pH of the connate water (White, 1959, written communication). Dr. K. B. Krauskopf (oral communication, 1959) has also suggested evaporites as a possible agent causing exceptionally high pH values in waters. No instances are known, however, of brines having pH of 11·6 after contact with evaporites, nor are evaporites known to underlie the area where Aqua de Ney emerges.

Another alternative, a connate water high in carbon dioxide and boron coming into contact with dedolomitized limestone at depth on or near igneous contact, has been suggested by White (1959, written communication). In this circumstance, dolomite might break down to form calcite and periclase, the carbon dioxide being driven off. Periclase may then hydrate to brucite. Later contact with connate water having excess carbon dioxide in the system, may substitute carbonate for hydroxide.

Another suggestion (Hem, 1959, written communication) requires a mechanism for removing hydrogen ions from solution. Reduction of sulphate, accompanied by oxidation of carbon and nitrogen in organic matter relatively poor in hydrogen, was proposed as a possibility. If the environment is noncalcareous so that restraint on the rising pH is absent, most of the other features of the water would then be explainable.

The possibility has been expressed by T. S. Lovering (oral communication, 1960) that the exceptional character of the water may reflect its origin as a mineralizing solution from a very deep source. In this hypothesis, elevated temperatures at depth would inhibit inclusion of CO_2 in the water and the high content of silica would be a direct expression of hydrothermal origin.

Some investigators consider that most oil-field brines originated primarily from diagenesis of entrapped sea water, and comparison of these waters with theoretical dilutions or concentrations of sea water is a common practice (DeSitter, 1947, pp. 2030–2040; White, 1957, pp. 1659–1692). The concentrations of chemical constituents in the waters to be compared are values obtained by calculations made assuming that the waters are of equal chloride concentrations.

The deuterium content of the water from Aqua de Ney is +2·6 (Friedman, 1958, written communication),* which is within the range typical for oil-field waters and connate waters of a similar salinity (White, 1959, written communication).

A comparison of the deuterium content of the water from Aqua de Ney with that of many California surface waters (−6·0 to −9·0) and a consideration of the dissolved-solids content indicate that the water has not been materially diluted by meteoritic waters in its ascent from the source. The low chloride concentration of the water from Aqua de Ney relative to that of sea water, suggests a possible mixture of the original source water for Aqua de Ney with other ground water having a comparable deuterium content. The ratios of chloride to other constituents in the

* The natural isotopic variations are customarily given in percent enrichment or depletion relative to a standard, as follows:

$$\delta D = \frac{D/H(\text{sample})}{D/H\ (\text{standard})} - 1 \times 100$$

The standard used for deuterium is water from Lake Michigan (Craig, 1957, p. 14).

water from Aqua de Ney show that considerable modification has occurred if the source water was originally entrapped sea water. The sodium, sulphide, carbonate and silica concentrations are very much in excess of amounts that would theoretically be present in a sea water of equal chloride content, and the calcium, magnesium, and sulphate contents are significantly less. If a sea-water origin is to be assumed, a mechanism must be sought that is capable of diminishing the concentrations of the alkaline earths while increasing those of the alkalis and silica, along with a mechanism for diminishing the sulphate and increasing the sulphide and carbonate concentrations.

If the presence of a material rich in exchangeable sodium and overlying the source of the water is assumed (Taylor, 1929, pp. 207–210), and the presence of sulphate-reducing bacteria such as have been reported in oil-field environments is postulated (Bastin, 1926, pp. 1270–1299), then a process of ion exchange that results in an increase of alkali at the expense of the alkaline earths can take place; and a process of sulphate reduction accompanied by an increase of carbonate and sulphide content can be visualized. The quantities of calcium, magnesium, and sulphate present in sea water when it is diluted to a chloride concentration equal to that of Aqua de Ney are not equivalent to the sodium, carbonate and sulphide found in Aqua de Ney. The writers therefore postulate admixture of an original connate water with a calcium magnesium sulphate type of ground water of such concentration as to account for the deficiencies. This assumption is considered reasonable in view of the relatively common occurrence of gypsiferous waters in oil fields (Crawford, 1942, p. 1318).

The chain of events postulated in the paragraphs which follow has been supported by calculations which show that a water having the composition of that from Aqua de Ney *could* originate in the manner suggested. The writers present the sequence as one hypothesis, among many, advanced to explain a phenomenon the origin of which remains unknown. The proposal is offered for consideration, not necessarily for acceptance by the readers.

If an ion-exchange process is to be considered, the relative replacing power of the ions involved is of paramount importance; this order has been given by Kelley (1955, p. 455) as: $Na < K < Mg < Ca < H$. Because of the apparently ready replacement of sodium ions by the other cations listed, and the widespread occurrence of calcium and magnesium salts in meteoric waters, clays that remain rich in exchangeable sodium are comparatively rare except at considerable depth below the ground surface, and hence below vigorously circulating meteoric waters (Kelley, 1955, p. 455). By designating the clays rich in exchangeable sodium as NaX, the summation of the exchange reactions may be written as follows:

(1) $$Ca\,SO_4 + 2\,NaX \rightleftharpoons CaX_2 + Na_2SO_4$$

(2) $$Mg\,SO_4 + 2\,NaX \rightleftharpoons MgX_2 + Na_2SO_4$$

With an abundance of sodium sulphate furnished by the above reactions, the sulphide and carbonate found in Aqua de Ney may be presumed to be the result of sulphate reduction. The uncombined gases furnished by such reactions may be instrumental in causing the water of Aqua de Ney to rise to ground level.

The non-thermal character of the spring suggests that the sulphate reduction occurred at relatively low temperature. The reduction of sulphate at low temperature and in the presence of oxidizable organic matter and of bacteria in oil-field environments has been reported from several sources. This process accordingly would seem a likely one for the production of the reduced sulphur species found in the water.

The relatively large concentration of boron found in the spring water may result from deposition of the host sediments of the hypothetical connate water under marine conditions in the presence of abundant organisms. Goldschmidt (1954. p. 289) has stated that boron is intimately connected with biological processes and has shown that nearly all siliceous organisms found in the sea contain relatively high concentrations of boron.

Another characteristic suggesting that metabolic processes may have influenced the chemical character of the water is the presence of ammonia. Ammonia is a constituent believed (White, 1957, p. 1671) to be characteristic of connate waters. Ammonia may be formed under conditions of anaerobic decomposition of organic material.

The chemical character of water of Aqua de Ney, then, is thought to be the result of processes of dilution, ion exchange, and sulphate reduction altering sea water originally entrapped in the sediments. The removal of hydrogen ions from solution by the processes of ion exchange and sulphate reduction has produced the high pH of Aqua de Ney.

The Redox potential of the water measured in E_h units was determined in the laboratory by the use of a Beckman model H-2 pH-meter. A platinum electrode was substitued for the glass electrode, and the meter was calibrated in terms of electromotive force (e.m.f.) by the use of a standard solution (Zobell, 1946). The observed e.m.f. value was referred to the standard half-cell by algebraic summation with the appropriate temperature correction value (Clark, 1928). The resulting value ($-0{\cdot}220$ V) confirmed the presence and persistence during storage of a strongly reducing environment in the water, as was anticipated from the presence of reduced forms of sulphur shown by the chemical analysis. Another E_h determination was made in February 1960 on a sample that had been in storage since May 1959. The E_h determined was $-0{\cdot}233$ V.

The ionic species of sulphur in the water of Aqua de Ney differ from the proportions expected at the prevailing pH and E_h. If the measured E_h represents the true condition in the water then sulphate should predominate over the sulphide species, according to stability diagrams given by Garrels and Naeser (1958, p. 128). The analysis of the water shows the reverse situation to be true. The reasons for this divergence are not known, but one might surmise that the reaction rates for the several stages in the reduction process are responsible for the non-equilibrium conditions, or that the measured E_h is not a true value.

The very high silica concentration is probable due to the high pH of the water. Krauskopf (1956) has shown that silica solubility increases very rapidly above a pH of 9. Solution of many forms of silica from rock walls should occur at this high pH.

The effect of reducing the pH by introducing carbon dioxide gas into a sample

of the water of Aqua de Ney was examined. Immediately before the test the pH of the water was 11·5. Carbon dioxide was generated and bubbled through the water sample for 20 min. During this time the pH steadily decreased. At the end of the test the pH was found to be 7·7. Within a few minutes after cessation of bubbling, a white suspension appeared. Several hours later the solution thickened and resembled a gel. Although no confirming analytical tests were made, the appearance of the gel and the high content of silica in the water suggest that the formation of the gel was due to the precipitation of silica.

The laboratory test suggests the possibility that if a great abundance of carbon dioxide had been present in the environment of the water of Aqua de Ney prior to its discharge at land surface, the pH and the silica concentration alike would have been much lower.

A portion of water from Aqua de Ney was placed in a flask and treated with an excess of calcium chloride. After 3 days during which the treated sample stood in the laboratory, a calcium determination was made, showing an increase of calcium of about 8 p.p.m. The following day a duplicate determination yielded the same result. It appears, therefore, that under conditions of storage at least, the water is not saturated with respect to calcium. This fact may support the hypothesis that base exchange removed calcium from Aqua de Ney water, but the evidence remains less than conclusive.

The term "alkalinity" is used variously by different authors. In the present discussion, the usage follows that accepted by the Quality of Water Branch of the U.S. Geological Survey (Hem, 1959, p. 92). Thus, alkalinity is defined as the capacity of a water containing a compound or compounds, with or without hydrolysis, for neutralizing strong acid to a titration end point of pH 4·5.

The routine determination of alkalinity failed to give consistent results; therefore, the alkalinity was determined by a modified titration procedure which allowed for the progressive hydrolysis of the titrated constituents and gave more nearly reproducible results.

An analysis of the total carbonate ionic species of this water was made in the Denver laboratory of the Quality of Water Branch (Hem, 1957, written communication). The Denver determination was by evolution and measurement of the CO_2 gas and was therefore not subject to errors introduced by titration of other weak acids. The total amount of dissolved carbonate in terms of carbon dioxide (2500 p.p.m.) so determined, was substantially lower than that calculated from the titration procedure and indicated that constituents in the water other than bicarbonate, carbonate, and hydroxide ions were contributing to the alkalinity. Compounds of boron and compounds of silica are probably largely present in dissociated states.

The concentrations of constituents shown in Table 1 do not accurately represent the ionic species actually in solution. As mentioned, boron and silica are probably present largely as dissociated ions. Likewise, the table also shows sulphide as hydrogen sulphide whereas in reality at pH 11·6 it is thought to be present as HS^-. On the other hand ammonia is reported as NH_4^+ when at pH 11·6 very little should be present in the ionized state but probably exists as undissociated NH_4OH.

The alkalinity titration yields a value for hydroxide (OH) of 1430 p.p.m.

(Table 1). The OH activity, calculated from the pH, is approximately equivalent to that of 70 p.p.m. OH. The activity coefficient for the ion in this solution is not known but it appears likely that the actual OH concentration cannot be greater than 100 to 200 p.p.m.

The effect of the water of Aqua de Ney upon the chemical character of water in Ney Springs Creek is shown by the comparison given below. Samples for analysis were taken at the points indicated upstream and downstream from the spring.

Table 3. Discharge, dissolved-solids content, and chloride concentrations along a portion of Ney Springs Creek

Sampling point	Discharge (g.p.m.)	Dissolved (p.p.m.) solids	Chloride (p.p.m.)
(1) Ney Springs Creek, 50 yd above Aqua de Ney	315 (measured)	83	6·1
(2) Aqua de Ney Spring	1 (estimated)	31,200	7180
(3) Ney Springs Creek, 0·5 mile below Aqua de Ney	316 (estimated)	136	20

The changes calculated from the above data and the following equations are:

Sampling point 1 + sampling point 2 = sampling point 3
p.p.m. × g.p.m. + p.p.m. × g.p.m. = p.p.m. × g.p.m.
Dissolved solids $83 \times 315 + 31{,}300 \times 1 = 136 \times 316$
$57{,}345 \neq 42{,}976$

The imbalance above presumably results from the inflow of water from a number of small springs seen downstream from Aqua de Ney Spring and upstream from sampling point (3)

Conclusions

The water of Aqua de Ney possesses unusual characteristics which distinguish it from other waters. These characteristics—namely, the low (Ca + Mg)/(Na + K) ratio, the pH (11·6), and the high silica content (4000 p.p.m.)—are thought to be related in cause and are accounted for, in theory, by alteration of a mixture of entrapped sea water and a calcium magnesium sulphate ground water. The abundance of alkali metals vs. the scarcity of alkaline earths suggests the occurrence of base exchange. The abundance of sulphides and of carbonates and the comparatively low sulphate content are probably indicative of sulphate reduction. There are many points of similarity to oil-field brines, and no evidence of thermal activity is associated with the water; hence, a metabolic reduction of sulphate such as is common in oil-field environments is assumed.

Alteration of the chemical constituents of the water by base exchange and sulphate reduction under the specified conditions has resulted in the removal of hydrogens ions from solution which, has caused alkaline conditions that result in the very high pH of the water. The high pH and the availability of siliceous minerals have contributed large amounts of silica to solution.

Acknowledgements—The writers acknowledge with sincere appreciation help received from many people who made independent determinations of chemical constituents in the water or of mineral content of the rocks as seen in thin section. Especially do they thank J. D. Hem, R. G. Coleman and R. A. Gulbrandsen, all of the Geological Survey, for their help. Appreciation is expressed also to K. B. Krauskopf, Stanford University, and D. E. White, W. L. Lamar and Ivan Barnes, all of the Geological Survey, for their helpful review of the manuscript. The responsibility for interpretation as well as for errors of commission or omission, however, rests with the writers.

References

Bastin E. S. (1926) The problem of natural reduction of sulphates. *Bull. Amer. Ass. Pet. Geol.* **10,** 1270–1299.

Bonham H. F., Jr. and Sharp J. V. A. (1958) Areal geology of Mount Shasta and vicinity, California. *Bull. Geol. Soc. Amer.* **69,** 1675 (Abstract).

Clark W. M. *et al.* (1928) Studies on oxidation-reduction. *U.S. Hygenic Bull.* 151, pp. 1–163.

Craig H. (1957) Deuterium-oxygen 18-tritium relationships in natural waters. *Proceedings of the* 1957 *Conference on New Research Methods in Hydrology, Comm. on Research in Water Resources, La Jolla, California.* p. 15. California University, Scripps Institute of Oceanography, La Jolla.

Crawford J. G. (1942) Oil-field waters of Montana plains. *Bull. Amer. Ass. Pet. Geol.* **26,** 1317–1374.

DeSitter L. U. (1947) Diagenesis of oil-field brines. *Bull. Amer. Ass. Pet. Geol.* **31,** no. 11, 2030–2040.

Garrels R. M. and Naeser C. R. (1957) Equilibrium distribution of dissolved sulphur species in water at 25°C and 1 atm total pressure. *Geochim. et Cosmochim. Acta* **15,** no. 1/2, 113–130.

Goldschmidt V. M. (1954) *Geochemistry.* Oxford University Press.

Hem J. D. (1959) Study and interpretation of the chemical characteristics of natural waters. *U.S. Geol. Survey Water-supply Paper* 1473, 269 p.

Hinds N. E. A. (1935) Mesozoic and Cenozoic eruptive rocks of the southern Klamath Mountains, California. *Calif. Univ., Dept. Geol. Sci. Bull.* **23,** no. 11, 313–380.

Hinds N. E. A. (1940) Paleozoic section of the southern Klamath Mountains, California. *Proceedings of the Sixth Pacific Science Congress* 1939, *Berkeley California.* Vol. 1, pp. 273–287. (Preprint).

Kelley W. P. (1955) Base exchange in relation to sediments. In *Recent Marine Sediments—a Symposium* p. 455. Society of Economic Paleontologists and Mineralogists, Spec. Pub. 4.

Kennedy G. C. (1950) A portion of the system silica-water. *Econ. Geol.* **45,** 629–653.

Krauskopf K. B. (1956) Dissolution and precipitation of silica at low temperatures. *Geochim. et Cosmochim. Acta* **10,** 1–26.

Nutting P. G. (1933) The bleaching clays. *U.S. Geol. Surv. Circ.* 3, 51 p.

Taylor E. McKenzie (1929) Papers on base exchange. *J. Pet. Technol.* **15,** 207–210.

Waring G. A. (1915) Springs of California. *U.S. Geol. Surv. Water-Supply Paper* 338, 410 p.

White D. E. (1957) Magmatic, connate, and metamorphic waters. *Bull. Geol. Soc. Amer.* **68,** 1659–1682

Zobell C. E. (1946) Studies on Redox potential of marine sediments. *Bull. Amer. Ass. Pet. Geol.* **30,** no. 4, 477–513.

Geochimica et Cosmochimica Acta, 1961, Vol. 22, pp. 87 to 93. Pergamon Press Ltd. Printed in Northern Ireland

The colorimetric and polarographic determination of some trace elements in the standard rocks G–1 and W–1

Ian Carmichael and Alison McDonald
Department of Geology, Imperial College of Science and Technology, London

(*Received* 10 *October* 1960)

Abstract—The elements Bi, Cd, Co, Cu, Ni, Pb, Sn and Zn have been determined colorimetrically and polarographically on the standard rocks G–1 and W–1, and the results are briefly compared with published data.

Introduction

At the same time that some trace elements in some natural acid glasses from the North Atlantic Tertiary volcanic province were being determined, the two standard rocks G–1 and W–1 were included with each batch, and the results obtained for these two standards are reported here. The inclusion of the two standards with series of samples provided a valuable control on the chemical techniques, and the quintuplicate determinations for Cu, Ni, Pb and Zn allow an estimate of the precision of the colorimetric methods at two different concentration levels to be made.

None of the colorimetric methods described below is new, and many of them are currently employed at the Geochemical Prospecting Research Centre, Imperial College. The final colorimetric comparison of the unknown solutions with standards has in all cases been made visually, thus allowing a very much smaller volume of solvent or coloured phase than that necessary for the smallest size of spectrophotometric cell. Visual comparison is particularly successful with mixed-colour complexes, such as are obtained with dithizone. In an attempt to eliminate personal bias, the first author alone prepared the rock samples from the initial decomposition to the stage of visual comparison which was done entirely by the second author. By varying the weights of sample and the dilution factors, a bias which may exist in visual comparison has been further minimized.

Analytical Methods

Cadmium, cobalt, copper, lead, nickel and zinc

A 1–2 g sample was decomposed by means of a hydrofluoric–perchloric acid mixture and the residue, having been evaporated to fumes, taken up in dilute hydrochloric acid. The solution was transferred to a separating funnel, and the pH adjusted to 9·5 using an ammoniacal sodium citrate–hydroxylamine hydrochloride buffer. The dithizone-reacting metals were extracted by repeated shaking with dithizone in CCl_4 until the organic phase remained green; the extracts were then evaporated to dryness. The organic residue was destroyed by heating with concentrated sulphuric–perchloric acids and fumed to dryness. The residue was taken up in 0·2 N hydrochloric acid and made up to a volume of 10 ml. This procedure is based on one described by Sandell (1950, pp. 405–406).

Cadmium. A 2 ml aliquot (W–1 only) was taken for the determination of Cd, the dithizonate being extracted from 4 N caustic soda. This method, which is slightly modified from that described by Sandell (1950, p. 238), enables 0·1 p.p.m. of Cd to be satisfactorily determined.

Cobalt. A 1–3 ml aliquot was taken for the estimation of Co, the thiocyanate complex being extracted into a 1:9 mixture of tri-*n*-butylamine and amyl alcohol at pH 5. This method will be submitted for publication later by the second author and others.

Copper. A 1–2 ml aliquot (G–1) was taken for the estimation of Cu by 2:2-diquinolyl using an acetate–tartrate hydroxylamine buffer solution (Almond 1955). Dithizone in benzene was also used and gave comparable results although the coloured organic phase is not very stable, and soon fades.

Nickel. A 1–2 ml aliquot was taken for the estimation of Ni by α-furil dioxime which was extracted into benzene at a pH of 9·5 using an ammonia–ammonium citrate buffer (Stanton and Coope, 1958). The coloured organic phase, as with the copper method, is very stable towards light and the yellow colours produced are easily matchable.

Lead and zinc. A 2 ml aliquot was adjusted to pH 9·5 in a separating funnel and the reacting metals extracted by dithizone in CCl_4. The dithizone extract was transferred to another funnel and shaken with an equal volume of 0·01 N hydrochloric acid. The dilute acid extract was concentrated on a water bath, made up to 10 ml, and the organic layer discarded. The authors have found it more convenient to separate the copper from the cadmium, lead and zinc by this procedure rather than from the initial dithizone extracts, because of the uncertain behaviour of cobalt and nickel. Lead and zinc were determined by dithizone in benzene using procedures very similar to those described by Sandell (1950, pp. 406 and 629).

Any remaining solution of the initial dithizone extraction may be used for the polarographic determination of Cd, Cu, Pb, Zn and perhaps Bi. A square wave Mervyn–Harwell polarograph was used by the authors, as the greatly enhanced sensitivity of this type of instrument over other polarographs (cf. Ferrett *et al.*, 1956) is necessary for the low concentrations involved.

Bismuth. A nitric acid-ammonium chloride electrolyte was used for the determination of Bi. As bismuth readily hydrolyses from dilute hydrochloric acid solutions to BiOCl, the solutions of G–1 and W–1 were run on the polarograph immediately on making up to volume after the destruction of the organic residue by perchloric–sulphuric acids (see above). The results obtained for G–1 (Table 2) are only to be treated as an order of magnitude, as the peaks obtained on the polarograms could not be reproduced after 2 or 3 hr standing of the original solutions. The peak for Bi in W–1 is unfortunately masked by the very large Cu peak, and it could not be determined.

Cadmium. A 1 ml aliquot of the initial dithizone extract solution was used for the determination of Cd in a phosphoric acid electrolyte. The interference of In was checked, although Iwantscheff (1958, p. 141) indicates that it is not extracted by dithizone in CCl_4 at pH 9·5.

Copper and lead. A further dilution of an aliquot of the initial extract was made, and copper and lead determined in an hydrochloric acid–potassium thiocyanate electrolyte.

Zinc. The most satisfactory electrolyte for the determination of Zn proved to be 0·02 N hydrochloric acid, so that as for Cu and Pb, an aliquot of the initial dithizone extract was further diluted by 10.

Several attempts have been made to determine thallium (which is also extracted by dithizone) polarographically, but the large amount of lead in relation to thallium in both G–1 and W–1 (Morris and Killick, 1960) necessitates the use of EDTA as a complexing agent, which in the electrolytes used reduced the sensitivity considerably. Several results were obtained for G–1, and while of the same order of magnitude were not particularly reproducible, and this problem is being further studied.

Tin. A 1 g sample of rock powder was heated in a long test tube with ammonium iodide, the sublimate leached with 1 N hydrochloric acid, and an aliquot taken for the determination of tin by gallein. This is a prospecting field method (Wood, 1957) and was only modified in detail.

In order to keep the reagent blanks to a minimum, all the reagents were examined polarographically before analysis. The added reagents were at all times carefully measured, and the reagent blank solutions were taken through the whole scheme of analysis.

With the exception of zinc as noted below, none of the polarographic determinations were made on the same solutions used for the colorimetric determinations.

Discussion of Results

The distinction between accuracy and precision is not always appreciated, for accuracy refers to the closeness of approach to the "true value", whereas precision is the ability to reproduce results. The precision and accuracy for the classical chemical determinations of the major elements in silicate rocks has been discussed by Fairbairn (1953) and for the rapid chemical methods by Mercy (1956). No such comprehensive study has yet been published of the chemical determination of the trace elements in silicate rocks.

The neutron activation determinations of many of the trace elements in G–1 and W–1, with their high sensitivity, specificity, and freedom from reagent blanks, probably yield the closest approach to the true value for a particular element. Using the radiochemical data of SMALES (1955), SMALES *et al.* (1957) and

Table 1. Colorimetric results for the granite G–I, Westerly, U.S.A.

Element	Values (p.p.m.)	$\bar{x}$	C	E	Previous data and source
Cobalt	1·3, 1·3	1·3	—	—	2·2 (all determinations) AHRENS and FLEISCHER (1960)
Copper	8·5, 10, 10, 10·5, 11	10	9·4	4·2	9·5 (radiochemical) SMALES (1955); 13 (all determinations) AHRENS and FLEISCHER (1960)
Lead	47, 48, 48, 50, 52	49	4·1	1·8	47 (colorimetric) FLANAGAN (1960)
Nickel	0·7, 0·9, 1·0, 1·0, 1·2	1·0	19	8·5	1·2 (radiochemical) SMALES *et al.* (1957)
Tin	3·0, 3·0, 3·3, 3·5, 3·5	3·3	7·9	3·5	2·3 (colorimetric) ONISHI and SANDELL (1957)
Zinc	37, 42, 43, 45, 45	42	7·9	3·5	40 (all determinations) AHREN and FLEISCHER (1960)

Table 2. Polarographic results for G–I

Element	Values (p.p.m.)	$\bar{x}$	C	E	Previous data
Bismuth	0·22, 0·27	0·25	—	—	None
Cadmium	0·06, 0·08, 0·09, 0·10	0·08	—	—	0·06 (radiochemical) VINCENT and BILEFIELD (1960)
Copper	9, 9, 10, 10, 12	10	12	5·4	9·5 and 13
Lead	44, 46, 46, 47, 50	47	4·7	2·1	47 } See Table 1
Zinc	36, 36, 36, 37	36	—	—	40

$\bar{x}$, arithmetic mean of the determinations.

C, relative deviation of a single determination $\frac{s}{\bar{x}} \times 100$, where s = standard deviation of a single determination.

E, relative error of the arithmetic mean, $C/\sqrt{n}$ where n = number of observations.

VINCENT and BILEFIELD (1960) it is thus possible to make some assessment of the accuracy of the colorimetric and polarographic results presented in Tables 1, 2, 3 and 4. The results of the computations on precision are also given, where five replicate determinations have been made, and in the discussion which follows, the precision, expressed as the relative deviation of a single observation (C) has been arbitrarily subdivided as follows:

C less than 5 per cent, precise; C between 5 per cent and 10 per cent, moderately precise; and C greater than 10 per cent lacking precision (cf. MERCY, 1956, p. 167).

Fairbairn *et al.* (1951, p. 27) have suggested that for spectrochemical analysis under ideal conditions, a relative deviation of 2 per cent may be attained, although this is believed to refer in the main to the major elements.

Both the polarographic and the colorimetric results for cadmium (Tables 2, 3 and 4) show fair agreement with the radiochemical determinations, although the results for G–1 (Table 2) are not so reliable in view of the reagent blank, as the acids used gave a measureable cadmium peak. However, the results suggest that the chemical techniques are reasonably accurate.

The colorimetric results for cobalt in W–1 (Table 3) indicate that single determinations are precise although, compared with the radiochemical results, not accurate. It is perhaps significant that other colorimetric results for cobalt in W–1 (Ahrens and Fleischer, 1960, p. 88) are also low, and in the writers' experience, the extraction of cobalt by dithizone is impeded by an excess of the citrate–hydroxylamine buffer in the aqueous solution, so that only the minimum necessary should be added (Sandell, 1950, p. 272). The results for both G–1 and W–1 (Tables 1 and 3) indicate that cobalt has been incompletely extracted by dithizone if compared to the radiochemical cobalt determinations, although the average of all cobalt determinations for W–1 (Table 3) is close to these new results.

The colorimetric values for copper in W–1 (Table 3) show that single determinations are both accurate and precise, the colorimetrically determined mean being in good agreement with the radiochemical mean, but at the lower level of copper in G–1 single determinations become only moderately precise and inaccurate. The polarographic results show excellent agreement with those obtained colorimetrically, and single polarographic determinations have comparable precision to the colorimetric observations.

The lead content of G–1 was in some doubt and led to the extensive colorimetric and spectrochemical re-examination reported by Flanagan (1960) with the result that the lead content, which originally was believed to be 27 p.p.m. (Ahrens, 1954), is now considered to be near 50 p.p.m.

Some of the results obtained by the writers for lead in G–1 are confusing, as the first five colorimetric determinations gave a mean value of 28 p.p.m. with C equal to 4·6. These five determinations used up the last of the powder from the bottle. In order to check these results polarographically, five samples were taken from a new bottle of G–1, and unwittingly, the buffer used for the initial dithizone extraction was modified to obtain the maximum extraction of cobalt (see above), and lead was determined polarographically with the results set down in Table 2. More samples were then taken for the colorimetric determination of lead, the results of which agree well with the polarographic determinations. At the moment it is not known whether an excess of citrate–hydroxylamine buffer prevents the complete extraction of lead by dithizone, or whether there was a difference between the two bottles of G–1 (Flanagan, 1960).

Both the colorimetric and polarographic results for lead for G–1 agree well with the average of the chemical determinations (Flanagan, 1960), although in neither case is the precision as good as that reported by Flanagan. The lead content of W–1 is less well known; these results (Tables 3 and 4) are in agreement with each other and with those obtained colorimetrically by Thompson and Nakagawa (1960).

The nickel results for W–1 (Table 3) indicate that single determinations are precise but not very accurate, the mean value being about 7 per cent higher than the radiochemical mean. This may in part be due to one rather low result used in the

Table 3. Colorimetric results for the diabase W–I, Centerville, U.S.A.

Element	Values (p.p.m.)	$\bar{x}$	C	E	Previous data and source
Cadmium	0·2, 0·4, 0·4	0·3	—	—	0·33 (radiochemical) Vincent and Bilefield (1960)
Cobalt	38, 40, 40, 42, 42,	40	4·3	1·9	51 (radiochemical) Ahrens and Fleischer (1960) 38 (all determinations)
Copper	108, 113, 114, 114, 115	113	2·4	1·9	112 (radiochemical) Smales (1955)
Lead	8, 8, 8, 9, 10	9	11	4·9	8 (colorimetric) Thompson and Nakagawa (1960)
Nickel	76, 78, 79, 79, 80	78	2·0	0·9	73 (radiochemical) Smales (1955) 82 (all determinations) Ahrens and Fleischer (1960)
Tin	2·5, 2·5	2·5	—	—	2·8 (colorimetric) Onishi and Sandell (1957)
Zinc	80, 83, 85, 85, 90	85	4·2	1·9	82 (all determinations) Ahrens and Fleischer (1960)

Table 4. Polarographic results for W–I

Element	Values (p.p.m.)	$\bar{x}$	C	E	Previous data
Cadmium	0·24, 0·27, 0·33, 0·35	0·30	—	—	0·33
Copper	108, 108, 110, 110, 111	109	1·3	0·6	112
Lead	8, 8, 10, 11, 12	10	18	8·0	8
Zinc	58, 63, 63, 64	62	—	—	82

See Table 3

$\bar{x}$, arithmetic mean of the determinations.
C, relative deviation of a single determination, $s/\bar{x} \times 100$ where s = standard deviation of a single determination.
E, relative error of the arithmetic mean $C/\sqrt{n}$ where n = number of observations.

compilation of the radiochemical mean (Smales, 1955) which if neglected would raise it to 75 p.p.m. The results for G–1 (Table 4) show that single colorimetric determinations lack precision and are inaccurate, although this is to be expected at this concentration level.

The results obtained by the rapid field method for tin are in surprisingly good agreement with those obtained by the more elegant method of Onishi and Sandell (1957). The precision of a single determination is also good (Table 1).

The results of the determination of zinc in both G–1 and W–1 are difficult to

assess. Sandell (1950, p. 620) indicates that copper, cobalt and nickel interfere in varying degrees in the colorimetric determination of zinc by dithizone. Copper and more or less of the cobalt and nickel may be separated from zinc by making a second dithizone extraction and shaking the dithizone extracts with 0·01 N hydrochloric acid, the zinc passing into the acid together with some of the cobalt and nickel.

Table 5. Determination of zinc in G–I and W–I

	Values (p.p.m.)	$\bar{x}$	C
G–I*	52, 52, 52, 53, 57	53	4·2
†	37, 42, 43, 45, 45	42	7·9
‡	36, 36, 36, 37	36	—
W–I*	113, 116, 116, 118, 118	116	1·6
†	80, 83, 85, 85, 90,	85	4·2
‡	58, 63, 63, 64	62	—

* Determinations of zinc without removal of copper, cobalt or nickel.
† Determination of zinc after removal of copper, some cobalt and nickel.
‡ Polarographic determinations without removal of copper, cobalt or nickel.

Zinc was determined in the acid extract, and also in the original solution before the second dithizone extraction, and the results for both rocks are given in Table 5. It may be concluded that copper, cobalt and nickel interfere seriously and lead to higher results, the lower zinc values of the acid extracts showing satisfactory agreement with other published data (Tables 1 and 3). The identical original solutions were then examined polarographically for zinc and the results are also given in Table 5. Although the polarographic zinc values for G–1 are only a little below the average of other determinations (Table 2), the results for W–1 are 20 p.p.m. below the average (Table 4) and would seem excessively low, although obtained on the identical solutions used for colorimetric analysis before the second dithizone extraction.

The authors conclude that although copper, together with some of the cobalt and nickel may be separated from zinc by the second dithizone extraction, the nickel and cobalt and possibly other elements which accompany zinc into the dilute acid interfere more seriously than is supposed, and it is considered that the polarographic results are probably a better approach to the true value for zinc in both G–1 and W–1.

Whether or not copper is separated before the determination of zinc, single determinations are precise for W–1, moderately precise for G–1, but where the prior separation of copper has been neglected, grossly inaccurate (Table 5). The data presented in Table 5 clearly illustrate the distinction between accuracy and precision.

Conclusions

The general measure of agreement between the polarographic results and those obtained colorimetrically, which although not completely independent of one another, for both rely on the same initial dithizone extraction, serve to show that the visual colorimetric methods for the determination of cadmium, copper and lead

are sufficiently precise and sensitive. The nickel determinations have no polarographic check but also seem satisfactory.

If the published radiochemical determinations of cobalt in both G–1 and W–1 are correct, then it would appear that the technique employed by the writers does not achieve a complete extraction of cobalt by dithizone.

It has been shown that copper, cobalt and nickel seriously interfere with the determination of zinc, and these elements must of necessity be separated by shaking a second dithizone extract with dilute acid. It is considered that even after this second separation, small amounts of nickel and cobalt and perhaps other elements which may accompany zinc, continue to interfere, and accordingly the polarographic determinations of zinc are believed to be more reliable.

Acknowledgements—The authors are indebted to Mr. R. E. Stanton of Imperial College for his advice and encouragement on analytical methods, and to Dr. E. A. Vincent for his criticism of the manuscript.

References

Ahrens L. H. (1954) *Quantitative Spectrochemical Analysis of Silicates.* Pergamon Press, London.

Ahrens L. H. and Fleischer M. (1960) Second report on a cooperative investigation of the composition of two silicate rocks. IV—Report on trace constituents in granite G–I and diabase W–I. *Bull. U.S. Geol. Surv.* 1113.

Almond H. (1955) Rapid field and laboratory method for the determination of copper in soils and rocks. *Bull. U.S. Geol. Surv.* 1036-A.

Fairbairn H. W., Schleet W. G., Stevens R. E., Dennen W. H., Ahrens L. H. and Chayes F. (1951) A cooperative investigation of precision and accuracy in chemical, spectrochemical and modal analysis of silicate rocks. *Bull. U.S. Geol. Surv.* 980.

Fairbairn H. W. (1953) Precision and accuracy of chemical analysis of silicate rocks. *Geochim. et Cosmochim. Acta* **4,** 143–156.

Ferrett D. J., Milner G. W. C., Shalgosky H. I. and Slee L. J. (1956) A comparative study of three recently developed polarographs. *Analyst.* **81,** 506–512.

Flanagan F. J. (1960) Second report on a cooperative investigation of the composition of two silicate rocks. V—The lead content of G–1. *Bull. U.S. Geol. Surv.* 1113.

Iwantscheff G. (1958) *Das dithizon und seine Anwendung in der Mikro- und Spurenanalyse.* Verlag Chemie, Weinheim/Bergstr.

Morris D. F. C. and Killick R. A. (1960) The determination of silver and thallium in rocks by neutron-activation analysis. *Talanta* **4,** 51–60.

Mercy E. L. P. (1956) The accuracy and precision of "rapid" methods of silicate analysis. *Geochim. et Cosmochim. Acta* **9,** 161–173.

Onishi H. and Sandell E. B. (1957) Meteoritic and terrestrial abundance of tin. *Geochim. et Cosmochim. Acta* **12,** 262–270.

Sandell E. B. (1950) *Colorimetric Determination of Traces of Metals* (2nd Ed.) Interscience, New York.

Smales A. A. (1955) Some trace element determinations in G–I and W–I by neutron activation. *Geochim. et Cosmochim. Acta* **8,** 300.

Smales A. A., Mapper D. and Wood A. J. (1957) The determination, by radioactivation, of small quantities of nickel, cobalt and copper in rocks, marine sediments and meteorites. *Analyst.* **82,** 75–88.

Stanton R. E. and Coope J. A. (1958) Modified field test for the determination of small amounts of nickel in soils and rocks. *Trans. Instn. Min. Metall. Lond.* **68,** 9–14.

Thompson C. E. and Nakagawa H. M. (1960) Spectrophotometric determination of traces of lead in igneous rocks. *Bull. U.S. Geol. Surv.* 1084-F.

Vincent E. A. and Bilefield L. I. (1960) Cadmium in rocks and minerals from the Skaergaard intrusion, East Greenland. *Geochim. et Cosmochim. Acta* **19,** 63–69.

Wood G. A. (1957) Studies on rapid analytical methods for use in geochemical prospecting. Ph.D. thesis, University of London.

Geochimica et Cosmochimica Acta, 1961, Vol. 22, pp. 94 to 98. Pergamon Press Ltd. Printed in Northern Ireland

Age measurements on pegmatites and a basic charnockite lens occurring near Lützow-Holm Bay, Antarctica

L. O. Nicolaysen,* A. J. Burger,† T. Tatsumi‡ and L. H. Ahrens§

(*Received* 17 *August* 1960)

Abstract—Rb^{87}-Sr^{87} age measurements were carried out on large biotite crystals from three granitic pegmatites and a basic charnockite lens occurring near Lützow—Holm Bay, Queen Maud Land. The mean age obtained (~ 515 million years) probably refers to the last major metamorphic episode in this region. The age data are also significant for the interpretation of palaeomagnetic results reported from this area.

The wintering team of the First Japanese Antarctic Expedition (1957–1958) explored rocky areas along the east coast of Lützow-Holm Bay, the Prince Harald Coast, and the western part of the Prince Olav Coast. Preliminary reports on geomorphologic and geologic studies have been published by Tatsumi and Kikuchi (1959a, b). The entire area surveyed consists of different kinds of metamorphic rock. Hornblende–pyroxene dioritic gneisses, showing a weak

Fig. 1.

* The Bernard Price Institute of Geophysical Research, Johannesburg.
† C.S.I.R., Pretoria.
‡ Geological Institute, Univeristy of Tokoyo, and
§ Department of Chemistry, University of Cape Town.

gneissic structure, occur extensively. These rocks show a close petrographic resemblance to the intermediate type of charnockite from neighbouring Enderby Land and from Adelie Land in Antarctica. Quartzo–feldspathic gneisses containing the assemblance pyralspite–biotite are widely distributed in this area, while marbles, quartzites and bands of basic metamorphic rock were also found. Lenticular masses and cross-cutting veins of pegmatite occur in all these rocks.

The location of Lützow-Holm Bay, Enderby Land and Adelie Land are shown in Fig. 1.

The age measurements reported here were carried out because there was no geologic information of any sort concerning the age of this great tract of metamorphic rocks. Interesting problems are posed by their unusual petrology, and their age has an additional significance in that systematic palaeomagnetic studies have been carried out in this region: Nagata and Shimizu (1959) reported concordant data on the natural remanent magnetization of biotite–hornblende granodioritic gneisses from the Ongul Islands, north of Lützow-Holm Bay.

Rb^{87}–Sr^{87} age measurements were carried out on extremely fresh biotite crystals, several centimetres in diameter, from the following occurrences:

Specimen No.	Lat.	Long.	Locality	Rock type
JARE 57112001	69°13′S	39°38′E	Lang Hovde district, Lützow-Holm Bay	Granitic pegmatite in granitic gneiss
JARE 57102622	69°38′S	39°18½′E	E. ridge of 190 m high mountain, Skallen district	Granitic pegmatite in dioritic gneiss (charnockite)
JARE 57110704	69°26′S	39°34′E	E. ridge of 410 m high mountain, Skarvsnes district	Granitic pegmatite in dioritic gneiss
JARE 57122307	69°1½′S	39°34′E	West Ongul Island	A small biotite rich mass in a basic charnockite lens, occurring in granodioritic gneiss

The concentrations of rubidium and radiogenic strontium were measured by the method of stable isotope dilution (Inghram, 1955). The Rb isotopic ratios were measured on a 6-in. radius-of-curvature mass spectrometer, using a balanced d.c. amplifier, and the Sr isotope measurements were carried out on a 12-in. machine equipped with an electron multiplier. The following results were obtained:

Mica specimen	Rb^{87} concentration (p.p.m.)	Radiogenic Sr^{87} concentration (p.p.m.)	Sr^{87} abundance	Age (million years)
57112001	250 ± 3	1·82 ± 0·13	0·139	525 ± 40
57102622	447 ± 9	3·29 ± 0·07	0·59	530 ± 16
57110704	182 ± 3 181 ± 2	1·28 ± 0·07	0·267	510 ± 30
57122307	248 ± 3	1·71 ± 0·09	0·170	500 ± 30

All ages calculated with λ for $Rb^{87} = 1{\cdot}386 \times 10^{-11}$ years^{-1}. Errors quoted are standard deviations.

The measurements on these biotites indicate that the three pegmatites and the basic charnockite lens (a metamorphic rock) are all of the same age, within the limits of the experimental errors. This agreement is significant; it indicates that the mean age ($\sim$515 million years) probably refers to the major metamorphic episode in this region. Specimen JARE 57102622 occurs in a pegmatite which also contained crystals of euxenite. The results of U, Pb measurements on this euxenite also indicate an age of $\sim$500 million years (Saito, Sato and Tatsumi, in press). Goldich *et al.* (1958) reported K^{40}–A^{40} age measurements on mica from a biotite–hornblende–augite paragneiss occurring on the west side of McMurdo Sound in Antarctica (see Fig. 1). Using the values $\lambda_\beta = 4{\cdot}72 \times 10^{-10}$ year^{-1}; $\lambda_e = 0{\cdot}585 \times 10^{-10}$ year^{-1} for the decay constants of K^{40} (see Aldrich and Wetherill, 1958), their data yield an age of 500 million years. This is very close to the ages of the five specimens from the Lützow-Holm Bay area. It appears probable that the metamorphism of the pyroxene granulites, amphibolites and granitic gneisses around McMurdo Sound took place at approximately the same time as the metamorphism in the Lützow-Holm Bay area. Further measurements from Antarctica have been reported by Tugarinov *et al.* (1959), who carried out determinations on orthite, biotite and muscovite, from a pegmatite in the Mirny region. These isotopic measurements indicated an age close to 1300 million years for this pegmatite.

The geologic time-scales published by Holmes (1959) and Kulp (1959) indicate that the date 500 million years ago is part of the Lower Palaeozoic Era. According to Holmes and Kulp, it occurred near the end of the Cambrian period. It has been widely assumed by petrologists that the charnockitic metamorphic rocks of Antarctica are of Pre-Cambrian age—see for example Fyfe *et al.* (1958, p. 232)—and this age was adopted by Tatsumi and Kikuchi (1959b), and by Nagata and Shimizu (1959) in their discussion of the palaeomagnetic results. This supposition for the rocks near Lützow-Holm Bay was based only on their petrographical features and not on field relations.

The many age determinations ranging from 450 to 520 million years have been reviewed by Holmes (1955, 1959) who has remarked that in parts of East Africa, Madagascar and Ceylon, and probably also in Travancore, there was extensive plutonic activity during the Cambrian and Lower Ordovician, now represented by vast swarms of pegmatites. Holmes has also noted that this activity was not confined to the present-day coastal lands of the Indian Ocean, but that it also characterized parts of South America.

The age measurements reported here indicate that part of Antarctica may be added to this list of "Gondwanaland" terrains densely impregnated by 500 million year old pegmatites. Several of these terrains consist of metamorphic rocks, among which pyroxene granulites and charnockitic gneisses are well represented. The chronologic history of these gneisses may now be systematically studied by isotope dilution techniques; such investigations may yield results of importance to the understanding of the petrologic problems.

In a review of Antarctic stratigraphy, Davies (1956) noted the presence of

Cambrian and Ordovician sedimentary rocks along the Scotia Arc of West Antarctica; fragments of unmetamorphosed Cambrian limestone have also been recovered from the debris along the Beardmore Glacier (which lies about 5° north of McMurdo Sound) and from the Weddell Sea area. The relationship between these Cambrian strata and the ~ 500 m.y. old metamorphism in East Antarctica remains undeciphered, and poses some interesting problems.

In their report on measurements of remanent magnetization of the gneiss from East Ongul Island, NAGATA and SHIMIZU (1959, p. 1473) calculated the pole position of the earths dipole in two different ways; assuming that the magnetic polarization occurred while the gneisses had their present structural alignment, the average position of the North pole is given as:

lat. = 19°N long. = 163°W.

However, assuming that the gneissosity planes were horizontal when the thermoremanent magnetization was produced, the average position of the North Pole (corresponding to the transformed magnetic polarizations) is:

lat. = 3°N long. = 107°W.

NAGATA and SHIMIZU then compared the latter position of the North Pole with results obtained by workers in South Africa and Australia on Pre-Cambrian rocks. A comparison with results on Lower Palaeozoic rocks from other areas now appears to be more relevant; for this purpose it is desirable to have further experimental evidence regarding the timing of the magnetic polarization and the structural deformation of the gneisses. BULL and IRVING (1960) have listed results of palaeomagnetic measurements from seven areas in Antarctica, and have noted that six of the mean palaeomagnetic pole positions differ appreciably from the present pole, but have longitudes varying over a relatively narrow range. If the magnetic polarization of the Ongul Island gneisses occurred while they had their present structural alignment, then the longitudes of these palaeomagnetic pole positions from Antarctica vary only between 132°W and 163°W; their latitudes vary by over 80°.

Acknowledgement—Dr. L. T. ALDRICH kindly made available to one of us (L .O. N.) the use of a mass spectrometer at the Dept. of Terrestial Magnetism for confirmatory isotopic measurements on one of the mica samples.

REFERENCES

ALDRICH L. T. and WETHERILL G. W. (1958) Geochronology by radioactive decay. *Ann. Rev. Nucl. Sci.* **8,** 257–258.

BULL C. and IRVING E. (1960) Palaeomagnetism in Antarctica. *Nature, Lond.* **185,** 834–835.

DAVIES, W. E. (1956) Antarctic stratigraphy and structure. *Amer. Geophs. Un.* Geophysical Monograph No. **1,** 44—51.

FYFE W. S., TURNER F. J. and VERHOOGEN J. (1958) Metamorphic reactions and metamorphic facies. *Geol. Soc. Amer. Mem.* **73,** 232—259.

GOLDICH S. S., NIER A. O. and WASHBURN A. L. (1958) A^{40}/K^{40} age of gneiss from McMurdo Sound, Antarctica. *Trans. Amer. Geophys. Un.* **39,** 956–958.

HOLMES A. (1955) Dating the Precambrian of Peninsular India and Ceylon. *Proc. Geol. Ass. Canad.* **7,** 103–104.

HOLMES A. (1959) A revised geological time-scale. *Trans. Edinb. Geol. Soc.* **17,** 183-216.

Inghram M. G. (1955) Stable isotope dilution analysis. *Annu. Rev. Nucl. Sci.* **4,** 81.
Kulp J. L. (1959) Geological time scale. (Abstract). *Geol. Soc. Amer. Bull.* **70,** 1634.
Nagata T. and Shimizu Y. (1959) Natural remanent magnetization of Pre-Cambrian gneiss of Ongul Island in the Antarctic. *Nature, Lond.* **184,** 1472.
Tatsumi T. and Kikuchi T. (1959a) Report of geomorphological and geological studies of the wintering team (1957–1958) of the First Japanese Antarctic Research Expedition—1. *The Antarctic Record.* No. 7, pp 373–388, Ministry of Education, Tokyo.
Tatsumi T. and Kikuchi T. (1959b) Report of geomorphological and geological studies of the wintering team (1957–1958) of the First Japanese Antarctic Research Expedition—II. *The Antarctic Record* No. 8, pp. 443–463. Ministry of Education, Tokyo.
Tugarinov A. I., Zhykov S. I., Zhirova V. V. and Knorre K. G. (1959) The age of ancient rock from Antarctica. *Geokhimiya* No. 6, 555–556.

Geochimica et Cosmochimica Acta, 1961, Vol. 22, pp. 99 to 105. Pergamon Press Ltd. Printed in Northern Ireland

Stable carbon isotope studies of crude oils and their porphyrin aggregates

R. Park
Division of Geology, California Institute of Technology*

H. N. Dunning
Petroleum Research Center, Bureau of Mines,
United States Department of the Interior, Bartlesville, Oklahoma

(*Received* 3 *June* 1960, *revised* 8 *August* 1960)

Introduction

The origin of porphyrin aggregates in petroleum is one of the intriguing problems of petroleum geochemistry since the origin of these aggregates is undoubtedly closely related to the origin of petroleum itself. Stevens (1956), in an extensive review on the origin of petroleum, concluded that petroleum is of organic origin and is probably formed by sedimentation and related processes in marine or brackish-water environments from marine and terrestrial organic matter. Extensive studies of porphyrins isolated from petroleum have yielded results which support this conclusion (Dunning and Moore, 1957). A large amount of laboratory data (Blumer, 1950; Dyemenkova and Kurbatskaya, 1957; Treibs, 1936) indicates that the metal–porphyrin complexes found in petroleums are related to porphyrins existing in living organisms and in their decay products. These data further indicate that the metal–porphyrin complexes originated during the sedimentation phase and the period of diagenesis before the petroleum moved from its source bed. Despite this almost overwhelming evidence, a few workers, notably Radchenko and Sheshina (1955) have maintained that the concentration of porphyrins, sulphur and vanadium in petroleum is a secondary process resulting from bacterial action.

Two developments in experimental technique over the past 20 years permit a new approach for studying the origin of porphyrins in petroleum. The first development is chemical and chromatographic methods for preparation and purification of porphyrin aggregates. The second development is an isotope ratio mass spectrometer for determining the C^{13}/C^{12} ratio of carbon dioxide with great precision (McKinney *et al.*, 1950). Utilization of these two methods now makes it possible to compare the C^{13}/C^{12} ratios of petroleums and their porphyrin aggregates with chemically similar substances in present-day organisms. Such a comparison may be expected to yield information concerning the origin of porphyrin aggregates in petroleum.

The C^{13}/C^{12} ratios of carbon from naturally occurring compounds are usually

* Present address: University of California, Lawrence Radiation Laboratory, Berkeley, California.

reported in terms of a δ-value. The term δ is the difference in per mil of the C^{13}/C^{12} ratios of a sample and a standard and is defined as:

$$\delta \text{ (in per mil, ‰)} = \frac{C^{13}/C^{12} \text{ sample} - C^{13}/C^{12} \text{ standard}}{C^{13}/C^{12} \text{ standard}} \times 10^3$$

For example, a δ-value of $+10$ indicates that the C^{13}/C^{12} ratio of the sample is greater than that of the standard by 10 per mil or 1 per cent. Conversely, a δ-value of -10 indicates a C^{13}/C^{12} ratio of the sample that is 10 per mil or 1 per cent less than that of the standard.

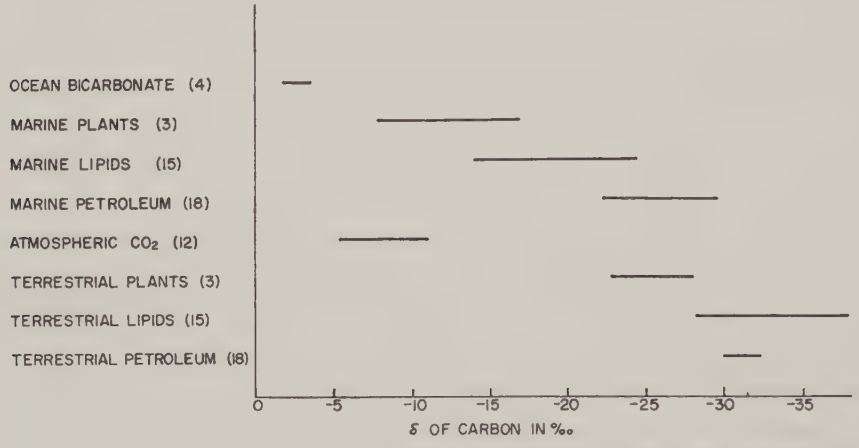

Fig. 1. The ranges C^{13}/C^{12} ratios for some carbon-containing materials in nature.

The standard used in this report is the C^{13}/C^{12} ratio of CO_2 prepared from the fossil skeleton of a cretaceous belemnite from the Peedee formation in North Carolina. This scale is referred to in the literature as the PDB scale (Craig, 1957).

Fig. 1 is a summary of some published C^{13}/C^{12} ratios for carbon containing materials in nature pertinent to this discussion (Craig, 1953, 1954; Park and Epstein, 1961 Silverman and Epstein, 1958; Keeling, 1958). The precision of these data is $\pm 0{\cdot}1$ per mil. These data show that many steps in the carbon cycle are accompanied by isotopic fractionation. For example, carbon dioxide fixation into sugars during photosynthesis is accompanied by a decrease in C^{13}/C^{12} ratio some 200 times greater than the precision with which the C^{13}/C^{12} ratio can be measured. The mechanisms of some of these fractionations are considered in detail elsewhere (Craig, 1954; Keeling, 1958; Park and Epstein 1960). Of special interest to this discussion is the relationship between the isotopic composition of petroleums and present-day plants. The data of Silverman and Epstein (1958) show that petroleums fall into two groups with respect to C^{13}/C^{12} ratio. Silverman and Epstein found that these groups were differentiated according to whether the petroleums originated from terrestrial or marine organic matter. The data show that petroleums of terrestrial and marine origin differ in δ-value by somewhat less than present-day terrestrial and marine plants. This may be due to contributions of terrestrial organic matter to the marine environment during sedimentation of the marine source bed. On the other hand contributions of marine organic matter to the terrestrial environment would not be expected.

Both terrestrial and marine petroleums are enriched in C^{12} compared to their parent material by 5 to 10 per mil. This apparent discrepancy can be explained by the results of Park and Epstein (1961) who found a similar difference of from 5 to 10 per mil between the lipid and carbohydrate fractions of present-day plants. The C^{13}/C^{12} ratios of petroleums correspond roughly to the C^{13}/C^{12} ratios of lipids in their plant sources. Thus the difference in C^{13}/C^{12} ratio between petroleums and present-day plant material could have occurred during sedimentation of the source bed, if the C^{12} enriched lipid material was preferentially preserved while nonlipid material was decomposed.

Park and Epstein (1961) explained C^{12} enrichment in plant lipids compared to the plant as a whole by proposing a model consistent with known biochemical pathways. The model proposed and supported by the experiments of Park and Epstein can also be used to predict the C^{13}/C^{12} ratio of porphyrins synthesized by plants. These workers suggested that isotopic discrimination during plant metabolism at the level of acetate or pyruvate could account for the relatively low C^{13}/C^{12} ratio of plant lipid as compared to the rest of the plant. To maintain a material balance, C^{12} enrichment in the acetate units used in lipid synthesis would necessarily result in a corresponding small increase in C^{13} in the remaining acetate units respired to CO_2 by the tricarboxylic acid cycle. Such a relationship was actually observed experimentally (Park and Epstein, 1961). Shemin and co-workers (1955) have shown that porphyrins are synthesized from the C^{13} rich fraction in this model. These workers showed that porphyrin biosynthesis involves condensation between succinate, a component of the tricarboxylic acid cycle, and glycine. This step is followed by cleavage of the glycine carboxyl to yield δ-aminolevulinic acid. The δ-aminolevulinic acids then condense to form pyrrole rings which subsequently form porphyrins. Thus it might be expected that whereas plant lipids have a smaller C^{13}/C^{12} ratio than the whole plant, plant porphyrins arising from the heavier fraction should have a C^{13}/C^{12} ratio similar to the whole plant. Initial experiments with chlorophyll isolated from tomato leaves confirmed this prediction. After removal of the phytol and magnesium, the C^{13}/C^{12} ratio of the resulting chlorin–e was only $+0{\cdot}5$ per mil with respect to the C^{13}/C^{12} ratio of the whole leaf.

The above considerations suggest that petroleum porphyrins arising from bacterial metabolism of the source lipid or petroleum hydrocarbon, should have a C^{13}/C^{12} ratio similar to that of the petroleum as a whole (Park and Epstein, 1961). On the other hand, porphyrins arising directly from porphyrins synthesized in the organic source material, or from bacterial degradation of the carbohydrate fractions of the source material, should have a C^{13}/C^{12} ratio larger than the petroleum hydrocarbon by about 5 per mil.

Several petroleums and highly purified porphyrin aggregates separated from them were analysed for C^{13}/C^{12} ratio to test these predictions.

Experimental

Some properties of the crude oils studied are summarized in Table 1. Porphyrin aggregates were isolated from these crude oils by the acetic acid–hydrogen bromide digestion method of Groennings (1953). Porphyrin contents were determined

spectrophotometrically by the method of Dunning *et al.* (1954) based on mesoetioporphyrin as a standard. Mesoporphyrin IX dimethyl ester was prepared by the method of Corwin and Erdman (1946).

Porphyrin aggregates isolated by the Groennings method seldom are of a purity higher than from 10 to 20 per cent by weight. Even careful chromatographic procedures (Fisher and Dunning, 1959) seldom produce a sample containing over from 40 to 50 per cent porphyrin. Therefore it was necessary to

Table 1. Crude oil properties

	Parts per million			Weight %		
	Porphyrin	Vanadium	Nickel	Nitrogen	Sulphur	Carbon residue
Boscan, Venez.	1700	900	70	0·61	5·53	4·1
Lagunillas, Venez.	170	320	40	0·29	2·12	4·4
Santa Maria Valley, Calif.	300	280	130	0·64	5·00	10·1
Tatums, Okla.	160	150	70	0·37	1·54	7·3

develop new methods of purification. Several methods were used to produce samples of various purities to allow determination of the effects of impurities on the C^{13}/C^{12} ratio.

Purification of porphyrin aggregates

Lagunillas. Sample A: Fraction 1 (Fisher and Dunning, 1959) obtained as the benzene eluate from a deactivated alumina column.

Sample B: Sample A, chromatographed on Alcoa H-41 alumina, eluted with 0·2 vol. per cent *iso*propanol in benzene. This fraction was collected, and the solvent removed. Then it was dissolved in benzene and chromatographed on Woelm basic alumina partly deactivated with 1 per cent water. Sample B was eluted with benzene from this column.

Sample C: The porphyrins of sample A were converted to a zinc complex by boiling with zinc acetate in glacial acetic acid. The complex was extracted into benzene after diluting the acid with water. The benzene was evaporated, then the zinc complex was dissolved in hexane and chromatographed on silica gel. The complex was eluted from this column with benzene. It then was shaken with dilute hydrochloric acid to cleave the complex and allow the porphyrin to enter the aqueous phase. The acid solution was washed with benzene, neutralized with sodium acetate and the porphyrin extracted into benzene. This solution was washed with water, dried, filtered, and the solvent evaporated to leave a few millilitres which was chromatographed on Woelm basic alumina, partly deactivated with 1 per cent water. This column was developed with benzene and increasing concentrations of *iso*propanol in benzene. The major fraction was eluted with 1 vol. per cent *iso*propanol in benzene.

Santa Maria Valley. Sample A: Fraction 1 (Fisher and Dunning, 1959) obtained as benzene eluate of deactivated alumina column. Sample B: This

sample was prepared by the same method as that used for Lagunillas, sample C. However, the degree of purity obtained was not as high.

Tatums. Sample A: Fraction 1 (Fisher and Dunning, 1959), obtained as the benzene eluate from a deactivated alumina column, was chromatographed on Woelm basic alumina, partly deactivated with 1 per cent water. Benzene and mixtures of benzene with isopropanol were used, as above, as eluents.

Sample B: Sample A was again chromatographed on Woelm basic alumina. It was then placed in a small molecular still (Dunning, 1956) and distilled to an equivalent atmospheric temperature of 500°C. This is considerably below the volatilization point of porphyrin complexes studied previously (Dunning, 1956) and no detectable amounts of porphyrins were volatilized.

Boscan. Sample A: This sample was prepared by the same method as that used for Tatums sample B.

Effect of distillation on the C^{13}/C^{12} *ratio of purified porphyrins*

The formation of the zinc complex and subsequent chromatography of the complex and free porphyrin, as in Lagunillas sample C, results in a considerable loss of porphyrin. This introduces the possibility that the C^{13}/C^{12} ratio of the pure porphyrins finally studied may not be representative of the C^{13}/C^{12} ratio of the porphyrin aggregate as a whole. Therefore, the molecular distillation method of purification also was needed. Since distillation might result in isotopic fractionation of the porphyrin aggregate, the C^{13}/C^{12} ratios of distilled fractions from pure, synthetic samples of mesoporphyrin IX dimethyl ester were measured. The C^{13}/C^{12} ratios of the feed, volatilized fractions, and residue are given in Table 2. The differences in C^{13}/C^{12} ratios of the fractions are barely detectable although the distillation was much more drastic than that used in removing non-porphyrin materials from the porphyrin aggregates.

Combustion of samples to CO_2

Samples were converted to CO_2 using the method described by Craig (1953). In this method, samples are combusted over copper oxide at 800°C under an oxygen atmosphere. The CO_2 from the combustion is collected in a trap at liquid nitrogen temperature. After several transfers between a trap at −78° and a trap cooled to liquid nitrogen temperature the sample is transferred to a mass spectrometer sample tube.

Mass spectrometry

The samples were analysed in a Nier sixty-degree sector-type mass spectrometer which incorporates the improvements described by McKinney *et al.* (1950), for determining C^{13}/C^{12} ratios to $\pm 0{\cdot}1$ per mil. All samples were corrected for the O^{17} contributions to the mass 45 peak and mixing of the sample and standard gas. These corrections are described by Craig (1957).

Results and Discussion

The C^{13}/C^{12} ratios of several crude oils and porphyrin aggregates isolated from them are given in Table 2. The data in Table 2 show that the δ-values for the

crude oils analysed in this study fall within the ranges reported by Silverman and Epstein (1958). Using Silverman and Epstein's values for marine and non-marine crude oils, the oils appear to be of marine origin except for the Tatums oil from Oklahoma. The geological history of the Deese sand, from which this oil is produced, is not entirely clear. It appears that while the area was a narrow sea area, and hence, marine, that the general trend was toward terrestrial conditions because of deltaic action. The relatively negative δ-value for the Tatums crude

Table 2. The C^{13}/C^{12} ratios of crude oils and their porphyrin aggregates

	δ (‰)* (crude oils)	Porphyrin aggregate	Purity (%)	δ (%) (porphyrins)
Lagunillas, Venezuela crude oil	−23·6	A	10	−24·0
		B	60	−21·6
		C	~100	−19·6
Santa Maria Valley, California crude oil	−23·3	A	20	−21·1
		B	70	−18·3
Tatums, Oklahoma crude oil	−30·9	A	60	−27·3
		B	~100	−26·0
Boscan, Venezuela crude oil	−26·7	A	89	−23·0
Syn. mesoporphyrin IX dimethyl ester		Feed	~100	−23·6
		< 650°C†	~100	−23·6
		650–700°C‡	~100	−23·5
		Residue	~100	−24·0

* δ (per mil) $= \dfrac{R \text{ sample} - R \text{ standard}}{R \text{ standard}} \times 1000$, where R is the C^{13}/C^{12} ratio.

† Molecularly distilled below equivalent atmosphere temperature of 650°C.

‡ Molecularly distilled between equivalent atmosphere temperature of 650°C and 700°C.

oil, typical of non-marine petroleum, is a further indication of the terrestrial origin of much of the organic matter from which this oil was formed.

The data in Table 2 also show that the C^{13}/C^{12} ratios of all the relatively pure porphyrin aggregates are from 4 to 5 per mil greater than the C^{13}/C^{12} ratio of the crude oils from which they were extracted. Furthermore, the differences in the C^{13}/C^{12} ratios are proportional to the purities of the samples from any given oil. These data leave little doubt that the porphyrin aggregates from crude oils are generally enriched in carbon-13 with respect to the petroleum hydrocarbon.

The fact that the petroleum and porphyrin aggregates differ by from 4 to 5 per mil in C^{13}/C^{12} ratio suggests strongly that porphyrin aggregates did not arise from the petroleum hydrocarbon by bacterial action. If, on the other hand, porphyrin aggregates in petroleum were contained in the original source material or were produced from bacterial destruction of the carbohydrate fraction of the source material during diagenesis a from 4 to 5 per mil difference in C^{13}/C^{12} ratio as shown in Table 2 would be expected. In either case these data indicate that the porphyrins from these petroleums were present during the formation and diagenesis of the oil. More data will be necessary to establish fully this interpretation

of the results. However, C^{13}/C^{12} ratio studies promise to be of great value in future research in this field.

Acknowledgements—The authors wish to thank Professor S. Epstein of the Geochemistry Department at the California Institute of Technology both for his generosity with laboratory equipment and for valuable criticisms of this work. The technical assistance of Lillie Fisher in preparation of the porphyrin aggregates is gratefully acknowledged. This research was financed in part by the AEC contract AT(11–1)208.

References

Blumer M. (1950) Porphyrin dyes and porphyrin-metal complexes in Swiss bitumens. *Helv. Chim. Acta* **33,** 1627–1637.

Corwin A. H. and Erdman J. G. (1946) A synthetic ferroporphyrin complex that is passive to oxygen. *J. Amer. Chem. Soc.* **68,** 2473–2478.

Craig H. (1953) The geochemistry of the stable carbon isotopes. *Geochim. et Cosmochim. Acta* **3,** 53–92.

Craig H. (1954) Carbon 13 in plants and the relationships between carbon 13 and carbon 14 variations in nature. *J. Geol.* **62,** 115–149.

Craig H. (1957) Isotopic standards for carbon and oxygen and correction factors for mass-spectrometric analysis of carbon dioxide. *Geochim. et Cosmochim. Acta* **12,** 133–149.

Dunning H. N., Moore J. W. and Myers A. T. (1954) Properties of porphyrins in petroleum. *Industr. Engng. Chem.* **46,** 2000–2007.

Dunning H. N. and Rabon N. A. (1956) Porphyrin-metal complexes in petroleum stocks. *Industr. Engng. Chem.* **48,** 951–955.

Dunning H. N. and Moore J. W. (1957) Porphyrin research and origin of petroleum. *Bull. Amer. Ass. Pet. Geol.* **41,** 2403–2412.

Dyemenkova P. Y. and Kurbatskaya A. P. (1957) The interrelation of the tar, asphaltene, vanadium, and nickel content in some crude oils and solid bitumens of a petroleum series. Geological Collection **1.** Gosteptekizclat, Leningrad, 335–364.

Fisher L. R. and Dunning H. N. (1959) Chromatographic resolution of petroleum porphyrin aggregates. *Industr. Engng. Chem.* **31,** 1194–1197.

Groennings S. (1953) Quantitative determination of the porphyrin aggregate in petroleum. *Analyt. Chem.* **25,** 938–941.

Keeling C. D. (1958) The concentration and isotopic abundances of atmospheric carbon dioxide in rural areas. *Geochim. et Cosmochim. Acta* **13,** 322–324.

McKinney C. R., McCrea J. M., Epstein S., Allen H. A. and Urey H. C. (1950) Improvements in mass spectrometers for measurement of small differences in isotopic abundance ratios. *Rev. Sci. Instrum.* **21,** 724–730.

Park R. and Epstein S. (1960) Carbon isotope fractionation during photosynthesis. *Geochim. et Cosmochim. Acta.* **21,** 110–126.

Park R. and Epstein S. (1961) Metabolic fractionation of C^{13} and C^{12} in plants. *Plant Physiol.* (In press).

Radchenko O. A. and Sheshina L. S. (1955) The genesis of porphyrins in crude oils *Dokl. Akad. Nauk S.S.S.R.* **105,** 1285–1288.

Shemin D. (1955) *Porphyrin Biosynthesis and Metabolism.* Ciba Foundation Symposium, London.

Silverman S. R. and Epstein S. (1958) Carbon isotopic compositions of petroleums and other sedimentary organic materials. *Bull Amer. Ass. Pet. Geol.* **42,** 998–1012.

Stevens N. P. (1956) Origin of petroleum—a review. *Bull. Amer. Ass. Pet. Geol.* **40,** 51–61.

Treibs A. (1936) Chlorophyll and hemin derivatives in organic mineral substances. *Angew. Chem.* **49,** 682–686.

Geochimica et Cosmochimica Acta, 1961, Vol. 22, pp. 106 to 132. Pergamon Press Ltd. Printed in Northern Ireland

The diffusion of helium through sedimentary rocks*

R. Newton† and G. F. Round‡
Petroleum research division, Research Council of Alberta, Edmonton, Canada

(*Received* 20 *May* 1960, *revised* 25 *July* 1960)

Abstract—Helium is produced by the radioactive decay of the nuclides of certain minerals and it is commonly assumed that a portion of this helium migrates from its source through overlying rocks to the atmosphere. In this paper the effect of diffusion control on the migration of helium in sediments has been evaluated by the construction of a series of mathematical models to represent a wide range of practical situations. These models range from that with a single infinite, uniform layer of sediment to that with n different, finite uniform layers of sediments. The problem has been reduced to one-dimensional diffusion with the Pre-Cambrian basement rocks as the source of helium and the diffusion equation has been solved for this system with differing boundary conditions. The n-layer models have been evaluated by a series of suitable approximations at each of the interfaces between the layers and in this way the relationship between the helium concentrations in successive layers has been obtained. The effect of these approximations has been illustrated by using them to evaluate some of the single-layer models. Some of the single-layer and two-layer models have been evaluated using representative values for the parameters introduced in the analysis.

Introduction

Helium occurs widely in nature in very low concentrations, being the third most abundant rare gas in the atmosphere. It is found entrapped in crystal structures, in accumulations of natural gases, in solution in ground waters and in the earth's atmosphere. The source of helium is a continuous one, since helium is being steadily generated by the radioactive decay of larger atoms. A small portion of the helium generated in the crust and mantle of the earth is lost to the atmosphere (Damon and Kulp, 1958) and a similar portion is lost from the atmosphere into space. A considerable amount of work has been done on the material balance of helium between the earth, the atmosphere and space, but little work has been done on the mode of migration of the helium within the earth to the atmosphere. It was the purpose of the present study to examine what appears to be the most likely means for this migration through sedimentary rocks. Sedimentary rocks are of particular interest, both because more is known about them and also because more is known about the distribution of helium in these rocks. In such a study it is necessary to define clearly both the helium source and the various mechanisms which might be operative as applied to the actual physical situation.

The Physical Situation

It is convenient to sub-divide the crustal rocks into two classes: The Pre-Cambrian rocks, which are termed "basement rocks" or "basement" and the Paleozoic and later rocks, which are termed "sediments" or "sedimentary rocks". This classification is one of age rather than geological nature.

The sediments are generally deposited in geosynclinal areas with a total thickness which can normally be regarded as small relative to the lateral extent. While

* Contribution 124 of the Research Council of Alberta.
† Research mathematician.
‡ Research engineer.

it is recognized that there are wide variations in lithology over a large area, for areas whose lateral extent is only three or four times the total sediment thickness it is fair to regard the lithology as being uniform. It is such localized regions which are considered in this study.

Although the sediments vary widely in character, the whole stratigraphic column may be regarded as a porous medium of which the pore size distribution varies throughout its length. The pores of the medium are largely filled by water, with dissolved quantities of mineral salts and natural gases and some quantities of oil and natural gases not in solution. The basement rocks are denser than the sediments but nevertheless are still porous and thus the migration of helium from its sources can be considered to take place throughout a porous medium.

Source of helium

Two classes of helium can be envisaged: primordial helium, and radiogenic helium produced since the formation of the earth. In view of the wide cosmic abundance of helium it is clear that primordial helium did exist in the early stages of the earth's formation and a portion of this helium is still present. Radiogenic helium is produced through the spontaneous decay of many elements. In such decay processes an α-particle readily picks up two electrons to form an atom of inert helium gas. The radioactive elements which can generate helium in this way are found for the most part in the uranium and thorium series of which the most important nuclides are U^{238}, U^{235} and Th^{232}. The half-lives of these nuclides are $4{\cdot}5 \times 10^9$ years, $7{\cdot}1 \times 10^8$ years and $1{\cdot}4 \times 10^{10}$ years, respectively, which are of the same order (10^9 years) as the age of the earth. Other possible source nuclides are Th^{230}, U^{233}, U^{234} with half-lives of the order of 10^5 years and U^{236} with a half-life of the order of 10^7 years. These nuclides do not occur naturally at the present time, but it is possible that they did exist at the early stages of the earth's formation. Consequently their helium contribution may be classed with primordial helium.

Helium is produced from these nuclides in radioactive minerals, which may be in the form of crystals in the rock or as an aqueous solution in the pores of the rock. The helium produced in crystals will be entrapped within the crystal structure and the possibility of its release is dependent upon the retentivity of the particular mineral. Retentivity varies widely for the range of helium-producing minerals and for any particular mineral it is dependent upon the amount of helium already produced (Hurley, 1952). Once this helium has been released from the crystal structure it may diffuse through the rock matrix into the pore structure of the rock, while the helium produced from radioactive minerals in aqueous solution is already in this pore structure.

Migration of helium

It is clear that the major portion of the movement of helium will take place within the pore structure in view of the disparity between the diffusivities of helium in solids and liquids. Since diffusion is the only means of mass transfer through the rock matrix, a comparison of the diffusivity in a solid, e.g. silica, of the order 10^{-10} cm^2/sec (Barrer, 1951) with the diffusivity in a liquid, e.g. water, of the

order of 10^{-5} cm^2/sec (Arnold, 1930) shows that movement through the rock matrix represents only a minor portion of the overall movement of helium. However, this portion of the helium movement is important as a controlling factor in the supply of helium to the pore structure. For example, a rock subjected to tensions resulting in microfracturing has a pore structure which presents a large surface area for the escape of helium from the rock matrix. Consequently in such regions of tension the concentration of helium in the pore space may be expected to be higher than that in a similar but undisturbed area.

Within the pore spaces helium exists in two ways: as discrete bubbles alone or in association with other gases, and in aqueous or hydrocarbon solution. Consequently there are three possible modes of helium migration: migration as bubbles, migration in solution due to fluid flow, and migration by molecular diffusion.

It is unlikely that helium moves as bubbles, since firstly, capillary action will mitigate against such movement and secondly, the geometry of the pore structure would be expected to cause the bubbles to be trapped. Consequently such a possible mode of migration has not been considered further in the present study.

There is a possibility that helium can migrate in solution due to the movement of the water, as it is known that in some layers of sediments there is a lateral flow of the ground water, which, for the upper sediments, may have a velocity as high as hundreds of feet per year. The proportion of the helium in the pore space which is in solution—and consequently the proportion of the helium which can migrate in this manner—is dependent on the partial pressure of the helium. The total pressure in the pores is mainly fixed by the overburden pressure and therefore the partial pressure of the helium depends on the quantities of other natural gases present. As helium is the least soluble of all the natural gas it is suggested that in general very little of the helium present is actually in solution. In addition, since the degree and extent of the flow of the groundwater is known only in certain limited cases it is not possible to generalize on this mode of migration. Consequently no attempt has been made to incorporate this in the subsequent analysis.

Diffusion as a means of helium migration has been suggested by Hitchon (1960) to account for the variation of helium concentration, with depth that he found in accumulations of natural gas. The cause of diffusion is the activational energy of each helium atom resulting in random motion. If in any particular region there is a higher concentration of helium atoms than in some other region then the random motion of the atoms will result in a mass transfer of the helium to the region of lower concentration. The rate of transfer is dependent upon the concentration gradient between the regions and the diffusion coefficient, or diffusivity, which is characteristic of the medium. Hence it is clear that molecular diffusion of helium does take place within the pore structure, under any conditions, and as a result it has seemed worthwhile to consider this in detail.

Helium concentrations in the basement and the sediments

The concentration level of helium in a porous medium for a diffusion process may be measured in terms of atoms of helium per unit volume of pore space, or for convenience in moles per litre of pore space. Helium atoms have been produced

since the formation of the earth and it is safe to assume that the bulk of these atoms have accumulated for the last 4 billion years. This would follow from the work of Damon and Kulp (1958) who calculated the present day rate loss of helium to the atmosphere as 7×10^{30} atoms per year* as opposed to the respective production rates in the crust and mantle of 191×10^{30} atoms per year and 934×10^{30} atoms per year. Although it is probably true that 4 billion years ago the earth was in a molten or plastic state, it seems likely that at that time the earth was sufficiently dense to retain helium, since some Pre-Cambrian rocks have been dated as old as 3·5 billion years. While the rate of loss of helium at that time was undoubtedly greater than the present day loss, the rate of production of helium was also greater, by a factor of 2·5 (calculated for Damon and Kulp's "average crust"). Thus, assuming substantial retention of the helium, it is possible to make a comparison between the contributions of helium from the basement and sedimentary rocks. At the time of sedimentation any helium which is free in the sedimentary material is lost to the atmosphere so that initially the concentration of helium in the sediments is zero, and the Paleozoic sediments, which first appeared about 500 million years ago, could accumulate only about one-tenth of the helium that is possible for the basement rocks over a period of 4 billion years. This calculated figure has also been obtained from the figures of Damon and Kulp on the abundances of source elements in their "average crust". If their values are used to calculate the helium concentration from the helium production over 4 billion years in a gneiss rock (a common basement rock) using Daly's (1933) values of 3 g/cm^3 for specific gravity and 3 per cent for porosity, then a value of 0·005 moles/l. of pore space is obtained. This is not an exceptionally high concentration but the value of 3 per cent for the porosity would seem to be high and in consequence far higher concentrations can be expected. Corresponding concentrations in sedimentary rocks will be far less, since production of helium is less, as already indicated, and the porosity of sedimentary rocks is generally greater than basement rocks. Consequently helium production from the sedimentary rocks will be ignored in the present study as far as the mathematical analysis of the diffusion process is concerned. However, it may be accounted for simply, by adding the small contribution from the sediments to that obtained from the diffusion process.

The diffusivity of the sediments

The diffusivity† may be thought of as a measure of the difficulty which a helium atom has in moving through the pore structure of the sediments while it is

* Figures for the rate of degassing of the earth have also been derived by Turekian (1959) which are in disagreement with those of Damon and Kulp. Turekian obtains his figures by a calculation, similar to that of Damon and Kulp but for argon, and then makes the assumption that the degassing constant—the ratio of the amount of argon lost in 1 year to the atmosphere to the total quantity of argon retained in the earth—is the same for helium as for argon. This assumption cannot be reasonably justified since argon will clearly behave in a similar manner to helium in its mode of migration but its rate of doing so is quite independent of that of helium. In consequence the figures of Damon and Kulp have been used throughout this paper.

† Diffusivity at a point in a porous medium is defined as the ratio between the rate of flow of helium per unit area of the medium, perpendicular to the flow, and the helium concentration gradient at that point.

in random motion. Thus the diffusivity can be said to be determined by two factors, the transfer medium and the geometry of the pore structure in which the transfer medium exists. The variation of diffusivity with transfer medium depends on the chemical nature of the medium, its temperature and pressure, and also the concentration of helium in the medium. A large amount of work has been done on these factors and while no simple concise theory has been put forward to combine them, sufficient is understood about them that it can be said that they are of minor importance in this particular problem. This conclusion is examined more closely in the next section. The variation of diffusivity with pore structure is not a subject which has been studied as such and the little information available usually comes from studies of flow through porous media. As for example the value of $1{\cdot}1 \times 10^{-5}$ cm^2/sec for the diffusivity of sodium iodide in water in a column packed with small glass beads obtained by Raimondi *et al.* (1959) which compares with their value of $0{\cdot}53 \times 10^{-5}$ cm^2/sec for sodium iodide in water in a sandstone. The diffusivity of a porous medium may be illustrated qualitatively by the following examples:

(a) A system of tubes: the diffusivity of this system is independent of tube diameter, but if at one point in each tube the diameter if reduced then the diffusivity of the system as a whole is reduced.

(b) A uniform granular system; if the granules are spherical, then the diffusivity of the system is independent of the size of the spheres. However, if the granules are disk-shaped, then the diffusivity varies widely with diameter and thickness of the discs.

Although for some particular porous systems it may be possible to determine the diffusivity theoretically, in practice it will be a matter for experiment.

Simplifications required for the mathematical analysis

The problem of the migration of the helium through sedimentary rocks has been described fairly completely and it is apparent that a number of simplifications are necessary before mathematical techniques can be applied. Thus far, the problem has been reduced to the local migration of helium from the basement rocks as a source, through overlying uniform layers of sediment which are considered as a porous medium. The mechanism of migration which is considered the most probable is diffusion, and as a consequence of the local uniformity the lateral effects can be ignored and the problem considered to be one-dimensional.

The time origin of the diffusion process is the onset of sedimentation. The sedimentation process is complex, but the rate of sedimentation is fast in comparison with the diffusional rate, as will be shown later, so, if the process is continued *ad infinitum* the situation is little different from that in which the sediments are infinite in extent and assumed to exist at the time origin. If at some time the sedimentation process effectively ceases, or is reversed by erosion, the situation is little different from that in which the sediments are finite in extent and assumed to exist at the time origin. These two situations, with sediments of finite and infinite thickness are the two basic problems considered in the analysis.

The process of sedimentation effects the diffusivity of the sediments in that at

any one point, as the thickness of sediment increases, the temperature and pressure rise while at the same time the compaction of the sediments increases. Diffusivity increases with absolute temperature (Glasstone *et al.*, 1941), so it is unlikely that variations of more than 25 per cent in the diffusivity would result at any particular point since the onset of sedimentation. The effect of pressure on diffusivity can be very little, since the water filling the major part of the pore structure is very nearly incompressible. Diffusivity is decreased by compaction, but since the major part of compaction takes place in a relatively short time any variation as a result has little effect on the much slower diffusion process. The effects of pressure and compaction together tend to offset the effect of temperature on diffusivity. The resultant effect can only be estimated but it is not significant in comparison with the variation of diffusivity with pore structure. The same is true of the variation of diffusivity with concentration and transfer medium.

The diffusivity of the sediments varies continuously throughout the stratigraphic column but as the layers of sediment are uniform it is convenient to assume an average or gross diffusivity for each of the layers.

Thus, the problems which are to be analysed are the one-dimensional diffusion of helium from the basement rocks, as the source, through overlying layers of sedimentary rocks which constitute a porous stratigraphic column both finite and infinite in extent. Each layer is characterized by a gross or average diffusivity and the complete sediments are assumed to exist at the time origin—the onset of sedimentation. In summary it can be said that these assumptions which have been made to reduce the problem to the above form have been made so that the mathematical analysis should not be more complex than the problem warranted. That is, with the present lack of knowledge concerning so many factors it would be unreasonable to complicate the analysis further.

Mathematical Models

All the models in this study are derived from the diffusion equation

$$D \frac{\partial^2 c}{\partial x^2} = \frac{\partial c}{\partial t} \tag{1}$$

to which a Laplace transformation (Churchill, 1944) on the variable t is applied giving:

$$\frac{\partial^2 \bar{c}}{\partial x^2} = \frac{p}{D} \bar{c} = q^2 \bar{c} \qquad \left(q^2 = \frac{p}{D}\right) \tag{2}$$

using the assumption made in the introduction that the initial concentration of helium in the sediments is zero. Here D is the diffusion coefficient, c the concentration and $\bar{c}$ its transformed form, x is distance, t is time, and p is the Laplace transform parameter.

Equation (2) will have solutions of the form:

$$\bar{c} = A \cosh qx + B \sinh qx \tag{3}$$

where A and B are constants to be determined by the boundary conditions of the problem. These boundary conditions will take one of the following forms

$$\left.\begin{aligned} c &= 0 \text{ for } t \geqslant 0 \text{ at some } x = x_0 \\ c &= C_0 \exp(-\beta t) \text{ for } t \geqslant 0 \text{ at some } x = x_0 \\ \frac{\partial c}{\partial x} &= 0 \text{ for } t \geqslant 0 \text{ at some } x = x_0 \\ \frac{\partial c}{\partial x} &= -f_0 \exp(-\lambda t) \text{ for } t \geqslant 0 \text{ at some } x = x_0 \end{aligned}\right\} \quad (4)$$

to which the Laplace transform is applied to give

$$\left.\begin{aligned} \bar{c} &= 0 \text{ for } p \geqslant 0 \text{ at some } x = x_0 \\ \bar{c} &= \frac{C_0}{p+\beta} \text{ for } p \geqslant 0 \text{ at some } x = x_0 \\ \frac{\partial \bar{c}}{\partial x} &= 0 \text{ for } p \geqslant 0 \text{ at some } x = x_0 \\ \frac{\partial \bar{c}}{\partial x} &= \frac{-f_0}{p+\beta} \text{ for } p \geqslant 0 \text{ at some } x = x_0 \end{aligned}\right\} \quad (5)$$

which will enable A and B to be determined directly. A and B will in general be functions of p and the resulting form for $\bar{c}$ can then be transformed back to c. This is done either by expressing the right-hand side of equation (3) as a sum of functions whose inverse transforms are known, or by applying the Laplace inversion formula to equation (3) and using the Theory of Residues to evaluate the resultant contour integral.

It has been assumed that the Pre-Cambrian basement is the source of helium from the decay of the three isotopes U^{238}, U^{235}, Th^{232}, with decay constants $1{\cdot}537 \times 10^{-10}$ year^{-1}, $9{\cdot}720 \times 10^{-10}$ year^{-1} and $0{\cdot}4985 \times 10^{-10}$ year^{-1}, respectively, and possibly also an initial distribution of primordial helium. Because radioactive decay is exponential it seems reasonable to assume that the flow of helium from the basement rocks can also be approximated by an exponential, i.e.

$$\frac{\partial c}{\partial x} = -f_0 \exp(-\lambda t) \qquad \text{for} \quad t \geqslant 0 \qquad \text{at} \quad x = 0 \quad (6)$$

where the origin $x = 0$ is taken as the basement surface and the parameters f_0 and λ are determined by the abundances of the source elements and their decay constants. If diffusion is the assumed transfer mechanism in the Pre-Cambrian basement then a lowest value of λ is estimated to be $0{\cdot}15 \times 10^{-17}$ sec^{-1} with an upper value probably in the region of $0{\cdot}5 \times 10^{-17}$ sec^{-1}.

However, as has already been mentioned earlier the helium accumulating in the Pre-Cambrian rocks can achieve very high concentrations. The figures previously calculated assumed average values for the abundances of the source elements, but as evidenced by Evans and Goodman (1941), and Murray and Adams (1958) the range of abundances is wide. In this case it cannot be asserted

positively that diffusion is the only controlling transfer mechanism in the basement rocks. To allow for this, that is to allow for an initial flow of helium from the basement rocks that is not governed solely by diffusion control and which is exceptionally high, an exponential decay of the helium concentration at the basement surface has been assumed, i.e.

$$c = C_0 \exp(-\beta t) \qquad \text{at} \quad x = 0 \qquad \text{for} \quad t \geqslant 0 \tag{7}$$

C_0 and β are determined by the abundances and decay constants of the source elements. This type of boundary condition gives an initially higher flow of helium into the sediments than is possible with the boundary condition (6). Since this condition is most likely to arise in situations with high abundances of the isotopes U^{238} and U^{235} the parameter β is taken to have a range corresponding to their decay constants, i.e. between $0{\cdot}5 \times 10^{-17}$ sec^{-1} and possibly as high as $1{\cdot}5 \times 10^{-17}$ sec^{-1}. The upper limit is determined by the contribution of U^{235}, and while at the present time the U^{238}/U^{235} ratio is in the region of 137·7 (Senftle *et al.*, 1957), over a period of 4 billion years the helium contribution from the U^{235} is some 40 per cent of that of the U^{238}. The other two boundary conditions to be used in the mathematical models are those for the surface of the sediments in the finite layer models, i.e.

$$c = 0 \qquad \text{at } x = l \qquad \text{for } t \geqslant 0$$

and

$$\frac{\partial c}{\partial x} = 0 \qquad \text{at} \quad x = l \qquad \text{for} \quad t \geqslant 0.$$

where $x = l$ is the position of the surface.

The first is the condition of zero helium concentration in the atmosphere which is a reasonable condition in that the present concentration is about 2×10^{-7} moles/l. The second is the condition of zero flow of helium through the surface—which corresponds to an impervious cap rock.

Model 1*a*. The sediments are considered to be semi-infinite and homogeneous with diffusivity D for all $x \geqslant 0$. The flow of helium into the sediments follows an exponential decay, i.e.

$$\frac{\partial c}{\partial x} = -f_0 \exp(-\lambda t) \qquad \text{at} \quad x = 0 \qquad \text{for} \quad t \geqslant 0$$

This has the transformed solution $\bar{c}$ given by,

$$\bar{c} = \frac{f_0}{q(p + \lambda)} \exp(-qx) \tag{8}$$

From this form c is obtained by expanding $(p + \lambda)^{-1}$ in powers of p^{-1} and inverting the sum into a sum of integral error functions (Crank 1956, *British Association Mathematical Tables*, 1931), i.e.

$$c = 2\sqrt{(Dt)} f_0 \sum_{r=0}^{\infty} (-4\lambda t)^r i^{2r+1} \operatorname{erfc} \frac{x}{2\sqrt{(Dt)}} \tag{9}$$

Model 1*b*. Semi-infinite homogeneous sediments, diffusivity D for $x \geqslant 0$, with an exponential decay of concentration being assumed at the basement surface, i.e.

$$c = C_0 \exp(-\beta t) \qquad \text{at} \quad x = 0 \qquad \text{for} \quad t \geqslant 0$$

this leads to the transformed solution

$$\bar{c} = \frac{C_0}{p + \beta} \exp(-qx) \tag{10}$$

and as in model 1a the result follows:

$$c = C_0 \sum_{r=0}^{\infty} (-4\beta t)^r i^{2r} \operatorname{erfc} \frac{x}{2\sqrt{(Dt)}} \tag{11}$$

Model 2*a*. Single finite homogeneous layer of sediments $0 \leqslant x \leqslant l$, diffusivity D, with

$$\frac{\partial c}{\partial x} = -f_0 \exp(-\lambda t) \qquad \text{at} \quad x = 0 \qquad \text{for} \quad t \geqslant 0$$

and

$$\frac{\partial c}{\partial x} = 0 \qquad \text{at} \quad x = l \qquad \text{for} \quad t \geqslant 0$$

which has the transformed solution

$$\bar{c} = \frac{f_0 \cosh q(l - x)}{q(p + \lambda) \sinh ql}$$

by putting

$$\frac{\cosh q(l - x)}{\sinh ql} = \frac{\exp(-qx) + \exp[-q(2l - x)]}{1 - \exp(-2ql)}$$

$$= \sum_{n=0}^{\infty} \{\exp -q(2nl + x) + \exp -q(2(n + 1)l - x)\}$$

the expression for $\bar{c}$ can be inverted as before to give

$$c = 2\sqrt{(Dt)} f_0 \sum_{r=0}^{\infty} \sum_{n=0}^{\infty} (-4\lambda t)^r \left[i^{2r+1} \operatorname{erfc} \frac{2nl + x}{2\sqrt{(Dt)}} + i^{2r+1} \operatorname{erfc} \frac{2(n + 1)l - x}{2\sqrt{(Dt)}} \right] \tag{12}$$

Model 2*b*. Finite homogeneous sediments $0 \leqslant x \leqslant l$, diffusivity D, with

$$c = C_0 \exp(-\beta t) \qquad \text{at} \quad x = 0 \qquad \text{for} \quad t \geqslant 0$$

and

$$\frac{\partial c}{\partial x} = 0 \qquad \text{at} \quad x = l \qquad \text{for} \quad t \geqslant 0$$

which has the transformed solution

$$\bar{c} = \frac{C_0 \cosh q(l - x)}{(p + \beta) \cosh ql}$$

which can be inverted to

$$c = C_0 \sum_{r=0}^{\infty} \sum_{n=0}^{\infty} (-4\beta t)^r (-1)^n \left[i^{2r} \operatorname{erfc} \frac{2nl + x}{2\sqrt{(Dt)}} + i^{2r} \operatorname{erfc} \frac{2(n+1)l - x}{2\sqrt{(Dt)}} \right] \quad (13)$$

Model 3*a*. Finite homogeneous sediments $0 \leqslant x \leqslant l$, diffusivity D, with

$$\frac{\partial c}{\partial x} = -f_0 \exp(-\lambda t) \qquad \text{at} \quad x = 0 \qquad \text{for} \quad t \geqslant 0$$

and

$$c = 0 \qquad \text{at} \quad x = l \qquad \text{for} \quad t \geqslant 0$$

which has the transformed solution

$$\bar{c} = \frac{f_0 \sinh q(l - x)}{q(p + \lambda) \cosh ql}$$

which can be inverted to

$$c = 2\sqrt{(Dt)} f_0 \sum_{r=0}^{\infty} \sum_{n=0}^{\infty} (-4\lambda t)^r (-1)^n \left[i^{2r+1} \operatorname{erfc} \frac{2nl + x}{2\sqrt{(Dt)}} - i^{2r+1} \operatorname{erfc} \frac{2(n+1)l - x}{2\sqrt{(Dt)}} \right] \quad (14)$$

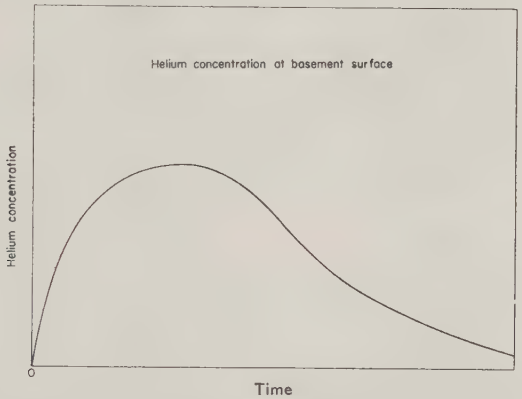

Fig. 1. The type of helium concentration–time curve that occurs for all points in the sediments.

Model 3*b*. Finite homogeneous sediments $0 \leqslant x \leqslant l$, diffusivity D, with

$$c = C_0 \exp(-\beta t) \qquad \text{at} \quad x = 0 \qquad \text{for} \quad t \geqslant 0$$

and

$$c = 0 \qquad \text{at} \quad x = l \qquad \text{for} \quad t \geqslant 0$$

which has the transformed solution

$$\bar{c} = \frac{C_0 \sinh q(l - x)}{(p + \beta) \sinh ql}$$

which can be inverted to

$$c = C_0 \sum_{n=0}^{\infty} \sum_{r=0}^{\infty} (-4\beta t)^r \left[i^{2r} \operatorname{erfc} \frac{2nl + x}{2\sqrt{(Dt)}} - i^{2r} \operatorname{erfc} \frac{2(n+1)l - x}{2\sqrt{(Dt)}} \right] \quad (15)$$

These first six models represent the problem in its simplest form. Their concentration/time curves are all of similar form, i.e. as in Fig. 1, and the peak

concentrations will occur after periods of 3×10^8 years up to 3×10^9 years, dependent mainly on the time constants of λ and β, the peak occurring earlier for larger values of λ and β. Each model is represented diagrammatically in Fig. 2,

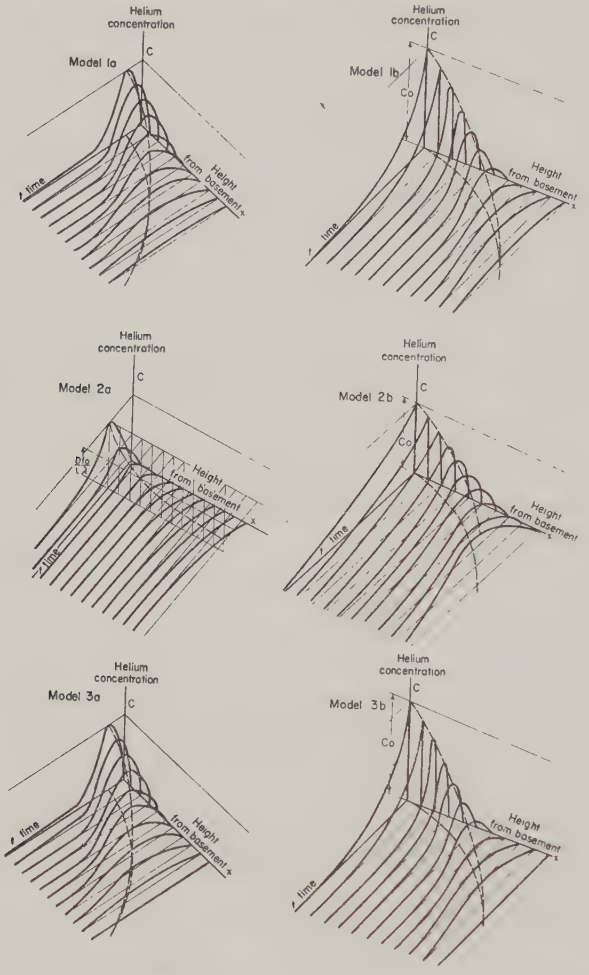

Fig. 2. Three-dimensional diagrams of the variation of helium concentration with time and distance from the basement. The letter a refers to models with an exponential decay of helium flow into the sediments and the letter b refers to models with an exponential decay of helium concentration at the basement. The numbers 1, 2 and 3 correspond, respectively, to models with semi-infinite sediments, finite sediments with zero helium flow through the surface and finite sediments with zero helium concentration at the surface.

concentration being measured against both time and distance from the basement surface. Models 1a and 1b are as might be expected and if these are truncated at $x = l$, they represent models with upper boundary conditions intermediate between those of models 2a, 2b and 3a, 3b. In model 2a with $\partial c/\partial x = 0$ at the surface of the sediments, no helium can escape and hence at infinite time a uniform distribution of helium is attained. In model 2b, however, at infinite time no

helium is left in the sediments and mathematically this would be attributed to back diffusion. In reality it is a result of the lower boundary condition

$$c = C_0 \exp(-\beta t) \qquad \text{at} \quad x = 0 \qquad \text{for} \quad t \geqslant 0$$

which is only an approximation. This could be adjusted by adding a constant to this boundary condition, but the result would be of academic interest only in that at the present time the helium concentrations at the most, can only be just beyond their peak values. Models 3a and 3b follow the expected patterns and it is worth noting that after periods of 500 million years the concentration/distance curves are nearly straight lines.

Two-layered models

Next in order of complexity are the two-layered models. The overall picture is the same as for the one-layered models but the relationship between the layers is of interest. The analysis is the same as that for the one-layered models except that in some cases it was found more practical to apply the theory of residues to the inverse Laplace transform integral in order to invert the transformed solutions. Without attempting to be rigorous, the theory of residues applied to this problem can be stated as:

$$\frac{1}{2\pi i}\int_{\gamma-i\infty}^{\gamma+i\infty}\frac{f(p)}{g(p)}\exp(pt)\,dp = \sum_{\xi_n}\frac{f(\xi_n)}{g'(\xi_n)}\exp(\xi_n t)$$

where

$$p = \xi_n \text{ are the roots of } g(p) = 0$$

Model 4a. Semi-infinite layer $l < x < \infty$, diffusivity D_2; on a finite layer $0 \leqslant x \leqslant l$, diffusivity D_1; with

$$\frac{\partial c}{\partial x} = -f_0 \exp(-\lambda t) \qquad \text{at} \quad x = 0 \qquad \text{for} \quad t \geqslant 0$$

This has the transformed solutions

$$\bar{c}_1 = \frac{f_0[\exp q_1(l-x) - \mu \exp -q_1(l-x)]}{q_1(p+\lambda)[\exp q_1 l + \mu \exp -q_1 l]} \qquad \text{for} \quad 0 \leqslant x \leqslant l$$

and

$$\bar{c}_2 = \frac{(1-\mu) f_0 \exp q_2(l-x)}{q_1(p+\lambda)[\exp q_1 l + \mu \exp -q_1 l]} \qquad \text{for} \quad l \leqslant x \leqslant \infty$$

where $q_1^2 = \dfrac{p}{D_1}$, $q_2^2 = \dfrac{p}{D_2}$, $k = \sqrt{\left(\dfrac{D_1}{D_2}\right)}$ and $\mu = \dfrac{1-k}{1+k}$.

This can be inverted by the previous methods to

$$c_1 = 2\sqrt{(D_1 t)} f_0 \sum_{n=0}^{\infty}\sum_{r=0}^{\infty}(-4\lambda t)^r(-\mu)^n \times \left\{ i^{2r+1}\operatorname{erfc}\frac{2nl+x}{2\sqrt{(D_1 t)}} - \mu i^{2r+1}\operatorname{erfc}\frac{2(n+1)l-x}{2\sqrt{(D_1 t)}}\right\} \qquad (16)$$

and

$$c_2 = 2(1-\mu) f_0 \sqrt{(D_1 t)} \sum_{n=0}^{\infty}\sum_{r=0}^{\infty}(-4\lambda t)^r(-\mu)^n i^{2r+1}\operatorname{erfc}\frac{[(2n+1)l - k(l-x)]}{2\sqrt{(D_1 t)}} \qquad (17)$$

Model 4b. Semi-infinite layer $l < x < \infty$, diffusivity D_2; on a finite layer $0 \leqslant x \leqslant l$, diffusivity D_1; with

$$c = C_0 \exp(-\beta t) \qquad \text{at} \quad x = 0 \qquad \text{for} \quad t \geqslant 0.$$

This has the transformed solutions

$$\bar{c}_1 = \frac{C_0[\exp q_1(l-x) - \mu \exp -q_1(l-x)]}{(p+\beta)[\exp q_1 l - \mu \exp -q_1 l]} \quad \text{for} \quad 0 \leqslant x \leqslant l$$

and

$$\bar{c}_2 = \frac{(1-\mu)C_0 \exp -q_2(x-l)}{(p+\beta)[\exp q_1 l - \mu \exp -q_1 l]} \quad \text{for} \quad l < x < \infty$$

which can be transformed to

$$c_1 = C_0 \sum_{n=0}^{\infty} \sum_{r=0}^{\infty} (-4\beta t)^r \mu^n \left[i^{2r} \operatorname{erfc} \frac{2nl + x}{2\sqrt{(D_1 t)}} - \mu i^{2r} \operatorname{erfc} \frac{2(n+1)l - x}{2\sqrt{(D_1 t)}} \right] \tag{18}$$

and

$$c_2 = C_0(1-\mu) \sum_{n=0}^{\infty} \sum_{r=0}^{\infty} (-4\beta t)^r \mu^n i^{2r} \operatorname{erfc} \frac{(2n+1)l - k(l-x)}{2\sqrt{(D_1 t)}} \tag{19}$$

Model 5a. One finite layer $l_1 < x \leqslant l_2$, diffusivity D_2; on a second finite layer $0 \leqslant x \leqslant l_1$, diffusivity D_1; with

$$\frac{\partial c}{\partial x} = -f_0 \exp(-\lambda t) \quad \text{at} \quad x = 0 \qquad \text{for} \quad t \geqslant 0$$

and

$$\frac{\partial c}{\partial x} = 0 \qquad \text{at} \quad x = l_2 \qquad \text{for} \quad t \geqslant 0$$

which has the transformed solutions:

$$\bar{c}_1 = \frac{f_0[k \cosh q_2(l_2 - l_1) \cosh q_1(l_1 - x) + \sinh q_2(l_2 - l_1) \sinh q_1(l_1 - x)]}{q_1(p+\lambda)[\sinh q_2(l_2 - l_1) \cosh q_1 l_1 + k \cosh q_2(l_2 - l_1) \sinh q_1 l_1]}$$

for $0 \leqslant x \leqslant l_1$

and

$$\bar{c}_2 = \frac{f_0 k \cosh q_2(l_2 - x)}{q_1(p+\lambda)[\sinh q_2(l_2 - l_1) \cosh q_1 l_1 + k \cosh q_2(l_2 - l_1) \sinh q_1 l_1]}$$

for $l_1 < x \leqslant l_2$

These are inverted by the theory of residues to give

$$c_1 = \frac{f_0 D_1}{\lambda l_2}$$

$$- \frac{f_0[k \cos \sqrt{(\lambda/D_1)} k(l_2 - l_1) \cos \sqrt{(\lambda/D_1)}(l_1 - x) - \sin \sqrt{(\lambda/D_1)} k(l_2 - l_1) \times \sin \sqrt{(\lambda/D_1)}(l_1 - x)] \exp(-\lambda t)}{\sqrt{(\lambda/D_1)}[\sin \sqrt{(\lambda/D_1)} k(l_2 - l_1) \cos \sqrt{(\lambda/D_1)} l_1 + k \cos \sqrt{(\lambda/D_1)} \times k(l_2 - l_1) \sin \sqrt{(\lambda/D_1)} l_1]}$$

$$+ \sum_{\xi_n > 0} \frac{f_0[k \cos \xi_n k(l_2 - l_1) \cos \xi_n(l_1 - x) - \sin \xi_n k(l_2 - l_1) \sin \xi_n(l_1 - x)] \times 2D_1 \exp(-\xi_n^2 D_1 t)}{(\lambda - \xi_n^2 D_1)\{k l_2 \cos \xi_n k(l_2 - l_1) \cos \xi_n l_1 - (l_1 + k^2(l_2 - l_1)) \times \sin \xi_n k(l_2 - l_1) \sin \xi_n l_1\}} \tag{20}$$

and

$$c_2 = \frac{f_0 D_1}{\lambda l_2}$$

$$- \frac{f_0 k \cos \sqrt{(\lambda/D_1)} k(l_2 - x) \exp(-\lambda t)}{\sqrt{(\lambda/D_1)}[\sin \sqrt{(\lambda/D_1)} k(l_2 - l_1) \cos \sqrt{(\lambda/D_1)} l_1 + k \cos \sqrt{(\lambda/D_1)} k(l_2 - l_1) \times \sin \sqrt{(\lambda/D_1)} l_1]}$$

$$+ \sum_{\xi_n > 0} \frac{f_0 k \cos \xi_n k(l_2 - x) 2 D_1 \exp(-\xi_n^2 D_1 t)}{(\lambda - \xi_n^2 D_1)[k l_2 \cos \xi_n k(l_2 - l_1) \cos \xi_n l_1 - (l_1 + k^2(l_2 - l_1)) \times \sin \xi_n k(l_2 - l_1) \sin \xi_n l_1]} \qquad (21)$$

where $q_1 = \xi_n$ are the positive roots of:

$$\sin q_1 k(l_2 - l_1) \cos q_1 l_1 + k \cos q_1 k(l_2 - l_1) \sin q_1 l_1 = 0$$

Model 5b. One finite layer $l_1 < x \leqslant l_2$, diffusivity D_2; on a second finite layer $0 \leqslant x \leqslant l_1$, diffusivity D_1; with

$$c = C_0 \exp(-\beta t) \qquad \text{at} \quad x = 0 \qquad \text{for} \quad t \geqslant 0$$

and

$$\frac{\partial c}{\partial x} = 0 \qquad \text{at} \quad x = l_2 \qquad \text{for} \quad t \geqslant 0$$

This has the transformed solutions

$$\bar{c}_1 = \frac{C_0[k \cosh q_2(l_2 - l_1) \cosh q_1(l_1 - x) + \sinh q_2(l_2 - l_1) \sinh q_1(l_1 - x)]}{(p + \beta)[k \cosh q_2(l_2 - l_1) \cosh q_1 l_1 + \sinh q_2(l_2 - l_1) \sinh q_1 l_1]}$$

and

$$\bar{c}_2 = \frac{C_0 k \cosh q_2(l_2 - x)}{(p + \beta)[k \cosh q_2(l_2 - l_1) \cosh q_1 l_1 + \sinh q_2(l_2 - l_1) \sinh q_1 l_1]}$$

which can be inverted by the theory of residues to give

$$c_1 = \frac{C_0\{k \cos \sqrt{(\lambda/D_1)} k(l_2 - l_1) \cos \sqrt{(\lambda/D_1)}(l_1 - x) - \sin \sqrt{(\lambda/D_1)} k(l_2 - l_1) \times \sin \sqrt{(\lambda/D_1)} x\} \exp(-\lambda t)}{\{k \cos \sqrt{(\lambda/D_1)} k(l_2 - l_1) \cos \sqrt{(\lambda/D_1)} l_1 - \sin \sqrt{(\lambda/D_1)} k(l_2 - l_1) \sin \sqrt{(\lambda/D_1)} l_1\}}$$

$$+ \sum_{\xi_n \geqslant 0} \frac{C_0\{k \cos \xi_n k(l_2 - l_1) \cos \xi_n(l_1 - x) - \sin \xi_n k(l_2 - l_1) \sin \xi_n(l_1 - x)\} \times 2 D_1 \xi_n \exp(-\xi_n^2 D_1 t)}{(\beta - \xi_n^2 D_1)[k l_2 \cos \xi_n k(l_2 - l_1) \sin \xi_n l_1 + (k^2(l_2 - l_1) + l_1) \times \sin \xi_n k(l_2 - l_1) \cos \xi_n l_1]} \qquad (22)$$

$$c_2 = \frac{C_0 k \cos \sqrt{(\lambda/D_1)} k(l_2 - x) \exp(-\lambda t)}{[k \cos \sqrt{(\lambda/D_1)} k(l_2 - l_1) \cos \sqrt{(\lambda/D_1)} l_1 - \sin \sqrt{(\lambda/D_1)} k(l_2 - l_1) \sin \sqrt{(\lambda/D_1)} l_1]}$$

$$+ \sum_{\xi_n \geqslant 0} \frac{C_0 k \cos \xi_n k(l_2 - x) 2 D_1 \xi_n \exp(-\xi_n^2 D_1 t)}{(\beta - \xi_n^2 D_1)[k l_2 \cos \xi_n k(l_2 - l_1) \sin \xi_n l_1 + (k^2(l_2 - l_1) + l_1) \times \sin \xi_n k(l_2 - l_1) \cos \xi_n l_1]} \qquad (23)$$

where $q_1 = \xi_n$ are the positive roots of:

$$k \cos q_1 k(l_2 - l_1) \cos q_1 l_1 - \sin q_1 k(l_2 - l_1) \sin q_1 l_1 = 0.$$

Model 6*a*. One finite layer $l_1 < x \leqslant l_2$, diffusivity D_2; on a second finite layer $0 \leqslant x \leqslant l_1$, diffusivity D_1; with

$$\frac{\partial c}{\partial x} = -f_0 \exp(-\lambda t) \qquad \text{at} \quad x = 0 \qquad \text{for} \quad t \geqslant 0$$

and

$$c = 0 \qquad \text{at} \quad x = l_2 \qquad \text{for} \quad t \geqslant 0$$

This has the transformed solutions

$$\bar{c}_1 = \frac{f_0[\cosh q_2(l_2 - l_1) \sinh q_1(l_1 - x) + k \sinh q_2(l_2 - l_1) \cosh q_1(l_1 - x)]}{q_1(p + \lambda)[\cosh q_2(l_2 - l_1) \cosh q_1 l_1 + k \sinh q_2(l_2 - l_1) \sinh q_1 l_1]}$$

$$\bar{c}_2 = \frac{f_0 k \sinh q_2(l_2 - x)}{q_1(p + \lambda)[\cosh q_2(l_2 - l_1) \cosh q_1 l_1 + k \sinh q_2(l_2 - l_1) \sinh q_1 l_1]}$$

which can be inverted by the theory of residues to give

$$c_1 = \frac{f_0\{\cos \sqrt{(\lambda/D_1)}k(l_2 - l_1) \sin \sqrt{(\lambda/D_1)}(l_1 - x) + k \sin \sqrt{(\lambda/D_1)}k(l_2 - l_1) \times \cos \sqrt{(\lambda/D_1)}(l_1 - x)\} \exp(-\lambda t)}{\sqrt{(\lambda/D_1)}[\cos \sqrt{(\lambda/D_1)}k(l_2 - l_1) \cos \sqrt{(\lambda/D_1)}l_1 - k \sin \sqrt{(\lambda/D_1)}k(l_2 - l_1) \times \sin \sqrt{(\lambda/D_1)}l_1]}$$

$$+ \sum_{\xi_n \geqslant 0} \frac{f_0\{\cos \xi_n k(l_2 - l_1) \sin \xi_n(l_1 - x) + k \sin \xi_n k(l_2 - l_1) \cos \xi_n(l_1 - x)\} 2D_1 \times \exp(-\xi_n^2 D_1 t)}{(\lambda - \xi_n^2 D_1)\{k l_2 \sin \xi_n k(l_2 - l_1) \cos \xi_n l_1 + [l_1 + k^2(l_2 - l_1)] \times \cos \xi_n k(l_2 - l_1) \sin \xi_n l_1\}} \tag{24}$$

and

$$c_2 = \frac{f_0 k \sin \sqrt{(\lambda/D_1)}k(l_2 - l_1) \exp(-\lambda t)}{\sqrt{(\lambda/D_1)}[\cos \sqrt{(\lambda/D_1)}k(l_2 - l_1) \cos \sqrt{(\lambda/D_1)}l_1 - k \sin \sqrt{(\lambda/D_1)}k(l_2 - l_1) \times \sin \sqrt{(\lambda/D_1)}l_1]}$$

$$+ \sum_{\xi_n \geqslant 0} \frac{f_0 k \sin \xi_n k(l_2 - x) 2D_1 \exp(-\xi_n^2 D_1 t)}{(\lambda - \xi_n^2 D_1)[k l_2 \sin \xi_n k(l_2 - l_1) \cos \xi_n l_1 + [l_1 + k^2(l_2 - l_1) \cos \xi_n k(l_2 - l_1)] \times \sin \xi_n l_1]} \tag{25}$$

where $q_1 = \xi_n$ are the positive roots of

$$\cos q_1 k(l_2 - l_1) \cos q_1 l_1 - k \sin q_1 k(l_2 - l_1) \sin q_1 l_1 = 0$$

Model 6*b*. One finite layer $l_1 < x \leqslant l_2$, diffusivity D_2; on a second finite layer $0 \leqslant x \leqslant l_1$, diffusivity D_1; with

$$c = C_0 \exp(-\beta t) \qquad \text{at} \quad x = 0 \qquad \text{for} \quad t > 0$$

and

$$c = 0 \qquad \text{at} \quad x = l_2 \qquad \text{for} \quad t > 0$$

This has the transformed solutions

$$\bar{c}_1 = \frac{C_0[k \sinh q_2(l_2 - l_1) \cosh q_1(l_1 - x) + \cosh q_2(l_2 - l_1) \sinh q_1(l_1 - x)]}{(p + \beta)[k \sinh q_2(l_2 - l_1) \cosh q_1 l_1 + \cosh q_2(l_2 - l_1) \sinh q_1 l_1]}$$

$$\bar{c}_2 = \frac{C_0 k \sinh q_2(l_2 - x)}{(p + \beta)[k \sinh q_2(l_2 - l_1) \cosh q_1 l_1 + \cosh q_2(l_2 - l_1) \sinh q_1 l_1]}$$

which can be inverted by the theory of residues to give

$$c_1 = \frac{C_0\{k \sin \sqrt{(\beta/D_1)}k(l_2 - l_1) \cos \sqrt{(\beta/D_1)}(l_1 - x) + \cos \sqrt{(\beta/D_1)}k(l_2 - l_1) \times \sin \sqrt{(\beta/D_1)}(l - x)\} \exp(-\beta t)}{\{k \sin \sqrt{(\beta/D_1)}k(l_2 - l_1) \cos \sqrt{(\beta/D_1)}l_1 + \cos \sqrt{(\beta/D_1)}k(l_2 - l_1) \sin \sqrt{(\beta/D_1)}l_1\}}$$

$$+ \sum_{\xi_n \geqslant 0} \frac{C_0\{k \sin \xi_n k(l_2 - l_1) \cos \xi_n(l_1 - x) + \cos \xi_n k(l_2 - l_1) \sin \xi_n(l_1 - x)\} \times 2D_1\xi_n \exp(-\xi_n^2 D_1 t)}{(\beta - \xi_n^2 D_1)\{kl_2 \sin \xi_n k(l_2 - l_1) \sin \xi_n l_1 - [l_1 + k^2(l_2 - l_1)] \times \cos \xi_n k(l_2 - l_1) \cos \xi_n l_1\}} \tag{26}$$

and

$$c_2 = \frac{C_0 k \sin \sqrt{(\beta/D_1)}k(l_2 - x) \exp(-\beta t)}{[k \sin \sqrt{(\beta/D_1)}k(l_2 - l_1) \cos \sqrt{(\beta/D_1)}l_1 + \cos \sqrt{(\beta/D_1)}(l_2 - l_1) \sin \sqrt{(\beta/D_1 l_1}]}$$

$$+ \sum_{\xi_n \geqslant 0} \frac{C_0 k \sin \xi_n k(l_2 - x) 2D_1\xi_n \exp(-\xi_n^2 D_1 t)}{(\beta - \xi_n^2 D_1)\{kl_2 \sin \xi_n k(l_2 - l_1) \sin \xi_n l_1 - (l_1 + k^2(l_2 - l_1)) \cos \xi_n k(l_2 - l_1) \times \cos \xi_n l_1\}} \tag{27}$$

where $q_1 = \xi_n$ are the positive roots of

$$k \sin q_1 k(l_2 - l_1) \cos q_1 l_1 + \cos q_1 k(l_2 - l_1) \sin q_1 l_1 = 0$$

The most notable feature about these models is the recurrence in each one of the factor k in conjunction with those distances which refer to the upper medium. Though the analogy is not exact, each model may be considered to be derived from its related one-layer model by a contraction in the upper medium, by the factor k. That is, the two-layered model is derived from the corresponding single-layered model, which has depth $l_1 + k(l_2 - l_1)$ and diffusivity D_1, by a contraction on the upper portion $k(l_2 - l_1)$ by the factor k. This has been represented diagrammatically in Fig. 3, which shows the contraction on some representative concentration = distance curve from any of the single-layered models. In the same way the overall effect of the same contraction on all the models represented in Fig. 2 can be visualized.

Multi-layered models

It might be inferred from the foregoing that a multi-layer system could be derived by a series of contractions on a single-layer system, but it is necessary to make a closer analysis. The previous method of analysis cannot be reasonably extended to more than a two-layered system, and it has been found necessary to

use an approximation technique. The system to be studied is the general one of n layers of sediments with differing diffusivities: $0 \leqslant x < l_1$, diffusivity D_1; $l_1 \leqslant x < l_2$, diffusivity D_2 and so on up to; $l_{n-1} \leqslant x \leqslant l_n$, diffusivity D_n. The same boundary conditions used in the previous models are applied at $x = 0$ and

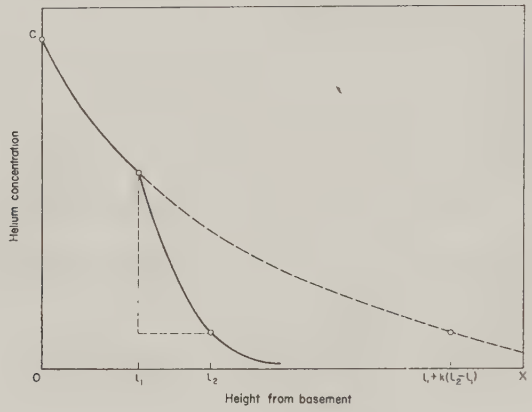

Fig. 3. An illustration of the type of contraction which may be used on a single-layered model (dotted line) to produce an approximation to the two-layered models (continuous line).

$x = l_n$ but at each interface $x = l_r (r = 1, 2, \ldots n - 1)$ an approximation is assumed which is of the same form as the boundary condition at $x = 0$, i.e. if

$$\frac{\partial c}{\partial x} = -f_0 \exp(-\lambda_0 t) \qquad \text{for} \quad t \geqslant 0 \qquad \text{at} \quad x = 0$$

then it is assumed that

$$\frac{\partial c}{\partial x} = -f_r \exp(-\lambda_r t) \quad \text{for} \quad t \geqslant 0 \quad \text{at} \quad x = l_r \quad (r = 1, 2, \ldots, n - 1)$$

These assumed forms are reasonable in exactly the same sense as the assumed initial boundary condition is reasonable. The parameters f_r and λ_r are determined by setting up a series of recurrence relations which ultimately determine each f_r and λ_r in terms of f_0 and λ_0. Similar approximations are then used to determine the helium concentrations at the interfaces.

Model 7a. The n-layered system of sediments described above with

$$\frac{\partial c}{\partial x} = f_0 \exp(-\lambda_0 t) \qquad \text{at} \quad x = 0 \qquad \text{for} \quad t \geqslant 0$$

and

$$\frac{\partial c}{\partial x} = 0 \qquad \text{at} \quad x = l_n \qquad \text{for} \quad t \geqslant 0$$

As previously stated it has been assumed that at each interface $x = l_r$, then

$$\frac{\partial c}{\partial x} = -f_r \exp(-\lambda_r t) \quad \text{for} \quad t \geqslant 0 \quad \text{and} \quad r = 1, 2, \ldots, n - 1$$

it would be better to write "at $x = l_{r-0}$", meaning on the side of the interface in the layer $l_{r-1} \leqslant x < l_r$. On the other side of the interface, in the layer $l_r \leqslant x < l_{r+1}$, $\partial c/\partial x = (-1/k_r^2) f_r \exp(-\lambda_r t)$ for while $\partial c/\partial x$ is discontinuous across the interface, the flow of helium $D(\partial c/\partial x)$ is continuous. k_r is defined by $k_r^2 = D_{r+1}/D_r$.

To obtain recurrence relations for f_r and λ_r the two layers of sediments $l_{r-1} \leqslant x < l_r$, D_r; $l_r \leqslant x < l_{r+1}$, D_{r+1} are studied,

assuming $\dfrac{\partial c}{\partial x} = -f_{r-1} \exp(-\lambda_{r-1} t)$ at $x = l_{r-1-0}$ for $t \geqslant 0$

or that $\dfrac{\partial c}{\partial x} = -\dfrac{1}{k_{r-1}^2} f_{r-1} \exp(-\lambda_{r-1} t)$ at $x = l_{r+1+0}$ for $t \geqslant 0$

and $\dfrac{\partial c}{\partial x} = -f_{r+1} \exp(-\lambda_{r+1} t)$ at $x = l_{r+1-0}$ for $t \geqslant 0$ (a)

For these two layers with the boundary conditions (a) it is possible to write down the transformed solutions as

$$\bar{c}_r = A \cosh q_r(l_r - x) + B \sinh q_r(l_r - x) \qquad \text{for} \quad l_{r-1} \leqslant x \leqslant l_r$$

and

$$\bar{c}_{r+1} = C \cosh q_{r+1}(x - l_r) + D \sinh q_{r+1}(x - l_r) \qquad \text{for} \quad l_r \leqslant x \leqslant l_{r+1}$$

the value of $\partial c/\partial x$ at $x = l_{r-0}$ is to be approximated by $-f_r \exp(-\lambda_r t)$, or

$$\frac{\partial \bar{c}}{\partial x} \simeq -\frac{f_r}{p + \lambda_r} \qquad \text{at} \quad x = l_{r-0} \qquad \text{for} \quad p > 0$$

but at $x = l_{r-0}$, $\dfrac{\partial \bar{c}}{\partial x} = \dfrac{\partial \bar{c}_r}{\partial x} = -Bq_r$

Thus it is only necessary to determine the coefficient B.

The following expression for B is found

$$B\left\{\cosh q_r\delta_r \sinh q_{r+1}\delta_{r+1} + \frac{1}{k_r} \cosh q_{r+1}\delta_{r+1} \sinh q_r\delta_r\right\}$$

$$= \frac{f_{r-1} \sinh q_{r+1}\delta_{r+1}}{k_{r-1}^2 q_r(p + \lambda_{r-1})} + \frac{f_{r+1} \sinh q_r\delta_r}{q_{r+1}(p + \lambda_{r+1})}$$

where $q_r^2 = \dfrac{p}{D_r}$, $\delta_r = l_r - l_{r-1}$, $k_r = \sqrt{\left(\dfrac{D_{r+1}}{D_r}\right)}$ $r = 1, 2, \ldots, n-1$

This expression for B can be expanded in terms of p and by comparing the initial coefficients with those of the expansion of $\dfrac{f_r}{q_r(p + \lambda_r)}$ the following recurrence relations result:

$$\frac{f_r}{\lambda_r} = \frac{\delta_{r+1} \cdot (1/k_{r-1}^2)(f_{r-1}/\lambda_{r-1}) + \delta_r \cdot k_r^2 (f_{r+1}/\lambda_{r+1})}{\delta_{r+1} + \delta_r} \tag{28}$$

and

$$\frac{f_r}{\lambda_r^2} = \frac{f_r}{\lambda_r} \cdot \frac{[\delta_{r+1}(\delta_r^2/2D_r + \delta_{r+1}^2/6D_{r+1}) + \delta_r(\delta_{r+1}^2/2D_{r+1} + \delta_r^2/6D_r)]}{\delta_{r+1} + \delta_r}$$

$$+ \frac{\delta_{r+1} \cdot (1/k_{r-1}^2)(f_{r-1}/\lambda_{r-1}^2 - f_{r-1}/\lambda_{r-1} \cdot \delta_{r+1}^2/6D_{r+1}) + \delta_r \cdot k_r^2(f_r/\lambda_r^2 - f_r/\lambda_r \cdot \delta_r^2/6D_r)}{\delta_{r+1} + \delta_r} \tag{29}$$

Since at $x = 0$ $\qquad \dfrac{\partial c}{\partial x} = -f_0 \exp(-\lambda_0 t) \quad$ for $\quad t \geqslant 0$

and at $x = l_r$ $\qquad \dfrac{\partial c}{\partial x} = -0\, x \exp(-\lambda_r t) \quad$ for $\quad t \geqslant 0$

each f_r and λ_r are determined by the above recurrence relations in terms of f_0 and λ_0.

If now the single layer of sediment $l_r \leqslant x < l_{r+1}$ is considered

with $\qquad \dfrac{\partial c}{\partial x} = -\dfrac{1}{k_r^2} f_r \exp(-\lambda_r t) \qquad$ at $\quad x = l_{r+0} \qquad$ for $\quad t \geqslant 0$

and

$$\frac{\partial c}{\partial x} = -f_{r+1} \exp(-\lambda_{r+1} t) \qquad \text{at} \quad x = l_{r+1-0} \qquad \text{for} \quad t \geqslant 0$$

it is possible to write down the transformed solution

$$\bar{c} = A \cosh q_{r+1}(x - l_r) + B \sinh q_{r+1}(x - l_r)$$

A and B are determined in terms of f_r, λ_r, f_{r+1}, λ_{r+1} and hence in terms of f_0 and λ_0. Thus $\bar{c}$ could be inverted and c known for each layer. However, as it is known how c will in general behave, it is more convenient to use another approximation. At each interface the approximation

$$c = C_r - C_r \exp(-\alpha_r t) \qquad \text{at} \quad x = l_r \qquad \text{for} \quad t \geqslant 0$$

or

$$\bar{c} = \frac{C_r}{p} - \frac{C_r}{p + \alpha_r} \qquad \text{at} \quad x = l_r \qquad \text{for} \quad p > 0$$

is assumed, and this approximates to the coefficient A. This then determines C_r and α_r in terms of f_r, λ_r, f_{r+1}, λ_{r+1}, i.e.

$$C_r = \frac{1}{\delta_{r+1}} \left\{ D_r \frac{f_r}{\lambda_r} - D_{r+1} \frac{f_{r+1}}{\lambda_{r+1}} \right\} \tag{30}$$

and

$$\frac{C_r}{\alpha_r} = \frac{1}{\delta_{r+1}} \left\{ \left(D_r \frac{f_r}{\lambda_r^2} - D_{r+1} \frac{f_{r+1}}{\lambda_{r+1}^2} \right) + \left(D_r \frac{f_r}{\lambda_r} - D_{r+1} \frac{f_{r+1}}{\lambda_{r+1}} \right) \frac{\delta_{r+1}^2}{6D_{r+1}} - D_r \frac{f_r}{\lambda_r} \cdot \frac{\delta_{r+1}^2}{2D_{r+1}} \right\} \tag{31}$$

Model 7b. The same n-layered system as in model 7a, with

$$\frac{\partial c}{\partial x} = -f_0 \exp(-\lambda_0 t) \qquad \text{at} \quad x = 0 \qquad \text{for} \quad t \geqslant 0$$

but with $c = 0$ at $x = l_n$ for $t \geqslant 0$

The same analysis applies except that at $x = l_n$, $\partial c/\partial x$ is not defined and thus it is necessary to consider separately the top layer of sediment $l_{n-1} \leqslant x \leqslant l_n$, D_n;

with $$\frac{\partial c}{\partial x} = -\frac{1}{k_{n-1}^2} f_{n-1} \exp(-\lambda_{n-1} t) \quad \text{at} \quad x = l_{n-1+0} \quad \text{for} \quad t \geqslant 0$$

and with $c = 0$ at $x = l_n$ for $t > 0$

This is a particular case of model 3a and therefore $\partial c/\partial x$ at $x = l_n$ can be written down in terms of f_{n-1} and λ_{n-1}. If $\partial c/\partial x$ is to be approximated by $-f_n \exp(-\lambda_n t)$ at $x = l_{n-0}$ then f_n and λ_n are determined in terms of f_{n-1} and λ_{n-1}. It is found that

$$\frac{f_n}{\lambda_n} = \frac{1}{k_{n-1}^2} \frac{f_{n-1}}{\lambda_{n-1}} \tag{32}$$

and

$$\frac{f_n}{\lambda_n^2} = \frac{1}{k_{n-1}^2} \frac{f_{n-1}}{\lambda_{n-1}^2} \left(1 + \lambda_{n-1} \cdot \frac{\delta_n^2}{2D_n}\right) \tag{33}$$

The approximations to the concentrations at the interfaces used in model 7a do not apply here and it is necessary to assume a form of

$$c = C_r \sqrt{(t)} \exp(-\alpha_r t) \quad \text{at} \quad x = l_r \quad \text{for} \quad t \geqslant 0$$

If it is now applied to the single layer $l_r \leqslant x < l_{r+1}$ as in model 7a, the following relations for C_r and α_r are obtained:

$$\frac{C_r \sqrt{\pi}}{\alpha_r^{3/2}} = \frac{1}{\delta_{r+1}} \left[\left(D_{r+1} \frac{f_{r+1}}{\lambda_{r+1}} - D_r \frac{f_r}{\lambda_r} \right) \cdot \frac{\delta_{r+1}^2}{6D_{r+1}} + \left(D_{r+1} \frac{f_{r+1}}{\lambda_{r+1}^2} - D_r \frac{f_r}{\lambda_r^2} \right) + D_r \frac{f_r}{\lambda_r} \cdot \frac{\delta_{r+1}^2}{2D_{r+1}} \right] \tag{34}$$

and

$$\frac{3C_r \sqrt{\pi}}{\alpha_r^{5/2}} = \frac{1}{\delta_{r+1}} \left\{ \left(D_{r+1} \frac{f_{r+1}}{\lambda_{r+1}} - D_r \frac{f_r}{\lambda_r} \right) \cdot \frac{2}{5!} \frac{\delta_{r+1}^4}{D_r^2} + \left(D_{r+1} \frac{f_{r+1}}{\lambda_{r+1}^2} - D_r \frac{f_r}{\lambda_r^2} \right) \frac{\delta_{r+1}^2}{6D_{r+1}} \right.$$
$$\left. + \left(D_{r+1} \frac{f_{r+1}}{\lambda_{r+1}^3} - D_r \frac{f_r}{\lambda_r^3} \right) + D_r \frac{f_r}{\lambda_r^2} \frac{\delta_{r+1}^2}{2D_{r+1}} - D_r \frac{f_r}{\lambda_r} \cdot \frac{\delta_{r+1}^4}{12D_{r+1}^2} \right\} \tag{35}$$

Model 8a. The same n-layer system of sediments as in model 7a

but with $c = C_0 \exp(-\beta_0 t)$ at $x = 0$ for $t \geqslant 0$

and

$$\frac{\partial c}{\partial x} = 0 \quad \text{at} \quad x = l_n \quad \text{for} \quad t \geqslant 0$$

It is first necessary to consider the lower boundary condition as having two parts

$$c = C_0 - C_0 \exp(-\infty t) = C_0 \quad \text{for} \quad t \quad \text{very small}$$

and

$$c = C_0 \exp(-\beta t) \quad \text{for all other values of} \quad t > 0$$

By doing this c follows the same pattern, rising to a maximum and then decreasing to zero, which c follows at all other points in the sediments. This form can then be approximated by

$$c = \mu C_0 - \mu C_0 \exp'(-\infty t) = \mu C_0 \qquad \text{for} \quad 0 \leqslant t < t_0$$

and $$c = C_0 \exp(-\beta_0 t) \qquad \text{for} \quad t \geqslant t_0$$

where $$\mu = \exp(-\beta_0 t_0) \qquad \text{for any suitable choice of } t_0$$

Then at each interface the approximations for the concentrations have the form

$$c = C_r - C_r \exp(-\beta_r t) \qquad \text{at} \quad x = l_r \qquad \text{for} \quad 0 \leqslant t < t_0 \qquad r = 1, 2, \ldots, n$$

and

$$c = C_r' \exp(-\beta_r' t) \qquad \text{at} \quad x = l_r \qquad \text{for} \quad t \geqslant t_0 \qquad r = 1, 2, \ldots, n$$

Then the two layers of sediments $l_{r-1} \leqslant x < l_r$, D_r; $l_r \leqslant x < l_{r+1}$, D_{r+1}; are considered as before with

(a) $$c = C_{r-1} - C_{r-1} \exp(-\beta_{r-1} t) \qquad \text{at} \quad x = l_{r-1} \quad \text{for} \quad 0 \leqslant t < t_0$$

and $$c = C_{r+1} - C_{r+1} \exp(-\beta_{r+1} t) \qquad \text{at} \quad x = l_{r+1} \quad \text{for} \quad 0 \leqslant t < t_0$$

and (b) $$c = C_{r-1}' \exp(-\beta_{r-1}' t) \qquad \text{at} \quad x = l_{r-1} \quad \text{for} \quad t \geqslant t_0$$

and $$c = C_{r+1}' \exp(-\beta_{r+1}' t) \qquad \text{at} \quad x = l_{r+1} \quad \text{for} \quad t \geqslant t_0$$

which leads to the following recurrence relations:

for (a)
$$C_r = \frac{\delta_{r+1} C_{r-1} + k_r^2 \delta_r C_{r+1}}{\delta_{r+1} + k_r^2 \delta_r} \tag{36}$$

and

$$\frac{C_r}{\beta_r} = C_r \cdot \frac{[\delta_{r+1}(\delta_r^2/2D_r + \delta_{r+1}^2/6D_{r+1}) + k_r^2 \delta_r(\delta_{r+1}^2/2D_{r+1} + \delta_r^2/6D_r)]}{\delta_{r+1} + k_r^2 \delta_r}$$
$$+ \frac{\delta_{r+1}[C_{r-1}/\beta_{r-1} - C_{r-1}(\delta_{r+1}^2/6D_{r+1})] + k_r^2 \delta_r[C_{r+1}/\beta_{r+1} - C_{r+1}(\delta_r^2/6D_r)]}{\delta_{r+1} + k_r^2 \delta_r} \tag{37}$$

and for (b)
$$\frac{C_r'}{\beta_r'} = \frac{\delta_{r+1}(C_{r-1}'/\beta_{r-1}') + k_r^2 \delta_r(C_{r+1}'/\beta_{r+1}')}{\delta_{r+1} + k_r^2 \delta_r} \tag{38}$$

and

$$\frac{C_r'}{\beta_r'^2} = \frac{C_r'}{\beta_r'} \cdot \frac{\{\delta_{r+1}[(\delta_r^2/2D_r) + (\delta_{r+1}^2/6D_{r+1})] + k_r^2 \delta_r[(\delta_{r+1}^2/2D_{r+1}) + (\delta_r^2/6D_r)]\}}{\delta_{r+1} + k_r^2 \delta_r}$$
$$+ \frac{\delta_{r+1}[(C_{r-1}'/\beta_{r-1}'^2) - C_{r-1}'(\delta_{r+1}^2/6D_{r+1})] + k_r^2 \delta_r[(C_{r+1}'/\beta_{r+1}'^2) - C_{r+1}'(\delta_r^2/6D_r)]}{\delta_{r+1} + k_r^2 \delta_r} \tag{39}$$

It remains only to consider the single layer of sediment at the surface $l_{n-1} \leqslant x \leqslant l_n$, D_n; with

(a) $$c = C_{n-1} - C_{n-1} \exp(-\beta_{n-1} t) \qquad \text{at} \quad x = l_{n-1} \quad \text{for} \quad 0 \leqslant t < t_0$$

and (b) $c = C'_{n-1} \exp(-\beta'_{n-1} t)$ at $x = l_{n-1}$ for $t \geqslant t_0$

and $\dfrac{\partial c}{\partial x} = 0$ at $x = l_n$ for $t \geqslant 0$

Assuming a form at $x = l_n$ of

for (a) $c = C_n - C_n \exp(-\beta_n t)$ for $0 \leqslant t < t_0$

and (b) $c = C_n' \exp(-\beta_n' t)$ for $t \geqslant t_0$

the following relations result:

for (a) $$C_n = C_{n-1} \tag{40}$$

and $$\frac{C_n}{\beta_n} = \frac{C_{n-1}}{\beta_{n-1}} + C_{n-1} \cdot \frac{\delta_n^2}{2D_n} \tag{41}$$

and for (b) $$\frac{C_n'}{\beta_n'} = \frac{C'_{n-1}}{\beta'_{n-1}} \tag{42}$$

and $$\frac{C_n'}{\beta_n'^2} = \frac{C'_{n-1}}{\beta_n'^2} + \frac{C'_{n-1}}{\beta'_{n-1}} \cdot \frac{\delta_n^2}{2D_n} \tag{43}$$

As the corresponding values at $x = 0$ are known, all the intermediate values of C_r, β_r, C_r', β_r' are determined.

Model 8b. The same n-layer system of sediments as in model 7a, but with

$c = C_0 \exp(-\beta_0 t)$ at $x = 0$ for $t \geqslant 0$

and $c = 0$ at $x = l_n$ for $t \geqslant 0$

This problem is treated in exactly the same manner as in model 8a, resulting in the same recurrence relations. Since the values at $x = 0$ and $x = l_n$ of C_r, β_r, C_r', β_r' are given, all the intermediate values are therefore determined.

In order to illustrate the nature of these approximations, models 7a, 7b, 8a and 8b, have been used to approximate to models 2a, 2b, 3a, and 3b. This was carried out by dividing the single uniform layer into ten uniform layers and using the recurrence relations obtained above to evaluate the system. The resultant forms are illustrated diagrammatically in Fig. 4 and are to be compared with the corresponding analytical forms in Fig. 2. The approximation to model 2a is the least like its corresponding analytical form but it best emphasizes the essential qualitative nature of this paper. For the multi-layer problem it is the relationship between successive layers which is of primary interest rather than the accurate overall picture. The overall picture is the same as that for a single layer and it is worthwhile to consider the multi-layer problem in terms of a contraction from the single layer problem. A fair representation will be gained by imagining a single layer $0 \leqslant x \leqslant l_n$ with diffusivity D_1 being expanded uniformly to a depth of

$$\delta_1 + \sqrt{\left(\frac{D_1}{D_2}\right)}\,\delta_2 + \ldots + \sqrt{\left(\frac{D_1}{D_n}\right)}\,\delta_n$$

and then being contracted sectionally—the length $\sqrt{(D_1/D_2)}\ \delta_2$ to δ_2, and so on, the length $\sqrt{(D_1/D_n)}\ \delta_n$ to δ_n—back to the length $\delta_1 + \delta_2 + \ldots + \delta_n \equiv l_n$. The recurrence relations give a more accurate relationship between the layers but the above representation is a useful illustration of the nature of the relationship.

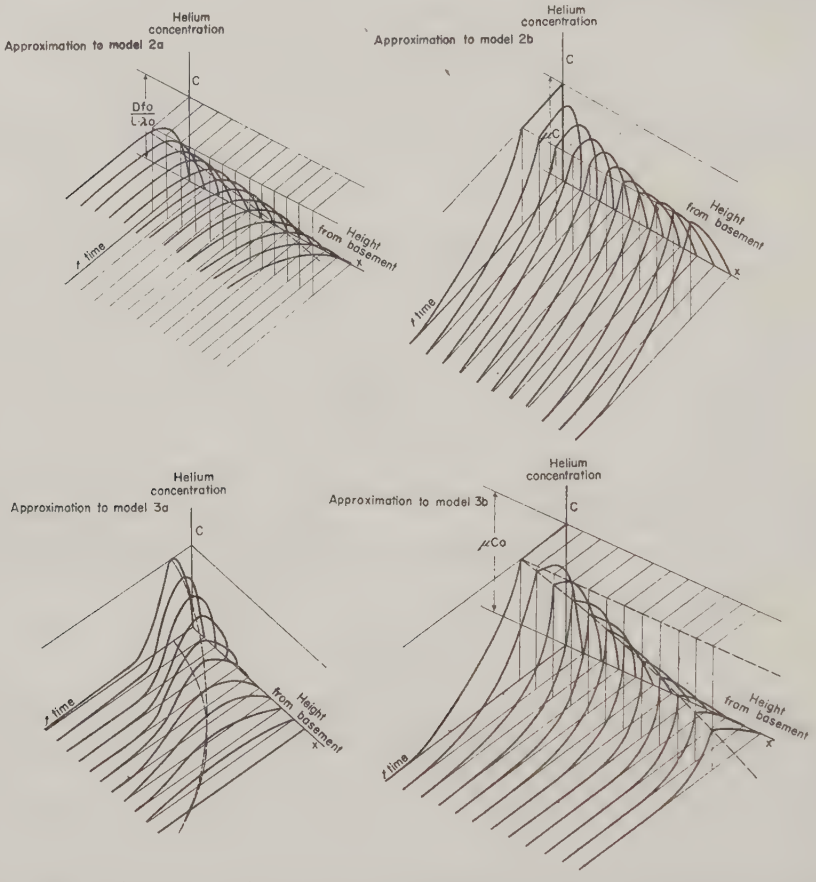

Fig. 4. Three-dimensional diagrams of the variation of helium concentration with time and distance from the basement, using the n-layer approximation techniques on the single finite layer models. These diagrams correspond to models 2a, 2b, 3a and 3b of Fig. 2.

Discussion

The very wide variation in the components of the problem limits any attempt at a quantitative analysis, but in order to provide a better understanding, some of the models have been evaluated numerically using representative values. Models 1a and 1b are plotted as concentration–distance curves in Fig. 5 for the three periods of 10^7, 10^8 and 10^9 years after the onset of sedimentation. The diffusivity was taken as 10^{-5} cm^2/sec and the values of λ and β as $0{\cdot}5 \times 10^{-17}$ sec^{-1} and $1{\cdot}5 \times 10^{-17}$ sec^{-1}, respectively. The area beneath the curves is a measure of the quantity of helium which has entered the sediments. Though the helium concentration scales are not directly comparable it is clear that the initial rate of

entry of helium is far greater in model 1b than in model 1a. This was the reason for choosing the exponential decay of concentration as a lower boundary condition for those situations where the initial helium concentration in the Pre-Cambrian is high. Models 4a and 4b are plotted as concentration–distance curves in Fig. 6 for the same three periods as before. The same values of λ and β were taken and the same diffusivity, 10^{-5} cm^2/sec, for the bottom layer of sediment, but for the upper layer a value of 10^{-7} cm^2/sec was used. The interface between the layers was taken

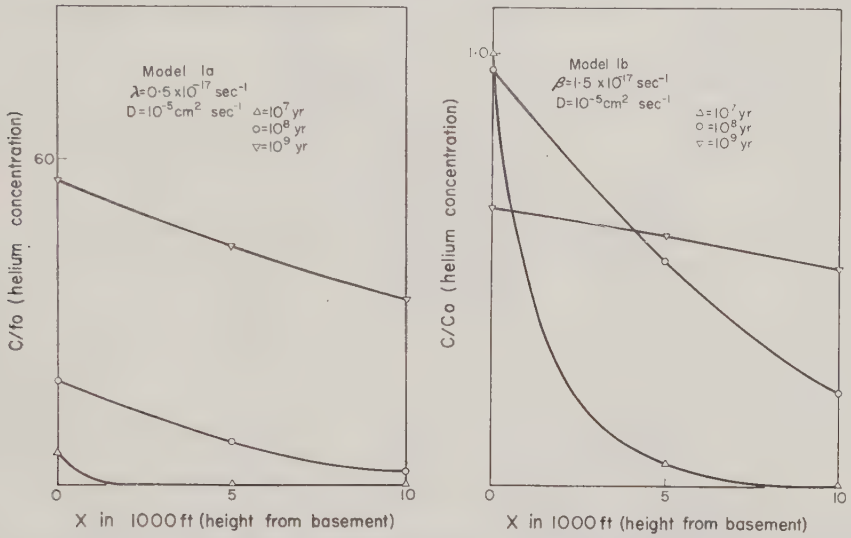

Fig. 5. Numerical examples of models 1a and 1b illustrating the difference between the lower boundary conditions of exponential decay of helium flow and exponential decay of helium concentration.

as 10,000 ft. from the basement. The upper layer is clearly, by comparison with the lower layer, nearly impermeable. Again it is of interest to note that the quantity of helium introduced into the sediments is initially high in model 4b and that in fact there is only a comparably slight increase between the periods of 10^8 and 10^9 years. A comparison with models 1a and 1b in Fig. 5 shows in each case a reduction in the concentration gradient in the lower layer.

Consideration of the above examples indicates the relationship between the rate of sedimentation and the rate of diffusion. The amount of helium reaching a specified level is determined by the diffusivity. The diffusivity of helium in water alone is about 3×10^{-5} cm^2/sec (Arnold, 1930) so that the value of 10^{-5} cm^2/sec used in these examples is probably a maximum value for porous media. As a result in practice far less helium reaches a specified level than is indicated in these examples and the assumption used in the introduction that the sedimentation rate is greater than the rate of diffusion is justified.

Summary

Helium migration through sedimentary rocks cannot be considered as anything but a complex problem. However, as with other problems of this type, considerable

advances can be made by breaking down the complex problem into a series of simpler problems from which the more complex forms can be compounded. By considering these simpler problems in detail, and as far as possible generalizing results, a worthwhile contribution can be made to the understanding of the problem as a whole. This has been the object of this paper for the migration of helium by diffusion, and within the limits of present-day knowledge it is felt that this has been achieved.

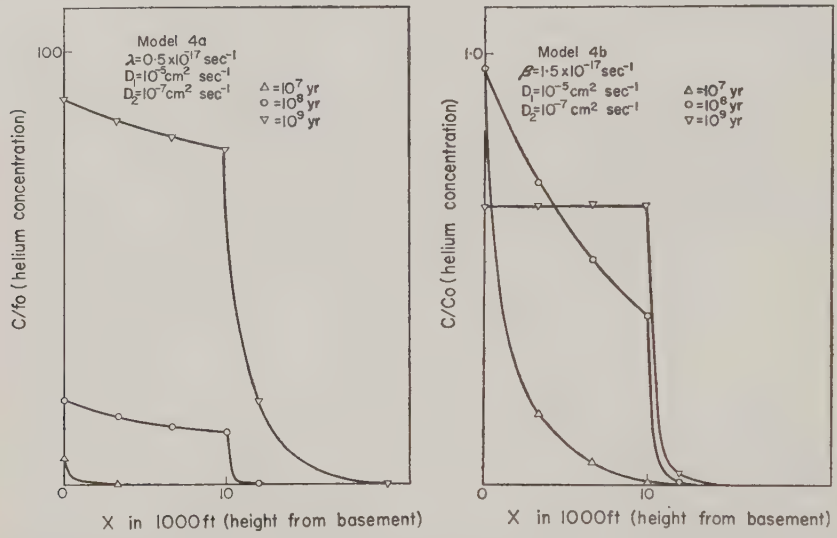

Fig. 6. Numerical examples of models 4a and 4b illustrating the effect of an upper medium of lower diffusivity.

Other modes of migration have not been ignored but it would appear that they are the exception, and diffusion is the general mode. The only other probable mode of migration is that due to the flow of water. If this flow is only 1 ft/year and if a significant proportion of the helium is in solution, then the migration of helium is entirely dominated by this flow. If in any particular region this mode is accepted then it follows that little or no helium can get above this flow and also that large accumulations of helium in regions such as natural gas reservoirs can be expected. Neither of these results appear to be generally true and it has seemed justified not to consider this mode in the general analysis of this paper.

Accepting diffusion as the mode of helium migration then it follows that in regions for which the lateral extent is three or four times the total sediment thickness and for which there is not extensive variation in lithology then the mathematical models developed in this paper can be applied. Within the same limitations this applies equally to orogenic and other regions of tectonic activity.

Although it may be estimated, the rate of introduction of helium into the sediments is an unknown factor. For the analysis it has been described in two ways, as an exponential flow decay, and as an exponential concentration decay. Together, these should adequately cover any situation which might occur in nature.

The process of sedimentation is rapid in relation to the diffusion process and

consequently little distortion of the concentration–distance curves obtained in this analysis would be expected to result in practice. It is apparent that even major breaks in sedimentation processes and erosional reverses would not result in marked distortions of the concentration-distance curves.

The determining effects for these curves are the gross diffusivities of each assumed layer and the boundary conditions assumed at the surface of the sediments. The gross diffusivity of any given layer affects the overall gradient of the curve in that layer, and the surface boundary condition affects the relationship of the whole curve to the basement and to the surface.

Nomenclature

D, D_r = diffusion coefficient (cm^2/sec).
c = concentration of helium (moles of helium per litre of available pore space).
x = distance measured from the Pre-Cambrian basement (cm).
t = time measured from onset of sedimentation (sec).
p = Laplace transformation parameter.
$\bar{c}$ = Laplace transform of c.
f_r, λ, λ_r = parameters to describe the exponential flow of helium.
C_r, C_r', β, β_r, β_r' = parameters to describe the exponential decay of helium concentration.
l, l_r = position of the surfaces of layers of sediments.
δ_r = thicknesses of the layers of sediments.

Acknowledgement—The writers are indebted to Dr. B. Hitchon for many valuable discussions clarifying our understanding of the geological nature of the problem and also to Dr. G. W. Hodgson for his helpful suggestions and criticisms.

References

Arnold J. H. (1930) A kinetic theory of diffusion in liquid systems. *J. Amer. Chem. Soc.* **52,** 3937–3955.

Barrer R. M. (1951) *Diffusion in and through Solids.* Cambridge University Press, Cambridge.

British Association Mathematical Tables (1931) Vol. 1, p. xxiv. British Association, London.

Churchill R. V. (1944) *Modern Operational Mathematics in Engineering.* McGraw-Hill, New York.

Crank J. (1956) *The Mathematics of Diffusion.* Clarendon Press, Oxford.

Daly R. A. (1933) *Igneous Rocks and the Depths of the Earth.* McGraw-Hill, New York.

Damon P. E. and Kulp J. L. (1958) Inert gases and the evolution of the atmosphere. *Geochim. et Cosmochim. Acta* **13,** 280–292.

Evans R. D. and Goodman C. (1941) Radioactivity of rocks. *Bull. Geol. Soc. Amer.* **52,** 459–490.

Glasstone S., Laidler K. J. and Eyring H. (1941) *Theory of Rate Processes.* McGraw-Hill, New York.

Hitchon B. (1960) Geochemistry of natural gas in Western Canada. *Geology of Natural Gas* (2nd Ed.) American Association of Petroleum Geologists. In preparation.

Hurley P. N. (1952) Alpha ionisation damage as a cause of low helium ratios. *Trans. Amer. Geophys. Un.* **33,** 174–183.

Murray E. G. and Adams J. A. S. (1958) Thorium, uranium and potassium in some sandstones. *Geochim. et Cosmochim. Acta* **13,** 260–269.

Raimondi P. G., Gardner G. F. H. and Petrick C. B. (1959) *Effect of Pore Structure and Molecular Diffusion on the Mixing of Miscible Liquids Flowing in Porous Media.* Paper presented at A.I.Ch.E.–S.P.E. Joint Symposium on Fundamental Concepts of Miscible Fluid Displacement Pt. II, San Francisco, December 1959.

Senftle F. E., Stieff L., Cuttitta F. and Kuroda P. K. (1957) Comparison of the isotopic abundances of U^{235} and U^{238} and the radioactivity ratios in Colorado Plateau uranium ores. *Geochim. et Cosmochim. Acta* **11**, 189–193.

Turekian K. K. (1959) The terrestrial economy of helium and argon. *Geochim. et Cosmochim. Acta* **17**, 27–43.

Geochimica et Cosmochimica Acta, 1961, Vol. 22, pp. 133 to 154. Pergamon Press Ltd. Printed in Northern Ireland

Radioactive species produced by cosmic rays in iron meteorites

M. Honda, J. P. Shedlovsky* and J. R. Arnold
School of Science and Engineering, University of California,
La Jolla, California

(*Received* 3 *April* 1960; *re-submitted* 11 *July* 1960)

Abstract—The radioactive isotopes Be^{10}, Al^{26}, Cl^{36}, K^{40}, and Mn^{53} have been measured in four iron meteorites: Grant, Williamstown, Odessa and Canyon Diablo. Each sample was recycled to constant activity, using a different chemistry for each recycle wherever possible. The samples were counted with a low-level β-counter, except for Mn^{53} whose X-rays were measured. The isotope ratios were approximately constant for each meteorite, except for Mn^{53} where a depth effect is visible. The cosmic-ray ages of Williamstown and Grant are about the same.

Since the pioneer work of Paneth *et al.*, 1953, the stable and radioactive products of cosmic-ray bombardment of meteorites have been intensively studied (see Begemann *et al.*, 1959; Ehmann and Kohman, 1958; Geiss, 1957, and Wänke, 1958 with the references given by them). The goal of these researches, speaking generally, has been to learn more about the history of the meteorites in space, and of the cosmic radiation itself.

As a contribution to this end, we have studied the content of Be^{10}, Al^{26}, Cl^{36}, K^{40} and Mn^{53} in several iron meteorites. In this paper we shall discuss the techniques used and the results obtained. A following paper will give a detailed analysis of the information which we can derive from them and the results of other workers, in particular concerning the production rate of these nuclides and the variation of cosmic-ray intensity with time over long periods.

We were especially interested in Mn^{53} (Sheline and Hooper, 1957), which has not been previously counted in the laboratory because of Mn^{54} contamination, and which is mainly a product of low-energy reactions. The work on K^{40} and Mn^{53} has been briefly described elsewhere (Honda, 1959, Shedlovsky, 1960a).

Samples

Odessa. A complete individual of 5·5 kg (similar to the one used by Ehmann and Kohman, 1958) was purchased from Ward's Scientific Establishment Inc. All but 200 g was consumed. Odessa is a coarse octahedrite found before 1922 at Odessa, Texas. From the existence of a crater 530 ft in diameter a very large mass must have fallen. More than 200 kg have been recovered. This meteorite has often been identified with the Canyon Diablo fall.

Grant. 500 g of cuttings from a slice completely through the meteorite were furnished through the courtesy of Dr. E. P. Henderson. All but 19 g was consumed. Grant is a fine octahedrite found near Grant, New Mexico, about 1929. One mass of 480 kg was recovered.

* Present address, Department of Chemistry, Carnegie Institute of Technology, Pittsburgh 13, Pa. Part of the work described is taken from a thesis submitted by J. P. Shedlovsky to Princeton University in partial fulfillment of the requirements for the Ph.D.

Williamstown. A slice of 406 g was furnished through the courtesy of Dr. Brian Mason. All but 12 g was consumed. This is a medium octahedrite found in 1892 near Williamstown, Kentucky. A mass of 68 kg was found.

Canyon Diablo. A piece of 800 g was purchased from Ward's Scientific Establishment Inc. (Ward Catalog No. 34-3763). About half, 429 g, was consumed. Canyon Diablo is a coarse octahedrite found in 1891 in Coconino County, Arizona, U.S.A., and associated with the "Meteor Crater". More than 30 tons have been recovered and the original mass is supposed to be very large.

General Procedures

(a) *Solution*

In the course of this research, and in more recent work, we have employed several different acid systems, including aqua regia, HNO_3, HCl and H_2SO_4. The aqua regia procedure described below is the most convenient when it can be applied, but it cannot be used when Cl^{36} is to be determined. For the next step elimination of all but traces of HNO_3 is essential. This requires repeated evaporation. Nitric acid allows the determination of all the nuclides studied. A convenient rate of solution is achieved by the use of 3 M HNO_3, adding stronger acid as required. As will be seen from our Williamstown experiments, HCl has some disadvantages. Special care must be used to oxidize Fe^{II} to Fe^{III}. We would now prefer H_2O_2 to HNO_3 for this purpose. Again Cl^{36} cannot be determined. The rate of solution in 6 M HCl is convenient. Sulphuric acid was used for the Cl^{36} determination only. In this case the sample was dissolved in 4–5 M H_2SO_4, and silver chloride precipitated. Use of this acid for work with other nuclides would be inconvenient.

Procedure for Grant

(1) The sample was washed with acetone, petroleum ether, acetone, H_2O, dilute HCl and H_2O, and dried with acetone. The weight was 467 g.

(2) It was placed in a 1-l. heat-resistant polyethylene beaker in an ice bath. From 100- to 600-ml portions of aqua regia were added, and the beaker covered with a watch glass. After reaction had nearly stopped the solution was decanted into a Pyrex beaker. Fresh portions were used until a very small mass remained. The final solution volume was 2·5 l.

(3) The solution was evaporated to near dryness; 2 l. of 6 M HCl were added and evaporated down to about 1·5 l.

(4) Residues from steps (1) and (3) were dissolved by adding 9 M HCl and the solutions centrifuged to remove insoluble material, mainly graphite. About 1 per cent of the solution was set aside for chemical analysis.

The following carriers were added: 10 mg Be as $Be(NO_3)_2$ solution, 27 mg Al as $AlCl_3$, 9·1 mg Mn as $MnCl_2$, 1·13 mg Cs as CsCl, and 11·5 mg Na as NaOH. The total volume of solution was just over 2 l.

Odessa

(1) The sample, a 3·6 kg portion of our specimen, was washed with water and acetone.

(2) The sample was dissolved in a 3-l. Pyrex beaker. The final solution volume was 20 l. Beryllium carrier was added (30 mg Be), and fresh HNO_3 (150 ml) to ensure that all iron was in the Fe^{III} state.

(3) The sample was evaporated in portions to near dryness in a porcelain dish, with repeated addition of small portions of HCl.

(4) After dissolving residues Al carrier (16 mg Al^{3+}) was added to the combined solutions. The final volume was about 20 l.

A separate sample was used for Cl^{36} (see below).

Williamstown

(1) The sample was washed with water and acetone.

(2) It was dissolved in 6 M HCl containing a small amount of HNO_3. About 3 l. of final solution resulted.

(3) After adding more HNO_3, to a total of 300 ml, the solution was evaporated in a Pyrex beaker to near dryness; 2 l. of 6 M HCl were added and the evaporation repeated.

(4) After dissolving residues 10 mg of Be and 27 mg of Al carrier were added. Final volume was 3 l.

Canyon Diablo

(1) The sample, 429 g, was washed with *iso*propyl alcohol, acetone, dilute nitric acid and water.

(2) About half of the sample was dissolved and the solution was separately processed from the rest, which was dissolved by further addition of the acid. For solution of the first part, 18 moles of HNO_3 were used, starting with 1 l. of 3 M and followed by 6 and 16 M acid. The vessel was a 4 l. flask fitted with a reflux condenser and an absorption tube filled with solid sodium hydroxide granules. No chlorine carrier was added. After the separation of the first part, 17·6 moles of nitric acid were used to dissolve the remaining sample as before. A small amount of insoluble substance was filtered off from the second part. Final volumes were about 2·5 l. for each part. The two sample solutions were treated in parallel. The fraction of the sample in each part was estimated by analyses of the iron content of the solutions. We found 60 per cent of the meteorite in part (1) and the rest in part (2) by subtraction. The carriers, 25 mg of Mn and 27 mg of Al, were added to each solution. An excess of $AgNO_3$ (5 m-mole) was added and the silver chloride precipitate was separated. Excess Ag^+ was removed by the addition of excess HCl (part 2). To the filtrate 13 mg of Be carrier was added.

(3) The silver chloride precipitate was treated by the same process as the Odessa sample and finally ammonium chloride was recovered (see below). In recycling, the combined NH_4Cl from both parts was resublimed.

(4) The filtrate was evaporated down to near dryness after the addition of 0·2 l. of concentrated HCl. About 1 l. of 8 M HCl was added and the solution was heated to decompose the remaining nitrate. By bubbling of HCl gas and addition of 8 M HCl, 1·2 l. of *ca.* 8 M HCl sample solution was prepared.

(b) *Extraction and anion exchange*

The solvent extraction of an $FeCl_3$ acid complex into *iso*propyl ether serves to

remove Fe with very few contaminants. This is the first step in bringing solution volumes down to small size.

The elements Be, Al and K are not removed from 9–10 M HCl solution by an anion exchange column, while Mn is adsorbed only weakly (Kraus *et al.*, 1954). Anion exchange serves to remove Co, the remaining Fe^{III}, and many other elements from the solution. The effluent contains the elements of interest, along with Ni. The adsorbed ions are eluted to give "Fe" and "Co" fractions.

(5) For Grant, Williamstown and Canyon Diablo, solvent extraction of each batch of solution with fresh portions of *iso*propyl ether was continued until the ether phase was nearly colourless (from three to four times). The aqueous phase was adjusted to ~8 M HCl when necessary. The ether phases were combined and back-extracted with water. The aqueous iron fraction was stored.

For Odessa a special extraction system was used (Shedlovsky, 1960b). A 5-l. flask was charged with 4 l. of meteorite solution. One litre of *iso*propyl ether and several hundred millilitres of water were placed in a 2-l. flask on a side arm, which was heated with a mantle. Ether was condensed in a reflux condenser, and was released through a glass frit at the bottom of the main flask. Iron was gradually transferred to the side flask. Occasionally it was necessary to add concentrated HCl to the main flask to maintain 8 M HCl. Here also a final H_2O back extraction was performed and an aqueous iron fraction stored.

(6) Ten millilitres of 30 per cent H_2O_2 were added to each extracted portion, and it was slowly evaporated to expel dissolved ether. The Odessa solutions were again evaporated in a porcelain dish. More 12 M HCl was added to dissolve crystallized salts.

(7) The solutions from step (6) were made up to 9 M by bubbling HCl gas through them. The total volumes were approximately: Grant, 2 l.; Williamstown, 750 ml; Odessa, 16 l.; Canyon Diablo, 1·1 l. (total).

(8) *Grant.* A 1-l. ion-exchange column of Dowex-1 X8 100–200-mesh was prepared after decantation to remove fines, and treated with H_2O, 3 l. 0·5 M HCl, and 1·5 l. 9 M HCl. The sample solution was passed through the column, which was washed with 1·5 l. of 9 M HCl (to remove Mn). The appropriate fractions were combined and evaporated down to about 500 ml. A "Co fraction" was eluted with 4 M HCl, and a "Fe fraction" with 0·5 M HCl. Both were stored.

Williamstown. After treatment as above the Williamstown sample contained a large amount of Fe^{II}. Twenty millilitres of HNO_3 was added to the solution and it was slowly heated. Rapid uncontrolled boiling occurred, and about 55 per cent of the solution spilled from the beaker.

Because the sample was irreplaceable, this was mopped up with filter paper, which was extracted with water and 6 M HCl. After filtering, 10 ml HNO_3 was added, and the solution boiled down to 1 l. The "spilled" and "unspilled" portions were treated separately from this point on. The fraction in each was estimated by nickel analysis.

*iso*Propyl ether extractions were carried out on both fractions for final removal of Fe. Anion exchange was carried out in the same way as for Grant.

Odessa. A 1·5 l. column of Dowex 1 was prepared as above. Eight litres of solution were passed through at 30 ml/min. The column was then nearly saturated.

It was washed with 1 l. of 9 M HCl, and this fraction combined with the previous effluent. Cobalt and iron fractions were eluted as above. Considerable irreversibly adsorbed Fe remained on the column after passing through 10 l. of 0·5 M HCl.

The column was then used again, but its adsorption capacity was greatly lowered. Only a few litres could be treated. A fresh 500-ml column was prepared and used twice for the remaining solution. All Ni fractions and Mn fractions were combined, and boiled down to 6 l.

Canyon Diablo. A 500-ml column of Dowex 1 was equilibrated with 10 M HCl for each part. The sample solution was passed through and the column washed with 10 M HCl. All effluents were collected, up to 1·5 l. for part 1 and 0·8 l. for part 2. Each solution was concentrated to 150 ml.

(c) *Separation of* Be, Al, Mn *and* K

To remove Ni, advantage is taken of the $Ni(NH_3)_4^{2+}$ complex ion. Successive precipitations with NH_3 leave Ni finally in solution, along with K and many other elements. Be, Al, and Mn are collected in a hydroxide fraction of small mass, along with other trace elements.

(9) To the solution from step (8), H_2O_2 was added, then NH_3 to make the pH 8·0. $Al(OH)_3$, $Be(OH)_2$ and hydrous MnO_2 precipitated along with phosphates and some $Ni(OH)_2$. About 10 ml H_2O_2 and 400 ml NH_3 were added, except in the case of Odessa, where 30 ml of H_2O_2 and 3 l. of NH_3 were added.

The basic solution was heated to near boiling and allowed to cool slowly. The hydroxides were filtered and washed with a 1 per cent NH_4NO_3–0·1 per cent NH_3 solution. They were then dissolved in 6 M HCl with a little H_2O_2 to reduce Mn to Mn^{II}. To remove the bulk of the nickel the precipitation was repeated twice more, keeping the NH_4Cl concentration about 1 M each time. The two parts of Canyon Diablo were combined at this point.

The filtrates from the three precipitation steps were combined and stored as a "Ni fraction". Potassium was later separated from this fraction (see below).

(d) *Isolation and purification of individual elements*

Manganese. Manganese was separated by basic H_2O_2 precipitation. It was purified by acid $NaBrO_3$ precipitation, scavenging and anion exchange in HCl, and finally again by $NaBrO_3$ precipitation.

(10) The final precipitate from step (9) was dissolved in 0·5 M H_2SO_4 with a little H_2O_2. The Mn in the Williamstown and Grant fractions was precipitated by the addition of NaOH to a final concentration of 5–10 per cent after adding 10 mg Fe^{III} carrier; 9·1 mg Mn^{2+} carrier was also added to the unspilled Williamstown fraction. Aluminate and beryllate remain in solution. The precipitate was centrifuged and washed with 1 per cent NaOH, and the washings added to the original solution. The cycle of solution and NaOH precipitation was repeated. All solutions were combined.

(11) The precipitate was dissolved in 0·5 M H_2SO_4–H_2O_2 and the solution boiled. Solid $NaBrO_3$ was added slowly and the solution boiled again until precipitation of MnO_2 was complete. The precipitate was centrifuged, washed with 0·5 M H_2SO_4, and redissolved in H_2SO_4–H_2O_2.

In the case of Odessa, step (10) was omitted, and the precipitate from step (9) was dissolved in 0·5 M H_2SO_4–H_2O_2 and MnO_2 precipitated with $NaBrO_3$. A large amount was required. In the case of Canyon Diablo, the step (9) precipitate was dissolved in dilute H_2SO_4–H_2O_2, partially neutralized with NaOH to pH ~0·5, and MnO_2 precipitated with $NaBrO_3$. Hydroxides were precipitated with NH_3–H_2O_2, filtered, and redissolved in H_2SO_4–H_2O_2. Further MnO_2 was recovered by the addition of $NaBrO_3$ to this solution. An appreciable amount of Mn was also recovered from the "Co fraction" of part 2. Iron carrier was added, and by repeated precipitation in strong NH_3 cobalt was separated as the ammine complex. Manganese was finally recovered with bromate.

(12) Fifty milligrams of Sr^{2+} carrier as $Sr(NO_3)_2$ solution was added and the solution heated to near boiling. After slow cooling, $SrSO_4$ was filtered off.

(13) The filtrate was adjusted to about 0·3 M H^+, and 10 mg of Cu^{2+} was added as $CuCl_2$ solution (50 mg for Odessa). After heating to 70°C, CuS was precipitated by bubbling through H_2S. The precipitate was filtered and washed with H_2S water. The filtrates were combined and boiled to remove H_2S.

(14) Iron carrier was added as $FeCl_3$ solution, (25 mg was used in the case of Odessa, 10 mg in other cases). A dilute Na_2CO_3 solution was slowly added until a faint opalescence persisted, at pH ~5. Three millilitres of acetic acid was added, and the clear solution diluted to 500 ml. The solution was boiled, 7 ml of 30 per cent NaAc added, and boiling continued for another minute. (The acetates of Fe, Al, Ti, V, Zr hydrolyse on boiling and their hydroxides precipitate. Manganous acetate is stable (Lundell and Hoffman, 1938). The hydroxides were filtered and washed with hot 5 per cent NaAc. The precipitate was redissolved in a minimum of hot dilute HCl and the procedure repeated. The filtrates are combined and made 0·5 M in H_2SO_4. Hydrous manganese dioxide was precipitated as in step (11). After centrifuging, it was washed twice with dilute H_2SO_4 and dissolved in a few millilitres of 9 M HCl with a drop of H_2O_2.

(15) A small anion column, 10–30 ml, was prepared as in step (8). The solution from step (14) was placed on the column, which was then washed with 9 M HCl. The Mn fractions were collected in the second and third column volumes of effluent. The combined fractions were evaporated to near dryness with H_2SO_4 to remove HCl.

(16) After dilution to about 25 ml, bringing the solution to about 0·5 M H_2SO_4, $NaBrO_3$ was added. After boiling the solution was centrifuged or filtered, washed free of sulphate, transferred to a crucible, and dried under an infra-red lamp (ignited in the case of Canyon Diablo).

This was the final form used for counting.

Recycle chemistry. This will be described only generally. Details are available (Shedlovsky, 1960b) for Mn, Al and Be.

For the first recycle, after dissolving the MnO_2 in H_2SO_4 with H_2O_2, the solution was titrated with EDTA to determine Mn content.* More H_2SO_4 was added and the solution evaporated to SO_3 fumes followed by decomposition of organic matter with H_2SO_4 and H_2O_2. Water was added, and MnO_2 precipitated

* This is not convenient for the following step. It is better to measure Mn, taking an aliquot, by a spectrophotometric method or EDTA titration.

with $NaBrO_3$. After scavenging with CuS and $Fe(OH)_3$, the precipitation was repeated and the solution in H_2SO_4 with H_2O_2 again evaporated to SO_3 fumes. These scavenging steps were omitted in the case of Odessa.

The manganese in solution was oxidized to MnO_4^- with $NaIO_4$ (boiling for 15 min). The solution was scavenged with $Fe(OH)_3$ in NH_3 solution. Some MnO_2 apparently precipitated with $Fe(OH)_3$ at this point. The filtrate was acidified and H_2O_2 added to reduce MnO_4^- to Mn^{2+}. Free I_2 was sublimed by heating. MnO_2 was again precipitated with $NaBrO_3$. The Odessa and Williamstown samples were dissolved in 9 M HCl with H_2O_2 and passed through an anion exchange column. Manganese was recovered in the second and third column volume of the effluent, and the solution evaporated to dryness. Finally MnO_2 was precipitated and dried.

The second recycle chemistry was similar to the first. Manganese was recovered from the $Fe(OH)_3$ scavenging steps of this and the previous recycle, carried through the scavenging procedure again and combined with the main Mn fraction. This was followed by anion exchange and MnO_2 precipitation.

Beryllium isolation and purification. Beryllium was separated from aluminium and other elements on a cation column by elution with 1·1 M HCl. Aluminium was eluted with 3 M HCl. Beryllium was purified by CuS scavenging and solvent extraction of the acetylacetone (AA) complex in the presence of EDTA (Merrill *et al.*, 1960).

(17) The final solution from step (10) was made acid with HCl, then brought to pH 8·0 with NH_3 (the Odessa solution in H_2SO_4 was brought to pH 8·0 with NH_3). The solution was boiled briefly. The precipitate was allowed to settle, centrifuged, washed twice with 1 per cent NH_4NO_3–0·1 per cent NH_4OH and dissolved in HCl. A second hydroxide precipitation was performed to remove most of the Na^+ and SO_4^{2-} ions. After dissolving in HCl the solutions were evaporated to near dryness and diluted with 1·1 M in HCl. (Ehmann and Kohman, 1958).

A 40 ml column of Dowex 50 X8, 100–200-mesh, cation resin was prepared (75 ml in the case of Odessa). The column was washed with more than three column volumes of 3 M HCl and finally with H_2O. The sample was put on the column, washed with one column volume of H_2O, and elution with 1·1 M HCl begun. Using a fraction collector, Be was eluted with 1·1 M HCl and Al with 3 M HCl.

(18) The Be fraction was made 0·3 M in hydrogen ion. A CuS scavenging was carried out as in step (13). $Be(OH)_2$ was precipitated with NH_3, heated, centrifuged, washed, and dissolved in warm 0·5 M HCl. This step was omitted in the case of Odessa.

Ten millilitres of 10 per cent Na_2EDTA was added and then NaOH solution dropwise to pH 7·0. Two millilitres of AA were added and the solution shaken until it dissolved. The solution was allowed to stand for ten minutes. The Be–AA complex was extracted with two 15 ml portions of $CHCl_3$. The organic solution was gently boiled down with 4 ml HCl until no organic phase remained. Nitric acid and HCl were added and the solution gently boiled to near dryness to destroy organic matter. A second extraction was performed as before after adding 10 ml

10 per cent Na_2EDTA and 2 ml AA. After evaporation and destruction of organic matter a final precipitation of $Be(OH)_2$ was performed in the presence of 0·05 m-moles of Na_2EDTA by the addition of NH_3 to pH 8. The white precipitate was heated and allowed to settle and cool. It was then filtered on Whatman no. 41H filter paper, washed, dried and ignited.

Recycle chemistry. The first recycle of beryllium was begun by fusing BeO with $NaHSO_4$, precipitating $Be(OH)_2$ from NH_3 solution, and CuS scavenging. A solution in 5 per cent NaOH was passed through a $Fe(OH)_3$ dispersed cation exchange column (Merrill *et al.*, 1960), which removes elements co-precipitating with Fe^{III} in this solution. After acidifying and precipitating $Be(OH)_2$ with NH_3, it was again dissolved and precipitation was carried out in the presence of EDTA. The precipitate was ignited and weighed.

In the second recycle, after fusing, precipitation, and CuS scavenging, the acid solution was put on a cation resin in the NH_4^+ form. The column was washed with water and treated with 1·5 column volumes of 0·1 M NH_4Ac–0·4 M HAc. After washing with water, Be was eluted with 0·5 M NH_4Ac–1 M HAc, the Be fraction lying between one and three column volumes (Merrill *et al.*, 1960). The hydroxide was precipitated, dissolved, and reprecipitated in the presence of EDTA.

Aluminium. The aluminium fraction was purified by CuS and $Fe(OH)_3$ scavenging, anion exchange with HCl, and finally the Gooch and Havens precipitation of $AlCl_36H_2O$ in HCl–ether (Hillebrand *et al.*, 1953).

(19) The Al fraction from step (17) was evaporated down to expel most of the HCl, and $Al(OH)_3$ precipitated with NH_3 at the methyl red end-point. The solution was heated, centrifuged, and the precipitate washed with 1 per cent NH_4NO_3–0·1 per cent NH_3. It was dissolved in a minimum of hot 0·5 M HCl.

(20) A CuS scavenging step was carried out as in step (13).

(21) Ten milligrams of Fe^{III} carrier was added and the solution made 5–10 per cent in NaOH. The precipitate after centrifuging was washed, and the solutions combined. The precipitate was redissolved in HCl. This step was repeated and all solutions combined. The solution was acidified with HCl, and NH_3 added to precipitate $Al(OH)_3$. After heating, centrifuging, and washing, the precipitate was dissolved in warm dilute HCl. To remove most of the Na^+ a second precipitation was carried out and the precipitate dissolved in 6 M HCl.

(22) A 5-ml Dowex 1 column was prepared and finally washed with 6 M HCl. The solution from step (21) was placed on the column, which was washed with 6 M HCl. All effluents were combined and evaporated down to about 10 ml.

(23) The solution, in a small beaker, was cooled in an ice bath and an equal volume of diethyl ether added. Hydrogen chloride gas was bubbled through until there was only one liquid phase. The precipitate was filtered on a fritted glass funnel.

(24) The precipitate was dissolved in water and $Al(OH)_3$ precipitated with NH_3 at the methyl red end-point. After heating and settling, the precipitate was filtered, washed and ignited.

Recycle chemistry. In the first recycle, Al_2O_3 was fused with $NaHSO_4$. The hydroxide was precipitated twice. A CuS scavenging was performed, and $Al(OH)_3$ precipitated in the presence of Mn^{2+} and Sr^{2+} holdback carriers. The solution

was made 5 per cent in NaOH and passed through a $Fe(OH)_3$ column as in the beryllium case. After two more $Al(OH)_3$ precipitations the solution was made 6 M in HCl and passed through an anion column. The solution and washings were combined, evaporated, precipitated with NH_3 and redissolved in HCl.

The Grant sample was further purified by putting the solution on a Dowex 50 cation column in the H^+ form. The column was eluted with 0·5 M oxalic acid (Merrill *et al.*, 1960). The Al fraction was collected over a range of 0·5 to 3 column volumes. The solution was boiled down with H_2SO_4 and H_2O_2 to destroy oxalic acid. After $Al(OH)_3$ precipitation the precipitation of $AlCl_3 \cdot 6H_2O$ was carried out as described in step (23).

A final hydroxide precipitation was performed and the precipitate ignited as before.

The chemistry of the second and third recycles was essentially the same. The Odessa and spilled Williamstown samples underwent the second recycle. The two Williamstown samples were combined for the third.

Potassium. The ammoniacal nickel fraction was put on a cation exchange column in the NH_4^+ form, and K^+ and other ions eluted with NH_4Ac before $Ni(NH_3)_4^{2+}$ (Honda, 1954, 1955). After decomposing NH_4^+ salts and scavenging, K^+ was separated by cation exchange and precipitated as the tetraphenylborate (Raff and Brotz, 1951). The salt was dissolved in acetone and recrystallized.

Reagents and procedures were checked for laboratory contamination with natural K. Reagent-grade NaOH and Cs salts were purified by cation exchange. A maximum of 100 μg of K could enter from steps (25) through (27). The milligram quantities found represent (1) natural K in the meteorite especially in troilite inclusions (Stoenner and Zähringer, 1958), (2) contamination of the original sample with terrestrial K, and (3) introduction of K in earlier steps of the procedure. The maximum amount of laboratory K introduced in our current procedures is not more than 1 mg/kg.

(25) *Grant.* A column of 1·8 l., Dowex 50 W-X 8, 100–200-mesh, was prepared in the NH_4R form by pretreatment with 3 M HCl, treatment with excess 2 M NH_4Ac–0·3 M NH_3, and washing with 0·3 M NH_3. About 1·2 l. of solution from step (9), containing 0·63 moles Ni and 3·9 moles Cl^-, were diluted to 3 l. with water, and passed through the column, which was then washed with 500 ml of 0·3 M NH_3. Potassium and cesium were eluted with 5·5 l. of 1 M NH_4Ac–0·3 M NH_3. At this point the front of the Ni band approached the bottom of the column. No nickel was eluted.

The nickel fraction was later eluted with 2 M HCl–2 M NH_4Cl.

Williamstown. The unspilled portion contained 0·18 mole Ni and 1·1 mole Cl^-, corresponding to 170 g of the sample. A 1·2 l. column was used, and 3 l. of eluent.

Odessa. Four fractions (nos. 1–4), each of 1·5 l. and containing 0·65 moles Ni and 3·7 moles Cl^-, were used. Fractions (1) and (2), after dilution to 3 l. were passed through a 1·2 l. column, and only the last 1·2 l. of effluent and 3 l. of eluate collected. Twenty milligrams of NaCl were added. Fractions (3) and (4) were treated almost exactly like Grant, except that 19·2 mg CsCl carrier was added to no. 3.

(26) The effluent was evaporated to dryness in a 3-l. Pyrex beaker. The residue was dissolved in 0·3 M HCl and filtered. After adding 2 mg Cu^{2+} carrier, CuS was precipitated. Excess H_2S was expelled and 2 mg Fe^{III} carrier added. The precipitate with NH_3 was composed of $Fe(OH)_3$ and other hydroxides, which were filtered off. The filtrate was evaporated in a Vycor dish and NH_4Cl decomposed by gentle heating.

In the case of Williamstown the evaporated solids were dissolved in aqua regia, and only $Fe(OH)_3$ scavenging was done. In the case of Odessa no. 1 and no. 2, the evaporation of the effluent from step (25) was completed, and NH_4Cl decomposed, in a platinum dish.

(27) The residue was extracted with saturated $Ca(OH)_2$ solution, and the extract passed through a 12-ml column of Dowex 50 X 8, 200–400-mesh, prepared by washing with 6 M HCl and water. The column was eluted with 1 M HCl, and K^+ recovered in the 60–85 ml fraction. The fraction was evaporated to KCl crystals, which were dissolved in 10 ml H_2O. One drop each of 1 M $MgCl_2$ solution, 0·5 M NaOH (potassium free), and phenolphthalein indicator were added along with one drop of HCHO to give an alkaline reaction. A small excess of 2 per cent sodium tetraphenylborate solution was added. The white precipitate $KB(C_6H_5)_4$, was filtered, and washed with 0·04 per cent $NaB(C_6H_5)_4$–0·04 M NaAc (Berkhout and Jongen, 1956). The precipitate was dried at 100°C. dissolved in acetone, filtered again, and the solution gently evaporated in a 10 ml beaker under an infra-red lamp. The salt was weighed and mounted.

From the 85–130 ml fraction, Cs was recovered in the same way.

In the case of Williamstown, no Cs carrier had been added, and the $KB(C_6H_5)_4$ precipitation was done directly after the $Fe(OH)_3$ scavenging, from an NaOH solution containing 0·3 m-moles of sodium in EDTA and two drops HCHO.* Two Odessa fractions (nos. 1–2) were treated in the same way. The others (nos. 3–4) were treated like Grant, except that the cation exchange purification of K required a second cycle because of high column loading.

Recycle chemistry. The recycle chemistry for Grant began with solution of the salt in acetone, to which an equal volume of H_2O was added. A cation column in the H^+ form was prepared as in step (27), and pretreated with acetone–water. The solution was put on the column which was washed with water and eluted with 1 M HCl. The K fraction was collected, 0·25 m-mole of NaOH carrier added, CuS and $Fe(OH)_3$ precipitations carried out, and $KB(C_6H_5)_4$ reprecipitated. For mass-spectrographic measurement a portion of recycled sample was purified using a 1·5 ml cation column as above, the eluent being 1 M HCl–0·05 M $HClO_4$. The K fraction was evaporated in a silica dish. The residue was dissolved in 1 ml H_2O. Special care was taken to avoid Ca contamination.

The Williamstown sample was recycled similarly, but no Na^+ carrier was added, and some NH_3 used in the $Fe(OH)_3$ scavenging step. This led to difficulties even with excess HCHO. Repurification of the final salt was necessary.

Chlorine. For Cl^{36} we used a separate portion of Odessa, of 298 g. It was washed with dilute H_2SO_4, dissolved in H_2SO_4, and AgCl precipitated and purified.

* The former procedure is preferred. MgEDTA seems to be better than the sodium salt.

A cation exchange column removed $Ag(NH_3)_2^+$, and NH_4Cl was purified by sublimation. The recovery was nearly quantitative. The Canyon Diablo sample is described above.

(1) Two litres of 4·5 M H_2SO_4 were used to dissolve the specimen in a flask fitted with a reflux condenser, after adding 107 mg equivalent of NH_4Cl carrier. The solution was heated until all but 55 g of the specimen had dissolved. The ferrous salts were dissolved in water and added to the main solution, which was filtered. An excess of $AgNO_3$ was added, and AgCl (with some Ag) was filtered off.

(2) The salt was dissolved with 5 M NH_3 and reprecipitated with HNO_3. It was dissolved again and the filtrate passed through a 10-ml cation exchange column in NH_4R form (Honda, 1955). The effluent was evaporated and a white residue, NH_4Cl, recovered. It was placed in a Vycor crucible and sublimed on the bottom of a water cooled flask used as a cover.

In recycling the Odessa sample, CuS and $Fe(OH)_3$ scavengings were performed. Silver chloride was precipitated from neutral solution in the presence of a small amount of EDTA. The precipitate was dissolved in NH_3 with a small amount of KI and digested. It was then purified as in step (2).

Chemical Analysis and Yield Determination

In the case of beryllium, the yield was calculated from the amount of added carrier and gravimetric determination of sample BeO. In all other cases the problem depended at least in part on chemical analysis of the meteorite or of our solutions. About 1 per cent of the original meteorite solution was saved for this purpose.

Manganese. Three aliquots of the original solution of each meteorite were taken, after ether extraction and anion exchange to remove Fe and Co. A few drops of Fe^{III} carrier were added and MnO_2 precipitated with $Fe(OH)_3$ by the addition of NH_3 and H_2O_2 to pH 8. The precipitate was washed and dissolved in 10 ml dilute H_2SO_4 with a little H_2O_2. The solution was heated to SO_3 fumes, cooled, water and 1 g $(NH_4)_2S_2O_8$ added and the solution boiled for 10 min. Then 0·5 g of $NaIO_4$ was added and the solution boiled 5 min. The solution was cooled, made up to 100 ml, and its absorbance measured at 525 mμ against H_2O in a 5 cm cell. One drop of HCl was added to destroy MnO_4^- and the absorbance again measured. This blank was subtracted, and the net readings compared to a calibration curve. The contents of Mn in parts per million were: Odessa 10·6, Williamstown 5·1, Grant (cuttings) 41·5, with an estimated precision of 0·5 p.p.m. for the first two and 1 p.p.m. for the last.

The samples were counted as MnO_2, which is not a suitable compound for gravimetric determination. Manganese was determined in them by EDTA titration (Schwarzenbach, 1956); the composition was close to MnO_2. Yields were determined based on the analyses above and added carrier if any.

Aluminium. Duplicate analyses of each solution for Al were performed by a fluorescence technique (Simons *et al.*, 1953), using the zinc salt of Pontachrome Blue Black R. Aluminium forms a complex which fluoresces over the region from 6365 to 6975 Å. An aliquot of the solution after removal of Fe and Co, and after addition of Be carrier for Al (2 mg BeO equivalent) was treated with NH_3 to

bring the pH to 7·6. After heating, centrifuging, and dissolving the precipitate in HCl, the precipitation was repeated. The precipitate was dissolved in HCl and the solution diluted to 10 ml.

Four 1 ml aliquots were taken and 1 μg of Al spike added to two of them. Each was diluted to 50 ml, and buffered to pH 5·0 with NH_4Ac–HAc. Two millilitres of 0·1 per cent dye solution in 95 per cent ethanol was added, and after 4 hr the fluorescence measured at 6675 Å with a Beckman DU spectrophotometer with photomultiplier attachment. From the difference in readings between the two pairs the amount of Al was calculated assuming a linear curve. Duplicate blanks were also measured. Plastic containers were used throughout. The values obtained for total Al in the three samples were: Odessa, 55 mg in 3540 g, Williamstown 0·5 mg in 170 g, and Grant 52 mg in 459 g. We believe that these quantities do not reflect the Al content of the original meteorites.

Yields were calculated based on these values and added Al carrier. In all cases except Canyon Diablo, these fell between 100–130 per cent. This indicates further laboratory contamination with Al, which we believe is mainly due to evaporation in porcelain and Pyrex ware. In the case of Canyon Diablo, the difficulties seemed to be small partly because of higher Al carrier content.

Because Al and Be are so similar chemically in all steps up to step (17), and because losses after this point should be small and similar, we have chosen a value of 75 per cent for the Al yields in all cases except Canyon Diablo, similar to the Be yields which approximate this value. The problem of Al yields also occurs in earlier work (Ehmann and Kohman, 1958); it can only be solved by more careful control of laboratory contamination (or larger amounts of Al carrier).

Potassium. Because of the radioactivity of natural K, it was impractical to add isotopic carrier. Caesium carrier was added in the case of Grant and Odessa fraction no. 3. This should give a rather accurate figure since the yield of both the ion exchange and tetraphenylborate precipitation steps is nearly quantitative (although the cation exchange behaviour of K and Cs is different). The K yield for Grant has been taken as 85 per cent, the same as the Cs yield. In the case of Odessa the yield of K for the four fractions was nearly identical. The Cs yield of fraction no. 3 was 81 per cent; we have taken 80 per cent for the combined K yield. The same yield was taken for Williamstown, based on the unspilled portion.

The amount of K found is probably much higher than the natural K content of the meteorite (Stoenner and Zähringer, 1958).

Chlorine. In the case of Odessa the recovery of NH_4Cl was 171 mg. Another 9 mg were recovered from solutions at various steps using $AgNO_3$. The total was taken to represent 100 per cent yield. Subtracting added carrier, this corresponds to 0·02 per cent Cl in our sample. In the case of Canyon Diablo no carrier was added. The yield was taken as 100 per cent. Part 1 of the solution, presumably the outside part of our specimen, showed 0·02 per cent Cl; part 2 showed 0·04 per cent. The specific activity in dpm Cl^{36}/kg meteorite seemed to be the same for both parts. The chloride mineral lawrencite occurs in some iron meteorites (Goldschmidt, 1954). On the internal evidence the results obtained may well represent the intrinsic Cl content of the two meteorites, rather than field contamination. Laboratory contamination is well below this figure.

Carrier Blanks

It does not appear reasonable that contamination with the actual nuclides under study could take place, since no man-made sources of these species were located in our neighbourhood. All carriers were checked for activity, however. The amounts found in our Mn, Al and Cl carriers without chemical purification could be safely neglected. The activity of our reagent KCl is in agreement with that of other samples and literature values. It was subtracted to obtain the excess cosmogenic K^{40}.

In the case of Be our carrier proved to contain about 250 p.p.m. U (based on $Be(NO_3)_2 \cdot 3H_2O$) along with its short-lived daughters. A direct count without chemistry gave 8 counts/min for 15 mg BeO. This is the same carrier used for all our Be^7 and Be^{10} studies (see Merrill *et al.*, 1960). Steps (8), (17) and (18) should each be efficient in removing U and Th from the final BeO. These contaminants are unimportant for Mn since only soft X-rays are measured. The occasional high Q-gas counts may be due to them. In the case of Al, the decontamination steps are (8), (21), (33) (for U only), and (23).

In the case of Canyon Diablo, a purified Be carrier was used. Except for this and a few differences in procedure in this case, the low and consistent results obtained for this meteorite are good evidence for general freedom from procedural and reagent blanks throughout this work.

Counting Procedures

All counting was done inside a low-level shield, consisting of an 8-in. low-carbon steel shield, with twelve cosmic-ray counters, surrounding the central counter, arranged in anticoincidence. The counters used were similar to those of Sugihara *et al.* (1953), with a metal-coated mylar cylindrical wall of thickness about 1 mg/cm^2. These were operated as flow counters at one atmosphere pressure with Q-gas (98·7 per cent helium, 1·3 per cent butane). Argon saturated with ethanol at 0°C was used for X-ray counting.* The counters were operated in the Geiger region using a battery power supply adjustable in small steps. The counter plateaus were at least 180 V long with a slope of 4–5 per cent/100 V. Usually the counters were operated about 50 V above threshold; a typical voltage (nominal) was 1035 V. The same Q-gas flows through the a.c. counters. Their anodes were tied together; the counters are well matched. The plateau of the a.c. assembly is more than 180 V long with a slope of 10 per cent/100 V. The counters are operated at 1335 V, 90 V above the threshold, also using a battery supply.

In most of our work a transistorized anticoincidence circuit was used.† This circuit, with a dead time of approximately 900 μsec, receives inputs from the central counter and the anticoincidence ring. It provides outputs for anticoincidence ring counts, total counts of the central counter, and counts in anticoincidence. Two central counters can be used in the same ring, providing a total of five outputs. All these are recorded on scalers. A strip chart recorder recorded the time for every 10 or 100 counts on a chosen channel.

* We are currently using 98·7 per cent Ar, 1·3 per cent ethylene for this purpose.
† Sharp Laboratories, La Jolla, California.

All transistorized circuits are powered by 6-V auto batteries. The only line current used is for the scalers.

Besides these counters, a NaI(Tl) crystal γ-ray spectrometer was used for auxiliary studies. The crystal and phototube are contained in a shield of 2 in. of mercury inside 2 in. of lead. Signals are measured on a 100-channel pulse-height analyser (R.I.D.L.).

Each sample for β-counting was mounted after weighing on a clean Lucite or copper cylinder, whose background had previously been compared at least once with that of a standard cylinder. The sample was ground in an agate mortar and pestle, transferred to the two halves of the cylinder, slurried with a few drops of 0·1 per cent agar solution (rubber cement solution in benzene for NH_4Cl) and spread with a thin rod. The total sample area approximated 20 cm^2; the sample length was about 3·5 cm (2·0 cm for K^{40}). The slurry was dried under an infra-red lamp and stored for at least several hours. Hands were always washed immediately before changing samples on the counter, and only the outside was handled. These precautions are necessary to avoid counts due to RaA, B and C.

In general, each sample was counted three times alternately with background. Each count was roughly 8 hr in length. The background of the first counter ranged from 0·17 to 0·24 counts/min during the course of the work; that of the second counter was about 0·35 counts/min. The statistical error of a 2-day run on a weak sample, with half of the time on sample and half on background, was about $\pm$0·017 counts/min. The Mn^{53} samples were treated differently. Here we compared sample with background using Q-gas. This gave a measure of any contamination present. Then the same measurements were made with argon-ethanol. The difference was taken to represent soft X-rays, since the counter efficiency is the same with both fillings for beta, alpha, and higher energy γ-radiation.

Counter Calibration

The efficiency of our counters for thin beta sources was measured using N.B.S. sources and natural K^{40}. The source length was 3·5 cm in all cases; source thickness was 1·5 mg/cm^2. The counting rate was corrected for self-absorption to zero sample thickness (see below), but no other corrections were applied. Back-scattering causes the efficiency to be higher for copper than for plastic sample holders. The resulting efficiencies for our first counter are shown in Table 1; similar data were obtained for the second counter.

The variation of counting efficiency with source length was measured using a point source. Corrections for (central) sources of finite length were obtained by integration. These values are given in Table 2.

The beta activities of our samples were determined by applying to the net Q-gas counting rate factors for the following variables: (1) thin source counting efficiency for this energy; (2) sample length; (3) self-absorption; and (4) chemical yield. The self-absorption corrections were made using the exponential equations of Libby (1956). The half-thicknesses used were 21·2 mg/cm^2 for Be^{10} (Arnold, 1956), 30 mg/cm^2 for Cl^{36}, and 63 mg/cm^2 for Al^{26}.

The data were further corrected for the following decay scheme factors: Al^{26}, 84 per cent β^+ emission; Cl^{36}, 98 per cent β^-; K^{40}, 89 per cent β^-.

Calibration for Mn^{53}, a pure X-ray emitter, was more difficult, as no accurate X-ray standards are available. W. S. Lyon kindly furnished us with an Oak Ridge standard of Fe^{55} assumed known to ± 25 per cent. Assuming a fluorescence yield of 0·27, we obtained 2·5 per cent for the efficiency of our counters filled with argon–ethanol, using a diluted standard (source length 2 cm) prepared from this

Table 1. Counting efficiency for thin β-sources
(Counter 1, source length = 3·5 cm)

Nuclide	Energy (MeV)	Counting efficiency Plexiglas (%)	Copper holder (%)
S^{35}	0·167	8·0	10·0
Co^{60}	0·31	18·0	23·5
Cs^{137}	0·51 (8% 1·17)	22·8	30·2
Tl^{204}	0·764	26·1	36·2
K^{40}	1·33*	28·5	37

* A disintegration rate of 1·72 dis/min β^-per/mg K was assumed

Table 2. Efficiency factor for sources of finite length (counter 2)
(Relative to 100% for 3·5 cm)

Length (cm)	Relative efficiency
0·0	118
1·0	117
2·0	112
2·5	109
3·0	105
3·5	100
4·0	94

source. We then performed an absolute calibration of this standard using a screen-wall counter (Libby, 1955) of 2·5-in. active diameter, using a drag-in voltage and argon–*iso*propanol at 1 atm (this gave better plateaus than argon–ethanol). The source was mounted near the centre of the 8-in. active length and covered with 1 mg/cm^2 Mylar (aluminium coated) to remove Auger electrons. Under these conditions this is very nearly an ideal 2π detector for the Fe^{55} X-rays. (Absorption due to the covering film was measured by using additional thicknesses.) The only important loss is the "wall effect" resulting from failure to count X-rays emitted in short paths close to the wall. We estimate this effect at 5 per cent. There are also small absorption corrections (see below). Using the counting rate obtained in this way and a fluorescence yield of 0·27, an efficiency of 3·0 per cent is obtained for the first counter for Fe^{55}.* For Mn^{53}, correcting for fluorescence yield and absorption coefficient, we obtain 2·8 per cent.

* R. Terwiel has made a Monte Carlo calculation of the efficiency of our counter for Fe^{55} X-rays and obtains 3·0 per cent, in good agreement with this measurement. Our value of $\alpha = 0{\cdot}27$ is meant to be based on the total number of disintegrations, including L-capture.

The counting efficiency of our counters for Fe^{55} with Q-gas filling is 0·07 per cent.

The Mn^{53} activity of each meteorite was calculated as follows. The net counting rate of the sample counted using Q-gas (representing any possible β-contamination) was subtracted from the net counting rate using Ar–EtOH. The Q-gas count was usually but not always zero within experimental error. This net counting rate was corrected as in the case of β-radiation. The mass absorption coefficients for Mn and O at this wavelength were taken to be 99·4 and 40·1, respectively. The half-thickness, for a collimated beam, is thus 8·9 mg/cm^2. For a source emitting isotropically the absorber equation

$$N/N_0 = e^{-\mu d} + \mu d Ei(-\mu d)$$

must be used (Campion, 1957). This was integrated numerically to the thickness of the sample.

Results

The data for the five nuclides are given in Tables 3 to 7.

Table 3. Be^{10} data

Sample	Weight (g)	Wt. sample counted BeO mg	% yield	Net counts/min	Counting efficiency (%)	dis/min per kg Be^{10}
Grant	459	18·4	61·3	0·232 ± 0·023	22	3·68 ± 0·36
Recycle		17·4	58·0	0·259 ± 0·023	22	4·34 ± 0·39
						Ave. 4·03 ± 0·27
Williamstown	386	22·0	73·4	0·201 ± 0·027	22	3·20 ± 0·43
Recycle		20·0	66·7	0·212 ± 0·020	22	3·70 ± 0·35
						Ave. 3·51 ± 0·35
Odessa	3540	81·3	77·3	1·060 ± 0·032	20	1·99 ± 0·06
Recycle		77·0	73·3	1·117 ± 0·039	20	2·18 ± 0·08
Recycle		71·0	67·6	0·957 ± 0·036	20	2·00 ± 0·08
						Ave. 2·06 ± 0·09
Canyon Diablo (combined)	420	44·2	63	0·064 ± 0·018	31	0·77 ± 0·22
Recycle		38·2	54·3	0·066 ± 0·017	31	0·91 ± 0·23
						Ave. 0·84 ± 0·16

Absorption curves were also determined for the Odessa samples of Be^{10} and Al^{26}, using plastic absorbers. The half-thicknesses determined by least squares fitting of a semi-log plot were 25 and 104 mg/cm^2, respectively, corresponding to energies of 0·63 and 1·61 MeV. The errors (standard deviations) of these determinations are estimated to be 0·1 and 0·3 MeV, respectively. The agreement is fairly satisfactory.

The γ-activity of each Mn sample was checked using a 2-in. well crystal and 100-channel γ-ray spectrometer. No peaks were found in any sample. The count

Table 4. Al^{26} data

Sample	Weight (g)	Wt. sample counted (Al_2O_3 mg)	% yield	Net counts/min	Counting efficiency (%)	dis/min per kg Al^{26}*
Grant	459	225·2	75	0·259 ± 0·022	26	4·10 ± 0·35
Recycle		162·2	54	0·219 ± 0·022	27	4·60 ± 0·46
						Ave. 4·29 ± 0·27
Williamstown						
Spilled	216	224·2	57·9	0·079 ± 0·016	26	3·43 ± 0·69
Unspilled	170	26·2	75	0·089 ± 0·012	30	3·28 ± 0·44
Combined	252	135·7	54·1	0·098 ± 0·020	28	3·61 ± 0·74
						Ave. 3·43 ± 0·46
Odessa	3540	164·4	75	0·677 ± 0·031	25	1·32 ± 0·06
Recycle		93·4	42·6	0·451 ± 0·022	29	1·48 ± 0·07
Recycle		72·4	33·0	0·305 ± 0·022	29	1·27 ± 0·10
						Ave. 1·37 ± 0·11
Canyon Diablo	420	42·3	40	0·065 ± 0·017	38	1·22 ± 0·31
Recycle		28·4	27	0·02 ± 0·014	38	0·56 ± 0·39
						Ave. 0·88 ± 0·25

* Assuming 84 per cent β^+ emission.

Table 5. Cl^{36} data

Sample	Weight (g)	Wt. sample counted (NH_4Cl mg)	Natural Cl content (%)	% yield	Net counts/min	Counting efficiency (%)	dis/min per kg Cl^{36}*
Odessa	243	171	0·02	95	0·26 ± 0·04	22	5·0 ± 0·8
Recycle		155		87	0·24 ± 0·03	22	5·1 ± 0·6
							Ave. 5·1 ± 0·5
Canyon Diablo							
Pt. 1	270	54·9	0·02	100	0·06 ± 0·014	25	0·84 ± 0·19
Pt. 2	150	94·8	0·045	100	0·03 ± 0·014	24	0·8 ± 0·37
Recycle (combined)	420	130·7		87	0·11 ± 0·02	25	1·26 ± 0·25
							Ave. 1·1 ± 0·2

* Assuming 98 per cent β^- emission.

rates in the Mn^{54} peak were all negative. The upper limit of Mn^{54} contamination in dis/min per kg is claculated to be (3σ confidence limit) 5 dis/min per kg for Odessa, and 15 dis/min per kg for Williamstown and Grant.

Discussion

The reliability of the final data, expressed in dis/min per kg, depends on the accuracy of the determination of chemical yield, the counting data, and the various factors entering into the counting efficiency. An effort has been made above to give the reader sufficient evidence to decide these questions.

The errors quoted are the statistical errors (standard deviations) of counting only. When these errors are less than 10 per cent, other errors in counting efficiency

Table 6. K^{40} data*

Sample	Weight (g)	Wt. of K collected (mg)	% yield	Wt. of K counted (mg)	Net counting rate (counts/min)	Specific activity of K (counts/min per mg)	Excess K^{40}† in meteorite (dis/min per kg)
Grant	459	1·58	85	1·53	1·20 ± 0·04	0·78 ± 0·03	4·9 ± 0·5
Recycle				1·33	0·99 ± 0·07	0·74 ± 0·05	4·3 ± 0·8
							Ave. 4·6 ± 0·5
Williamstown	170	1·08	80	1·02	0·69 ± 0·03	0·68 ± 0·03	6·4 ± 1·0
Recycle				0·57	0·33 ± 0·02	0·58 ± 0·04	3·5 ± 1·2
							Ave. 5·0 ± 1·0
Odessa							
Pts. 1 and 2	1100	5·56	80	4·29	2·43 ± 0·10	0·57 ± 0·02	2·4 ± 0·7
Pts. 3 and 4	1100	5·45	80	5·04	2·70 ± 0·06	0·54 ± 0·01	1·4 ± 0·6
							Ave. 1·9 ± 0·5
Reagent KB $(C_6H_5)_4$ (1)				1·96	0·90 ± 0·04	0·46 ± 0·02	
(2)				1·11	0·53 ± 0·02	0·48 ± 0·02	

* Dr. Wasserburg has measured the enrichment factor of K^{40} to K^{41} and K^{39} by a mass spectrographic method. The samples, $KClO_4$, were prepared from our recycled samples. The enrichment factor in our samples was measured to be 1·36 and 1·17 in Grant and Williamstown, respectively. When we compare these data with our measurements agreement is found to be good within the statistical error. A small discrepancy might be indicated in the case of Grant which could be attributed to dilution by introduction of natural potassium during processing.

† Assuming 89 per cent β^- emission.

Table 7. Mn^{53} data

Sample	Weight (g)	Wt. sample counted (mg Mn)	% yield	Net counts/min Q-gas	Net counts/min Argon	Counting efficiency	dis/min per kg Mn^{53}
Grant	459	24·9	88·3	0·25 ± 0·07	3·05 ± 0·24	1·84	375 ± 34
Recycle		8·0	28·4	0·096 ± 0·032	0·98 ± 0·11	2·21	306 ± 39
Recycle		17·4	61·7	0·123 ± 0·037	1·79 ± 0·05	1·99	296 ± 12
							Ave. 299 ± 11
Williamstown	170	3·4	34·0	0·34 ± 0·04	0·726 ± 0·064	2·34	288 ± 53
Recycle		1·2	12·0	0·011 ± 0·025	0·15 ± 0·026	2·41	282 ± 71
							Ave. 285 ± 43
Odessa	3540	19·8	52·8	0·060 ± 0·045	7·17 ± 0·36	1·95	196 ± 10
Recycle		10·0	26·7	0·11 ± 0·05	4·03 ± 0·11	2·16	192 ± 6
Recycle		10·9	29·1	0·064 ± 0·037	4·63 ± 0·16	2·14	208 ± 8
							Ave. 197 ± 5
Canyon Diablo (combined)	420	14	25	0·171 ± 0·025	0·426 ± 0·043	2·52	94 ± 19
Recycle		8·2	15	0·010 ± 0·15	0·163 ± 0·017	2·69	90 ± 13
							Ave. 92 ± 12

and chemical yield probably are greater in most cases. Absolute errors are then probably in the general region of 10 per cent, or greater if the counting error is greater. However, ratios may be more accurate. The internal consistency of the results supports this view.

Two special cases call for comment. On a percentage basis the Al^{26} data are less accurate than the others. The Williamstown results show larger error. This results from a combination of the lowest counting rates and the least satisfactory chemistry. The Odessa K^{40} measurement is of low accuracy because of the small

difference between the counting rate and that of the natural standard. Errors due to differences in mounting are greatly magnified in this instance.

In our opinion, the most important requirement for accuracy is the use of large samples, which not only results in comparatively high and reliable counting data, but also creates the possibility of such auxiliary tests as absorption curves and tests for γ-impurities. In the sample purification process we have usually used a different chemistry for each recycle step, to guard against a high yield for any contaminant. Contamination with the nuclides studied is most unlikely to occur at the location of our laboratory.

The question of sampling is important in the interpretation of the results. Fireman (1959) reports that the He^3 content of Grant ranges from $6{\cdot}6.10^{-6}$ cm^3(s.t.p.)/g meteorite at one edge to $5{\cdot}0.10^{-6}$ at the centre. Hoffman and Nier (1958) find a range from 6·0 to $4{\cdot}7.10^{-6}$ for He^3 and from 21·0 to $18{\cdot}2.10^{-6}$ for He^4. Our sample of saw cuttings should be a good average. Williamstown is a small meteorite, and large variations are not to be expected, even if it is a fragment of a larger fall. Schaeffer and Zähringer, (1959, 1960) give values of 4·8 and $6{\cdot}3.10^{-6}$ cm^3/g for the He^3 content as determined by two methods.

The comparison of our results for Be^{10} and Al^{26} in Odessa with those of Ehmann and Kohman (1958) is made difficult by the large size of this meteorite. Their results were $0{\cdot}7 \pm 0{\cdot}2$ dis/min per kg Be^{10} and $5{\cdot}5 \pm 1{\cdot}0$ dis/min per Al^{26}. The difference in the Be^{10} results may well be due to the difference in position of the two specimens. It is also possible that the chemical yield of Be in their work was rather low. Their result on Al^{26}, however, is in disagreement with our data: it exceeds the Al^{26} activity found in Grant and Williamstown, and it disagrees with the Al^{26}/Be^{10} ratio of 0·7–1·1 found in all our meteorites. In view of the small activity observed, their Al^{26} value may be due to contamination.

It should be noted that the production of Al^{26} by spallation of sulphur and phosphorus in an iron meteorite may be significant compared to the production from iron, because of the much higher cross-section in these elements. This may be a source of variation in the Al^{26} data.

Sprenkel (1959) has found 7·8 dis/min per kg Cl^{36} in Odessa, 3·3 dis/min per kg in Williamstown, and 6·8 and 8·9 dis/min per kg for the Canyon Diablo I and II. This species can be formed not only by high-energy reactions but also, in sufficiently large meteorites, by neutron capture in Cl^{35}. The chlorine content of iron meteorites is highly variable, and large meteorites may be quite inhomogeneous with respect to this element. An excess of Cl^{36} produced by neutron capture would result in a shift in the ratio A^{36}/A^{38} to values higher than 0·7 (Geiss, 1957). Since Schaeffer and Zähringer (1960) report the ratio of A^{36}/A^{38} to be 0·58, 0·61, and 0·67 for their specimens of Odessa, Canyon Diablo I and Williamstown, this source seems to be ruled out. Williamstown is a small meteorite (see below), and even if their specimens of Odessa and Canyon Diablo came from the outer skin, their Cl^{36} contents (from Fe spallation) should be lower than that for Williamstown because bombardment takes places from one side only. We conclude that this is probably a real experimental discrepancy, and that the cosmic-ray age reported for Williamstown is too large.

A study of Cl^{36} in Sikhote-Alin has been reported by Gfeller *et al.* (1960).

The relative concentration of K^{40} and K^{41} in Carbo and Treysa has been measured by Voshage and Hintenberger (1959).

It is instructive to consider the ratio of activities in our four meteorites (Table 8). The ratio Williamstown/Grant is near unity for all species. For the short-lived species this is consistent with the results of other workers (Begemann *et al.*, 1959, Geiss *et al.*, 1958) for meteorites of a few hundred kilograms or less. The agreement in K^{40} results indicates a similar cosmic-ray age for the two meteorites.

In Odessa and Canyon Diablo the amount of Mn^{53} is relatively higher than that of the other species. This nuclide, because of its proximity in mass and charge to

Table 8. Ratio of activities in meteorites

	Be^{10}	Al^{26}	K^{40}	Mn^{53}
Williamstown / Grant	0·87 ± 0·11	0·80 ± 0·13	1·1 ± 0·3	0·95 ± 0·15
Odessa / Grant	0·51 ± 0·04	0·32 ± 0·04	0·4 ± 0·15	0·66 ± 0·03
Canyon Diablo / Grant	0·21 ± 0·04	0·20 ± 0·06		0·31 ± 0·04

the target species, must be produced by low-energy secondary particles to a much greater extent than the others. A high value for its activity in large meteorites is consistent with our expectations, since the ratio secondaries/primaries must increase with depth. The K^{40} value for Odessa may indicate an age similar to that of Williamstown, but the error is large.

So far as we are aware, our samples of Mn^{53} are the first sources of this nuclide which have been counted. Synthetic samples so far prepared contain too much Mn^{54} for counting. We hope it will be possible to determine the half-life of Mn^{53} by measuring Mn^{53}/Mn^{55} mass-spectrometrically in our meteorite samples.

In a following paper we will discuss the cosmic-ray age, the depth effect, and the time variation of the cosmic-ray intensity.

Note added in proof

Using a fresh sample we have obtained a value of 3·8 ± 0·7 dis/min per kg Cl^{36} in Williamstown, in agreement with Sprenkel (1959). The result is difficult to interpret; perhaps Williamstown has a long terrestrial age.

Acknowledgements—The authors are grateful to E. P. Henderson and to Brian Mason for making available the large samples of Grant and Williamstown which made this work possible.

We are indebted to G. J. Wasserburg for the mass-spectrometric K^{40} analyses, to E. D. Goldberg and W. Sackett for assistance with γ-ray measurements and Al analyses respectively, and to M. C. Anderson for assistance with the Canyon Diablo chemistry. We have profited by discussions with them and with D. Lal, R A. Naumann and H. C. Urey. This research was supported by the Office of Ordnance Research, U.S. Army.

References

Arnold J. R. (1956) Beryllium-10 produced by cosmic rays. *Science* **124,** 584.

Begemann F., Eberhardt P. and Hess D. C. (1959) He^3–H^3 radiation age of a stone meteorite. *Z. Naturf.* **14a,** 500.

Berkhout H. W. and Jongen G. H. (1956) Determination of potassium by precipitation and titration of its tetraphenylboron salt. *Chem. Anal.* **45,** 6.

Campion P. J. (1957) *In National Academy of Sciences-National Research Council Publication* No. 573, p. 88.

Ehmann W. D. and Kohman T. P. (1958) Cosmic-ray-induced radioactivities in meteorites. *Geochim. et Cosmochim. Acta* **14,** 340, 364.

Fireman E. L. (1959) The distribution of helium-3 in the Grant meteorite and a determination of the original mass. *Planet. Space Sci.* **1,** 66.

Geiss J. (1957) On the history of the meteorites from isotope measurements. *Chimia* **11,** 349.

Geiss J., Oeschger H. and Signer P. (1958) Helium-3-hydrogen-3 measurements on a stone meteorite. *Helv. Phys. Acta* **31,** 322.

Gfeller C., Herr W., Houtermans F. G. and Oeschger H. (1960) Cl^{36} in meteorites. *Helv. Phys. Acta.* In press.

Goldschmidt V. M. (1954) *Geochemistry* (Edited by A. Muir) Clarendon Press, Oxford.

Hillebrand W. F., Lundell G. E. F., Bright H. A. and Hoffman J. I. (1953) *Applied Inorganic Analysis* (2nd Ed.). John Wiley, New York.

Hoffman J. H. and Nier A. O. (1958) Production of helium in iron meteorites by the action of cosmic rays. *Phys. Rev.* **112,** 2112.

Honda M. (1954) Separation of alkaline earth cations by ion-exchange resin. *Japan Analyst* **3,** 132.

Honda M. (1955) Separation and determination of transition metals with cation-exchange resin *Japan Analyst* **4,** 384.

Honda M. (1959) Cosmogenic K^{40} in iron meteorites. *Geochim. et Cosmochim. Acta* **17,** 148.

Kraus K. A., Nelson F. and Smith G. W. (1954) Anion exchange studies IX. Adsorbability of a number of metals in hydrochloric-acid solution. *J. Phys. Chem.* **58,** 11.

Libby W. F. (1955) *Radiocarbon Dating* (2nd Ed.). University of Chicago Press, Chicago.

Libby W. F. (1956) Relation between energy and half-thicknesses for absorption of β-radiation. *Phys. Rev.* **103,** 1900.

Lundell G. E. F. and Hoffman J. I. (1938) *Outlines of Methods of Chemical Analysis.* John Wiley, New York.

Merrill J. R., Honda M. and Arnold J. R. (1960) Methods for separation and determination of beryllium in sediments and natural waters. *Analyt. Chem.* **32,** 1420.

Paneth F. A., Reasbeck P. and Mayne K. I. (1953) Production by cosmic rays of helium-3 in meteorites. *Nature, Lond.* **172,** 200.

Raff P. and Brotz E. (1951) Determination of potassium as the salt of tetraphenylboron. *Z. anal. Chem.* **133,** 241.

Schaeffer O. A. and Zähringer J. (1959) High-sensitivity mass spectrometric measurements of stable helium and argon isotopes produced by high-energy protons in iron. *Phys. Rev.* **113,** 674.

Schaeffer O. A. and Zähringer J. (1960) Helium, neon, and argon isotopes in some iron meteorites. *Geochim. et Cosmochim. Acta.* **19,** 94–99.

Schwarzenbach G. (1956) *Complexometric Titration* (2nd Ed.). F. Enke, Stuttgart.

Shedlovsky J. P. (1960a) Cosmic ray produced Mn^{53} in iron meteorites *Geochim. et Cosmochim. Acta.* **21,** 156–158.

Shedlovsky J. P. (1960b) Thesis, Princeton University.

Sheline R. and Hooper J. E. (1957) Probable existence of Mn^{53} in iron meteorites. *Nature, Lond.* **179,** 85.

Simons L. H., Monaghan P. H. and Taggart M. S., Jr. (1953) Aluminum and iron in Atlantic and Gulf of Mexico surface water—determination and occurrence. *Analyt. Chem.* **25,** 989.

Sprenkel E. L. (1959) *Cosmic-ray Produced Chlorine-36 Activities in Iron Meteorites.* Unpublished Thesis.

Stoenner R. W. and Zähringer J. (1958) Potassium-argon age of iron meteorites. *Geochim. et Cosmochim. Acta* **15,** 40.

Sugihara T. T., Wolfgang R. L. and Libby W. F. (1953) Large thin-wall Geiger Counter *Rev. Sci. Instrum.* **24,** 511.

Voshage H. and Hintenberger H. (1959) Potassium as a reaction product of cosmic radiation in iron meteorites. *Z. Naturf.* **14a,** 828.

Wänke H. (1958) Scandium-45 as a reaction product of cosmic radiation in iron meteorites. *Z Naturf.* **13a,** 645.

Geochimica et Cosmochimica Acta, 1961, Vol. 22, pp. 155 to 163. Pergamon Press Ltd. Printed in Northern Ireland

Studies of tektite composition—I

Inverse relationship between SiO_2 and the other major constituents

S. R. Taylor,* Maureen Sachs** and R. D. Cherry†

(*Received* 19 *August* 1960)

Abstract The relation of SiO_2 to the other major constituents in tektites has been studied. For the australites, SiO_2 is shown to vary inversely with Al_2O_3, FeO, MgO, CaO and K_2O, but not Na_2O. These relationships are shown graphically and are statistically significant. The lack of a significant relation between SiO_2 and Na_2O is attributed to the poor quality of the sodium determinations.

The averages of the australites, philippinites, billitonites, indochinites, moldavites and Ivory Coast tektites show inverse relationships between SiO_2 and Al_2O_3, MgO, FeO and Na_2O; similar relationships exist between SiO_2 and Al_2O_3, MgO, FeO, CaO and Na_2O for sixty-seven analyses of individual tektites.

It is concluded that a significant inverse relationship exists between SiO_2 and the other major constituents in tektites, and that Al_2O_3, FeO, MgO, CaO, Na_2O and K_2O display positive correlations among themselves.

1. Introduction

The observed variation in composition between individual tektites is small‡ but is greater than the limits of precision of the determinations. Taylor (1960) showed that the alkali elements varied significantly in concentration in individual tektites and there seems to be little doubt that there are real differences in composition. In the study of the abundance and distribution of the alkali elements Li, Na, K, Rb and Cs in australites, Taylor (1960) showed that a close coherence exists between these five elements. Such close sympathetic variation among the alkali elements is not in accord with their usual geochemical behaviour. It is the sort of pattern which might result from physical mixing of two phases, one containing the alkali elements and the other sensibly lacking in them.

Such a mixing hypothesis was proposed by Cherry and Taylor (1959), the two components being chondritic silicate (from a comet head) and arkose. If this mixing occurred, an inverse relationship should exist between the constituents provided by the comet (notably magnesium) and those from the arkose (for example, the alkali elements). Determinations of magnesium in the samples used by Taylor (1960) showed, contrary to expectation, that a strong *positive* correlation exists between Mg and the alkali elements. On the basis of a mixing hypothesis, this indicates that Mg and the alkali elements are provided by the same component of the mix. The correlation coefficient between Mg and K for our determinations is $+0{\cdot}766$ which is significant at the 0·1 per cent level. Such a high degree of coherence is not apparent from the published analyses; this is presumably due to lack of precision in this data. Our data were obtained by emission spectrochemical methods of analysis, using the inter-laboratory standards G–1 and W–1 (Fairbairn *et al.*,

* Dept. of Geophysics, Australian National University, Canberra, Australia.
** Dept. of Geochemistry, University of Capetown.
† Dept of Physics, University of Capetown.

‡ For example, the published analyses of australites show the following ranges: 68·91–79·51% SiO_2; 9·97–15·42% Al_2O_3; 1·35–2·49% MgO; 1·48–3·88% CaO; 0·91–1·54% Na_2O; 1·25–2·56% K_2O(Barnes, 1940).

1951; Fairbairn, 1953) for calibration. Full details will be published subsequently, when comparison will be made with chemical determinations of magnesium by Dr. H. B. Wiik on the same samples.

The positive correlations observed between the alkali elements and magnesium are not readily explainable in conventional geological terms, and led us to examine the published analyses of tektites to see which constituents showed inverse relationships with the above elements. It is the purpose of this paper to draw attention to the inverse relationship which was found to exist between SiO_2 and the other major constituents in tektites.*

2. Evidence from Lechatelierite Particles

Although tektites are glassy objects, they are nevertheless inhomogeneous, since they contain variously shaped lechatelierite particles. These are held to represent fused grains of quartz (Barnes, 1940, p. 506) which is, of course, widespread enough on the earth to make the presence of these particles a limiting factor in theories of the extraterrestrial origin of tektites. Although grains of quartz are extremely common on the earth, they are the end result of a set of complicated processes, restricted to planets similar to the earth. Illustrations of lechatelierite particles are given in Figs. 22 (p. 85) and 23 (p. 86), and Plates 7 (p. 281) and 17 (p. 301) of Baker (1959). Barnes (1958, Plate 1, p. 270) shows stereoscopic pairs of a moldavite, a bediasite, and some glass produced by the explosion of an atomic bomb at Alamogordo, New Mexico, all of which show lechatelierite particles.

Barnes (1958) has emphasized the implications for theories of tektite origin, of the presence of lechatelierite particles which indicate that a temperature of at least 1713°C was reached at the time of formation. He shows that such particles cannot represent originally immiscible liquid drops since they disappear in a few hours at a temperature of about 1600°C, and thus concludes that the initial melting of tektites took place quickly. This conclusion is reinforced by the presence of the alkali elements which would surely distil out of molten silicate if such temperatures were maintained. In relatively cool d.c. arcs, operated at temperatures of 3000–4000°C, the alkali elements are selectively lost from silicate powders in times of the order of a few minutes (Ahrens and Taylor, 1960, pp. 185–188).

3. Relation between SiO_2 and the Other Major Constituents in Australites

The presence of the lechatelierite particles suggested to the authors that an investigation of the relation between SiO_2 and the other constituents in tektites might prove of interest. The analytical data for the australite group of tektites were selected for study for several reasons.

(1) They show a wider spread in composition, and are better preserved than any other single group.

(2) Although only eleven analyses are available, the other two groups for which more data are available (indochinites, with twenty-four analyses and

* This relationship has been noted by Baker and Forster (1943, p. 395) and may be deduced from graphs of SiO_2 versus the other major constituents in Barnes (1940) and Cassidy (1958).

moldavites, with thirteen analyses) are much more restricted in composition. Fourteen australites, for which TAYLOR (1960) has published determinations of the alkali elements, are being analysed for major and trace elements, and this body of data will provide a check on the present conclusions.

(3) The australites are distributed over a wide area (2×10^6 miles^2, BAKER,

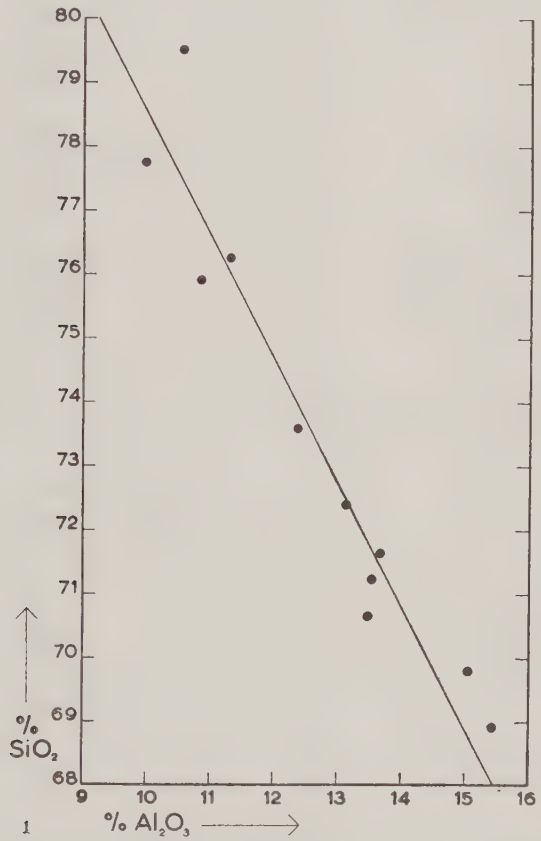

Fig. 1. Inverse relation between SiO_2 and Al_2O_3 for australites. The correlation coefficient is −0·968. For Figs. 1 and 2, the regression lines have been calculated, and the line shown is the mean of the two calculated lines. The eleven analyses plotted in Figs. 1 and 2 are from BARNES (1940) and BAKER (1956).

1959) and show a regional variation in composition from east to west. The other groups are much more restricted geographicallly.

It was thus felt that facts concerning the australites would be of use in studying the more obscure occurrences.

When SiO_2 was plotted against the other oxides, an inverse correlation was found. Fig. 1 is a plot of weight per cent SiO_2 vs. Al_2O_3 for australites; data are from BARNES (1940) and BAKER (1956). It is apparent that there is a regular inverse relation. The correlation coefficients are given in Table 1, and show that the inverse relation for SiO_2–Al_2O_3 in australites is above the 0·01 per cent significance level. The SiO_2–MgO relation is shown in Fig. 2 and here again, lies well

Table 1. Values of correlation coefficients (r) and levels of significance, for various pairs of elements in australites

A	r	Percentage level of significance* (%)
SiO_2–Al_2O_3	−0·969	< 0·01
SiO_2–MgO	−0·944	< 0·01
SiO_2–CaO	−0·839	0·12
SiO_2–FeO	−0·718	1·3
SiO_2–K_2O	−0·663	2·6
SiO_2–Na_2O	−0·420	> 10
Al_2O_3–MgO	+0·927	<0·01
Al_2O_3–CaO	+0·732	1·0
Al_2O_3–FeO	+0·561	7·4
Al_2O_3–K_2O	+0·619	4·2
Al_2O_3–Na_2O	+0·345	> 10
CaO–MgO	+0·693	1·8
CaO–FeO	+0·626	4·0
CaO–K_2O	+0·508	12·0
CaO–Na_2O	+0·304	> 10
FeO–K_2O	+0·415	> 10
FeO–Na_2O	+0·215	> 10
FeO–MgO	+0·615	2·6
MgO–K_2O	+0·677	2·2
MgO–Na_2O	+0·448	> 10
K_2O–Na_2O	+0·426	> 10
B		
MgO–K_2O	+0·766	0·14
MgO–Na_2O	+0·809	0·05
K_2O–Na_2O	+0·962	< 0·01

* A significance level of 1·0 per cent indicates that there is one possibility in 100 of the correlation arising by chance; a level of 0·1 per cent, one in 1000; a level of 0·01 per cent, one in 10,000, etc.
A: Published data for eleven australites from Barnes (1940) and Baker (1956).
B: Data for fourteen australites from Taylor (1960) and unpublished determinations.

above the 0·01 per cent significance level. The SiO_2–CaO relation, the SiO_2–FeO relation (total iron expressed as FeO), and the SiO_2–K_2O relationship are all statistically significant. In contrast to the above, the correlation for the pair SiO_2–Na_2O is not significant (>10 per cent level). The correlation coefficients for the other pairs of elements are also given in Table 1. It can be seen that the correlations are in general significantly positive, with the exception of the pair FeO–K_2O, and of the five pairs that include Na_2O.

To summarize, silica displays negative correlations with the other major constituents, which show positive correlations among themselves. The lack of

significance in those pairs which include Na_2O probably results from the poor quality of the Na_2O determinations (except for two analyses quoted by Baker (1956) the analyses were performed before 1913). Supporting evidence for this suggestion was provided by new determinations of Na and K in fourteen australites

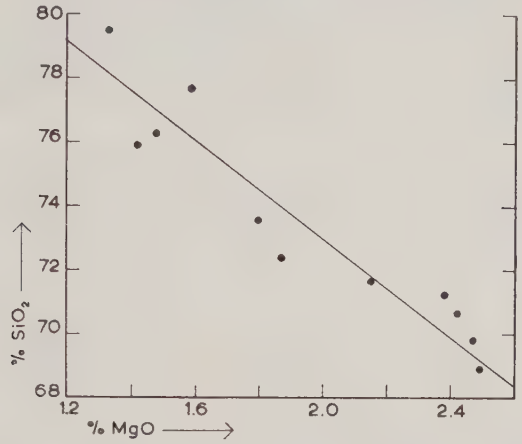

Fig. 2. Inverse relation between SiO_2 and MgO for australites. The correlation coefficient is −0·944.

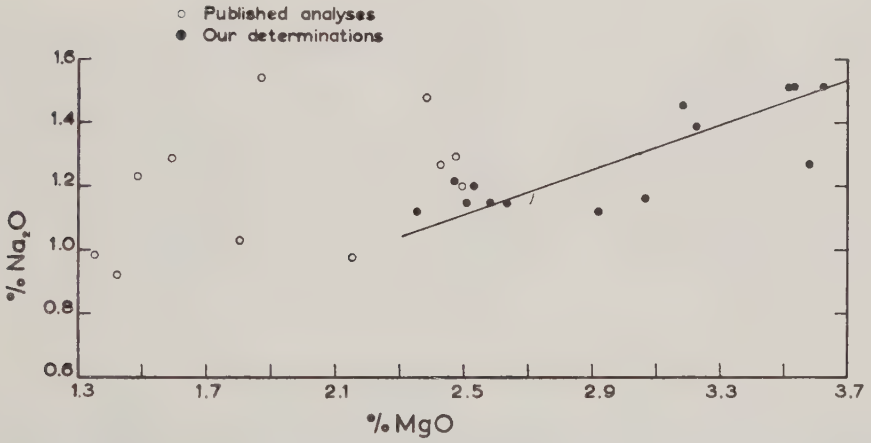

Fig. 3. The relation between Na_2O and MgO for australites. The open circles (○) represent data from Barnes (1940) and Baker (1956). The correlation coefficient for these determinations is +0·448, and no statistically significant relation exists. The filled circles (●) represent analyses by Taylor (1960) and unpublished determinations. For these the correlation coefficient is +0·809 and a positive correlation exists; the average of the regression lines for this data is shown. All the samples with MgO greater than 3·10 per cent come from Western Australia; those with less than 2·2 per cent are from Victoria or Tasmania.

(Taylor, 1960, Fig. 3). These show a very close coherence ($r = +0{\cdot}962$) and there is also a significant correlation with Mg. All the correlations lie above the 1 per cent significance level (see Table 1B). Fig. 3 shows a comparison of the relationship between Na_2O and MgO in the published analyses of australites, with those results obtained on the fourteen australites by the authors. The regression

lines for MgO on Na_2O and vice versa have been calculated and the average of these is shown on Fig. 3. It can be seen that there is a close coherence ($r = +0{\cdot}809$), in contrast to the wide scatter of the published analyses (from Barnes, 1940; Baker, 1956) which do not show such a coherence and for which the correlation is not significant ($r = +0{\cdot}448$). The difference is attributed to analytical error in the published data. Ahrens (1957) showed that the quality of determinations of major elements in silicates deteriorates with decreasing concentration. For analyses of silicate material by different analysts, using the methods by which the

Table 2. Mean compositions of six groups of tektites calculated from the data of Barnes (1940)

	n	SiO_2	Al_2O_3	MgO	K_2O	CaO	FeO*	Na_2O
Moldavites	10	79·60	11·02	1·30	2·90	1·92	2·45	0·51
Australites	9	73·33	12·75	1·98	2·05	3·01	4·70	1·25
Indochinites	24	73·14	12·48	2·00	2·40	2·51	5·02	1·45
Philippinites	4	71·21	12·57	2·90	1·93	3·19	5·18	1·52
Billitonites	7	70·50	12·53	3·07	2·28	3·14	5·84	1·75
Ivory Coast tektites	3	71·05	14·60	3·29	1·53	1·67	5·62	1·71

* Total iron expressed as FeO.
n = number of analyses available for calculation of mean.

standard granite and diabase were analysed (Fairbairn, 1953), it may be predicted that the relative deviation at the 2 per cent concentration level will be at least 10 per cent. This increases to about 15 per cent at the 1 per cent concentration level. These figures are derived from Table 1 and Fig. 1 of Ahrens (1957) and should be regarded as minima. For example, the relative deviations for determinations at the same levels in chondrites are 25 per cent and 40 per cent, respectively. *We may conclude that an inverse relationship exists between SiO_2 and the other major constituents in australites. This relationship adds another limiting factor to theories of tektite origin.*

4. Major Element Relations for other Groups of Tektites

The above discussion has centred around the australite group of tektites, for the reasons already given. It is logical to enquire whether the foregoing considerations apply to the other groups of tektites as well. We have performed similar calculations using the *mean* compositions of tektites in each of six groups: australites, indochinites, moldavites, philippinites, billitonites and Ivory Coast tektites. These averages have been obtained from the data of Barnes; the six groups chosen are all those for which Barnes gives more than two analyses. The means are listed in Table 2. The inverse correlation between SiO_2 and MgO contents of the different tektite groups is immediately apparent, and similar correlations exist (and are significant at the 10 per cent level or better) between SiO_2 and all the other major constituents except CaO and K_2O. Further, a positive correlation is found to exist between all pairs of the group of constituents MgO, Al_2O_3, FeO and Na_2O, and surprisingly, also between SiO_2 and K_2O. The correlation coefficients

and levels of significance are given in Table 3. It is seen that the levels of significance are not as high as in the case of the individual group (the australites) considered above; this we feel is only to be expected on account of the paucity of the data for some of the groups (e.g. the Ivory Coast tektites for which means are based on only three analyses). The 10 per cent significance level can, in the circumstances, be regarded as a satisfactory test.

Since the *averages* of the various groups show the same type of negative correlation (except as discussed below) between SiO_2 and the other major constituents

Table 3. Values of correlation coefficients (r) and levels of significance for various pairs of elements in tektites, using the group means of Table 2

	r	Percentage level of significance (%)
SiO_2–Al_2O_3	−0·733	9·5
SiO_2–MgO	−0·898	1·5
SiO_2–K_2O	+0·792	6·2
SiO_2–CaO	−0·448	not significant
SiO_2–FeO	−0·989	< 0·1
SiO_2–Na_2O	−0·986	< 0·1
Al_2O_3–MgO	+0·771	7·4
Al_2O_3–K_2O	−0·936	0·6
Al_2O_3–FeO	+0·747	8·8
Al_2O_3–Na_2O	+0·762	8·0
Al_2O_3–CaO	−0·203	not significant
K_2O–CaO	−0·033	not significant
K_2O–FeO	−0·751	8·6
K_2O–Na_2O	−0·760	8·1
K_2O–MgO	−0·807	5·3
MgO–CaO	+0·173	not significant
MgO–FeO	+0·878	2·2
MgO–Na_2O	+0·899	1·5
CaO–FeO	+0·380	not significant
CaO–Na_2O	+0·340	not significant
FeO–Na_2O	+0·999	< 0·1

as do the individual values of the australites, it is most likely that an explanation which holds for the australites is also valid for the other groups. The chances against the *averages* displaying this correlation are very high unless identical causes operated. The situation with respect to all tektites is thus the same as for the individual group (australites) with the notable exceptions of (a) the positive SiO_2–K_2O correlation between the groups and (b) the lack of significance in the group SiO_2–CaO correlation. It seems likely that (a) is connected with the varying loss of K_2O which might be distilled off selectively in different mixing processes. This positive correlation in the group means arises principally because the moldavites contain similar amounts of K_2O to the other groups, although higher in SiO_2 content. This is perhaps the most significant compositional difference between the various groups. The lack of significance in the group SiO_2–CaO

relation is probably due to a similar cause, although the difference in composition is less distinct and may be due to imprecise data.

Finally, we have considered all the available analyses of the individual tektites, including sixty-one from Barnes (1940, Table 5, but not the analyses of Darwin glass and Libyan Desert glass), two from Baker (1956, p. 114, nos. 1 and 2) and four from Spencer (1939, p. 426, nos. 14, 29, 32 and 33) which are not in Barnes' list. The doubtful tektite from Peru (Spencer, 1939, no. 7) has been excluded. Fig. 4 shows the inverse correlation between SiO_2 and Al_2O_3 for these sixty-seven

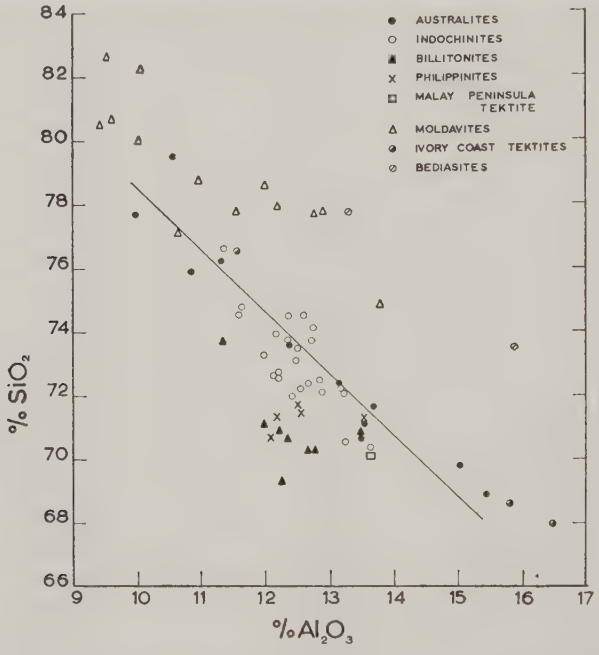

Fig. 4. The inverse relation between SiO_2 and Al_2O_3 for sixty-seven analyses of tektites. The sources of data are given in the text. The line shown is the average of the regression lines for australite data.

samples. It should be compared with Fig. 1 where the australite data is presented. Similar graphs are obtained for SiO_2 vs. the other major constituents except that in the case of K_2O, and to some extent for CaO as well, the data for the moldavites is displaced from the average line. Such graphs of SiO_2 vs. the other major constituents have been presented by Barnes (1940, Figs. 93 and 94) and Cassidy (1958, Figs. 1 to 6) and are not repeated here.

In Fig. 4, a regional grouping can be observed, with the data for the moldavites, philippinites, indochinites and billitonites tending to cluster in rather distinct areas, whereas the australites cover most of the observed range in composition. The indochinites, philippinites, billitonites and the Malay Peninsula tektites together form a single group on Fig. 4, and the possibility of a common origin for these groups of tektites should be investigated.

In Table 4, the correlation coefficients and percentage levels of significance for the individual analyses are given. A very high level of significance ($<0{\cdot}01$ per

cent) is observed for the inverse relationships between SiO_2 and Al_2O_3, MgO, FeO, CaO and Na_2O. The SiO_2–K_2O relation is inverse and significant at the 0·85 per cent level, if the moldavite data are excluded. When all analyses are considered, a positive correlation, significant at the 6·0 per cent level, is found

Table 4. Correlation coefficients (r) and percentage levels of significance for sixty-seven analyses of tektites (The source of the data is given in the text.)

	r	Percentage level of significance (%)
SiO_2–Al_2O_3	−0·742	< 0·01
SiO_2–MgO	−0·678	< 0·01
SiO_2–FeO	−0·952	< 0·01
SiO_2–CaO	−0·471	< 0·01
SiO_2–Na_2O	−0·694	< 0·01
SiO_2–K_2O*	+0·245	6·0
SiO_2–K_2O†	−0·365	0·85

* All determinations. A positive correlation exists at a rather low level of significance.

† Fifty-four determinations, excluding those for the moldavites.

between SiO_2 and K_2O. This minor anomaly, due to the significant difference, already referred to, between the moldavites and the other groups, explains the positive correlation observed between SiO_2 and K_2O in the group means.

Acknowledgement—The authors are grateful to Professor L. H. Ahrens and Dr. N. E. Taylor for helpful discussions.

References

Ahrens L. H. (1957) A survey of the quality of some of the principal abundance data of geochemistry. *Physics and Chemistry of the Earth* Vol. II, pp. 30–45. Pergamon Press, London.

Ahrens L. H. and Taylor S. R. (1960) *Spectrochemical Analysis* (2nd Ed.) Addison-Wesley, Reading, Mass.

Baker G. (1956) Nirranda strewn field australites, south-east of Warrnambool, Western Victoria. *Mem. Nat. Mus. Victoria.* **20,** 59–172.

Baker G. (1959) Tektites. *Mem. Nat. Mus. Victoria.* **23,** 1–313.

Baker G. and Forster H. C. (1943). The specific gravity relationships of australites. *Amer. J. Sci.* **241,** 377–406.

Barnes V. E. (1940) *North American Tektites.* University of Texas Publication No. 3945, pp. 477–656.

Barnes V. E. (1958) Properties of tektites pertinent to their origin. *Geochim. et Cosmochim. Acta* **14,** 267–278.

Cassidy W. A. (1958) Achondrite investigations and their bearing on the origin of tektites. *Geochim. et Cosmochim. Acta* **14,** 304–315.

Cherry R. D. and Taylor S. R. (1959) Origin of Al^{26} and Be^{10} in tektites. *Geochim. et Cosmochim. Acta* **17,** 176–185.

Fairbairn H. W. (1953) Precision and accuracy of chemical analysis of silicate rocks. *Geochim. et Cosmochim. Acta* **4,** 143–156.

Fairbairn H. W. *et al.* (1951) A cooperative investigation of precision, and accuracy in chemical, spectrochemical and modal analyses of silicate rocks. *Bull. U.S. Geol. Surv.* 980.

Spencer L. J. (1939) Tektites and silica-glass. *Miner. Mag.* **25,** 425–440.

Taylor S. R. (1960) Abundance and distribution of alkali elements in australites. *Geochim. et Cosmochim. Acta* **20,** 85–100.

Geochimica et Cosmochimica Acta, 1961, Vol. 22, pp. 164 to 168. Pergamon Press Ltd. Printed in Northern Ireland

Studies of tektite composition—II

Derivation from a quartz–shale mixture

R. D. Cherry and S. R. Taylor*
Department of Physics and Department of Geochemistry, University of Cape Town.

(*Received* 19 *August* 1960)

Abstract—The evidence of an inverse relation between SiO_2 and the other major constituents discussed in Part I of this series, together with the presence of particles of fused silica (lechatelierite) in tektites is explained on the basis of a physical mixing process. A mixture of 25 per cent quartz and 75 per cent of the non-volatile (at 1700°C) constituents of shale is shown to produce a close match to the average composition of tektites.

Introduction

Many workers have compared the chemical composition of tektites with that of the common rocks of the earth's crust. The nearest compositional equivalent among terrestrial materials is arkose, which is presumably the "more acid" sedimentary rock of some investigators. This sedimentary rock contains amounts of SiO_2 and Al_2O_3 similar to those found in tektites, together with more K_2O than Na_2O. The MgO content of arkoses is, however, much too low (average: 0·23 per cent, Pettijohn, 1957, p. 324) to match that of tektites which average 2·12 per cent. The MgO content of tektites is also much higher than in igneous rocks which contain similar amounts of silica (see Cherry and Taylor, 1959, Figs. 1 and 2 and pp. 179–183), although Mason (1959) was able to match individual analyses of tektites with igneous rocks of rather unusual composition. In fact, the attainment of an exact match between tektite composition and that of common terrestrial rocks has proved elusive, although several workers (Urey, 1957, 1958; Barnes, 1940, 1958; Taylor and Ahrens, 1959; Spencer, 1933; Friedman, 1958) have emphasized that the chemical composition of these black glassy bodies is strong evidence for either a terrestrial origin for tektites, or their derivation from the surface of a planet similar to the earth.

In order to account for the unusual composition (in particular the high MgO content) and the reported presence of unstable nuclides, Cherry and Taylor (1959) were led to propose that tektites were the result of mixing of two separate materials. Ehmann and Kohman (1958) had reported the presence of the radioactive nuclides Al^{26} and Be^{10} in australites, in quantities that precluded a terrestrial source. Cherry and Taylor (1959) suggested that these unstable nuclides might have been derived from a comet, which collided with the earth, melting surface material, as postulated by Urey (1957). Based on the assumption that the non-volatile constituents of the comet were similar in composition to the average silicate phase of chondrites, Cherry and Taylor showed that a mixing of one part of this with thirteen parts of arkose, assumed to be the surface cover of a desert terrain, gave a major element composition closely matching that of tektites.

* Now at the Department of Geophysics, The Australian National University, Canberra.

Based on reasonable assumptions of the rate of production of the radioactive nuclides in material of chondritic silicate composition exposed to cosmic radiation, it was possible, on mixing with the terrestrial material, to produce a concentration of Be^{10} close to that found by EHMANN and KOHMAN. Our figure for Al^{26} was lower by a factor of about 10 as compared with the experimental figure. More recent work by ANDERS (1960), using γ-γ coincidence spectrometry, has shown that the "most probable value for the Al^{26} content of australites would appear to be zero". If this is so, we no longer need to expose some or all of the australite material to cosmic radiation outside the earth's atmosphere, and the basic evidence for including chondritic silicate in the tektite "mix" falls away. Furthermore, in a study of the relations between the major elements of tektites (part I of this series, TAYLOR, SACHS and CHERRY, 1961), the authors have shown that their earlier mixing theory is untenable because of the lack of a required negative correlation between the MgO content and, for example, the K_2O content. The same study has shown that a strong inverse relationship exists between SiO_2 content and the amounts of the other major constituents; it is the purpose of the present paper to demonstrate that a mixture of quartz and the non-volatile constituents of shale will produce the observed relations and provide a very close match to the average composition of tektites.

2. Origin of Tektite Composition from a Mixture

It is at this stage convenient to summarize the more notable features of the chemical composition of tektites. Any theory of tektite origin must account for: (a) a high content of *both* silica and alumina; (b) a relatively high MgO content; (c) a K_2O:Na_2O ratio which is greater than unity (except for the Ivory Coast tektites) and which may be as high as 5·7 (for the moldavites); and (d) the strong negative correlation between SiO_2 content and the amounts of all the other major constituents.

The last-named feature, supported by consideration (a), suggested to us that tektites could have been derived from a mixture of quartz and some parent material. Such a mixture would not only account for the observed inverse correlation between SiO_2 and the other materials, but would also account for the presence of lechatelierite particles in tektites. The regression lines for SiO_2 on Al_2O_3 and vice versa have been drawn for the australite data. These lines pass through 96·9 and 98·4 per cent SiO_2, respectively (see Fig. 1) a fact which supports the idea that one component in the mixing process consists essentially of SiO_2 (i.e. quartz).

The nature of the other component does not pose a major problem. Its composition must presumably be fixed (since the significant negative correlation can scarcely arise if SiO_2 is mixed with several different materials) and a study of the compositions of geologically common materials indicated that the non-volatile (at 1700°C)* constituents of shale best fitted the requirements. The data given by PETTIJOHN (1957) were used for the composition of the shale. It was assumed that the constituents H_2O, CO_2, SO_3 and organic matter (totalling 9·19 per cent of the

* The presence of lechatelierite particles indicates that a temperature of about 1700°C was reached momentarily during tektite formation (BARNES, 1958; TAYLOR, SACHS and CHERRY, 1961)

whole) would be evaporated at temperatures of the order of 1700°C; the remaining constituents were then multiplied up to give a total of 100 per cent, and this material (column (1), Table 1) was then mixed in with SiO_2 (quartz) in various ratios. A mixture of 75 per cent shale and 25 per cent quartz resulted in the very

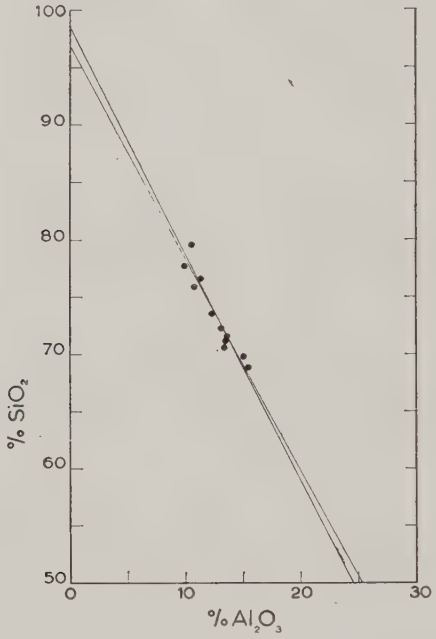

Fig. 1. Inverse relationship between SiO_2 and Al_2O_3 for the australites.

Table 1. Comparison of composition of tektites with that of a mixture of SiO_2 with the non-volatile constituents of shales

	(1)	(2)	(3)
SiO_2	64·32	73·24	73·73
TiO_2	0·72	0·54	0·86
Al_2O_3	17·05	12·79	12·47
FeO	6·72	5·04	4·92
MgO	2·70	2·03	2·12
CaO	3·44	2·58	2·50
Na_2O	1·44	1·08	1·32
K_2O	3·59	2·69	2·32
Total	99·98	99·99	100·24

(1) Composition of average shale from Pettijohn (1957), Table 61, p. 344 recalculated as follows: H_2O + and −, (5·00 per cent), CO_2 (2·63 per cent) SO_3 (0·64 per cent) and organic matter (0·80 per cent) omitted from total, being regarded as volatile constituents at 1700°C. Total iron is expressed as FeO. P_2O_5 (0·17 per cent) is omitted because of lack of data in tektites. The constituents listed in Column (1) total 90·31 per cent of the shale and have been recalculated to 100 per cent. Pettijohn's average is taken from Clarke (1924), p. 30, not p. 24 as stated.

(2) Composition of a mixture of three parts of Column (1) with one part of SiO_2.

(3) Average composition of sixty-one tektites from Barnes (1940). The analyses of Darwin glass and Libyan Desert glass quoted by Barnes are excluded from this average.

satisfactory overall composition given in column (2) of Table 1. Comparison with the tektite figures given in column (3) of the same table shows an almost exact match. If the above "mixture" theory is correct it must of course account for the minor constituents as well. We are determining the trace elements in some australites and preliminary results are not inconsistent with derivation from shale by dilution with quartz (Taylor and Sachs, 1960). Details will be published in a subsequent paper, together with major element determinations by Dr. H. B. Wiik. It is concluded that an origin of the average major element composition of tektites from a mixture of 75 per cent shale and 25 per cent quartz will explain: (a) the chemical composition of tektites, (b) the inverse correlation between SiO_2 content and the contents of the other major constituents of tektites; and (c) the presence of lechatelierite particles in tektites. Shale and quartz are of course geologically very common, and we feel that no serious objection could be raised on the grounds of lack of availability of these materials.

There remains the problem of providing a mechanism for the mixing process. Presumably temperatures of the order of 1700°C are required; anything lower would probably not yield the required melting of SiO_2, while temperatures which were too high would perhaps lead to a complete loss of sodium and potassium. The Urey comet hypothesis (viz., a collision between the head of a comet and the earth, resulting in a chemical explosion above the earth's surface) still seems the most satisfactory mechanism postulated to date, although we must now introduce the restriction that no appreciable* mixing between comet material and earth material is allowed. In this connection it should perhaps be mentioned that (a) the original Urey theory did *not* postulate mixing between the comet head and the material on the surface of the earth—Urey (1958, p. 1078) has in fact stated that he is "not particularly fond" of the idea of material being brought from the comet head—and (b) the mixing in of material from the comet head was originally introduced by us in an attempt to explain the reported presence of Al^{26} in tektites. As mentioned earlier, subsequent work of high reliability (Anders, 1960) disputes the earlier evidence in favour of the presence of Al^{26}, and it therefore appears unlikely that comet head material will be required to be incorporated in tektites even on these grounds.

In conclusion we mention a point in connexion with what is often considered to be the most serious objection to the Urey theory, viz., the fact that several distinct groups of tektites exist, ranging in age from Eocene to Recent (Baker, 1959) (a span of 60×10^6 years) whereas Urey (1957) predicts a "collision frequency" for comets with the earth of only one every 50 million years. Dr. J. D. Fernie of the Astronomy Department of this University has, however, drawn our attention to the fact that collision frequencies from one comet every 15 million years (Spencer-Jones, 1934; Duncan, 1955) to one every 200 million years (Struve *et al.*, 1959) have been quoted in text-books on astronomy. It is clear that the uncertainties involved in estimating the frequency of comet collisions are such that it is unreasonable to expect anything better than an order of magnitude result until such time as a more exact calculation can be performed.

* Certainly a 1/13 mixing ratio as suggested by us previously (Cherry and Taylor, 1959) is far too high.

Acknowledgements—The authors are grateful to Professor L. H. Ahrens and Dr. J. D. Fernie for helpful discussions.

References

Anders E. (1960) The record in the meteorites. II—On the presence of aluminium-26 in meteorites and tektites. *Geochim. et Cosmochim. Acta* **19,** 53–62

Baker G. (1959) Tektites. *Mem. Nat. Mus. Victoria* **23,** 1–313.

Barnes V. E. (1940) *North American Tektites*. University of Texas Publication No. 3945, pp. 477–656.

Barnes V. E. (1958) Properties of tektites pertinent to their origin. *Geochim. et Cosmochim. Acta* **14,** 267–278.

Cherry R. D. and Taylor S. R. (1959) Origin of Al^{16} and Be^{10} in tektites. *Geochim. et Cosmochim. Acta* **17,** 176–185.

Clarke F. W. (1924) The data of geochemistry. *Bull. U.S. Geol. Surv.* 770.

Duncan J. C. (1955) *Astronomy* (5th Ed.). Harper & Bros., New York.

Ehmann W. D. and Kohman T. P. (1958) Cosmic-ray-induced radioactivities in meteorites II. Al^{26}, Be^{10} and Co^{60} in aerolites, siderites and tektites. *Geochim. et Cosmochim. Acta* **14,** 364–379.

Friedman I. (1958) The water, deuterium, gas and uranium content of tektites. *Geochim. et Cosmochim. Acta* **14,** 316–322.

Mason B. H. (1959) Chemical composition of tektites. *Nature, Lond.* **183,** 254–255.

Pettijohn F. J. (1957) *Sedimentary Rocks* (2nd Ed.). Harper & Bros., New York.

Spencer L. J. (1933) Origin of tektites. *Nature, Lond.* **131,** 117.

Spencer-Jones H. (1934) *General Astronomy* (2nd Ed.). Edward Arnold, London.

Struve O., Lynds B. and Pillars H. (1959) *Elementary Astronomy*. Oxford University Press.

Taylor S. R. and Ahrens L. H. (1959) The significance of K/Rb ratios for theories of tektite origin. *Geochim. et Cosmochim. Acta* **15,** No. 4, 370–372.

Taylor S. R. and Sachs M. (1960) Trace elements in Australites. *Nature, Lond.* 188, 387–388.

Taylor S. R., Sachs M. and Cherry R. D. (1961) Studies of tektite composition. I—Inverse relation between SiO_2 and the other major constituents. *Geochim. et Cosmochim. Acta.* **22,** 155–163.

Urey H. C. (1957) Origin of tektites. *Nature, Lond.* **179,** 556–557.

Urey H. C. (1958) Origin of tektites. *Nature, Lond.* **182,** 1078.

Geochimica et Cosmochimica Acta, 1961, Vol. 22, pp. 169 to 175. Pergamon Press Ltd. Printed in Northern Ireland

Meteorite analysis: the search for diamond

D. V. N. Sarma* and T. Mayeda
University of Chicago and University of California, La Jolla, California
and
University of Chicago, Chicago, Ill.

(*Received in final form*, 13 August 1960)

Abstract—An investigation of various chemical methods involving non-oxidizing conditions for separation of diamonds in stone meteorites was continued. A new technique which employs KHF_2 fusion was successful in recovering graphite from several meteorites. No diamonds were found in seventeen meteorites using the methods described.

The presence of diamonds in meteorites was first reported by Jerofejeff and Latschinoff (1888) in the achondritic stone meteorite, Novo Urei. They reported 1 per cent by weight of small black diamonds. This was confirmed by Kunz (1888). von Sandberger (1889) reported that he observed a small black diamond in the crystalline bronzite chondrite from Carcote. Urey *et al.* (1957) found diamonds in Goalpara but were unable to confirm their existence in Carcote or in other chondrites. Foote (1891) reported diamonds in the Canyon Diablo octahedrite and subsequent study by several workers has confirmed these findings. Graphite with a cubic form, considered to be a pseudomorph of diamonds, has been reported by Haidinger and Partsch (1846) in Magura, by Fletcher (1887) in Youndegin and Crosby Creek, by Cohen and Weinschenk (1891) in Toluca, and by Huntington (1894) in Smithville. Urey *et al.* (1957) were unable to find diamonds in Richardton (chond.), Forest City (chond.), Holbrook (chond.), Warrenton (carb. chond.), Indarch (carb. chond.), Cold Bokkeveld (carb. chond.), and Cape Girardeaux (chond.). The lower limits for diamond could not be determined as the chemical treatment failed to decompose certain resistant minerals, presumably chromites.

In the current phase of this work, carbon in the pure form has been successfully isolated from a large number of chondritic meteorites, by a careful exploration of the methods of mineral attack under non-oxidizing conditions.

Experimental

The procedure followed initially was the same as the one adopted by Mrs. T. Mayeda. It was a modification of the method described in the earlier paper (1957). The meteorite sample was examined under the microscope to determine the physical appearance and then with a magnet to determine the proportion of magnetic material present. A piece, approximately 10 g, was broken with a chisel and powdered in a steel mortar, to so small a particle size that it could be easily attacked by acids. No sieve was used. The sample was transferred to a Pyrex beaker after weighing and treated with 100 ml of an acid mixture of HCl and

* At present at Atomic Energy Establishment, Chemistry Division, Bombay, India.

HNO_3 (2:1) and diluted by an equal volume of water, a water bath being used for heating. After 24 hr, the acid was changed and the attack continued for another day. The residue was centrifuged, washed with dilute HCl and transferred to a platinum dish. The silica was driven off with HF + H_2SO_4 and the residue, which was black, was centrifuged in a plastic tube. The washed sample was dried and weighed. This was always less than 100 mg. Any solids left in the collected washings were added to the residue.

After examination under a microscope, it was treated with 1 ml of $HClO_4$ and 1 ml of H_2SO_4 for 1 hr on a water bath. The residue was washed with water and dried with alcohol.

A gravity separation of graphite was next made using bromoform as separating liquid (bromoform s.g. 2·85, graphite s.g. 2·25 and diamond s.g. 2·8 to 3·5; density of chromite, 5·5). The supernatant liquid from the centrifuge tube was drawn off and the residue at the bottom washed with a little alcohol. The denser residue was studied by X-ray diffraction.

The procedure left some spinels unattacked and the presence of diamond, if any, was masked. Repeated treatment using $HClO_4$ dissolved very little more spinels. Sometimes no residue is left and it is difficult to be sure that oxidation did not occur.

Alternate procedures were tried simultaneously with the analysis, the last stage being different. A small quantity of one of the processed samples (Channing) was analysed spectrographically to learn the nature of the residues. The data are given in Table 1.

Table 1. Spectrographic analysis of Channing residue*

Element detected	Estimated weight (%)
Cr	Principal constituent
Mn, Si, Fe, Mg, Al, Ti	1–10 each
V	0·5
Ca, Zn, Na	0·1

* By A. J. Leoni, Enrico Fermi Institute for Nuclear Studies, University of Chicago.

With the analysis as a guide the following procedures were tried.

(1) A trial run on graphite and diamond using $HClO_4$ and H_2SO_4 after preliminary treatment with dilute HCl + HNO_3 and HF showed 60 and 7·5 per cent loss, respectively.

(2) Weighed graphite and diamond samples were treated with dilute HCl + HNO_3 and the residue fused with boric oxide in a platinum dish at 800°C under nitrogen (non-oxidizing), eluted with dil. HCl, washed with water and alcohol, dried and weighed. The recovery was found to be quantitative with diamond and 95 per cent with graphite. However, when the same procedure was tried on the meteorite residues, it failed to attack the spinels as was found by X-ray analysis.

(3) Potassium bisulphate fusion at 500°C was next tried. It was found that graphite was oxidized up to 58 per cent though this could be diminished somewhat in a nitrogen atmosphere.

(4) As KHF_2 is known to attack minerals very effectively, and has a low fusion temperature (250°C), it was selected for trial. Weighed samples of diamond and graphite were fused with KHF_2, for 1 hr at 250–300°C, and then evaporated with HCl repeatedly, to drive off HF. The residue was centrifuged, washed with water, then with alcohol and dried. The recovery of both diamond and graphite were found to be quantitative. The method showed promise and was tried on the sample from Richardton and was found to dissolve the entire black residue of spinels. The above procedures were tried on carborundum which is a possible impurity and found to be ineffective in decomposing it. Results are given in Table 2.

Table 2.

Method	Sample	Initial weight (g)	Final weight (g)	Recovery (%)
1	Diamond	0·0027	0·0025	92·5
	Graphite	0·0267	0·0118	40
2	Graphite	0·0060	0·0057	95
	Diamond	0·0027	0·0027	~100
3	Graphite	0·0341	0·0143	68
4	Graphite	0·0047	0·0047	~100
	Diamond	0·0027	0·0027	~100
2	Carborundum	was unattacked		
4	Carborundum	was unattacked		
$HF + HNO_3$	Carborundum	was unattacked		
2	Richardton residue	0·0095	0·0069	72·6 (spinels)
4	Richardton residue	0·0069	Nil.	complete solution

The final procedure adopted was as follows: The finely powdered mineral sample was weighed into a pyrex beaker and digested with (1:1) HCl for 6 hr, followed by concentrated HCl for another 6 hr. The residue was centrifuged, washed with dilute HCl and transferred to platinum. The silica was driven off with HF and the residue evaporated with HCl to drive off HF, centrifuged and washed. The residue left now was black (less than 100 mg). It was fused in platinum with KHF_2 at 250 to 300°C, for 1 hr and the fluoride driven off with HCl. The residue was centrifuged, the few black grains left were powdered in a small tool steel mortar and the fusion with KHF_2 repeated, with addition of HF towards end of fusion. After evaporating with HCl to drive off HF, the residue was centrifuged with a high-speed centrifuge, washed with distilled water, then with alcohol and dried. The very small sample, if any is left (usually less than 1 mg), was centrifuged with bromoform, the heavier and lighter fractions separated,

Table 3. Tests for diamonds

Ser. no.	Sample	Type	Weight (g)	Method	Remarks
1	Adrian	Vein, cry. sph. ch.	12·9564	(1)	No diamond present†
2	Arapahoe*	Blk. cho.	10·0632	(1)	No diamond present
				(2)	No diamond present
				(4)	No residue
3	Arriba	Polymict Brec. Int. cho.	9·3777	(1)	No diamond present
4	Barratta	Blk. hyp. cho.	6·7476	(1)	No diamond present
5	Beenham	Int. cho.	12·2725	(1)	No diamond present
6	Brewster	Int. cho.	11·1928	(1)	No residue
7	Channing*	Blk. cho.	9·6614	(1)	No diamond present
			3·6365	(2)	No diamond present
8	Coldwater	Oct.	10·2732	(1)	No residue
9	Coon Butte	Brec. gr. cho.	3·2452	(4)	No residue
10	De Nova	Wht. vein. cry. sph. cho.	8·9697	(4)	No residue
11	Diamonds from Goalpara	Urelitite	0·0026	(4)	Quantitative recovery
				(2)	75% recovery
12	Hat Creek	Vein. gr. cho.	8·0913	(4)	No residue
13	Hugoton	Polymict brec. Blk. Cho.	11·2314	(4)	No residue
14	Kelly*	Wht. Gr. brec. cho.	7·2348	(1)	Residue to small to
				(4)	analyse
15	Ness Co.*	Cry. bronz. cho.	8·4873	(1)	Residue to small to
				(4)	analyse
16	Peetz Co.	Blk. cho.	13·4001	(4)	Coincidences for
			10·1243		diamond in residue ~0·005 to 0·015 per cent
17	Residue from Richardton	Vein. sph.	0·0095	(2)	No diamond present
		Bronz. Cho.	0·0069	(4)	No residue
18	Taiban	Blk. cho.	7·9068	(4)	Only 1st diamond line, sample too small

* In X-ray diffraction patterns, the more intense of diamond lines appear weak and the less intense lines are not detected. However, the diamond coincidences could also be ascribed to a mixture of spinels in the absence of a complete diamond pattern.

† The remark "No diamond present" means that a residue remained giving a diffraction pattern mostly of spinels but no consistent pattern of even weak lines characteristic of diamond was observed.

individually washed with alcohol and dried. The fractions were then studied by X-ray diffraction.

It may be seen that there is no positive evidence for diamond to within 0·015 per cent of a 10 g sample. In the case of Peetz, the residue which still had a large spinel concentration after the first fusion with KHF_2 showed coincidences with all the diamond lines. However, their intensities showed a departure from the expected, perhaps due to interference by impurity lines. The approximate concentration may be estimated to be about 0·005 to 0·015 per cent of the total meteorite. In this connexion it may be noted that a sample from Taiban, which was carefully purified, showed a single line coincident with the most intense diamond line, but the amount of sample (0·1 mg or less) was inadequate to develop the other lines over the background. Taiban belongs to the same type as Peetz, i.e. black chondrite.

A typical analysis for Peetz is given in Table 4.

Conclusion

It is concluded that the evidence for diamond is uncertain within the limits of the experiment. Further work with larger samples is likely to show their presence at least in the black chondrites.

Notes

The programme involved the development of a chemical method to dissolve the chromites without burning up the carbon. Most procedures for chromite attack involve oxidizing agents. The isolation of extremely small amounts of carbon in its original and unaltered physical form has presented a formidable chemical problem. The further handling of the isolated sample without introduction of mechanical impurities while centrifuging from large amount of wash liquids to the final sealing into the X-ray capillary requires special techniques, and the transition from a macro- to a micro-scale towards the end needs great care. A few notes are given below to indicate some of the methods employed.

(1) The treatment with HF leaves a residue which requires repeated evaporation with HCl, not only to drive off all HF, but also to dissolve a few difficultly soluble materials like TiO_2.

(2) Centrifuging the solutions is a major problem in the analysis. Unless a sufficient centrifugal force is present, small quantities of material remain floating under the action of surface tension and are incapable of precipitation by other means. A minimum of 5000 g is required to break the force of surface tension. Use of alcohol is of no great help.

(3) The densities of graphite and amorphous carbon being low, the whorl action in centrifuging lifts them from the bottom. Also, very fine particles (100 Å or so) require adsorption to bring them down. The use of a solution of gelatin with addition of alcohol to precipitate it can bring these particles down on centrifuging. In the present investigation, advantage was taken of a little fluoride left in solution, that dissolved silica from the walls, which was precipitated by HCl. In the last stage a very high speed centrifuge was used.

Table 4. X-ray data*

Ser. no.	Spacing (Å)	Intensity	Cu–K_2, dispersion (3·154°/mm)	
			Diamond Spacings	Intensity†
1. Peetz with considerable spinel concentration Diamond estimate not more than 0·015%	2·91	m.		
	2.48	v.s.		
	2·063	m.s.	2·060	100
	1·687	w.		
	1·592	s.		
	1·465	s.v.s.		
	1·309	v.v.w.		
	1·268	w.	1·261	27
	1·197	v.v.w.		
	1·112	v.w.		
	1·0825	m.	1·0754	16
	1·041	w.		
	0·981	v.v.w.		
	0·964	m.		
	0·957	v.w.		
	0·9305	v.w.		
	0·8944	v.v.w.	0·8916	7
	0·876	m.		
	0·8527	m.s.		
	0·8174	v.w.	0·8182	15
	0·8078	m.		
	0·8057	v.w.		
2 Taiban	2·063		2·060	100

s, strong; m, medium; w, weak; v, very.
* Data from patterns taken by Miss Ann Plettinger.
† H. E. Swanson and R. K. Fuyat, *U.S. Bur. Stand. Circular* 539, Vol. II, p. 5.

(4) The use of plastic centrifuge tubes is to be avoided, as hard substances scratch the walls and get imbedded.

(5) The final sample centrifuge tube is transferred to a special capillary drawn from the end of a 1-cm Pyrex tube. The outer diameter of the capillary was 0·5 mm and with as thin walls as could be drawn.

(6) Two different methods of transference were used. In the wet method which permitted washing of the sample, the lower end of the capillary was fitted with a 1-mm filter of finely powdered Pyrex glass supported by a broken capillary fragment. The design was taken from a radiochemical technique for isolating small samples for X-ray analysis.

In the dry method the tube with the capillary was carefully cleaned from grease, etc., washed with absolute alcohol and dried at 80°C. The tip of the capillary was

sealed and the dry sample from a similarly cleaned centrifuge tube was transferred by gentle knocking on the walls, while still warm. The cleaning and drying permitted the sample to fall into the capillary without loss by sticking to the walls of the tube. This method is more convenient than the previous one as the preparation of a satisfactory filter of the capillary tip is difficult. A dense filter makes the filtration extremely slow even when centrifuged.

Acknowledgement—The authors are indebted to Dr. H. H. Nininger for his co-operation in securing the samples used in this work. We are grateful to Dr. Harold C. Urey in whose laboratory the entire work was performed. We also thank him for his suggestion for the research and his continued interest in our progress. We are indebted to Miss Ann Plettinger, Physics Department, University of Chicago, for the numerous X-ray diffraction determinations. The work was financed by the Atomic Energy Commission Contract No. AT(11–1)–101.

References

Cohen E. and Weinschenk E. (1891) Meteoreisenstudien. *Ann. K. K. Naturh. Hofmus., Wien,* **6,** 131–165.

Fletcher L. (1887) On a meteoric iron found in 1884 in the Sub-District of Youndegin, Western Australia, and containing cliftonite, a cubic form of graphitic carbon. *Miner. Mag.* **7,** 124.

Foote A. E. (1891) Meteoric iron of Cañon Diablo. *Amer. J. Sci.* **42,** 413–417.

Haidinger W. and Partsch C. (1846) Graphit, Pseudomorph Nach Schwefelkies. *Ann. Phys. Chim., Lpz.* **67,** 437–439.

Huntington O. W. (1894) The Smithville meteoric iron. *Proc. Amer. Acad. Arts Sci.* **29,** 251–260.

Jerofejeff M. and Latschinoff P. (1888) Der Meteorit von Nowo-Urei. *Verh. Russ. Kais. Miner. Gesells., St. Petersburg* **24,** 272–292.

Kunz G. F. (1888) Diamonds in meteorites. *Science* **11,** 118–119.

Urey H. C. (1956) Diamonds, meteorites, and the origin of the solar system. *Astrophys. J.* **124,** 623–637.

Urey H. C., Mele A. and Mayeda T. (1957) Diamonds in stone meteorites. *Geochim. et Cosmochim. Acta* **13,** 1–4.

von Sandberger F. (1889) Ein Neuer Meteorit aus Chile. *Neues Jb. Min. Geol.* **2,** 173–180.

Geochimica et Cosmochimica Acta, 1961, Vol. 22, pp. 176 to 199. Pergamon Press Ltd. Printed in Northern Ireland

Graphic and algebraic solutions of the discordant lead-uranium age problem†

L. R. Stieff and T. W. Stern
U.S. Geological Survey, Washington 25, D.C.

Received 21 *April* 1960

Abstract—Uranium-bearing minerals that give lead–uranium and lead–lead ages that are essentially in agreement, i.e. concordant, generally are considered to have had a relatively simple geologic history and to have been unaltered since their deposition. The concordant ages obtained on such materials are, therefore, assumed to approach closely the actual age of the minerals. Many uranium-bearing samples, particularly uranium ores, give the following discordant age sequences; $Pb^{206}/U^{238} < Pb^{207}/U^{235} \ll Pb^{207}/Pb^{206}$ or, less frequently, $Pb^{207}/Pb^{206} \ll Pb^{207}/U^{235} < Pb^{206}/U^{238}$. These discordant age sequences have been attributed most often to uncertainties in the common lead correction, selective loss of radioactive daughter products, loss or gain of lead or uranium, or contamination by an older generation of radiogenic lead.

The evaluation of discordant lead isotope age data may be separated into two operations. The first operation, with which this paper is concerned, is mechanical in nature and involves the calculation of the different possible concordant ages corresponding to the various processes assumed to have produced the discordant ages. The second operation is more difficult to define and requires, in part, some personal judgement. It includes a synthesis of the possible concordant age solutions with other independent geologic and isotopic evidence. The concordant age ultimately chosen as most acceptable should be consistent not only with the known events in the geologic history of the area, the age relations of the enclosing rocks, and the mineralogic and paragenetic evidence, but also with other independent age measurements and the isotopic data obtained on the lead in related or associated non-radioactive minerals.

The calculation of the possible concordant ages from discordant age data has been greatly simplified by Wetherill's graphical method of plotting the mole ratios of radiogenic Pb^{206}/U^{238} (N_{206}/N_{238}) vs. radiogenic Pb^{207}/U^{235} (N_{207}/N_{235}) after correcting for the contaminating common Pb^{206} and Pb^{207}. The linear relationships noted in this graphical procedure have been extended to plots of the mole ratios of total Pb^{206}/U^{238} ($^tN_{206}/N_{238}$) vs. total Pb^{207}/U^{235} ($^tN_{207}/N_{235}$). This modification permits the calculation of concordant ages for unaltered samples using only the Pb^{207}/Pb^{206} ratio of the contaminating common lead.

If isotopic data are available for two samples of the same age, x and y, from the same or related deposits or outcrops, graphs of the normalized difference ratios

$$\left[\frac{(N_{206}/N_{204})x - (N_{206}/N_{204})y}{(N_{238}/N_{204})x - (N_{238}/N_{204})y}\right] \text{ vs. } \left[\frac{(N_{207}/N_{204})x - (N_{207}/N_{204})y}{(N_{235}/N_{204})x - (N_{235}/N_{204})y}\right]$$

can give concordant ages corrected for unknown amounts of a common lead with an unknown Pb^{207}/Pb^{206} ratio. (If thorium is absent the difference ratios may be normalized with the more abundant index isotope, Pb^{208}.) Similar plots of the normalized, difference ratios for three genetically related samples ($x - y$) and($x - z$), will give concordant ages corrected, in addition, for either one unknown period of past alteration or initial contamination by an older generation of radiogenic lead of unknown Pb^{207}/Pb^{206} ratio.

Practical numerical solutions for many of the concordant age calculations are not currently available. However, the algebraic equivalents of these new graphical methods give equations which may be programmed for computing machines. For geologically probable parameters the equations of higher order have two positive real roots that rapidly converge on the exact concordant ages corrected for original radiogenic lead and for loss or gain of lead or uranium. Modifications of these general age equations expanded only to the second degree have been derived for use with desk calculators.

These graphical and algebraic methods clearly suggest both the type and minimum number of samples necessary for adequate mathematical analysis of discordant lead isotope age data. This mathematical treatment also makes it clear that discordant lead isotope data alone cannot provide the basis for the choice of one of the possible concordant age solutions. The new equations, in particular, provide an incentive to improve our physical constants, analytical techniques and sampling methods in order that we may derive all of the useful geologic information that is available in a comprehensive lead isotope age study.

† Publication authorized by the Director, U.S. Geological Survey.

Introduction

The calculated lead-isotope ages of many uranium-bearing minerals, particularly uranium ores, yield the following discordant age sequence: $Pb^{206}/U^{238} < Pb^{207}/U^{235} \ll Pb^{207}/Pb^{206}$. Much less frequently, the reverse age sequence, $Pb^{207}/Pb^{206} \ll Pb^{207}/U^{235} < Pb^{206}/U^{238}$, is observed. Agreement among these three lead isotope ages, i.e. concordant ages, are rarely obtained for uranium ores but are found more often for pegmatitic uraninite and zircon.

Unfortunately, the first discordant age sequence may be explained equally well by the continuous, selective loss of one or more radioactive daughter products, loss of radiogenic lead or additions of uranium at one time in the history of the minerals, or initial contamination by relatively small amounts of an older generation of radiogenic lead. The reverse age sequence can be interpreted as evidence for loss of uranium, addition of radiogenic lead, or initial contamination by relatively large amounts of an older radiogenic lead. It should be added that accidental concordance may occur either as a result of contamination by large amounts of an older generation of radiogenic lead or as a result of processes of leaching and alteration in which compensating amounts of lead and uranium have been added or removed.

General papers on the interpretation of lead isotope ages have been published by Kulp *et al.* (1954), Ahrens (1955a, b), Wetherill (1956), Stieff and Stern (1956), Kulp and Eckelmann (1957), and Aldrich and Wetherill (1958). Explanation of discordant isotopic age data using the radon-loss hypothesis has been published by Wickman (1942), Robinson (1955), Louw and Strelow (1955), Giletti and Kulp (1955), and Greenhalgh and Jeffery (1959). Interpretation of discordant age sequences using the lead-loss hypothesis has been published by Collins *et al.* (1954), Eckelmann and Kulp (1956), and Gerling (1958). Horne and Davidson (1955) have suggested a hypothesis based on multiple periods of uranium deposition to explain the age anomalies found for a single specimen of Witwatersrand uraninite concentrate. Attempts to interpret the discrepancies between the lead–uranium and lead–lead ages on the basis of contamination by an older generation of radiogenic lead have been made by Stieff *et al.* (1953), Tugarinov (1954), and more recently by Horne (1957a, b).

Present methods for making concordant numerical solutions of discordant lead isotope age data are both tedious and difficult. Existing graphical solutions also have their limitations. It is the purpose of this paper to review briefly the literature on the graphical procedures used in the analysis of discordant age data, and to present a new and more generalized graphical treatment of this problem. In addition, a new set of algebraic equations equivalent to these new graphical solutions which permit relatively simple numerical calculation of concordant ages is also included. A detail discussion of both the algebraic and graphic treatments is in preparation and will be published elsewhere.

Uranium-bearing minerals that yield directly concordant ages are usually assumed to have been unaltered by geologic processes and the concordant ages are considered to approximate closely the actual ages of the samples. The first operation in the evaluation of a discordant age sequence is, therefore, the adjustment, either numerically or graphically, of the data until the lead–uranium and

lead–lead ages are in agreement. This is done in the belief that one of the recalculated concordant ages will more nearly approach the true age of the mineral. Thus, the criterion of concordance underlies the mathematical analysis of the observed age discrepancy, and requires assumptions concerning the different processes which could have produced the age discordancies.

It is abundantly evident, however, that no amount of mathematical manipulation of the discordant age data will, in itself, provide the basis for the choice of the most probable age. The choice of one of the equally possible recalculated concordant ages can be made only on the basis of additional evidence. The second operation, therefore, consists of testing the validity of these recalculated concordant ages in terms of the geologic history of the area, the geologic age relation of the enclosing rock, the petrographic, paragenetic and mineralogic data on the uranium-bearing minerals being studied, the probable sources of the uranium and contaminating lead, the isotopic composition of lead in the associated non-radioactive minerals, and other independent age measurements which are considered to be reliable. In the event that available geologic evidence is equivocal, either the alternative concordant age solutions should be presented as equally possible or, following a clear statement of the investigator's own prejudice, a preference stated for one of the concordant ages.

Graphical Methods

Graphs of N_{207}/N_{204} *vs.* N_{206}/N_{204}

Perhaps the simplest graphical treatment of the regularity in lead isotope data was first suggested by Houtermans (1946, 1947). In an analysis of the natural variation in isotopic composition of common lead he plotted the atom or mole ratios of Pb^{207}/Pb^{204}, (N_{207}/N_{204}), against similar ratios of Pb^{206}/Pb^{204}, (N_{206}/N_{204}). See Fig. 1(a). In graphs of this type or in graphs of Pb^{207}/Pb^{208} vs. Pb^{206}/Pb^{208} (where thorium has not contributed radiogenic Pb^{208}) the mixture of a single common lead, A, having uniform N_{207}/N_{204} and N_{206}/N_{204} ratios, with varying amounts (points B, C and D) of a single radiogenic lead of uniform Pb^{207}/Pb^{206} ratio, R^*, will lie on a straight line. These straight lines were called "isochrones" by Houtermans and the slope of the isochrones passing through these points is the Pb^{207}/Pb^{206} ratio of the added radiogenic lead.

It is readily apparent from Fig. 1 that, if isotopic data are available for at least two radiogenically enriched samples, such as B and C, resulting from the mixture of just two components, R^c and R^*, the Pb^{207}/Pb^{206} ratio of the added radiogenic lead, R^*, may be obtained from the slope of the line passing through B and C. Knowledge of the isotopic composition of the contaminating common lead, A, is not necessary. If the two components consist of the radiogenic lead produced by uranium-bearing minerals and its contaminating common lead, it follows that the slope of the line passing through the plotted points of the two samples will give the Pb^{207}/Pb^{206} age of the samples. This age is independent of either recent loss or gain of lead or uranium because: (1) isotopic fractionation of Pb^{206} and Pb^{207} is not known to occur as a result of the chemical processes of alteration, and (2) the quantitative amounts of lead and uranium do not appear in these graphs.

It can also be seen from Fig. 1(a) that the addition of varying amounts of a third radiogenic component whose Pb^{207}/Pb^{206} ratio is R, will give points E, F and G, for which no simple linear relationship can be derived. The graphical presentation of the three-component mixtures (R^c, R^* and R) is typical of all discordant age sequences not produced by recent gain or loss of lead or uranium. The absence of any systematic relations between three or more samples, each of which contains a mixture of three different leads, indicates that additional data,

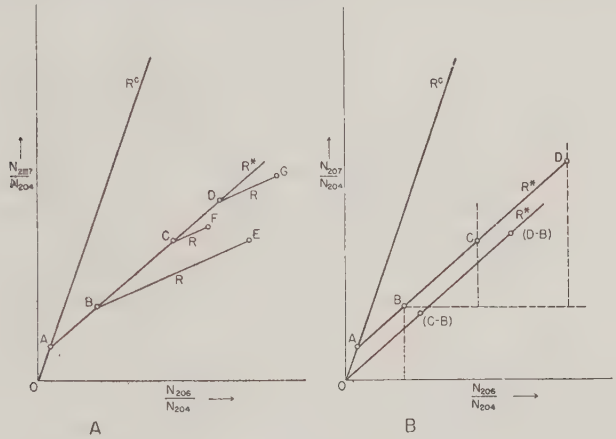

Fig. 1(a). Graph of N_{207}/N_{204} vs. N_{206}/N_{204} for two- and three-component lead mixtures.
Fig. 1(b). Graph of N_{207}/N_{204} vs. N_{206}/N_{204} for two-component lead mixtures and their difference plots.

specifically the quantitative amounts of lead and uranium in the sample, are required before a unique solution can be obtained.

In Fig. 1(b), the differences between the coordinates for samples (C minus B) and (D minus B) are plotted. These difference points for the two-component mixtures, R^c and R^*, must also lie on a straight line passing through the origin. The slope of this line, R^*, is equal to the slope of the line passing through the original points B, C and D. This obvious analytical relationship is mentioned here in order to simplify the presentation of some of the graphical procedures which follow.

Graphs of radiogenic N_{207}/N_{235} vs. radiogenic N_{206}/N_{238}

Ahrens (1955b) first noticed the linear relationships that are obtained in plots of the ratios of radiogenic N_{207}/N_{235} against radiogenic N_{206}/N_{238} among related samples giving discordant age sequences. Wetherill (1956) developed Ahrens' suggestion into a rigorous graphical analysis of discordant lead–uranium ages resulting from multiple episodes of lead–uranium fractionation and presented a detailed mathematical proof of the graphical procedures.

To Ahrens' plot of the mole ratios of N_{207}/N_{235} vs. N_{206}/N_{238} Wetherill added a curve which he called "Concordia" (see Fig. 2a). Within this graph the coordinates of all points may be given by a Pb^{207}/U^{235} and a Pb^{206}/U^{238} age equivalent

to the two ratios, N_{207}/N_{235} and N_{206}/N_{238}. The curve, Concordia, is the locus of all points having equal Pb^{207}/U^{235} and Pb^{206}/U^{238} ages. Thus, a plot of the N_{207}/N_{235} and N_{206}/N_{238} ratios of any sample falling on this curve are, by definition, concordant, i.e. the Pb^{206}/U^{238} age = Pb^{207}/U^{235} age = the Pb^{207}/Pb^{206} age.

Conversely, any point not lying on this curve must represent a discordant age sequence. It should be stressed that before it is possible to use a graph of this type it is first necessary to make a correction for the contaminating common lead as the values N_{207} and N_{206} represent only the radiogenic remainders. In those

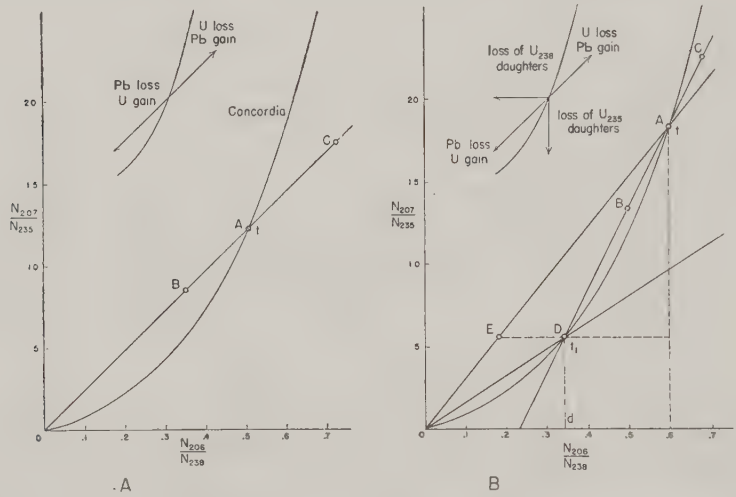

Fig. 2(a). Graph of N_{207}/N_{235} vs. N_{206}/N_{238} for uranium-bearing samples which have recently lost or gained lead or uranium.

Fig. 2(b). Graph of N_{207}/N_{235} vs. N_{206}/N_{238} for uranium-bearing samples which lost or gained lead or uranium at a time, t_1, in the past.

age calculations in which the common lead corrections are significant but have been incorrectly made, a discordant age sequence will result that is indistinguishable from those produced by the other causes already mentioned.

The mathematical proofs of the properties of these ratio plots (Wetherill, 1956) are not easy to follow, whereas the discussion of Russell and Ahrens (1957) is quite brief. Referring to Fig. 2(a), a relatively simple proof can be presented as follows. Assume that:

(a) Samples A, B and C were formed at the same time, t.

(b) Sample A is unaltered.

(c) Sample B has recently lost lead or gained uranium while sample C has recently lost uranium or gained radiogenic lead.

(d) Recent loss or gain of lead or uranium will not significantly alter the Pb^{207}/Pb^{206} ratios of samples B and C by isotopic fractionation of Pb^{206} or Pb^{207}.

(1) The curve Concordia is the locus of those points whose N_{207}/N_{235} and

N_{206}/N_{238} ratios are equal to the same age, t, and it is defined by the parametric equation:

$$N_{207}/N_{235} = \exp(\lambda^{235}t) - 1$$

$$N_{206}/N_{238} = \exp(\lambda^{238}t) - 1$$

for values of t between 0 and infinity.

(2) The plot of the unaltered sample, A, lies on the curve Concordia and its Pb^{206}/U^{238}, Pb^{207}/U^{235}, and Pb^{207}/Pb^{206} ages are equal.

(3) The points B and C do not lie on the concordant age curve because their Pb^{206}/U^{238} and Pb^{207}/U^{235} age are not equal.

(4) The slope of the line connecting point A with the origin times the atom ratio of the present-day relative abundance of U^{235}/U^{238}, 1:137·7, must give the Pb^{207}/Pb^{206} ratio of the radiogenic lead in sample A. ($N_{207}/N_{235} \times 1/137{\cdot}7 \times N_{238}/N_{206} = N_{207}/N_{206}$).

(5) The slope of the lines passing through the origin and the points B and C times 1/137·7 will give the N_{207}/N_{206} ratios of B and C.

(6) The radiogenic Pb^{207}/Pb^{206} ratios of A, B and C, are equal (assumptions (a) and (c)).

(7) Therefore, the points B and C must lie on a single line passing through the origin and intersecting the curve, Concordia, at point A.

(8) The concordant age for samples B or C corrected for recent loss or gain of lead or uranium will therefore be given by the N_{207}/N_{235} and N_{206}/N_{238} ratios at the intersection of the line passing through the origin and the points B or C and the curve Concordia.

The quantitative aspects of the loss or gain of lead and uranium may also be obtained directly from this graphical treatment.

(9) The length of the cord OA is directly proportional to the ratio of the total number of atoms of lead and uranium required to produce a concordant age, t.

(10) The segment OB lying on the cord OA and the segment OC lying on OA extended are also directly proportional to the ratios of the lead and uranium remaining after recent processes of alteration.

(11) Therefore, the ratio of the length of the line segment BA to OA times 100 will give the percentage of lead loss or uranium gained recently. The ratio of the length of the line OC to the line OA times 100 will give the percentage of uranium lost or lead gained recently.

This simple analysis demonstrates that plots of the ratios of radiogenic lead to uranium for a suite of cogenetic uranium-bearing minerals which have been recently altered will lie on a straight line passing through the origin, the intersection of this line with Concordia will equal the Pb^{207}/Pb^{206} age of the sample, and the extent of the recent alteration may be determined graphically by measuring the ratios of the length of the line between the origin and the intersection with Concordia and the line segments determined by plots of the discordant lead–uranium ratios. As has been mentioned (see Fig. 1), the same age can also be obtained by plots of N_{207}/N_{204} vs. N_{206}/N_{204} with the further advantage that corrections for the original contaminating common lead need not be made.

In graphs of N_{207}/N_{204} vs. N_{206}/N_{204} the slope of the line passing through coordinates of a set of cogenetic minerals will give the Pb^{207}/Pb^{206} age independent of any processes of recent alteration.

The case of loss or gain of lead or uranium at one specific time in the past history of the mineral is shown in Fig. 2(b). Using arguments similar to those given for the case of recent loss or gain of uranium and assuming that:

(a) Samples A, B and C were formed at the same time, t.

(b) Sample A has not been altered during its history.

(c) Sample B lost lead or gained uranium at the time, t_1, while sample C lost uranium or gained lead at the time, t_1, in the past.

(d) Chemical alteration at some time in the past would not significantly alter the Pb^{207}/Pb^{206} ratios of samples B and C by isotopic fractionation of Pb^{206} or Pb^{207}.

Then the following relations can be demonstrated:

(1) The Pb^{207}/Pb^{206} ratio of the radiogenic lead produced by the unaltered sample, A, during the time interval, t-t_1 is equal to the slope of the line passing through the points A and D, on Concordia times 1/137·7, the present-day relative abundance of U^{235}/U^{238}.

(2) The slopes of the line passing through the point D and the points B, and C times 1/137·7, will give the Pb^{207}/Pb^{206} ratio of samples B and C.

(3) At the time of loss or gain of lead and uranium in the past, t_1, the radiogenic Pb^{207}/Pb^{206} ratios of the samples A, B and C were equal (assumptions (a) and (d)).

(4) Therefore, the points B and C must lie on a single line passing through the points D and A.

(5) The concordant age for samples B or C corrected for lost or gained lead or uranium at one time in the past, t_1, will therefore be given by the N_{207}/N_{235} and N_{206}/N_{238} ratios at the intersection of the line passing through the point, t_1, on Concordia the point B or C and cutting the concordant age curve at t.

The graphical representation of the selective loss of significant amounts of one or more of the radioactive daughter products in either the U^{238} or the U^{235} series throughout a major portion of the history of a uranium-bearing sample is shown in Fig. 2(b). If, for example, selective loss by diffusion of radon (Em^{222}) in the U^{238} series compared to actinon (Em^{223}) in the U^{235} series had occurred, the sample would be ultimately depleted in Pb^{206} while the Pb^{207} content of the sample would remain unchanged. Assuming in Fig. 2(b) that sample E lost extensive amounts of radon, the concordant age corrected for this loss would be obtained by noting the intersection of a horizontal line passing through the point E and cutting the curve Concordia. Similarly, selective loss of radioactive daughter products in the U^{235} series would be restored by passing vertical lines through the points until they cut the concordant age curve. The amount of Pb^{206} that must be restored in order to give sample E a concordant age may be obtained graphically from the ratio of the length of the line ED to the line OD.

Graphical representation of the correction for the presence of an older generation of radiogenic lead is shown in the Fig. 3(a). Sample A gives concordant lead–uranium ages and has a Pb^{207}/Pb^{206} ratio equal to R. Samples B and C could correspond to the discordant lead–uranium ages of two uranium ore specimens

that have received at the time of their formation different amounts of an older radiogenic lead with a Pb^{207}/Pb^{206} ratio equal to R^*. In lead isotope age studies on the accessory minerals in igneous and metamorphic rocks, the presence of relict minerals, such as relict zircon, could correspond to the deposition of an older generation of radiogenic lead in uranium ores. Age studies on the radioactive detrital minerals in sedimentary rocks would also give similar discordant age

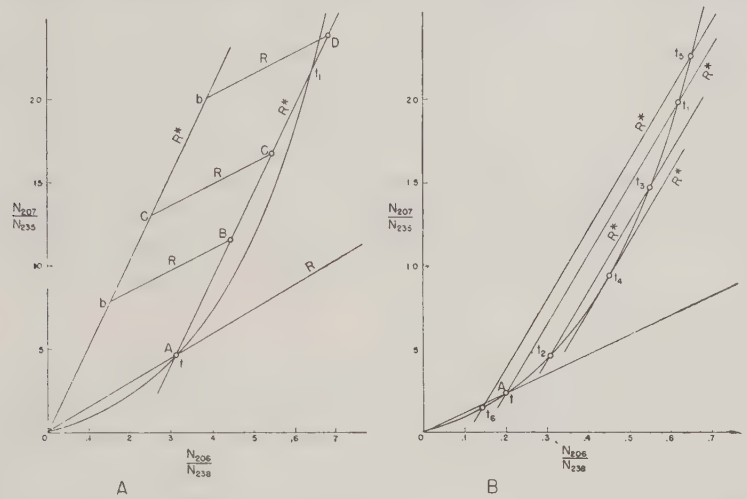

Fig. 3(a). Graph of N_{207}/N_{235} vs. N_{206}/N_{238} for uranium-bearing samples contaminated with an original radiogenic lead having a Pb^{207}/Pb^{206} ratio, R^*.
Fig. 3(b). Graph of N_{207}/N_{235} vs. N_{206}/N_{238} showing the family of time intervals producing radiogenic lead having a Pb^{207}/Pb^{206} ratio, R^*.

sequences if, for example, zircon from source rocks of two different ages were being mixed in varying proportions in the sediments.

If isotopic data are available for at least two discordant samples that were originally formed at the same time, B and C (Fig. 3a), the concordant age corrected for the presence of an older generation of radiogenic lead can be obtained by passing a line through the two points and noting the intersection, t, with the concordant age curve having the smallest N_{206}/N_{238} and N_{207}/N_{235} ratios. The slope of this straight line divided by 137·7 will equal the Pb^{207}/Pb^{206} ratio of the older radiogenic lead. The intersection giving the higher age value, t_1, corresponds to the age obtained after correcting for the gain or losses of lead or uranium as previously described. This graph makes it clear that the two concordant age solutions t and t_1 are mathematically equally acceptable. The choice of either t or t_1 as the most probable concordant age for both C and B must be based on other evidence. If the discordant ages of B and C are a result of the presence of relict minerals, t_1 would give the age of the earlier period of mineral formation. Should sample B and C represent mixtures of two zircons in a sedimentary sequence the points t and t_1 would correspond to the two ages of the igneous rocks contributing the accessory minerals.

The maximum time interval during which an older generation of radiogenic

lead with a Pb^{207}/Pb^{206} ratio of R^* could have been produced and still have been deposited at the time of formation of sample A is given by the time interval t-t_1 (see Fig. 3b). The limiting case for the production of a radiogenic lead whose Pb^{207}/Pb^{206} ratio equals R^*, t_4, is given by the tangent to the concordant age curve whose slope is R^*. In other words, t_4 represents the instantaneous rate of production of radiogenic lead having a Pb^{207}/Pb^{206} ratio R^*. Between the time t_4 and the time interval t-t_1 lie all of the possible time intervals during which a radiogenic lead with a Pb^{207}/Pb^{206} ratio of R^* could be produced and then redeposited at the time of formation of a new mineral. These values are given by the family of lines parallel to t-t_1 and intersecting the concordant age curve, for example, at t_2-t_3. It can be seen in Fig. 3(b) that radiogenic lead with a Pb^{207}/Pb^{206} ratio of R^* could also be introduced into the sample whose age is t at some time after the formation of the mineral, for example, at the time t_6. Paragenetic studies of polished sections of uranium ores should help to distinguish this latter case from the deposition of radiogenic lead at the time of formation of the uranium ore.

Graph of total N_{207}/N_{235} vs. total N_{206}/N_{238}

The discordant lead-isotope age problem may be further generalized by plotting the total N_{207}/N_{235} vs. total N_{206}/N_{238} instead of the graphs of radiogenic N_{207}/N_{235} vs. radiogenic N_{206}/N_{238} used by Ahrens (1955a, b) and Wetherill (1956). Both the concordant and discordant ages of a sample corrected for varying amounts of a common lead with a specific Pb^{207}/Pb^{206} ratio can now be made from this new graph (see Fig. 4a). The concordant age curve still represents the locus of those points whose N_{207}/N_{235} and N_{206}/N_{238} ratios give the same age, t. In this graph the concordant age of an unaltered sample, A, corrected for a common lead with a specific Pb^{207}/Pb^{206} ratio, R^c is obtained by passing a line whose slope is equal to $R^c \times 137{\cdot}7$ through the point A and noting the intersection of this line with the concordant age curve, t. It should be stressed that this concordant age, t, is obtained without use of either Pb^{204} or Pb^{208} as the index of the common lead present.

This concordant age, t, may now be compared graphically with the ages obtained by the more conventional methods of correcting for contaminating common lead (Stieff *et al.*, 1959) using either Pb^{204} or Pb^{208} as the index isotope (Fig. 4a). First, the radiogenic Pb^{207}/Pb^{206} ratio is obtained using the appropriate index isotope, Pb^{204} or Pb^{208}, and a common lead having the same Pb^{207}/Pb^{206} ratio, R^c. Then, with the aid of either the nomographs or the age tables that are available (Wickman, 1939; Kulp *et al.*, 1954; Greenhalgh and Jeffery, 1959; or Stieff *et al.*, 1959), a point, c, is obtained on the concordant age curve whose N_{206}/N_{238} or N_{207}/N_{235} ratio is equivalent in age to the radiogenic Pb^{207}/Pb^{206} ratio age just calculated. A line is now drawn from the origin to this equivalent point, c, on the concordant age curve. The co-ordinates of the intersection, a, of the cord, Oc, and the line passing through A with the slope $R^c \times 137{\cdot}7$ will give the corresponding N_{207}/N_{235} and N_{206}/N_{238} ratios that would be obtained using the conventional index isotope method of common lead correction. A comparison of the age equivalents of the co-ordinates of the intersections a and t may also

help in a partial evaluation of the experimental errors encountered in the isotopic analysis of the generally far less abundant index isotopes.

The availability of analytical data for two or more unaltered samples whose ages are assumed to be the same and which have been assumed to be contaminated only by a common lead having the same Pb^{207}/Pb^{206} ratio will permit a concordant age solution without knowledge of the amount of, or the Pb^{207}/Pb^{206} ratio of the contaminating common leads. This concordant age can easily be obtained by passing a line through the co-ordinates of the points A and B (Fig. 4a) and observing the intersection of this line with the concordant age curve. The slope

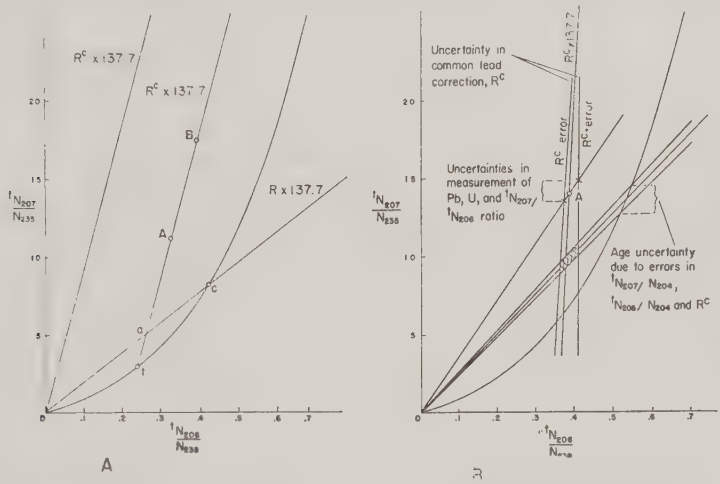

Fig. 4(a). Graph of $^tN_{207}/N_{235}$ vs. $^tN_{206}/N_{238}$ for unaltered uranium-bearing samples contaminated with a common lead having a Pb^{207}/Pb^{206} ratio, R^c.
Fig. 4(b). Graph of $^tN_{207}/N_{235}$ vs. $^tN_{206}/N_{238}$ showing the errors in age produced by uncertainties in the analytical results and the common lead correction.

of this line divided by 137·7 will obviously be the Pb^{207}/Pb^{206} ratio of the contaminating lead which will give the same concordant age for both samples A and B. This ratio may now be directly compared with the experimentally determined Pb^{207}/Pb^{206} ratio of the lead in related non-radioactive minerals, such as galena, pyrite or feldspar. Failure of the experimentally and graphically determined Pb^{207}/Pb^{206} ratios to agree or an abnormal graphic value for R^c will indicate a more complex geologic history than was initially assumed. As was mentioned at the conclusion of the discussion of Fig. 2(a), the same age can be obtained graphically from plots of N_{207}/N_{204} (Fig. 1a) even though the samples have been recently altered.

The overall error in an age determination resulting from uncertainties in the analytical measurements as well as in the assumed Pb^{207}/Pb^{206} ratio of the common lead correction is shown in Fig. 4(b). If the possible age sequences represented by the shaded area in this figure do not cut the concordant age curve it must be concluded that the sample yields truly discordant lead isotope ages and has been involved in some more complex geological process than was first assumed. If the shaded area does intersect the concordant age curve it is reasonable to conclude that the sample has had a relatively simple geologic history and that the

true age of the sample probably lies somewhere within the limit of the concordant ages that have been obtained.

$$\textit{Graphs of } \frac{(N_{207}/N_{204})x - (N_{207}/N_{204})y}{(N_{235}/N_{204})x - (N_{235}/N_{204})y} \text{ vs. } \frac{(N_{206}/N_{204})x - (N_{206}/N_{204})y}{(N_{238}/N_{204})x - (N_{238}/N_{204})y}$$

If the ratios involving total N_{206} and total N_{207} are now normalized with the index isotope N_{204} (or N_{208} if Th is absent), the necessity of considering the isotopic composition of the contaminating common lead can be completely eliminated. It was shown in Fig. 1(b) that, given isotopic data on at least two lead samples, B and C, both containing different amounts of a common lead and a

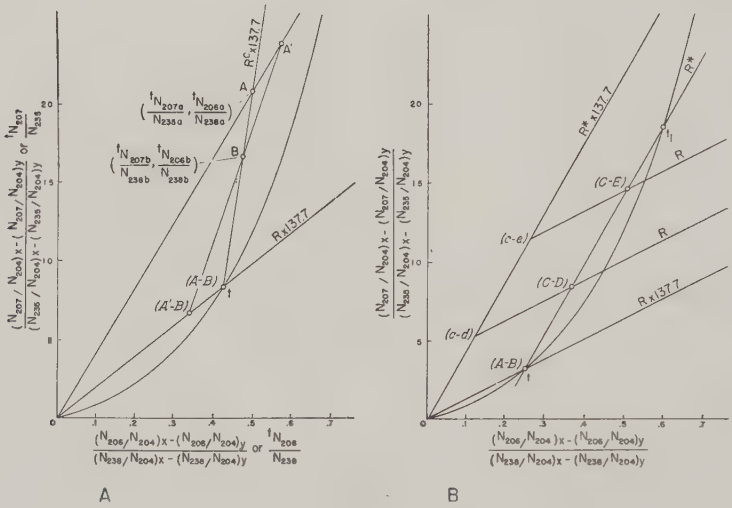

Fig. 5(a). Graph of $\dfrac{(N_{207}/N_{204})x - (N_{207}/N_{204})y}{(N_{235}/N_{204})x - (N_{235}/N_{204})y}$ vs. $\dfrac{(N_{206}/N_{204})x - (N_{206}/N_{204})y}{(N_{238}/N_{204})x - (N_{238}/N_{204})y}$ for recently altered uranium-bearing samples contaminated only with common lead.

Fig. 5(b). Graph of $\dfrac{(N_{207}/N_{204})x - (N_{207}/N_{204})y}{(N_{235}/N_{204})x - (N_{235}/N_{204})y}$ vs. $\dfrac{(N_{206}/N_{204})x - (N_{206}/N_{204})y}{(N_{238}/N_{204})x - (N_{238}/N_{204})y}$ for common lead contaminated uranium-bearing samples which, in addition, were altered at a time, t, in the past or contain an older radiogenic lead, R.*

radiogenic lead with Pb^{207}/Pb^{206} ratios R^c and R^*, respectively, a plot of $[(N_{207}/N_{204})_C - (N_{207}/N_{204})_B]$ vs. $[(N_{206}/N_{204})_C - (N_{206}/N_{204})_B]$ would lie on a straight line passing through the origin with a slope, R^*, equal to the Pb^{207}/Pb^{206} ratio of the added radiogenic lead. Turning now to Fig. 5(a), it can be shown that, if two unaltered samples, A and B, containing different amounts of lead and uranium were formed at the same time and were contaminated only with a common lead of uniform Pb^{207}/Pb^{206} ratio, R^c, the point $(A\text{-}B)$ given by the co-ordinates

$$\left[\frac{(N_{207}/N_{204})_A - (N_{207}/N_{204})_B}{(N_{235}/N_{204})_A - (N_{235}/N_{204})_B}\right] \quad \text{and} \quad \left[\frac{(N_{206}/N_{204})_A - (N_{206}/N_{204})_B}{(N_{238}/N_{204})_A - (N_{238}/N_{204})_B}\right]$$

would lie on the concordant age curve.

The point $(A\text{-}B)$ has the additional property that it must lie on the line passing

through the co-ordinates $({}^{t}N_{207a}/N_{235a}, {}^{t}N_{206a}/N_{238a})$ and $({}^{t}N_{207b}/N_{235b}, {}^{t}N_{206b}/N_{238b})$ of the points A and B, respectively. In the case just described the slope of the line passing through the co-ordinates of points A and B divided by 137·7 would equal the Pb^{207}/Pb^{206} ratio, R^c, of the contaminating common lead. However, if either or both of the samples had been recently altered: for example, if sample A had lost uranium and moved to A', then the point $(A'\text{-}B)$ would still lie on the line through the points A' and B but the slope of this line would not be related to the Pb^{207}/Pb^{206} ratio of the contaminating common lead. As in the previous discussion of recent alteration, the point $(A'\text{-}B)$ would lie on a line passing through the origin with a slope divided by 137·7 and equal to the Pb^{207}/Pb^{206} ratio, R, of radiogenic lead in samples A and B.

The problem of the three-component lead mixtures, R^c, R^*, and R can now be considered (Fig. 5b). Assume that in addition to a common lead having the same Pb^{207}/Pb^{206} ratio R^c, samples A and B have received different amounts of an older generation of radiogenic lead with a Pb^{207}/Pb^{206} ratio, R^*. Then the normalized difference ratios of this two component mixture, R^c and R^*, would lie on a line passing through the origin whose slope is equal to $R^* \times 137{\cdot}7$; for example, the point $(c\text{-}d)$. The amounts of radiogenic Pb^{206} and Pb^{207} produced in the time interval $0\text{-}t$ may now be added graphically to the point $(c\text{-}d)$ by passing a line through the point $(c\text{-}d)$ with the slope, R, and of length equal to the line segment from the origin to the point $(A\text{-}B)$. The co-ordinates of the point $(C\text{-}D)$ thus represent the discordant ages that are obtained when the normalized difference ratios are plotted for a pair of samples each containing three-component lead mixtures.

The graphical concordant ages obtained using normalized difference plots for not less than three samples, C, D and E, formed at the same time, is shown in Fig. 5(b). Assuming, in addition, that the samples contain different amounts of lead and uranium, and were contaminated by a common lead having a uniform Pb^{207}/Pb^{206} ratio, a line passing through the co-ordinates of the points $(C\text{-}D)$ and $(C\text{-}E)$ cuts the concordant age curve at t and t_1. The concordant age, t, is the age that would be obtained after correcting for the addition of an older generation of radiogenic lead formed, perhaps, in the time interval $t\text{-}t_1$. The concordant age, t_1, would correspond to the correction of samples C, D and E for loss or gain of lead or uranium at one time in the past, t. Thus it is possible to obtain concordant ages for a suite of at least three cogenetic uranium-bearing minerals without knowledge of either the amount or isotopic composition of the contaminating common lead, and either the effects of a single period of alteration or the presence of yet an older generation of radiogenic lead.

Once again it becomes clear that the calculation of the two concordant ages cannot in itself provide the basis for the choice of one age against the other. If an alteration hypothesis at some time, t, can be supported by independent geologic and laboratory evidence, the age of the enclosing host rock will be more nearly defined by t_1. If the independent evidence supports the presence of at least two generations of radiogenic lead the age of the host rock will be set more nearly by the age t, while t_1 will set a maximum age of the older source of radiogenic lead.

Algebraic Methods

Although it is not difficult to obtain an approximately concordant age from discordant isotopic lead–uranium data by graphical methods, there are geologic problems for which the exact algebraic solutions may be preferred. Furthermore, as Aldrich and Wetherill (1958) have noted, "the algebraic expressions involved are frequently so complex that it is difficult to visualize the physical processes (Wetherill, 1956; and Wickman, 1955).", Finally, practical algebraic solutions provide an incentive to improve the measurement of the physical decay constants used in our calculations, the analytical techniques, and sampling methods in order that we may derive all of the useful geologic information that is available in a comprehensive lead isotope age study. For these reasons a set of algebraic expressions have been derived which are exact equivalents of the graphical procedures described above. In these equations the role of the possible geologic processes can be visualized and it is possible to obtain as exact a concordant age solution as is required by the specific geologic problem.

To the writers' knowledge only one simple algebraic solution has been published and it was specifically intended for the original radiogenic lead problem. The lead–uranium isotope age equations derived by Keevil (1939):

$$t\,(\text{yrs}) = 1{\cdot}515 \times 10^{10} \log \left(1 + \frac{1{\cdot}15\ \text{Pb}^{206}}{\text{U}^{238}}\right) \tag{1}$$

and

$$t\,(\text{yrs}) = 2{\cdot}37 \times 10^{9} \log \left(1 + \frac{158\ \text{Pb}^{207}}{\text{U}^{238}}\right) \tag{2}$$

were modified by Tugarinov (1954) to include corrections for original radiogenic lead. The suggested modifications took the form of the following system of equations:

$$\begin{aligned} t_m &= 15{\cdot}15 \times 10^{9} \log \left[\left(\frac{\text{Pb}^{206} - \text{X Pb}^{206*}}{\text{U}}\right) \times 1{\cdot}158 + 1\right] \\ &= 2{\cdot}37 \times 10^{9} \log \left[\left(\frac{\text{Pb}^{207} - \text{X Pb}^{207*}}{\text{U}}\right) \times 159{\cdot}6 + 1\right] \end{aligned} \tag{3}$$

where Pb^{206*} and Pb^{207*} are the percent abundances of the original radiogenic lead, X is the percentage of the occluded original radiogenic lead in the uranium-bearing material and t_m is the corrected concordant age of the mineral.

Tugarinov's age equations, because of their log form, cannot be solved for "X", the amount of original radiogenic lead present. In addition, it is necessary to know independently the $\text{Pb}^{207}/\text{Pb}^{206}$ ratio of the original radiogenic lead. Given Pb^{206*} and Pb^{207*}, repeated substitutions of different values for "X" must be made until a value of "X" is found which will make the $\text{Pb}^{206}/\text{U}^{238}$ age equal to the $\text{Pb}^{207}/\text{U}^{235}$ age. The $\text{Pb}^{207}/\text{Pb}^{206}$ age, corrected for the same amounts of original radiogenic lead, will then be in agreement with the two lead–uranium ages.

An alternative approach to Tugarinov's specific algebraic solution of the problem of original radiogenic lead which is also both simple and generally

applicable to the discordant age problem, may be derived by using a series expansion of the exponential term in the general age equation,

$$e^{\lambda t} = \frac{N_d}{N_p} + 1 \tag{4}$$

In this equation N_d and N_p represent the number of atoms of stable daughter product and radioactive parent, respectively; λ represents the decay constant times 10^{-10} years^{-1}; and t, the age in 10^{10} years equivalent to the atom ratio N_d/N_p. The value $e^{\lambda t}$ may be approximated as closely as desired by the series:

$$e^{\lambda t} = (1 + \lambda t) + \frac{(\lambda t)^2}{2!} + \frac{(\lambda t)^3}{3!} \cdots \frac{(\lambda t)^n}{n!}$$

Substituting this series for $e^{\lambda t}$, the age equation (4) may be written in the form,

$$1 + \lambda t + \frac{(\lambda t)^2}{2!} + \frac{(\lambda t)^3}{3!} \cdots \frac{(\lambda t)^n}{n!} = \frac{N_d}{N_p} + 1$$

$$\lambda t + \frac{(\lambda t)^2}{2!} + \frac{(\lambda t)^3}{3!} \cdots \frac{(\lambda t)^n}{n!} = \frac{N_d}{N_p} \tag{5}$$

Introducing the term, N_d* for the number of atoms of stable original radiogenic daughter present at the time of mineral formation, to, equation (5) can be written,

$$N_d - N_p\left(\lambda t + \frac{(\lambda t^2)}{2!} + \frac{(\lambda t)^3}{3!} \cdots \frac{(\lambda t)^n}{n!}\right) = N_d^* \tag{5a}$$

and where N_d represents the total number of atoms of stable radiogenic daughter now in the sample.

Where values of t are small, less than 250 million years, equation (5) may be carried only to the second term without introducing serious errors. As t increases, however, it is necessary either to include a larger number of terms in the expansion of $e^{\lambda t}$ and to work with equations of higher degree than two or to include an additional factor, f, which may be obtained from Table 1:

$$f + \frac{(\lambda t)^2}{2} + \lambda t = \frac{N_d}{N_p} \tag{6}$$

This factor represents, for a number of values of t_1, the difference between the two term expansion of exp (λt_1) for the U^{235} and U^{238} series and the actual value of exp (λt_1) for the particular value of t_1. The decision to use equation (5) or (6) will be determined in part by the computing facilities available, the requirements of the specific geologic age problem and by the section of the geologic time scale involved in the age calculations. Depending on the assumed cause of the age discordancies, the trial Pb^{206}/U^{238} or the Pb^{207}/Pb^{206} age calculations made to determine the extent and type of lead–uranium age discordancies, can be used to guide the selection of the initial age, t_1 and the corresponding values of f_1 and f_2 from Table 1. Should the nature of the geologic problem require a further refinement in the first calculated age, a second choice of t_1 based on the first calculated age, t, can be made. With experience in the initial choice of t_1, it has been found that two age calculations will usually suffice for most geologic problems.

Table 1. Factors for use with equations of the second degree

$t_1 \times 10^6$ years	f_1	f_2	$t_1 \times 10^6$ years	f_1	f_2	$t_1 \times 10^6$ years	f_1	f_2
0	$0{\cdot}0000_0$	$0{\cdot}0000_0$	500	$0{\cdot}0000_8$	$0{\cdot}0217_1$	900	$0{\cdot}0004_6$	$0{\cdot}1410_2$
20	$0{\cdot}0000_0$	$0{\cdot}0000_0$	10	$0{\cdot}0000_8$	$0{\cdot}0231_0$	10	$0{\cdot}0004_7$	$0{\cdot}1461_9$
40	$0{\cdot}0000_0$	$0{\cdot}0000_1$	20	$0{\cdot}0000_9$	$0{\cdot}0245_5$	20	$0{\cdot}0004_9$	$0{\cdot}1514_8$
60	$0{\cdot}0000_0$	$0{\cdot}0000_3$	30	$0{\cdot}0000_9$	$0{\cdot}0260_6$	30	$0{\cdot}0005_0$	$0{\cdot}1569_1$
80	$0{\cdot}0000_0$	$0{\cdot}0000_8$	40	$0{\cdot}0001_0$	$0{\cdot}0276_4$	40	$0{\cdot}0005_2$	$0{\cdot}1624_8$
100	$0{\cdot}0000_0$	$0{\cdot}0001_6$	50	$0{\cdot}0001_0$	$0{\cdot}0292_8$	50	$0{\cdot}0005_4$	$0{\cdot}1681_9$
20	$0{\cdot}0000_0$	$0{\cdot}0002_7$	60	$0{\cdot}0001_1$	$0{\cdot}0309_9$	60	$0{\cdot}0005_6$	$0{\cdot}1740_4$
40	$0{\cdot}0000_0$	$0{\cdot}0004_3$	70	$0{\cdot}0001_1$	$0{\cdot}0327_6$	70	$0{\cdot}0005_7$	$0{\cdot}1800_4$
60	$0{\cdot}0000_0$	$0{\cdot}0006_5$	80	$0{\cdot}0001_2$	$0{\cdot}0346_1$	80	$0{\cdot}0005_9$	$0{\cdot}1861_9$
80	$0{\cdot}0000_0$	$0{\cdot}0009_3$	90	$0{\cdot}0001_3$	$0{\cdot}0365_3$	90	$0{\cdot}0006_1$	$0{\cdot}1924_9$
200	$0{\cdot}0000_0$	$0{\cdot}0012_8$	600	$0{\cdot}0001_3$	$0{\cdot}0385_2$	1000	$0{\cdot}0006_3$	$0{\cdot}1989_3$
10	$0{\cdot}0000_1$	$0{\cdot}0014_9$	10	$0{\cdot}0001_4$	$0{\cdot}0405_8$	10	$0{\cdot}0006_5$	$0{\cdot}2055_4$
20	$0{\cdot}0000_1$	$0{\cdot}0017_2$	20	$0{\cdot}0001_5$	$0{\cdot}0427_3$	20	$0{\cdot}0006_7$	$0{\cdot}2123_1$
30	$0{\cdot}0000_1$	$0{\cdot}0019_7$	30	$0{\cdot}0001_6$	$0{\cdot}0449_5$	30	$0{\cdot}0006_9$	$0{\cdot}2192_3$
40	$0{\cdot}0000_1$	$0{\cdot}0022_4$	40	$0{\cdot}0001_6$	$0{\cdot}0472_5$	40	$0{\cdot}0007_1$	$0{\cdot}2263_2$
50	$0{\cdot}0000_1$	$0{\cdot}0025_4$	50	$0{\cdot}0001_7$	$0{\cdot}0496_3$	50	$0{\cdot}0007_3$	$0{\cdot}2335_7$
60	$0{\cdot}0000_1$	$0{\cdot}0028_7$	60	$0{\cdot}0001_8$	$0{\cdot}0521_0$	60	$0{\cdot}0007_5$	$0{\cdot}2409_9$
70	$0{\cdot}0000_1$	$0{\cdot}0032_2$	70	$0{\cdot}0001_9$	$0{\cdot}0546_4$	70	$0{\cdot}0007_7$	$0{\cdot}2485_8$
80	$0{\cdot}0000_1$	$0{\cdot}0036_0$	80	$0{\cdot}0002_0$	$0{\cdot}0572_8$	80	$0{\cdot}0008_0$	$0{\cdot}2563_4$
90	$0{\cdot}0000_1$	$0{\cdot}0040_1$	90	$0{\cdot}0002_0$	$0{\cdot}0600_1$	90	$0{\cdot}0008_2$	$0{\cdot}2642_8$
300	$0{\cdot}0000_2$	$0{\cdot}0044_5$	700	$0{\cdot}0002_1$	$0{\cdot}0628_2$	1100	$0{\cdot}0008_4$	$0{\cdot}2723_9$
10	$0{\cdot}0000_2$	$0{\cdot}0049_2$	10	$0{\cdot}0002_2$	$0{\cdot}0657_3$	10	$0{\cdot}0008_6$	$0{\cdot}2806_9$
20	$0{\cdot}0000_2$	$0{\cdot}0054_3$	20	$0{\cdot}0002_3$	$0{\cdot}0687_4$	20	$0{\cdot}0008_9$	$0{\cdot}2891_8$
30	$0{\cdot}0000_2$	$0{\cdot}0059_7$	30	$0{\cdot}0002_4$	$0{\cdot}0718_3$	30	$0{\cdot}0009_1$	$0{\cdot}2978_4$
40	$0{\cdot}0000_2$	$0{\cdot}0065_4$	40	$0{\cdot}0002_5$	$0{\cdot}0750_3$	40	$0{\cdot}0009_3$	$0{\cdot}3067_0$
50	$0{\cdot}0000_3$	$0{\cdot}0071_6$	50	$0{\cdot}0002_6$	$0{\cdot}0783_2$	50	$0{\cdot}0009_6$	$0{\cdot}3157_4$
60	$0{\cdot}0000_3$	$0{\cdot}0078_1$	60	$0{\cdot}0002_7$	$0{\cdot}0817_2$	60	$0{\cdot}0009_9$	$0{\cdot}3249_9$
70	$0{\cdot}0000_3$	$0{\cdot}0085_0$	70	$0{\cdot}0002_8$	$0{\cdot}0852_2$	70	$0{\cdot}0010_2$	$0{\cdot}3344_3$
80	$0{\cdot}0000_3$	$0{\cdot}0092_4$	80	$0{\cdot}0003_0$	$0{\cdot}0888_3$	80	$0{\cdot}0010_4$	$0{\cdot}3440_7$
90	$0{\cdot}0000_4$	$0{\cdot}0100_1$	90	$0{\cdot}0003_1$	$0{\cdot}0925_4$	90	$0{\cdot}0010_7$	$0{\cdot}3539_2$
400	$0{\cdot}0000_4$	$0{\cdot}0108_3$	800	$0{\cdot}0003_2$	$0{\cdot}0963_6$	1200	$0{\cdot}0011_0$	$0{\cdot}3639_6$
10	$0{\cdot}0000_4$	$0{\cdot}0116_9$	10	$0{\cdot}0003_3$	$0{\cdot}1002_9$	10	$0{\cdot}0011_2$	$0{\cdot}3742_2$
20	$0{\cdot}0000_5$	$0{\cdot}0126_0$	20	$0{\cdot}0003_4$	$0{\cdot}1043_4$	20	$0{\cdot}0011_5$	$0{\cdot}3846_9$
30	$0{\cdot}0000_5$	$0{\cdot}0135_6$	30	$0{\cdot}0003_6$	$0{\cdot}1085_0$	30	$0{\cdot}0011_8$	$0{\cdot}3953_8$
40	$0{\cdot}0000_5$	$0{\cdot}0145_6$	40	$0{\cdot}0003_7$	$0{\cdot}1127_8$	40	$0{\cdot}0012_1$	$0{\cdot}4062_8$
50	$0{\cdot}0000_6$	$0{\cdot}0156_2$	50	$0{\cdot}0003_9$	$0{\cdot}1171_7$	50	$0{\cdot}0012_4$	$0{\cdot}4174_0$
60	$0{\cdot}0000_6$	$0{\cdot}0167_3$	60	$0{\cdot}0004_0$	$0{\cdot}1216_9$	60	$0{\cdot}0012_7$	$0{\cdot}4287_6$
70	$0{\cdot}0000_6$	$0{\cdot}0178_9$	70	$0{\cdot}0004_1$	$0{\cdot}1263_4$	70	$0{\cdot}0013_0$	$0{\cdot}4403_3$
80	$0{\cdot}0000_7$	$0{\cdot}0191_1$	80	$0{\cdot}0004_3$	$0{\cdot}1311_1$	80	$0{\cdot}0013_4$	$0{\cdot}4521_4$
90	$0{\cdot}0000_7$	$0{\cdot}0203_8$	90	$0{\cdot}0004_4$	$0{\cdot}1360_0$	90	$0{\cdot}0013_7$	$0{\cdot}4641_8$

Calculation of concordant ages for one sample, given the Pb^{207}/Pb^{206} *ratio,* R^*

If discordant analytical age data are available for only one sample an exact concordant age may be calculated, given the Pb^{207}/Pb^{206} ratio, R^*, of the contaminating original radiogenic lead or the radiogenic lead lost at one time in the past. The value, R^*, may be assumed or may be inferred from independent evidence, such as the isotopic study of the lead in associated non-radioactive minerals. From such data, it is possible to derive an age equation which will yield two

Table 1 (*continued*)

$t_1 \times 10^6$ years	f_1	f_2	$t_1 \times 10^6$ years	f_1	f_2	$t_1 \times 10^6$ years	f_1	f_2
1300	$0{\cdot}0014_0$	$0{\cdot}4764_5$	2100	$0{\cdot}0060_9$	$2{\cdot}576_9$	2900	$0{\cdot}0165_6$	$8{\cdot}971_1$
20	$0{\cdot}0014_7$	$0{\cdot}5017_3$	20	$0{\cdot}0062_7$	$2{\cdot}668_8$	20	$0{\cdot}0169_2$	$9{\cdot}225_8$
40	$0{\cdot}0015_4$	$0{\cdot}5279_9$	40	$0{\cdot}0064_5$	$2{\cdot}763_3$	40	$0{\cdot}0172_9$	$9{\cdot}486_6$
60	$0{\cdot}0016_0$	$0{\cdot}5552_6$	60	$0{\cdot}0066_4$	$2{\cdot}860_5$	60	$0{\cdot}0176_6$	$9{\cdot}753_6$
80	$0{\cdot}0016_8$	$0{\cdot}5835_8$	80	$0{\cdot}0068_3$	$2{\cdot}960_3$	80	$0{\cdot}0180_3$	$10{\cdot}02_7$
1400	$0{\cdot}0017_5$	$0{\cdot}6129_6$	2200	$0{\cdot}0070_3$	$3{\cdot}062_9$	3000	$0{\cdot}0184_1$	$10{\cdot}30_7$
20	$0{\cdot}0018_3$	$0{\cdot}6434_4$	20	$0{\cdot}0072_3$	$3{\cdot}168_4$	20	$0{\cdot}0188_0$	$10{\cdot}59_3$
40	$0{\cdot}0019_1$	$0{\cdot}6750_4$	40	$0{\cdot}0074_3$	$3{\cdot}276_7$	40	$0{\cdot}0191_9$	$10{\cdot}88_6$
60	$0{\cdot}0020_0$	$0{\cdot}7078_1$	60	$0{\cdot}0076_4$	$3{\cdot}388_0$	60	$0{\cdot}0195_9$	$11{\cdot}18_6$
80	$0{\cdot}0020_8$	$0{\cdot}7417_5$	80	$0{\cdot}0078_5$	$3{\cdot}502_4$	80	$0{\cdot}0199_9$	$11{\cdot}49_3$
1500	$0{\cdot}0021_7$	$0{\cdot}7769_0$	2300	$0{\cdot}0080_6$	$3{\cdot}619_8$	3100	$0{\cdot}0204_0$	$11{\cdot}80_8$
20	$0{\cdot}0022_6$	$0{\cdot}8133_2$	20	$0{\cdot}0082_8$	$3{\cdot}740_3$	20	$0{\cdot}0208_1$	$12{\cdot}12_9$
40	$0{\cdot}0023_5$	$0{\cdot}8510_0$	40	$0{\cdot}0085_1$	$3{\cdot}864_2$	40	$0{\cdot}0212_4$	$12{\cdot}45_8$
60	$0{\cdot}0024_4$	$0{\cdot}8900_0$	60	$0{\cdot}0087_3$	$3{\cdot}991_2$	60	$0{\cdot}0216_6$	$12{\cdot}79_5$
80	$0{\cdot}0025_4$	$0{\cdot}9303_4$	80	$0{\cdot}0089_6$	$4{\cdot}121_7$	80	$0{\cdot}0220_9$	$13{\cdot}13_9$
1600	$0{\cdot}0026_4$	$0{\cdot}9720_6$	2400	$0{\cdot}0092_0$	$4{\cdot}255_6$	3200	$0{\cdot}0225_3$	$13{\cdot}49_2$
20	$0{\cdot}0027_4$	$1{\cdot}015_2$	20	$0{\cdot}0094_4$	$4{\cdot}393_1$	20	$0{\cdot}0229_8$	$13{\cdot}85_2$
40	$0{\cdot}0028_5$	$1{\cdot}059_8$	40	$0{\cdot}0096_8$	$4{\cdot}534_1$	40	$0{\cdot}0234_3$	$14{\cdot}22_1$
60	$0{\cdot}0029_6$	$1{\cdot}105_8$	60	$0{\cdot}0099_3$	$4{\cdot}678_8$	60	$0{\cdot}0238_8$	$14{\cdot}59_8$
80	$0{\cdot}0030_7$	$1{\cdot}153_4$	80	$0{\cdot}0101_8$	$4{\cdot}827_3$	80	$0{\cdot}0243_4$	$14{\cdot}98_4$
1700	$0{\cdot}0031_8$	$1{\cdot}202_6$	2500	$0{\cdot}0104_4$	$4{\cdot}979_6$	3300	$0{\cdot}0248_1$	$15{\cdot}37_8$
20	$0{\cdot}0033_0$	$1{\cdot}253_3$	20	$0{\cdot}0107_0$	$5{\cdot}135_8$	20	$0{\cdot}0252_9$	$15{\cdot}78_2$
40	$0{\cdot}0034_1$	$1{\cdot}305_7$	40	$0{\cdot}0109_7$	$5{\cdot}296_0$	40	$0{\cdot}0257_7$	$16{\cdot}19_5$
60	$0{\cdot}0035_4$	$1{\cdot}359_7$	60	$0{\cdot}0112_4$	$5{\cdot}460_3$	60	$0{\cdot}0262_5$	$16{\cdot}61_7$
80	$0{\cdot}0036_6$	$1{\cdot}415_5$	80	$0{\cdot}0115_1$	$5{\cdot}628_8$	80	$0{\cdot}0267_5$	$17{\cdot}04_8$
1800	$0{\cdot}0037_9$	$1{\cdot}473_0$	2600	$0{\cdot}0117_9$	$5{\cdot}801_6$	3400	$0{\cdot}0272_5$	$17{\cdot}49_0$
20	$0{\cdot}0039_2$	$1{\cdot}532_3$	20	$0{\cdot}0120_8$	$5{\cdot}978_6$	20	$0{\cdot}0277_6$	$17{\cdot}94_1$
40	$0{\cdot}0040_5$	$1{\cdot}593_5$	40	$0{\cdot}0123_6$	$6{\cdot}160_2$	40	$0{\cdot}0282_7$	$18{\cdot}40_3$
60	$0{\cdot}0041_9$	$1{\cdot}656_5$	60	$0{\cdot}0126_6$	$6{\cdot}346_3$	60	$0{\cdot}0287_9$	$18{\cdot}87_4$
80	$0{\cdot}0043_3$	$1{\cdot}721_5$	80	$0{\cdot}0129_6$	$6{\cdot}537_1$	80	$0{\cdot}0293_1$	$19{\cdot}35_6$
1900	$0{\cdot}0044_7$	$1{\cdot}788_4$	2700	$0{\cdot}0132_6$	$6{\cdot}732_5$	3500	$0{\cdot}0298_5$	$19{\cdot}84_9$
20	$0{\cdot}0046_2$	$1{\cdot}857_4$	20	$0{\cdot}0135_7$	$6{\cdot}932_8$	20	$0{\cdot}0303_9$	$20{\cdot}35_4$
40	$0{\cdot}0047_7$	$1{\cdot}928_4$	40	$0{\cdot}0138_8$	$7{\cdot}138_1$	40	$0{\cdot}0309_3$	$20{\cdot}86_9$
60	$0{\cdot}0049_2$	$2{\cdot}001_5$	60	$0{\cdot}0142_0$	$7{\cdot}348_4$	60	$0{\cdot}0314_9$	$21{\cdot}39_5$
80	$0{\cdot}0050_8$	$2{\cdot}076_8$	80	$0{\cdot}0145_2$	$7{\cdot}563_9$	80	$0{\cdot}0320_5$	$21{\cdot}93_4$
2000	$0{\cdot}0052_4$	$2{\cdot}154_4$	2800	$0{\cdot}0148_5$	$7{\cdot}784_6$	3600	$0{\cdot}0326_2$	$22{\cdot}48_4$
20	$0{\cdot}0054_0$	$2{\cdot}234_1$	20	$0{\cdot}0151_8$	$8{\cdot}010_7$	20	$0{\cdot}0331_9$	$23{\cdot}04_6$
40	$0{\cdot}0055_7$	$2{\cdot}316_2$	40	$0{\cdot}0155_2$	$8{\cdot}242_3$	40	$0{\cdot}0337_7$	$23{\cdot}62_1$
60	$0{\cdot}0057_4$	$2{\cdot}400_7$	60	$0{\cdot}0158_6$	$8{\cdot}479_5$	60	$0{\cdot}0343_6$	$24{\cdot}20_8$
80	$0{\cdot}0059_1$	$2{\cdot}487_6$	80	$0{\cdot}0162_1$	$8{\cdot}722_4$	80	$0{\cdot}0349_6$	$24{\cdot}80_9$

concordant age solutions for a single sample without knowledge either of the amount of original radiogenic Pb^{206} and Pb^{207} present in the sample or the amount of lead lost in the past. The derivation of the equations given in this and the following paragraphs, as well as examples of their use, will be presented in detail elsewhere. The numerical solutions obtained from equation (7) will be valid only, if in addition.

(a) The sample has not recently lost or gained lead or uranium.

(b) The initial correction for common lead has been correctly made so that the remaining Pb^{206} and Pb^{207} represent only the total radiogenic lead in the sample.

Writing equation (5a) for the N_{206}/N_{238} and N_{207}/N_{235} ratios, respectively, and dividing one equation by the other one obtains the following expression:

$$\left.\begin{aligned}\left(\frac{R^*\lambda_1^{\,n}}{n!} - \frac{R\lambda_2^{\,n}}{n!}\right)t^n \cdots + \left(\frac{R^*\lambda_1^{\,3}}{3!} - \frac{R\lambda_2^{\,3}}{3!}\right)t^3 \\ + \left(\frac{R^*\lambda_1^{\,2}}{2!} - \frac{R\lambda_2^{\,2}}{2!}\right)t^2 + (R^*\lambda_1 - R\lambda_2)t + RR_5 - R^*R_8) = 0\end{aligned}\right\} \quad (7)$$

where t = the concordant age (times 10^{10} years);

$R^* = \dfrac{N_{207}}{N_{206}}$, the ratio of the number of atoms of older radiogenic lead.

$R = \dfrac{N_{235}}{N_{238}} = \dfrac{1}{137{\cdot}7} = 0{\cdot}00726_2$, the present-day abundance ratio of the number of atoms of the two uranium isotopes;

$R_5 = \dfrac{N_{207}}{N_{235}}$, the ratio of the number of atoms of radiogenic Pb^{207} to U^{235};

$R_8 = \dfrac{N_{206}}{N_{238}}$, the ratio of the number of atoms of radiogenic Pb^{206} to U^{238};

λ_1 = decay constant for U^{238} (times 10^{-10} years^{-1});

λ_2 = decay constant for U^{235} (times 10^{-10} years^{-1}).

If computing facilities are available equation (7) may be easily programmed to solve directly for t. The degree of the equation used is determined in each case by the approximate age range of the sample being dated and generally will not exceed 10. For values of R^*, R_5 and R_8 of geologic interest equation (7) has two positive, real roots. As the degree of this equation increases, the smaller positive root approaches the concordant age, t_1, corrected for original radiogenic lead shown in Fig. 2(b). The larger positive root approaches the value t as shown in Fig. 2(b) and is the concordant age obtained by correcting for loss of lead or addition of uranium at some time, t_1, in the past. In the latter case R^* is the Pb^{207}/Pb^{206} ratio of the radiogenic lead lost in the time interval t-t_1.

If computing facilities are not available equation (7) may be taken only to the second power of t. As in equation (6), when t is greater than 250 million years two factors, f_1 and f_2, should be added for the U^{238} and U^{235} series, respectively. These factors, obtained from Table 1 for different values of t_1, compensate for the failure of equation (8) to approximate closely enough the actual value of $e^{\lambda t}$ for a specific value of t.

Equation (7) then takes the form,

$$\left(\frac{R^*\lambda_1^{\,2}}{2!} - \frac{R\lambda_2^{\,2}}{2!}\right)t^2 + (R^*\lambda_1 - R\lambda_2)t + (RR_5 - R^*R_8 + R^*f_1 - Rf_2) = 0$$

solving for t,

$$t = \frac{-b \pm \sqrt{(b^2 - 4ac)}}{2a} \tag{8}$$

where $2a = (R^*\lambda_1^2 - R\lambda_2^2)$
$b = (R^*\lambda_1 - R\lambda_2)$
$c = (RR_5 - R^*R_8 - Rf_2 + R^*f_1)$

and where

f_1 = the factor for the U^{238} series depending on t_1.
f_2 = the factor for the U^{235} series depending on t_1.

For values of R^*, R_5 and R_8 of geologic interest, equation (8) also has two positive real roots. The smaller root can be made to approach the concordant age corrected for original radiogenic lead while the larger root can be made to approach the concordant age corrected for lead loss or gain of uranium. In using equation (8) to calculate the concordant age corrected for original radiogenic lead, values of f_1 and f_2 are selected from Table 1 for a t_1 less than the trial Pb^{206}/U^{238} age. With even approximately correct values for f_1 and f_2, the smaller root will fall close to the actual age of the sample corrected for original radiogenic lead.

The larger root, however, depending on the extent of the lead–uranium age discordancy, may depart substantially from the concordant "lead-loss age". If it is desired to calculate exactly the "lead-loss age" using equation (8), values of f_1 and f_2 must be chosen from Table 1 for t_1 greater than the Pb^{207}/Pb^{206} age. Because the terms f_1 and f_2 become increasingly important as t increases, it may be desirable to make a rough graphical lead-loss solution to guide the initial choice of t_1. The departure of the first calculated age, t, from the exact lead-loss solution may be tested by comparing the calculated value of R^* with the given value of R^* using the following equation:

$$R\,\frac{\{R_5 - [f_2 + (\lambda_2 t)^2/2! + \lambda_2 t]\}}{\{R_8 - [f_1 + (\lambda_1 t)^2/2! + \lambda_1 t]\}} = R^* \tag{9}$$

The first calculated value of t along with the appropriate values of f_1 and f_2 for this calculated t from Table 1 may be substituted in equation (9). If the "Tables for the calculation of lead-isotope ages," STIEFF *et al.* (1959) are available, the term $[f_1 + (\lambda_1 t)^2/2! + \lambda_1 t]$ and $[f_2 + (\lambda_2 t)^2/2! + \lambda_2 t)$ may be replaced by the appropriate numerical values of the N_{206}/N_{238} and N_{207}/N_{235} ratios using the calculated value of t. If for the particular geologic problem the agreement between the calculated R^* and the given R^* is not satisfactory, a new t_1 is chosen and the lead-loss age recalculated. This calculation may be repeated until the desired degree of agreement between the calculated R^* and the given R^* is obtained.

Equation (7) may be extended to the calculation of concordant ages of unaltered samples in a manner directly analogous to the modification of WETHERILL's graphical procedure shown in Fig. 4(a). Equation (7) then becomes:

$$\left(\frac{R^c\lambda_1^n}{n!} - \frac{R\lambda_2^n}{n!}\right) t^n \cdots + \left(\frac{R^c\lambda_1^2}{2!} - \frac{R\lambda_2^2}{2!}\right) t^2 + (R^c\lambda_1 - R\lambda_2)t + RR_{5t} - R^cR_{t8} = 0 \tag{10}$$

where

$R^c = \frac{N_{207}}{N_{206}}$, the ratio of the number of atoms Pb^{206} and Pb^{207} in the contaminating common lead;

$R_{5t} = \frac{{}^tN_{207}}{N_{235}}$, the ratio of the total number of atoms of Pb^{207} to U^{235};

$R_{8t} = \frac{{}^tN_{206}}{N_{238}}$, the ratio of the total number of atoms of Pb^{206} to U^{238}.

For geologically possible values of R^c, R_{5t}, and R_{8t} equation (10) expanded to the third degree or higher has two positive real roots. The equations of odd degree also have one negative real root. The smaller positive root rapidly approaches the concordant age corrected for a common lead having a Pb^{207}/Pb^{206} ratio, R^c. The larger root generally has values in excess of current estimates of the age of the earth; is geologically impossible and consequently can be neglected. The real negative root does not have any geologic significance.

If computing facilities are not available equation (10) also can be taken only to the second power of t and the terms f_1 and f_2 added. One then obtains for the R^c

$$R\frac{\{R_{5t} - [f_2 + (\lambda_2 t)^2/2! + \lambda_2 t]\}}{\{R_{8t} - [f_1 + (\lambda_1 t)^2/2! + \lambda_1 t]\}} = R^c \tag{11}$$

Expanding (11) and solving for t,

$$t = \frac{-b \pm \sqrt{(b^2 - 4ac)}}{2a} \tag{12}$$

where $2a = (R^c\lambda_1{}^2 - R\lambda_2{}^2)$

$b = (R^c\lambda_1 - R\lambda_2)$

$c = (RR_{5t} - R^cR_{8t} + R^cf_1 - Rf_2)$

Equation (12) has one positive and one negative root for geologically possible values of R^c, R_{5t}, and R_{8t}. With approximately correct values for f_1 and f_2 from Table 1, the age t will closely approach the concordant age t for a specific value of R^c.

Calculation of concordant ages using two samples, the amount and Pb^{207}/Pb^{206} *ratio, R*, being unknown*

From the graphical treatment (Fig. 2b) it was shown that discordant age data on two samples will yield a concordant age without knowledge of the amount or the ratio of the original radiogenic lead contamination, or the lead lost at one time in the past. The calculations will be valid if the lead isotope data are available from at least two samples giving different ages and meeting the following conditions:

(a) The samples were deposited at the same time.
(b) The samples were contaminated by an original radiogenic lead having the same Pb^{207}/Pb^{206} ratio.
(c) The samples were altered, at one time in the past.

(d) The samples have been corrected for common lead so that N_{206} and N_{207} represent only the total radiogenic lead in the sample.

The algebraic equivalent of the two sample problem becomes:

$$\left.\begin{aligned}&\left[\frac{\lambda_2{}^n}{n!}(R_{8a}-R_{8b})+\frac{\lambda_1{}^n}{n!}(R_{5b}-R_{5a})\right]t^n\ldots\\&\quad+\left[\frac{\lambda_2{}^2}{2!}(R_{8a}-R_{8b})+\frac{\lambda_1}{2!}(R_{5b}-R_{5a})\right]t^2\\&\quad+[\lambda_2(R_{8a}-R_{8b})+\lambda_1(R_{5b}-R_{5a})]\,t+R_{5a}R_{8b}-R_{5b}R_{8a}=0\end{aligned}\right\}\quad(13)$$

where

$R_{5a}=\dfrac{N_{207a}}{N_{235a}}$, the ratio of the number of atoms of radiogenic Pb^{207} to U^{235} in sample A;

$R_{8a}=\dfrac{N_{206a}}{N_{238a}}$, the ratio of the number of atoms of radiogenic Pb^{206} to U^{238} in sample A;

$R_{5b}=\dfrac{N_{207b}}{N_{235b}}$ = the ratio of the number of atoms of radiogenic Pb^{207} to U^{235} in sample B;

$R_{8b}=\dfrac{N_{206b}}{N_{238b}}$ — the ratio of the number of atoms of radiogenic Pb^{206} to U^{238} in sample B.

If computing facilities are not available, equation (13) may be taken to the second degree and the terms f_1 and f_2 added.

Solving for t one obtains:

$$t=\frac{-b\pm\sqrt{(b^2-4ac)}}{2a}\quad(14)$$

where

$$2a=\lambda_1{}^2(R_{5b}-R_{5a})+\lambda_2{}^2(R_{8a}-R_{8b})$$
$$b=\lambda_1(R_{5b}-R_{5a})+\lambda_2(R_{8a}-R_{8b})$$
$$c=R_{5a}R_{8b}-R_{5b}R_{8a}+f_2(R_{8a}-R_{8b})+f_1(R_{5b}-R_{5a})$$

For geologically possible values of R_{5a}, R_{8a}, R_{5b}, and R_{8b}, fulfilling assumptions (a) through (d) given above, equations (13) and (14) have two positive real roots. Analogous to equations (7) and (8) the two positive roots of these equations approach the concordant ages corrected for original radiogenic lead and loss of lead or gain of uranium.

Calculation of concordant ages using normalized difference ratios

If discordant analytical age data are available for two samples, A and B, concordant ages can be calculated using normalized difference ratios without first correcting for a specific common lead. However, the Pb^{207}/Pb^{206} ratio, R^*, must be either assumed or determined from independent isotopic data. In order

for this calculation to be valid it is necessary, as in the previous cases, for the two or more samples in question to meet the following conditions:

(a) The samples must have different amounts of lead and uranium.
(b) The samples were formed at essentially the same time.
(c) The samples contained at the time of their formation a common lead with the same Pb^{207}/Pb^{206} ratio.
(d) The samples contained at the time of their formation an original radiogenic lead with the same Pb^{207}/Pb^{206} ratio, or
(e) The samples were altered at one time in the past.
(f) If either (c) or (d) applies, the samples must not have been subjected to recent loss or gain of lead or uranium.
(g) The samples must not contain thorium if Pb^{208} is used as the index isotope.

The graphical concordant age solution shown in Fig. 5(a) and (b) may be obtained algebraically from the following equation:

$$\left(\frac{R^*\lambda_1{}^n}{n!} - \frac{R\lambda_2{}^n}{n!}\right)t^n \ldots + \left(\frac{R^*\lambda_1{}^2}{2!} - \frac{R\lambda_2{}^2}{2!}\right)t^2 + (R^*\lambda_1 - R\lambda_2)t + RR_{5(a-b)} - R^*R_{8(a-b)} = 0 \qquad (15)$$

where

$$R_{5(a-b)} = \frac{(N_{207}/N_{204})a - (N_{207}/N_{204})b}{(N_{235}/N_{204})a - (N_{235}/N_{204})b},$$

the ratio of the difference of the total number of atoms of Pb^{207} to U^{235} normalized with the index isotope, Pb^{204} in samples A and B; and

$$R_{8(a-b)} = \frac{(N_{206}/N_{204})a - (N_{206}/N_{204})b}{(N_{238}/N_{204})a - (N_{238}/N_{204})b},$$

the ratio of the difference of the total number of atoms of Pb^{206} to U^{238} normalized with the index isotope, Pb^{204}, in samples A and B.

If computing facilities are not available equation (15) may be carried only to the second power of t and the terms f_1 and f_2 added. Solving this equation for t one obtains,

$$t = \frac{-b \pm \sqrt{(b^2 - 4ac)}}{2a} \qquad (16)$$

where

$$2a = (R^*\lambda_1{}^2 - R\lambda_2{}^2)$$
$$b = (R^*\lambda_1 - R\lambda_2)$$
$$c = (RR_{5a-b} - R^*R_{8a-b} - R^*f_1 + Rf_2)$$

For geologically possible values of R^*, $R_{5(a-b)}$ and $R_{8(a-b)}$ fulfilling the assumptions (a) to (f), equation (15) has two positive roots. If original radiogenic lead is assumed to be responsible for the discordant trial ages obtained for samples A and B, the smaller root will approach, as the degree of the equation increased, a concordant age corrected both for the presence of an original radiogenic lead having a Pb^{207}/Pb^{206} ratio, R^*, and a single common lead. The isotopic composition of the common lead need not be known. If past alteration is assumed

to be responsible for the discordant trial ages, the larger root will approach the concordant "lead-loss" age as the degree of the equation increases. For the latter assumption, the smaller root will approach the time in the past when the alteration took place and R^* would now become the Pb^{207}/Pb^{206} ratio of the radiogenic lead produced by the uranium in the interval given by the two roots. Similarly, equation (16) also has two positive roots. Depending on the choice of t_1, f_1 and f_2, the smaller root will approach the concordant age corrected for original radiogenic lead or the larger root the lead-loss age.

If discordant analytical age data are available for three samples, A, B and C meeting the conditions (a) to (f) set forth above, concordant ages can be calculated from the normalized difference ratios as before, without knowledge of either the amounts or the Pb^{207}/Pb^{206} ratio of the contaminating common lead. In addition, the effects of either a single period of past loss or gain of lead or uranium, or the presence of an older generation of radiogenic lead can also be treated. Following the same notation used in equation (15), this equation takes the form:

$$\left.\begin{aligned}&\left[\frac{\lambda_1^{\,n}}{n!}\left(R_{5(a-c)}-R_{5(a-b)}\right)+\frac{\lambda_2^{\,n}}{n!}\left(R_{8(a-b)}-R_{8(a-c)}\right)\right]t^n\ldots\\&\quad+\left[\frac{\lambda_1^{\,2}}{2!}\left(R_{5(a-c)}-R_{5(a-b)}\right)+\frac{\lambda_2^{\,2}}{2!}\left(R_{8(a-b)}-R_{8(a-c)}\right)\right]t^2\\&\qquad+\left[\lambda_1\left(R_{5(a-c)}-R_{5(a-b)}\right)+\lambda_2\left(R_{8(a-b)}-R_{8(a-c)}\right)\right]t\\&\qquad\quad+R_{5(a-b)}R_{8(a-c)}-R_{5(a-c)}R_{(a-b)}=0\end{aligned}\right\}\quad(17)$$

If computing facilities are not available equation (17) may be taken only to the second degree and the terms f_1 and f_2 added. Solving for t, one obtains:

$$t=\frac{-b\pm\sqrt{(b^2-4ac)}}{2a}\qquad(18)$$

where

$$\begin{aligned}2a&=\lambda_1{}^2\left(R_{5(a-c)}-R_{5(a-b)}\right)+\lambda_2{}^2\left(R_{8(a-b)}-R_{8(a-c)}\right)\\b&=\lambda_1R_{5(a-c)}-R_{5(a-b)}\right)+\lambda_2\left(R_{8(a-b)}-R_{8(a-c)}\right)\\c&=R_{5(a-b)}R_{8(a-c)}-R_{5(a-c)}R_{8(a-b)}+f_1\left(R_{5(a-c)}-R_{5(a-b)}\right)+f_2\left(R_{8(a-b)}-R_{8(a-c)}\right)\end{aligned}$$

Equation (17) taken to the third degree or higher has two positive roots for values of the normalized difference ratios, $R_{5(a-b)}$, $R_{8(a-b)}$, $R_{5(a-c)}$ and $R_{8(a-c)}$, that are geologically significant. As in the previous case these roots approach, with increase in the degree of the equations, the exact concordant age corrected for original radiogenic lead or loss of lead. For most geologically significant values for the ratios equation (18) will also have two positive roots. The smaller root will for values of t_1 less than the lowest trial lead–uranium age rapidly approach the exact concordant age corrected for original radiogenic lead. With this value of t_1, the larger root, however, has no geologic meaning. In order to obtain the "lead-loss" age different values of t_1 equal to, or greater than, the largest trial lead–lead age must be substituted. The initial choice of t_1 may be guided by an approximate graphical solution of $R_{5(x-y)}$ versus $R_{8(x-y)}$ as shown in Fig. 5(b).

Acknowledgements –The writers are grateful to their many colleagues whose discussions and helpful criticism have contributed to this paper. In particular, we are indebted to Edward Monasterski, U.S. Geological Survey, for preparing Table 1 and for programming the expanded age equations. This work is part of a programme being conducted by the U.S. Geological Survey on behalf of the Division of Research, U.S. Atomic Energy Commission.

References

Ahrens L. H. (1955a) The convergent lead ages of the oldest monazites and uraninites (Rhodesia, Manitoba, Madagascar, and Transvaal). *Geochim. et Cosmochim. Acta* **7,** 294–300.

Ahrens L. H. (1955b) Implications of the Rhodesia age pattern. *Geochim. et Cosmochim. Acta* **8,** 1–15.

Aldrich L. T. and Wetherill G. W. (1958) Geochronology by radioactive decay. *Annu. Rev. Nucl. Sci.* **8,** 257–298.

Collins C. B., Farquhar R. M. and Russell R. D. (1954) Isotopic constitution of radiogenic leads and the measurement of geologic time. *Geol. Soc. Amer. Bull.* **65,** 1–21.

Eckelmann W. R. and Kulp J. L. (1956) Uranium–lead method of age determination—I. Lake Athabasca problem. *Bull. Geol. Soc. Amer.* **67,** 35–54.

Gerling E. K. (1958) Effect of metamorphism on geologic age as determined by the lead method. *Geochemistry* No. 4, 363–373. (Translation).

Giletti B. J. and Kulp J. L. (1955) Radon Leakage from radioactive minerals. *Amer. Min.* **40,** 481–496.

Greenhalgh D. and Jeffery P. M. (1959) A contribution to the Pre-Cambrian chronology of Australia. *Geochim. et Cosmochim. Acta* **16,** 39–57.

Horne J. E. T. and Davidson C. F. (1955) The age of the mineralization of the Witwatersrand. *Great Britain Geol. Survey Bull.* **10,** 58–73.

Horne J. E. T. (1957a) *Age of a Later Uraninite from the Witwatersrand.* Great Britain Geological Survey Age Determination Report 2, 1–4. (Unpublished).

Horne J. E. T. (1957b) *Ages of Uraninites from Nkana, Northern Rhodesia and from Shinkolobwe, Belgian Congo.* Great Britain Geological Survey Age Determination Report 3, 1–3. (Unpublished).

Houtermans F. G. (1946) Die Isotopenhäufigkeiten im natürlichen Blei und das Alter des Urans. *Naturwissenschaften* **33,** 185–186.

Houtermans F. G. (1947) Das Alter des Urans. *Z. Naturforf.* **2a,** 322–328.

Keevil N. B. (1939) The calculation of geological age. *Amer. J. Sci.* **237,** 195–214.

Kulp J. L., Bate G. L. and Broecker W. S. (1954) Present status of the lead method of age determination. *Amer. J. Sci.* **252,** 345–365.

Kulp J. L. and Eckelmann R. W. (1957) Discordant U–Pb ages and mineral type. *Amer. Min.* **42,** 154–164.

Louw J. D. and Strelow F. W. E. (1955) Geological age determinations on Witwatersrand uraninites using the lead-isotope method. *S. Afr. Geol. Soc. Trans.* **57,** 209–230.

Robinson S. C. (1955) Mineralogy of uranium deposits, Goldfields, Saskatchewan. *Bull. Canad. Geol. Surv.* **31,** 1–128.

Russell R. D. and Ahrens L. H. (1957) Additional regularities among discordant lead–uranium ages. *Geochim. et Cosmochim. Acta* **11,** 213–218.

Stieff L. R. and Stern T. W. (1956) Interpretation of the discordant age sequence of uranium ores. In Page L. R. *et al.* (Compilers) *Contributions to the Geology of Uranium and Thorium by the U.S. Geological Survey and Atomic Energy Commission for the United Nations International Conference on Peaceful Uses of Atomic Energy, Geneva, Switzerland,* 1955. U.S. Geol. Survey Prof. Paper 300, 549–555.

Stieff L. R., Stern T. W. and Milkey R. G. (1953) A preliminary determination of the age of some uranium ores of the Colorado Plateau by the lead–uranium method. *U.S. Geol. Surv. Circ.* 271, 1–19.

Stieff L. R., Stern T. W., Oshiro Seiki and Senftle, F. E. (1959) *Tables for the Calculation of Lead Isotope Ages.* U.S. Geol. Survey Prof. Paper 334-A, 1–40.

Tugarinov A. I. (1954) Reliability of the absolute age of uranium minerals from the ratio of lead isotopes. *Dokl. Akad. Nauk SSSR* **99,** 1061–1063.

Wetherill G. W. (1956) Discordant uranium–lead ages—I. *Trans. Amer. Geophys. Un.* **37,** 320–326.

Wickman F. E. (1939) Some graphs on the calculation of geological age. *Sveriges Geol. Undersökn. Årsbok* **33,** No. 7, 1–8.

Wickman F. E. (1942) On the emanating power and the measurement of geological time. *Geol. Fören. Stockholm Förh.* **64,** 465–476.

Wickman F. E. (1955) Leakage of uranium and lead and the measurement of geologic time. *Nuclear Processes in Geologic Setting.* NAS–NRC Publication 400, 62.

Geochimica et Cosmochimica Acta, 1961, Vol. 22, pp. 200 to 243. Pergamon Press Ltd. Printed in Northern Ireland

Geochemistry of the turbidites of the Normanskill and Charny formations—I

Effect of turbidity currents on the chemical differentiation of turbidites

J. N. Weber and G. V. Middleton
Department of Geology, McMaster University, Hamilton, Canada

(*Received in final form* 20 *May*, 1960)

Abstract—Thirty-one Normanskill greywackes and twenty-four Quebec group (Charny formation) arkoses have been analysed spectrographically to determine the concentrations of Ag, B, Ba, Be, Co, Cr, Cu, Ga, La, Mg, Mn, Mo, Ni, Sc, Sr, Ti, V, Y and Zr, of which Ag, Be, La, Mo and Y were rarely or never detected. The analyses indicate the nature and magnitude of chemical variations within turbidite beds, between beds in a stratigraphic section, between sections and between formations.

Despite the grading of turbidite strata, variation in concentration from the top to the bottom of a bed is small except for zirconium which is relatively concentrated at the base. Variation between beds and between sections is greatest as a result of the relative distances of the samples from successive turbidity flows and variation between formations is small, reflecting the uniformity of turbidite sediments derived from many terrestrial rock types with little chemical differentiation.

Introduction

To determine the role of turbidity currents as agents of sedimentological chemical differentiation of greywackes and other turbidite deposits, thirty-one samples of greywacke from the Normanskill formation near Normanskill, Catskill, New Baltimore and Mechanicville, New York, and twenty-four specimens of the feldspathic turbidites of the Charny formation near Quebec City and St. Romuald,* Quebec, Canada, were analysed spectrographically for eighteen minor and trace elements and one major element. The analyses were used to estimate the nature and magnitude of the variation within turbidite beds and between beds, between stratigraphic sections and between formations.

The effect of the source area upon the chemical composition of the turbidite deposits is shown by comparison of the analyses of the Normanskill and Charny formations with basic and acid igneous provenance, respectively.

When the analyses are compared with estimates of crustal abundances of the elements, the Normanskill and Charny turbidites appear to be undifferentiated crustal material which has been rapidly eroded and deposited upon the continental shelf. Periodic oversteepening of the slope gave rise to large turbidity currents which exhibited a laterally differentiated chemical composition from which turbidite beds were deposited.

Methods

1. *Sampling*

Samples of greywackes were taken from the Normanskill formation of Ordovician age of New York State from four carefully measured stratigraphic sections consisting of sequences of interbedded shales and greywackes. Intervals

* See sample localities in appendix for exact locations.

were measured to a tenth of a foot and the position of the sample in the interval was recorded. Only large samples of fresh material were collected.

Greywacke and shale samples were also taken from the Quebec group (Charny formation), from two stratigraphic sections, near Quebec City.

The Rensselaer formation was sampled by collecting from one large quarry in New York state. Several miscellaneous greywackes were analysed; these represent "grab samples" donated by various persons.

Several thin-sections were cut from each greywacke sample and most of the remainder was crushed using a steel hand crusher to a powder less than 200-mesh size. After mixing, 50 mg of the powder was combined with a palladium–graphite mixture and prepared for spectrographic analysis.

2. *Spectrographic methods*

Powdered specimens were mixed with equal parts of an internal standard mixture consisting of 0·1% palladium chloride in graphite, according to a method developed by Shaw (1960). The samples were ignited in the d.c. arc, using a Stallwood air jet, and the light was directed through a JACO 21-ft grating spectrograph with a Wadsworth mount and with first-order dispersion of 5·2 Å/mm. The condensing optics comprised a cylindrical lens (horizontal axis) with a focal length of 25 cm, a cylindrical lens (vertical axis) with a focal length of 6·7 cm placed 16·1 cm from the slit, a diaphragm with a 5 mm aperture placed 27·5 cm from the slit and a spherical lens with a focal length of 10 cm placed 58·1 cm from the slit. The distance from the arc to the slit was 72·5 cm. Light emitted by the excited atoms, directed through a slit 30μ wide and 6 mm long, was controlled in intensity by one wire-mesh screen and four steps (3, 4, 5, 6) of a seven-step rotating sector at the slit, adjacent steps having a log–intensity ratio of 0·2. Using "Special" grade graphite electrodes produced by the National Carbon Company, the samples were arced for approximately 100–110 secs at 220 V open circuit direct current with an amperage ranging from 3 A at the start to 7 A at the completion of the burn. Air passed through the Stallwood air jet at a rate of 1 l/min.

The portion of the spectrum from 2200 Å to 4900 Å was recorded on two photographic plates, Kodak emulsion SAI for wavelengths from 2200 to 3550 Å and emulsion IIIF for wavelengths of from 3550 to 4900 Å, and the plates were developed for exactly 3 min in D-19 developer at 20°C. Samples were arced in triplicate, each replicate on a different set of photographic plates. Photometric measurements were made using an ARL microdensitometer, and emulsion calibration curves were constructed at various intervals covering the spectrum. Background corrections selected by Shaw were applied to the spectral lines. A standard, either the granite G1 or the dibase W1, was added to each set of photographic plates.

Computation was carried out with a standard calculation board and working curves were constructed from values obtained from artificial standards.

The spectral lines measured are listed in Table 1.

Precision is measured as the magnitude of the difference between three replicate analyses of one sample, and is calculated by the method given in Shaw

and Bankier (1954) and Shaw (1954). Precision was calculated for several elements using either twenty-two G1 standards or ten W1 standards and the values are given in Table 2. Because the values differ little from those obtained by Shaw, and inasmuch as the same method, spectrograph, calibration and working curves were used, the table of precision (Table 3) given by Shaw (1960) is applicable here.

Accuracy or the magnitude of the difference between the values of the natural standards G1 and W1 determined by the writer and the values of G1 and W1 generally agreed upon by spectrographers* is given in Table 4 where "nd" indicates that the spectral line was not detected, "tr" denotes that the line was too faint to measure accurately and "s" shows that the spectral line was too intense to measure its density. Twenty-two samples of G1 and ten samples of W1 were burned.

The concentrations of the elements in G1 and W1 agree fairly closely with the accepted values except in the case of strontium where the figures are abnormally high. The cause of the high values determined from a line of average intensity in a spectral region of very little background and very few spectral lines, is unknown. However, rather than use the abnormally high values of strontium, it appears appropriate to apply a correction factor reducing the strontium concentrations, and the following method was used. Plotting strontium values determined in this paper on the abscissa and strontium values determined by Herzog and Pinson on the ordinate, two points (W1 and G1) can be placed on the graph. After the points are joined by a straight line, the authors' strontium values read on the abscissa are corrected by reading off the ordinate. The correction factor assumes, of course, that a linear relationship exists between the true and the determined values of strontium, and as no basis for this assumption is known, both the determined and the corrected values for this element are given in the analyses.

All concentrations are expressed in parts per million (p.p.m.) except magnesium which is written in per cent (%).

3. *Statistical methods*

Several statistical techniques were used in the treatment of data.

(a) An "F-test" was applied to sets of populations to determine if two populations in question had a common standard deviation, s. Unless two populations possess nearly identical standard deviations, a further procedure to test whether or not the means of the two populations differ is invalid. The equations used are:

$$F = s_1^2/s_2^2 \quad \text{assuming} \quad s_1^2 > s_2^2$$

where:

$$s_1^2 = \sum \frac{(x_1 - \bar{x}_1)^2}{N-1} \qquad s_2^2 = \sum \frac{(x_2 - \bar{x}_2)^2}{N-1}$$

where x_1 denotes observations from the first population and x_2 from the second, each with N observations. If the populations have the same standard deviation, F will be less than $F\alpha(N-1)$.

* Ahrens (1955), Degenhardt (1957), Fairbairn (1953), Fleischer (unpublished), Herzog and Pinson (1955), Mackenzie *et al.* (1958), Shaw (1960), Smales (1955), Young (1958).

(b) To determine whether or not two populations had identical means, a "Student t-test", H: $u_T = u_B$ was applied. A value t was calculated from the following formulae and the means were considered to be equal if t fell between two values $\pm t_{1/2\alpha,(2N-2)}$

$$t = \frac{\bar{X}_T - \bar{X}_B}{S_p\sqrt{(1/N_T + 1/N_B)}}$$

$$S_p^2 = \frac{(N_T - 1)S_T^2 + (N_B - 1)S_B^2}{N_T + N_B - 2}$$

$$S_B^2 = \sum \frac{(X_B - \bar{X}_B)^2}{N - 1} \qquad S_T^2 = \sum \frac{(X_T - \bar{X}_T)^2}{N - 1}$$

where X_T denotes observations from the T population, X_B from the B population; $\bar{X}_T$ is the average of the X_T observations; N_T is the number of observations in the T population.

Turbidites of the Normanskill and Charny formations. Two formations consisting of shale and greywacke or shale and arkose sequences were selected to illustrate the effect of turbidity currents on the chemical homogeneity of turbidites, the Normanskill formation of New York state and the Charny formation of the Quebec group of the province of Quebec, Canada.

The Normanskill formation is estimated by RUEDEMANN (1930) to contain close to 2000 ft of "mostly dark grey to black argillaceous shales, but also red and green shales and heavy beds of chert and grit". The "grit" beds, containing a variety of rock fragments, "are ever present in the Normanskill shale" and range in thickness from "two feet to thirty feet". The occurrence of mud-pellet intraformational conglomerates, the regular alternations of grit and shale, the "ripple marks", cross-bedding and mud flow structures "give the impression that this formation was deposited in shallow water, probably near shore, where the velocity of the currents was frequently and rapidly changing" (RUEDEMANN, 1942). The only fossils found are graptolites, seaweed and eurypterids, the latter being fragmentary remains found only at one locality.

It is noteworthy that earlier authors, who did not understand the significance of graded bedding, nowhere mention this, the dominant sedimentary structure found in the Normanskill greywackes, and abundant flute casts and other bedding plane markings are uncommonly described. On the other hand, cross-bedding, which is rare in the Normanskill is frequently mentioned. The maximum bed thickness quoted by RUEDEMANN is probably in excess of the true maximum thickness, since RUEDEMANN did not recognize the composite nature of the beds not separated by any shale parting. The maximum thickness observed was one bed 10 ft thick measured in a stratigraphic section.

Field studies have clearly shown that the Normanskill greywackes are typical turbidites produced by the settling of a turbid mixture of sediment and water which slumped from the shelf environment probably because of local over-steepening of the slope, and moved as a dense current into deeper water. Local over-steepening apparently took place where relatively unweathered sedimentary

material derived from a nearby land mass was supplied at a rate greater than could be redistributed by normal current action.

Structures and features which are characteristic of turbidite rocks are described from field evidence:

(1) Graded bedding. Every greywacke bed in the formation shows a sharp well-defined contact with the underlying shale (or greywacke). Some beds show well-defined grading and pass up gradually into the overlying shale. Most beds are not well-graded in the main part of the bed (at least, the grading is not apparent in the field) but show a rather poorly defined gradational upper contact. In many cases the upper surface shows a peculiar "ripple marking". The structure is here described noncommitally as "wavy bedding", because it is on a larger scale than normal ripple marking, shows the typical cross-sectional shapes neither of current nor of oscillation ripples and is irregularly patterned in plan (i.e. it does not show the regular linear crests typical of normal ripples). The rippled material is always of silt or very fine sand size, weathering brownish grey, and shows fine cross-bedding in cross-section. In some cases an undisturbed parallel lamination is developed. It appears that these structures are developed by the action of currents acting on the finer "tail" after the main body of the turbidity current had passed.

(2) Flute and load casts are typically developed. The size of the flute casting does not appear to be directly related either to the thickness of the overlying bed, or to its grain size.

(3) Drag marks and gouge channels.

(4) Mud-Pellet conglomerates.

(5) Very regular bedding and the absence of cut-and-fill structures, other than those which are a result of exaggerated flute or load casting.

(6) Rare cross-bedding. Where it occurs, it is of the variety known as "torrential" and is always developed in the upper parts of thick beds.

(7) The scarcity of fossils, especially within the sandstones. Where fossils occur they are found in the shale interbeds and are of planktonic organisms such as graptolites and seaweed.

In summary, the Normanskill formation comprises marine greywacke deposits of undoubted turbidity current origin.

The Charny formation of the Quebec group, a series of pre-Silurian Paleozoic rocks in the Appalachian Highlands of Quebec, also shows sedimentary structures and petrographic features which indicate a turbidite origin for the arkosic beds. Osborne (1953) mentions heterogeneous, poorly sorted sandstone beds from 6 in. to 40 ft thick, containing mingled grains of diverse sizes and showing a tendency to have more of the larger grains toward the bottom of a bed.

Mineral grains of generally unstable species such as diopside, augite and hypersthene are present and, along with other evidence, lead Osborne to the conclusion that the sandstones were formed by "downslope mass movement of marine sediments which were ultimately deposited with shales and siltstones".

In a later paper (Osborne, 1956) "it is inferred that the materials were inshore accumulations which intermittently became unstable and slid, lubricated with water, downslope to form the sandstones. The final deposits at depth have thick beds, in many places graded bedding, fluting of the underlying bed and other

features suggesting rapid accumulation. . . . They are the result of a structural condition, viz., a steep slope on which sediments and sedimentary rocks accumulated and down which the accumulated material slid intermittently".

"The beds of sandstone support the contention that the site of final accumulation of the rocks was in deep water, for otherwise the original sediments would not have the potential energy for the mixing of the materials and their spread across the sea bottom".

Petrography. The composition of the sandstones, as determined by modal analysis, will be given in Part II of the present paper. Further detailed work on the petrography of the Normanskill and Quebec rocks is in progress, and will be the subject of later communications. A brief summary of the main points follows.

Both the Normanskill and Quebec rocks show the heterogenous composition and poor sorting and rounding of grains typical of many turbidites. The grading of the beds, which may not be apparent in the field, is clearly demonstrated by the decrease in maximum grain size towards the top of the bed, as determined in thin section and on sliced hand specimens. The decrease in grain size is commonly correlated with a change in the mineralogical composition of the rock: most beds have less quartz and more clay or argillaceous rock fragments at the top, than at the bottom. The Quebec sandstones are generally coarser and occur in thicker beds than the Normanskill sandstones. Preliminary investigations show that the median grain size, and sorting, are not subject to such regular variation within the bed as the maximum size.

The Quebec Group rocks are compositionally simpler than the Normanskill. The former consist of quartz (27–77 per cent), polysynthetically twinned plagioclase feldspar (up to 4 per cent), other feldspar, including perthite (up to 18 per cent), a recrystallized chloritic "clay matrix" (7–53 per cent) and minor amounts of fine-grained rock fragments (less than 3 per cent), zircon, tourmaline, garnet, biotite, white mica, goethite, ilmenite, leucoxene and other heavy minerals. Carbonates may also be present, usually in minor quantities, but in some cases forming as much as 37 per cent of the rock.

The Normanskill rocks are more difficult to analyse owing to the abundance and diversity of the different rock fragments, which may very easily be confused with the clay matrix. Experiments have shown that operator error is so high that a distinction between clay matrix and fine-grained rock fragments has little objective significance for these rocks. Modal analyses indicate that the rocks are composed of quartz (15–42 per cent), feldspar (up to 4 per cent), clay and fine-grained rock fragments (30–63 per cent), carbonates, both as rock fragments and as cement (6–37 per cent), and minor amounts of zircon, tourmaline, leucoxene, biotite and other heavy minerals. An analysis of the different rock types found as fragments in one bed (analysis 6) indicates the following relative abundances: shales and slates 40 per cent, dark biopelites 8 per cent, sandstones and siltstones 8 per cent, limestones 25 per cent, siliceous metamorphic rocks 13 per cent, volcanic rocks 7 per cent. The figures given should be regarded as subject to large variance and operator error: nevertheless, it is clear that the fragments are mainly of fine-grained sedimentary and low-grade metamorphic rocks, with a small fraction of basic and intermediate volcanic rocks.

According to Krynine's classification (1948) the Normanskill sandstones are low rank greywackes, and the Quebec sandstones fall on or near the boundaries between low- and high-rank greywackes and arkoses.

Inasmuch as these two rock groups, the Normanskill and Quebec, were produced by gravity settling of a turbid suspension of relatively unsorted and little weathered rock material, it might be expected that heavier or larger grains would be the first to settle and that the finest material would come to rest only after a considerable period of time had passed. The heaviest grains are usually those containing high concentrations of the less abundant elements such as zirconium, titanium and nickel, as well as common elements such as iron, and it might be expected that elements characteristic of the "heavy mineral suite" of minerals would be highly enriched at the base of each turbidite bed. In a similar manner it might be expected that elements such as boron, barium and vanadium, which are precipitated slowly from the sea or are adsorbed on clays, would be concentrated in the upper, relatively clay-rich part of the bed.

This study proposes to outline the distribution of selected elements: (1) between the top and bottom of a turbidite bed, (2) between turbidite beds in a stratigraphic section, (3) between several stratigraphic sections in one formation, and (4) between different turbidite formations.

The distribution of elements within a turbidite bed. Samples from near the top and bottom of eleven individual beds were analysed. The results are given in Table 5 and are presented pictorially in Fig. 1. If the statistical test to determine whether the means of the concentrations of elements at the top and bottom are identical is applied (Tables 6 and 7), zirconium is found to be the only element which is consistently concentrated at the base relative to the top of a bed at the 1 per cent level of significance. Although the F-test indicates that the standard deviations for zirconium are different, the graph in Fig. 1(n) shows that the segregation of zirconium is real. At the 10 per cent level of significance, only copper shows a difference and at 40 per cent, a very low level of significance, a difference is suggested for chromium, nickel, strontium, titanium and vanadium.

t values can indicate in a general way, the order in which elements tend to differentiate between the top and bottom of a bed and this tendency is shown in Table 7.

Arithmetic means and standard deviations using top and bottom values of each bed are listed in Table 8.

Distribution of elements between beds. Two stratigraphic sections were selected to illustrate the extent of variation in concentration of elements between different beds. Section 1 comprises 66 ft of strata and section 2 contains about 145 ft of beds. Samples were collected from the beds at random, either at the top, bottom or somewhere in between. Because there appears to be little variation, consistent or inconsistent, from top to bottom of a bed, except for zirconium, this sampling method appears to be valid.

The analytical results are given in Tables 9 and 10 and are shown pictorially in Figs. 2 and 3.

Distribution of elements between sections. Comparison of two stratigraphic sections of the Quebec group is made in Table 11 showing an average of twenty-four

analysed specimens. The Normanskill formation (Table 12) is represented by four stratigraphic sections from which samples were taken from each bed crushed, weighted according to the thickness of the bed and mixed together to form a composite sample of each section. The composite samples were subsequently analyzed.

Variation between formations. A mean for the Normanskill was derived by taking the arithmetic average of four stratigraphic sections. The mean for the Quebec Group includes twenty-four samples from two stratigraphic sections.

One other rock unit, the Rensselaer formation of New York State is represented by four randomly chosen samples, from one section.

Macpherson (1958) analysed eleven arkosic greywackes, five feldspathic greywackes and thirteen volcanic greywackes, all of Pre-Cambrian age and probably of turbidite origin, for boron, chromium, vanadium, nickel, copper, manganese and barium. Because no information on the accuracy of his results is published, three of Macpherson's samples, one of each greywacke rock type, were analysed in this paper. The results are shown in Table 13. A large discrepancy exists for manganese, vanadium and barium. Macpherson's values for vanadium are probably too high because the concentrations were obtained by using spectral line V 3185·4 which, as shown by Shaw (1958) is coincident with a line of calcium. The spectral line used for manganese, Mn 4034·5 occurs in a region of high background intensity, and Macpherson makes no mention of applying background corrections. However, because agreement for boron, chromium, nickel and copper is reasonably good, the averages of his volcanic, feldspathic and arkosic greywackes may be used. It should be remembered that the great majority of the samples analysed by the writers came from two Paleozoic formations only, whereas Macpherson's averages represent a collection of greywackes, which although they are alike petrographically, come from a variety of formations which may have been deposited at periods of time separated by many hundreds of millions of years.

The Rensselaer analyses are shown in Table 14. Comparison of the means of several formations is made in Table 15.

Nine miscellaneous greywackes, most of them probably of turbidite origin, were donated by various persons and analyses of them are shown in Table 16. Because many of the formations are represented by only one or two samples, the analyses are not used except for general comparison purposes.

Discussion and Summary

The degree of variation within beds and between beds, between sections and between formations is summarized in Tables 17 and 18. The figures in Table 18 are the standard deviation given as the per cent of the mean (i.e., coefficient of variation). In order to produce a figure for variation within a bed, eleven means and eleven standard deviations were calculated for each element and the average was taken.

The results are rather unexpected. Because turbidites originate by the settling of grains of many sizes and compositions from turbulent moving suspensions, it might be expected that the heavier grains, which are those showing extremely

high concentrations of relatively uncommon elements such as zirconium and chromium, would rapidly sink to the bottom, leaving the lighter quartz and feldspar grains and the much smaller clay particles to settle later. Thus a heavy concentration of elements which are abundant in heavy minerals could be expected at the base of turbidite beds. Such is not the case, at least in the Normanskill formation, except for zirconium which even at the 1 per cent level of significance appears to be highly concentrated at the base of a stratum. Copper may behave in a similar manner but the results are not conclusive. Zirconium is present largely as the resistant heavy mineral zircon which was reported frequently from thin-section point counts and was shown to constitute at least 50 per cent of the transparent heavy minerals separated from one Normanskill greywacke.

Not only do the Normanskill greywackes show little consistent variation from top to bottom, but they show very little total variation in concentration of any kind. From Table 18, it can be seen that variation within beds is generally less than variation in any of the other units studied.

Within a bed, variation in concentration is least for elements such as nickel, boron, vanadium, barium, copper and chromium, that is, elements which are notably enriched in hydrolysate sediments as well as in heavy minerals. While the heavy mineral content may decrease upwards in a bed, the hydrolysate or clay content will increase. Boron, for example, may occur largely in tourmaline at the base of a bed. As tourmaline decreases in amount upwards, boron may be largely present in the clay fraction and the total boron content will vary little. The small percentage of the heavy minerals compared to the clay is offset by the much greater concentration of minor elements which they contain.

On the other hand, elements like zirconium and magnesium show no such counter-balancing action. Zirconium, present in high concentration as zircon at the base of a bed is only moderately concentrated from marine waters by clays, largely because little zirconium is available in soluble form.

Variation between beds is fairly large, much larger than could be explained by the sampling method. Figs. 2 and 3 indicate the absence of marked secular variations in composition in the Quebec Group over the time interval necessary to deposit about 150 ft of beds. Any small trends, if they do exist, are obscured by sampling and analytical methods. A change in the nature and composition of the source area is unlikely over the small period of time in which these beds were deposited. However, because it is unlikely that two successive turbidite flows or slides might originate at exactly the same position on the shelf area, super-position of flows originating many miles apart may not only account for the differences in composition but also for the considerable range of bed thickness. For example, at the location where the section was measured, one thick bed may represent a flow originating close at hand while a much thinner bed may be the record of the "tail" of a turbidity flow originating a hundred miles further along the shelf. If the reason for over-steepening of the shelf was the growth of a large river delta, certain areas of the delta where organic matter may be relatively abundant are quite sufficient to account for differences in copper and other elements which are rapidly deposited in the presence of decaying organic material. It is especially noteworthy in this regard that copper shows the greatest variation between beds,

as copper forms sulphide deposits at the first opportunity; very little hydrogen sulphide from decaying organisms is necessary for precipitation as a sulphide.

A considerable variation exists between sections. The Normanskill and Quebec sections show different degrees of variation but as the Quebec Group is represented by only two sections, the results are not very significant. The large variation in the Normanskill formation is probably a result of the position of the section relative to the source. A section far from the source of slumping would contain relatively little of the heavier and larger mineral grains. If zirconium may be taken to represent the heavy mineral fraction and boron the clay fraction, it will be seen that, generally speaking, the sections with high zirconium content have less boron, suggesting that zirconium-rich sections were closer to the source area. The results, however, are not conclusive.

The variation in concentration between formations is relatively small but larger than that within beds. Certain elements such as strontium, nickel, copper and barium have standard deviations about 50 per cent of the mean value whereas manganese and boron show very little variation having standard deviations of only 15 per cent of the mean. The lack of considerable variation is probably a reflection of the general similarity of turbidite material. The sediment is simply a mixture of debris weathered from a great many rock types with relatively unstable minerals such as feldspar included with others such as zircon and tourmaline. Strontium, the greatest variant, is probably present in the carbonate cement. Nickel, copper and barium which also vary considerably are a function of the quantity supplied by weathering of the source area as these elements are rapidly deposited in hydrolysate material included in the turbidites.

Boron, manganese and vanadium show relatively little variation within beds and between beds, between sections and between formations, although boron variation in the Normanskill sections for some reason is rather high.

In summary, greatest variation is shown between beds and between sections, probably as a result of super-position of turbidity flows originating many miles apart along a delta-shelf area and because of the location of sections at various positions away from the source. Variation between formations is smaller because turbidites are intimate mixtures of many types of weathered igneous metamorphic and sedimentary rock types and many geochemical segregations that fractional crystallization or other processes had accomplished in the crystallization of igneous rocks are destroyed by the process of sedimentological recombination. In other words, weathered material from all major igneous rock types is deposited together without the intervention of segregational sedimentary processes and no major differences are to be expected between one turbidite formation and another except for elements like strontium, calcium and magnesium which might be diagenetically redistributed as cement. Variation within beds is least, possibly because of a counter-balancing effect of elements which are contained both in the heavy mineral suite and in the hydrolysate fraction.

The best average representing the chemical composition, as far as minor elements are concerned, of a formation is apparently obtained by collecting grab samples distributed throughout the length, breadth and thickness of a formation, disregarding the position of the sample in a bed.

Effect of provenance on chemical composition

The Quebec group derived the bulk of its sediment from a crystalline granite–gneiss shield which is largely acidic in composition. The Normanskill greywackes, on the other hand, were supplied with a relatively more basic provenance comprising sedimentary, metamorphic and igneous source rocks.

Because certain elements are characteristically more highly concentrated in basic rocks than in acidic rocks, while the reverse is true of other elements, it is interesting to see whether or not the turbidites which are formed from the weathering products of these rocks retain the minor element distribution pattern of the parent.

Table 19 compares the distribution pattern of elements in acidic and basic rocks given by Rankama and Sahama (1950) and Nockolds and Allen (1953), with that of G1–W1 and of the Quebec and Normanskill turbidites. It is uncertain whether boron, gallium and strontium are more concentrated in acidic or basic rocks. However, cobalt, chromium, copper, magnesium, manganese, nickel, scandium and vanadium are more concentrated in basic rocks and have higher values in the Normanskill than in the Quebec turbidites. Zirconium is typical of acidic rocks and is higher in concentration in the Quebec group. The element which does not follow the pattern is barium which is high in acidic rocks but low in the average given for the Quebec group. This is undoubtedly caused by the bias in ignoring several analyses for barium in the average for the formation. In several analyses, barium was present in too high a concentration to be measured. Titanium is another element which fails for some reason to fit the pattern. With the exception of titanium, the Normanskill greywackes have higher concentrations of elements which are characteristically more abundant in basic rocks while the Quebec group derived largely from acidic rocks shows higher concentrations of elements from that clan.

The Rensselaer formation is also derived from a granite–gneiss provenance. Although only four analyses are available for comparison, it is clear that the Rensselaer greywackes are higher in barium and zirconium and lower in cobalt, chromium, copper, nickel, strontium and vanadium than the Normanskill greywackes.

Comparison with crustal abundance

In Table 20 are listed the estimates of crustal abundance by nine authors. Table 21 contains, perhaps, the most reliable estimate. If the formation means of the Normanskill and Quebec turbidites (Table 15) are compared with these figures it is apparent that no striking enrichment or impoverishment of the minor elements studied has taken place during the formation of turbidites from crustal material. A slight enrichment is shown for boron and zirconium and a slight decrease for chromium, magnesium, manganese, nickel and vanadium.

Comparison of shales and sandstones with the Normanskill and Quebec turbidites

Table 22 summarizes the average minor element content of shales, sandstones and the Normanskill and Quebec turbidites. In most cases, the concentration of elements in turbidites falls between the concentration in shales and sandstones.

This is quite expected inasmuch as turbidites are essentially mixtures of sandstone and shale.

Notable exceptions are cobalt, nickel and titanium. It is probable that cobalt and nickel values for the average shale need revising upwards. This is suggested both by the writers' unpublished analyses and also by analyses of pelites by SHAW (1954).

SUMMARY

Variation of the concentration of elements from the top to the bottom of a turbidite bed is very small and inconsistent except for zirconium which is concentrated near the base. Variation within beds is minimized by a compensation effect of elements which occur in both the clay matrix and heavy minerals. Variation between beds and sections is of a greater magnitude and results from the difference in distance from the origin of the slumping to the sample as in the case of beds in one section, or from the difference in distance from the source area to the sample as in the case of sections since turbidity currents are inhomogeneous both laterally and vertically.

In chemical composition, the turbidites fall between shales and sandstones and represent mixtures of these two rock types.

Acknowledgements—The writers are indebted to Dr. D. M. SHAW who supervised and directed the spectrographic analysis which was carried out in his spectrographic laboratories at McMaster University. The spectrographic analysis was undertaken by J. N. WEBER while most of the greywacke samples were collected and preliminary petrographic analysis undertaken by G. V. MIDDLETON.

PHILIP S. SIMONY is thanked for donation of several samples of the Gowganda formation including point-counts and for many helpful discussions. Dr. G. E. G. WESTERMANN and Dr. PH. KUENEN provided several European greywacke samples and Dr. W. H. WILLIAMS made helpful suggestions regarding the statistical manipulations.

Financial support was generously provided by Imperial Oil Company and the Woodrow Wilson National Fellowship Foundation during the period 1959–1960. Research funds of the National Research Council and the Geological Survey of Canada were gratefully accepted to cover the high costs of crushing and of spectrographic materials.

REFERENCES

AHRENS L. H. (1955) *Quantitative Spectrochemical Analysis of Silicates.* Addison-Wesley, London.

ANDERSON J. S. (1945) Chemistry of the Earth. *J. Proc. Roy. Soc. N.S. Wales* **76,** 329–345.

BERG G. (1929) *Vorkommen und Geochemie der Mineralischen Rohstoffe.* Leipzig.

CLARKE F. W. and WASHINGTON H. S. (1924) *The Composition of the Earth's Crust.* U.S. Geol. Surv. Prof. Paper 127.

DEGENHARDT H. (1957) Untersuchungen zur geochemischen Verteilung des Zirkoniums in der Lithosphäre. *Geochim. et Cosmochim. Acta* **11,** 279–309.

FAIRBAIRN H. W. (1953) Precision and accuracy of chemical analyses of silicate rocks. *Geochim. et Cosmochim. Acta* **4,** 143–156.

FERSMAN A. E. (1933) *Geokhimia.* Leningrad.

FLEISCHER M. (1955) Estimates of the abundances of some chemical elements and their reliability. In A. POLDERVAART (Editor) *Crust of the Earth.* Special Paper 62 Geological Society of America.

FLEISCHER M. (unpublished) Personal communication to D. M. SHAW.

GOLDSCHMIDT V. M. (1937) The laws of geochemical distribution of the elements. IX—The abundance of the elements. *Norske vidensk. Akad. Oslo. Math.-Nat. Klasse* **4,** 1–148.

GREEN J. (1953) Geochemical table of the elements for 1953. *Bull. Geol. Soc. Amer.* **64,** 1001–1012.

Herzog L. F. and Pinson W. H. (1955) The strontium and rubidium contents of the Granite G1 and the Diabase W1. *Geochim. et Cosmochim. Acta* **8,** 295–298.

Krynine P. D. (1948) The megascopic study and field classification of sedimentary rocks. *J. Geol.* **56,** 130–165.

McKenzie R. M., Oertal A. C. and Tiller K. G. (1958) Analyses of the standard rocks G1 and W1. *Geochim. et Cosmochim.* **14,** 68–72.

Macpherson H. G. (1958) A chemical and petrographic study of Precambrian sediments. *Geochim. et Cosmochim. Acta* **14,** 73–92.

Mason B. (1952) *Principles of Geochemistry.* John Wiley, New York.

Nockolds S. R. and Allen R. (1953) The geochemistry of some igneous rock series. *Geochim. et Cosmochim. Acta* **4,** 105–142.

Osborne F. F. (1953) Concretion conglomerate in the Charny Sandstone, Quebec. *Trans. Roy. Soc. Canada* Ser. 3, Sect. LV, **47,** 55–60.

Osborne F. F. (1956) Geology near Quebec City. *Canad. Naturalist* **83,** 157–223.

Polanski A. (1948) A new essay of evaluation of the chemical composition of the earth. *Soc. des Amis des Sci. Lettres de Posnan* Ser. B, **9,** 39–40.

Rankama R. and Sahama Th. G. (1950) *Geochemistry.* Univ. of Chicago Press, Chicago.

Ruedemann R. (1930) Geology of the Capital district. *Bull. N.Y. State Mus.* 285.

Ruedemann R. (1942) Geology of the Catskill and Kaaterskill Quadrangles—I. *Bull. N.Y. State Mus.* 331.

Schneiderhöhn H. (1934) Die ausnutzungsmöglichkeiten der deutschen Erzlagerstatten. *Metallwirtschaft* **13,** 151–157.

Shaw D. M. (1954) Trace elements in pelitic rocks—I and II. *Bull. Geol. Soc. Amer.* **65,** 1151–1182.

Shaw D. M. (1958) A vanadium-calcium spectral line coincidence at 3185 Å and its effect on vanadium abundance data. *Geochim. et Cosmochim. Acta* **15,** 159–161.

Shaw D. M. (1960) Spectrochemical analysis of silicates using the Stallwood Jet. Canad. Min. **6** (4), 467–482.

Shaw D. M. and Bankier J. D. (1954) Statistical methods applied to geochemistry. *Geochim. et Cosmochim. Acta* **5,** 111–123.

Smales A. A. (1955) Some trace elements in G1 and W1 by neutron activation. *Geochim. et Cosmochim. Acta* **8,** 300.

Turekian K. K. and Kulp J. L. (1956) The geochemistry of strontium. *Geochim. et Cosmochim. Acta* **10,** 245–296.

Young E. J. (1958) G1 and W1 values—spectrochemical determination using an internal standard. *Geochim. et Cosmochim. Acta* **13,** 339–340.

Statement of Analyses

(Concentration of all elements except magnesium is given in parts per million (p.p.m.). Magnesium is stated in per cent (%). Sr* indicates corrected concentration values of strontium.)

Analysis	B	Ba	Co	Cr	Cu	Ga	Mg	Mn	Ni	Sc	Sr	Sr*	Ti	V	Zr
1	120	410	24	100	26	2	1·7	490	45	11	240	170	9000	66	710
2	120	410	19	91	24	10	1·8	480	41	9	290	200	7200	59	360
3	55	380	24	130	27	25	2·0	800	50	9	430	260	7600	90	480
4	61	350	22	120	25	9	1·7	670	44	8	250	180	6600	86	550
5	33	220	15	120	24	8	0·56	810	29	7	670	380	3700	59	480
6	56	240	14	93	25	9	1·2	440	32	6	140	120	4300	49	490
7	74	280	15	95	22	9	1·3	520	32	6	140	120	4600	54	410
8	73	320	17	100	25	11	1·6	560	35	8	230	170	5000	53	480
9	84	270	14	73	27	4	1·8	420	33	6	180	140	5700	45	430
10	79	300	18	99	24	5	2·2	590	37	4	240	170	5400	40	310
11	42	430	23	210	52	15	0·96	740	50	12	300	200	6700	97	830
12	38	380	16	140	31	14	1·0	560	39	9	300	200	4300	91	330
13	85	320	16	85	21	6	1·9	440	35	6	280	190	7000	51	530
14	96	270	20	86	25	11	2·6	430	38	7	210	150	6600	48	430
15	98	330	20	100	25	tr	1·8	600	44	10	250	180	8600	56	640
16	91	320	20	80	23	tr	1·5	410	43	9	200	150	6800	59	380
17	76	410	22	100	26	3	1·8	500	44	10	270	180	7700	61	560
18	91	360	18	85	23	11	2·3	490	39	10	260	180	7700	49	370
19	83	390	20	98	26	3	1·7	500	44	10	320	210	8000	65	560
20	99	400	16	82	23	3	1·6	420	38	10	240	170	7000	58	420
21	89	420	21	85	30	14	2·5	350	39	8	190	150	5400	61	330
22	63	320	21	120	28	18	1·7	520	39	5	350	220	5200	62	470
23	77	330	18	94	24	11	1·9	500	36	8	220	160	5300	57	320
24	77	370	19	100	27	18	1·9	490	40	8	240	170	5300	58	270
25	89	150	9	87	30	tr	0·47	520	31	2	52	77	23,000	56	1100
26	110	350	18	56	2	5	0·83	500	28	5	110	110	13,000	50	720
27	74	280	24	57	8	6	1·8	—	29	6	180	140	7700	39	310
28	21	450	27	180	43	18	1·0	640	53	7	610	350	5600	62	610
29	24	230	18	120	32	14	0·97	590	34	7	240	170	3600	61	280
30	33	400	20	140	26	14	1·1	550	39	9	470	280	4400	64	290
31	61	440	21	120	30	11	1·7	650	47	10	330	210	6600	82	410
32	39	s	tr	120	4	4	0·19	480	9	nd	120	110	5300	34	650
33	62	110	14	93	tr	3	0·71	660	20	5	160	130	7600	40	670
34	68	86	4	170	7	tr	0·52	800	13	nd	59	81	8800	49	820
35	85	71	14	130	5	5	0·91	860	27	5	84	94	16,000	47	2000
36	63	180	17	110	13	4	0·70	940	28	nd	100	100	6100	45	510
37	73	210	32	110	32	18	1·5	830	40	8	120	110	11,000	43	530
38	76	290	22	110	7	13	1·2	900	27	5	110	110	13,000	47	790
39	57	400	16	110	9	14	1·3	1000	20	6	150	130	12,000	51	650

Statement of Analyses (*contd*).

Analysis	B	Ba	Co	Cr	Cu	Ga	Mg	Mn	Ni	Sc	Sr	Sr*	Ti	V	Zr
40	51	630	14	87	5	6	1·1	980	23	5	130	120	8700	38	530
41	49	200	18	100	4	10	1·3	s	31	5	110	110	14,000	49	790
42	49	s	16	77	6	tr	0·72	1000	20	tr	160	130	8000	33	450
43	69	—	8	54	19	3	0·40	370	14	3	100	100	7100	32	470
44	55	580	19	67	10	16	1·1	630	33	8	140	120	8600	49	410
45	60	—	7	79	14	3	0·42	350	14	1	84	93	7300	45	660
46	89	150	9	87	30	tr	0·47	520	31	3	52	77	23,000	56	1100
47	110	350	18	56	2	5	0·83	500	28	5	110	110	13,000	50	720
48	74	280	24	57	8	6	1·8	—	29	6	180	140	7700	40	310
49	94	48	tr	83	5	tr	0·55	130	42	7	92	98	5500	45	2000
50	100	120	10	66	5	14	0·68	76	22	5	95	99	3100	51	710
51	140	260	29	84	12	36	1·7	93	48	12	130	120	3800	52	810
52	80	92	8	61	5	10	0·61	92	33	6	72	87	3700	41	1500
53	43	99	tr	51	4	tr	0·30	89	19	4	63	83	2800	27	830
54	64	61	10	81	6	tr	0·40	87	47	6	73	88	3000	49	670
55	51	81	11	66	3	6	0·45	150	22	5	130	120	5600	30	890
56	23	800	20	140	24	13	1·9	950	30	7	330	220	7400	51	580
57	17	510	tr	130	5	tr	0·74	600	15	8	260	180	5600	41	460
58	32	840	13	110	11	8	1·2	630	21	5	340	220	5300	43	450
59	56	830	21	130	14	14	2·2	840	34	10	220	160	7000	59	360
60	91	420	25	140	9	13	1·7	610	65	11	120	110	10,000	88	560
61	140	510	31	150	260	6	2·0	1200	70	15	150	130	13,000	100	520
62	74	s	19	110	12	tr	0·99	720	42	tr	110	110	5400	57	220
63	170	660	36	580	160	5	3·0	870	130	19	160	130	15,000	100	430
64	20	150	59	320	56	15	0·69	120	100	20	350	220	4800	96	230
65	30	120	27	180	46	13	0·58	110	84	9	230	170	3800	64	200
66	30	170	33	230	35	14	0·61	120	110	11	510	300	3800	71	190
67	69	270	16	130	4	8	3·3	670	32	8	140	120	5500	54	340
68	70	400	21	120	5	14	4·0	620	38	10	160	130	6400	66	250
69	34	620	11	130	8	3	4·3	680	59	9	270	180	3700	48	200
70	45	250	tr	92	5	tr	4·4	590	33	7	600	340	4500	42	340
71	63	570	29	87	7	6	2·1	s	37	10	110	110	8000	62	330
72	26	500	31	170	150	10	4·0	320	55	9	130	120	4700	77	200
73	tr	290	tr	64	5	6	1·1	110	11	tr	92	98	1100	24	tr
74	15	470	18	190	2	16	3·8	510	52	7	170	140	4200	55	200
75	13	470	15	150	tr	13	2·2	230	32	5	130	120	2500	42	210
76	nd	240	nd	tr	35	nd	3·8	2400	tr	50	2800	—	nd	tr	nd
77	tr	200	tr	tr	23	tr	tr	tr	tr	tr	tr	—	tr	tr	1100
78	120	340	16	100	25	14	3·0	100	33	8	100	100	6400	68	310
79	26	410	700	900	75	tr	0·70	260	260	28	400	250	11,000	320	s

Sample Localities

Analysis	Location
1	Greywacke. Normanskill formation. Section 1; 10·5–13·2 ft interval. Base.
2	Greywacke. Normanskill formation. Section 1; 10·5–13·2 ft interval. Near top.
3	Greywacke. Normanskill formation. Section 1; 0–4·5 ft interval. Base.
4	Greywacke. Normanskill formation. Section 1; 0–4·5 ft interval. About 1·5 ft from top.
5	Greywacke. Normanskill formation. Section 1; 0–4·5 ft interval. Top
6	Greywacke. Normanskill formation. Section 2; 82·5–92·5 ft interval. Near base.
7	Greywacke. Normanskill formation. Section 2; 82·5–92·5 ft interval. Middle.
8	Greywacke. Normanskill formation. Section 2; 82·5–92·5 ft interval. Near top.
9	Greywacke. Normanskill formation. Section 2; 58·4–63·4 ft interval. 1 ft from base.
10	Greywacke. Normanskill formation. Section 2; 58·4–63·4 ft interval. Near top.
11	Greywacke. Normanskill formation. Section 2; 29·1–32·2 ft interval. Base.
12	Greywacke. Normanskill formation. Section 2; 29·1–32·2 ft interval. Near top.
13	Greywacke. Normanskill formation. Section 3; 4·8–8·2 ft interval. Base.
14	Greywacke. Normanskill formation. Section 3; 4·8–8·2 ft interval. 1 ft from top.
15	Greywacke. Normanskill formation. Section 3; 11·8–16·0 ft interval. Base.
16	Greywacke. Normanskill formation. Section 3; 11·8–16·0 ft interval. 1 ft below top.
17	Greywacke. Normanskill formation. Section 3; 61·2–62·5 ft interval. Near base.
18	Greywacke. Normanskill formation. Section 3; 61·2–62·5 ft interval. Top.
19	Greywacke. Normanskill formation. Section 3; 37·0–41·3 ft interval. Base.
20	Greywacke. Normanskill formation. Section 3; 37·0–41·3 ft interval. Near top.
21	Greywacke. Normanskill formation. Section 4; 0–6·0 ft interval. Base.
22	Greywacke. Normanskill formation. Section 4; 0–6·0 ft interval. Near base.
23	Greywacke. Normanskill formation. Section 4; 0–6·0 ft interval. 3 ft from top.
24	Greywacke. Normanskill formation. Section 4; 0–6·0 ft interval. 1 ft from top.
25	Greywacke. Quebec group. Section 2; 140–147 ft interval. Base.
26	Greywacke. Quebec group. Section 2; 140–147 ft interval. 15 to 18 in. above base.
27	Greywacke. Quebec group. Section 2; 140–147 ft interval. 2–2·5 ft below top.

Sample Localities (*contd*)

Analysis	Location
28	Greywacke. Composite of 11 samples of section 1 of the Normanskill formation. Section measured on south-west side of Normanskill, New York, west of old bridge.
29	Greywacke. Composite of 46 samples of section 2 of the Normanskill formation. Section measured at Austin's Glen near Catskill, New York.
30	Greywacke. Composite of 26 samples of section 3 of the Normanskill formation. Section measured at quarry $1\frac{1}{4}$ miles south of New Baltimore, New York.
31	Greywacke. Composite of 7 samples of section 4 of the Normanskill formation. Section measured at road-cut south-west of Mechanicville, New York on Highway 146 about 2 miles east of Clifton Park.
32	Greywacke. Quebec group. Section 2; 1·0–2·0 ft interval
33	Greywacke. Quebec group. Section 2; 2·0–8·5 ft interval. Top.
34	Greywacke. Quebec group. Section 2; 14·5–15·5 ft interval. Base.
35	Greywacke. Quebec group. Section 2; 19·0–19·5 ft interval.
36	Greywacke. Quebec group. Section 2; 33·2–37·1 ft interval. Base.
37	Greywacke. Quebec group. Section 2; 37·1–38·5 ft interval. About 0·2 ft from top.
38	Greywacke. Quebec group. Section 2; 42·2–46·9 ft interval. Just above middle.
39	Greywacke. Quebec group. Section 2; 58·5–66·0 ft interval. Above centre.
40	Greywacke. Quebec group. Section 2; 66·5–78·0 ft interval. Top.
41	Greywacke. Quebec group. Section 2; 82·5–94·5 ft interval. 1·0 ft from top.
42	Greywacke. Quebec group. Section 2; 101·0–102·3 ft interval. 0·4 ft from top.
43	Greywacke. Quebec group. Section 2; 111·6–112·0 ft interval.
44	Greywacke. Quebec group. Section 2; 115·6–117·5 ft interval. Top.
45	Greywacke. Quebec group. Section 2; 125·9–128·5 ft interval. 0·2 ft from base.
46	Greywacke. Quebec group. Section 2; 140–147 ft interval. Base. Identical with analysis 25.
47	Greywacke. Quebec group. Section 2; 140–147 ft interval. 15–18 in. above base. Identical with analysis 26.
48	Greywacke. Quebec group. Section 2; 140–147 ft interval. 2–2·5 ft below top. Identical with analysis 27.
49	Greywacke. Quebec group. Section 1; 0–37 ft interval. 6–7 ft above base.
50	Greywacke. Quebec group. Section 1; 0–37 ft interval. About 10·0 ft below top.
51	Greywacke. Quebec group. Section 1; 37–45 ft interval. 5–6 ft below top.
52	Greywacke. Quebec group. Section 1; 37–45 ft interval. About 2 ft below top.
53	Greywacke. Quebec group. Section 1; 45–62 ft interval. Top.
54	Greywacke. Quebec group. Section 1; 62–63 ft interval.
55	Greywacke. Quebec group. Section 1; 65·5–67·0 ft interval.
56	Greywacke. Rensselaer formation. Quarry at East Nassau, New York.
57	Greywacke. Rensselaer formation. Quarry at East Nassau, New York.
58	Greywacke. Rensselaer formation. Quarry at East Nassau, New York.
59	Greywacke. Rensselaer formation. Quarry at East Nassau, New York.
60	Greywacke. Kiskatom formation. Highway 23 A, west of Kaaterskill Falls, New York.

Sample Localities (*contd*).

Analysis	Location
61	Greywacke. Kiskatom formation. Small falls below Kaaterskill Falls, Highway 23 A, New York.
62	Greywacke. Kiskatom formation. Highway 23 A, west of Kaaterskill Falls, New York.
63	Greywacke. Kiskatom formation. Small falls below Kaaterskill Falls, Highway 23 A, New York.
64	Arkosic greywacke. Pre-Cambrian. $\frac{3}{4}$ mile south of New Liskeard, Northern Ontario. From H. G. Macpherson (analysis no. 6).
65	Feldspathic greywacke. Pre-Cambrian. $1\frac{1}{2}$ miles south-west of the south end of Porcupine Lake, Ontario. From H. G. Macpherson (analysis no. 14).
66	Volcanic greywacke. Pre-Cambrian. $\frac{3}{4}$ mile south of New Liskeard, Northern Ontario. From H. G. Macpherson (analysis no. 21).
67	Greywacke. Quarry south of Wildemann, Ober-Harz, north-west Germany. Upper Mississippian "Kulm". From G. E. G. Westermann.
68	Greywacke. Quarry south of Wildemann, Ober-Harz, north-west Germany. Upper Mississippian "Kulm". From G. E. G. Westermann.
69	Greywacke. Macigno (Oligocene). Reno Valley, south of Poretta Terme, between Bologna and Pisa, Italy. From Ph. Kuenen.
70	Greywacke. Formazione "Marnoso-Arenacea" (Lower Miocene). Upper Tiber River, between Pieve S. Tefano and Verghereto, Italy. From Ph. Kuenen.
71	Greywacke. Barmouth Grit (Cambrian) Bryn-Anas, north of Barmouth, Northern Wales. From Ph. Kuenen.
72	Greywacke. Gowganda formation. Northern part of township 143, Blind River, Ontario. From P. S. Simony.
73	Greywacke. Gowganda formation (upper). South shore of west arm of Quirke Lake, township 144, Blind River, Ontario. From P. S. Simony.
74	Greywacke. Gowganda formation (lower). North-east of Hough Lake, township 143, Blind River, Ontario. From P. S. Simony.
75	Greywacke. Gowganda formation (about 500 ft from the base). Stan Rock Mines near tip of Peninsula between the bays of Quirke Lake, township 143, Blind River, Ontario. From P. S. Simony.
76	Carbonate material from greywacke. Normanskill formation. Section 1; 10·5–13·2 ft interval.
77	Quartz–feldspar fraction of greywacke. Normanskill formation. Section 1; 10·5–13·2 ft interval.
78	Clay matrix from greywacke. Normanskill formation. Section 1; 10·5–13·2 ft interval.
79	Heavy mineral fraction of greywacke. Normanskill formation. Section 1; 10·5–13·2 ft interval.

Description of Stratigraphic Sections of the Normanskill Formation and the Quebec Group

Normanskill section 1

Location: South-west side of Normanskill, west of the old bridge.
Measured from the top down.

0–4·5	*Greywacke*	very coarse, lower bedding plane has poorly exposed flow-marks. Top 1·5 ft are cross-bedded, remainder massive. Sharp contrast at 4·5 ft with truncated cross-bedding.
4·5–6·5	*Siltstone*	dark grey, laminated, grading from very fine sandstone at base to shale above. Ripple marked.
6·5–7·3	*Shale*	dark grey, breaking with uneven, hackley fracture. Slickensides.
7·3–8·9	*Greywacke*	medium to fine-grained, probably slightly graded.
	Shale parting	
8·9–9·6	*Greywacke*	medium to coarse-grained, strong flow-markings at base.
9·6–10·5	*Greywacke*	medium-grained. Upper half finely cross-bedded and may be welded onto base of bed above. Base shows flow-markings.
10·5–13·2	*Greywacke*	very coarse-grained at base, grading upwards. A little intra-formational conglomerate near the top.
13·2–14·3	*Greywacke*	medium-grained. Massive.
14·3–16·1	*Greywacke*	laminated and showing small scale cross-bedding, especially near the top.
16·1–21·0	*Greywacke*	laminated and showing small scale cross-bedding, passing down into beds disturbed by folding and slumping.

Normanskill section 2

Location: Austin's Glen, near Catskill, N.Y. Section begins on north bank.
Measured from top to base. Beds strike 040° magnetic and dip 60° NW.

0–0·4	*Greywacke*	dark grey, coarse, graded at very top only. Fine markings on lower surface, horizontal, strike 040° magnetic.
0·4–0·8	*Siltstone*	poorly cleaved, with a central poorly defined bed of fine greywacke.
0·8–1·6	*Greywacke*	coarse, massive, no apparent grading. Base of bed with fine flow markings plunging to 235° magnetic.
1·6–1·8	*Siltstone*	cleaved, as above.
1·8–2·3	*Greywacke*	coarse, massive, graded slightly.
2·3–3·2	*Shale*	very dark brown or purplish brown, poorly cleaved.
3·2–3·4	*Greywacke*	or siltstone. Very fine-grained.
3·4–3·9	*Shale*	as above.
3·9–4·5	*Greywacke*	coarse-grained, very slightly graded.
4·5–6·2	*Shale*	as above.
6·2–6·7	*Greywacke*	massive. Large (?) ripple marks on top surface. Base flat or with faint flow-markings plunging to 235° magnetic.
6·7–7·4	*Shale*	at top grading down into micromicaceous siltstone.
7·4–8·8	*Greywacke*	coarse to very coarse-grained. Massive base may be slightly coarser-grained than the top which is welded onto the siltstone above. Fine flow-markings on the base plunge to 235°.
8·8–9·0	*Shale*	as above.
9·0–10·8	*Greywacke*	medium to coarse-grained. Massive. Not graded.
10·8–11·6	*Siltstone*	grading down into bed below.
11·6–12·8	*Greywacke*	gradational contact above, sharp below. Graded from coarse to medium grain.
12·8–14·5	*Shale*	in upper 0·5 ft grading down into *siltstone* which is welded on to the top of the bed below.

14·5–15·2	*Greywacke*	fine-grained, massive.
15·2–15·8	*Shale*	and siltstone or very fine greywacke.
15·8–16·5	*Greywacke*	coarse to very coarse-grained. Fine flow-marks on base plunge to 230° magnetic.
16·5–16·8	*Shale*	silty, grey.
16·8–17·6	*Greywacke*	medium to coarse-grained, massive; sharp contact with thin shale below.
17·6–17·7	*Shale*	grey.
17·7–18·4	*Greywacke*	coarse-grained, grading slightly to very coarse-grained at the base. Fine flow-markings.
18·4–19·0	*Shale*	grey, cleaved.
19·0–19·9	*Greywacke*	very coarse-grained, with fragments of green shale. No variation in thickness or in grain size could be determined in this bed, when traced 150 ft along strike to the south.
19·9–20·2	*Shale*	grey.
20·2–21·7	*Greywacke*	vary coarse-grained, massive. Flow marks on base plunge to 50° magnetic.
21·7–21·9	*Shale*	grey. Appears to pinch out to the south.
21·9–23·7	*Greywacke*	massive. Coarse to very coarse-grained.
23·7–25·5	*Shale*	grey, cleaved.
25·5–26·6	*Greywacke*	varies in thickness from 1·0 ft to 1·2 ft because of large scale flow-marks at the base. At the top there is 0·1 ft of laminated sandstone. Very coarse-grained, massive.
26·6–27·4	*Siltstone*	laminated. Large shale intraclasts (1 in. across) occur along the junction with the bed below.
27·4–28·5	*Greywacke*	very coarse-grained, massive. Medium-sized, well-developed flow-marks on base.
28·5–29·1	*Shale*	silty, grey.
29·1–32·2	*Greywacke*	grades up into siltstone at top. Large flow-marks on the base.
32·2–34·3	*Siltstone*	finely cross-laminated (large ? ripples). Upper 0·5 ft is more shaly.
34·3–35·4	*Greywacke*	very coarse-grained, contact with bed above marked by plane of large shale intraclasts (up to 3 in. across). Lower contact sharp, welded into shale below, and with flow-marks.
35·4–37·4	*Siltstone*	laminated and ? rippled as above.
37·4–37·9	*Greywacke*	medium to coarse-grained. Sheared.
37·9–40·7	*Siltstone*	as above.
40·7–43·3	*Greywacke*	very coarse-grained with well developed medium-sized flow-marks on the base. Massive, grading at the top into siltstone. Flow-markings nearly horizontal.
43·3–47·5	*Siltstone*	as above.
47·5–50·4	*Greywacke*	very coarse-grained grading up into siltstone at the top. Base sharp, showing large shallow flow-marks.
50·4–51·5	*Siltstone*	as above.
51·5–52·6	*Greywacke*	coarse-grained, with large flow-marks on the base.
52·6–53·3	*Greywacke*	or siltstone. Laminated, medium to fine-grained.
53·3–56·1	*Siltstone*	or shale with lenses of greywacke. May be disturbed by shearing.
56·1–57·2	*Greywacke*	medium-grained. Massive. May be slightly graded.
57·2–58·4	*Shale*	grey. In the centre is an irregular bed of greywacke which further south appears to merge with the one above.
58·4–63·4	*Greywacke*	graded. Pebbles 2–3 mm across at base grading up into siltstone at the very top. Welded onto the top of the bed below but with a sharp, though irregular, contact.
63·4–67·9	*Greywacke*	grades from conglomerate with pebbles 2–3 mm across at the base, to coarse-grained at the top. Large flow marks at the base.
67·9–68·2	*Greywacke*	fine-grained. Acts as a parting.

68·2–71·7	*Greywacke*	coarse to very coarse-grained with fine conglomerate streaks irregularly distributed in the centre of the bed. No regular grading.
71·7–73·2	*Siltstone*	cross-laminated.
73·2–74·5	*Greywacke*	graded from fine conglomerate at the base to coarse to very coarse-grained sandstone at the top. Sharp contact at the base, in some places with greywacke and in others with shale.
74·5–75·2	*Greywacke*	in some places with a thin shale above it. Irregular in thickness.
75·2–75·5	*Shale*	grey.
75·5–77·3	*Greywacke*	very coarse-grained. Graded. Large flow-markings on the base.
77·3–79·8	*Greywacke*	very coarse-grained with medium-grained streaks. May be more than one bed.
79·8–80·5	*Shale*	or siltstone. Irregular but sharp contact with bed below.
80·5–82·5	*Greywacke*	with large scale cross-bedding. Conglomeratic (pebbles 2–4 mm across).
82·5–92·5	*Greywacke*	very coarse-grained, massive. Base with medium-sized flow-marks.
92·5–	*Shale*	

Section at this point is disturbed by a small anticline.

Normanskill section 3

Location: Quarry 1¼ miles south of New Baltimore, N.Y. Section measured from top to base. Above the top of the measured section, and inaccessible, is approximately 10 ft of massive greywacke.

0–3·1	*Greywacke*	fine-grained. Laminated and cross-bedded on a small scale (foresets 0·2 ft high).
3·1–3·3	*Siltstone*	parting.
3·3–4·3	*Greywacke*	fine to medium-grained. Shows lamination and some irregular cross-bedding.
4·3–4·8	*Siltstone*	laminated and cross-bedded.
4·8–8·2	*Greywacke*	coarse-grained, massive, with flow-marks on the base.
8·2–8·7	*Siltstone*	argillaceous.
8·7–9·8	*Greywacke*	top transitional to siltstone above.
9·8–10·0	*Siltstone*	parting.
10·0–11·2	*Greywacke*	coarse-grained.
11·2–11·8	*Siltstone*	cross-bedded at the base, more argillaceous above.
11·8–16·0	*Greywacke*	coarse, massive, large flow-markings on the base.
16·0–16·5	*Shale*	dark grey, argillaceous.
16·5–17·3	*Greywacke*	coarse-grained, massive, with fine flow-markings on the base.
17·3–18·6	*Shale*	as above.
18·6–19·2	*Greywacke*	
19·2–19·4	*Shale*	as above.
19·4–20·2	*Greywacke*	
20·2–20·3	*Shale*	parting.
20·3–20·9	*Greywacke*	
20·9–29·0	*Shale*	and siltstone interbedded. Poorly exposed.
29·0–29·6	*Greywacke*	
29·6–37·0	*Shale*	with thin interbeds of siltstone and greywacke. Poorly exposed.
37·0–41·3	*Greywacke*	coarse-grained, massive. Medium-sized flow-marks on base.
41·3–42·7	*Shale*	with siltstone.
42·7–46·7	*Greywacke*	graded slightly, from coarse to very coarse-grained at the base. Base welded to siltstone below.
46·7–50·5	*Siltstone*	or very fine-grained greywacke. Laminated and cross-bedded.
50·5–50·6	*Siltstone*	parting.
50·6–51·3	*Greywacke*	fine-grained, or siltstone. Some cross-bedding at top. Flow marks at base.

51·3–51·9	*Siltstone*	or fine-grained greywacke. Cross-bedded. Partings above and below this bed.
51·9–54·5	*Siltstone*	or fine-grained greywacke. Cross-bedded. Cross-bedding in the two beds above is very irregular and may be a slump structure.
54·5–54·6	*Siltstone*	parting.
54·6–55·0	*Siltstone*	or fine-grained greywacke as above. Parting at base.
55·0–56·2	*Siltstone*	as above.
56·2–56·9	*Siltstone*	interbedded with shale.
56·9–57·8	*Greywacke*	fine-grained, massive, with flow-markings on the base.
57·8 -59·3	*Siltstone*	interbedded with shale.
59·3–59·7	*Siltstone*	
59·7–59·8	*Siltstone*	parting.
59·8–60·7	*Siltstone*	with cross-bedding.
60·7–61·2	*Siltstone*	or fine-grained greywacke with irregular cross-bedding (? slumping).
61·2–62·5	*Greywacke*	coarse to very coarse-grained, showing slight grading near the top (?). Possibly flow-markings on the base (not well exposed).
62·5–63·3	*Siltstone*	laminated.
63·3–66·6	*Greywacke*	medium to coarse-grained, massive, with occasional shale intraclasts.

Normanskill section 4

Location: Roadcut, south-west of Mechanicville. Highway No. 146 about 2 miles east of Clifton Park, N.Y.

0–6·0	*Greywacke*	coarse to very coarse-grained. At 1·8 ft from base there is a bed full of shale intraclasts, which does not appear to continue along the cut to the east. Flow-markings at base plunge to 100° magnetic. Beds dip 28° S, strike 80° magnetic.
6·0–6·7	*Shale*	dark grey, fissile.
6·7–8·0	*Greywacke*	coarse to very coarse-grained with fragments of shale. Flow-markings on base plunge to 170° magnetic.
8·0–8·9	*Shale*	as above.
8·9–11·9	*Greywacke*	coarse to very coarse-grained with shale intraclasts. Flow-markings on base plunge to 095° magnetic.
11·9–13·3	*Shale*	as above.
13·3–14·0	*Greywacke*	medium to coarse-grained.

Quebec group section 1

Location: Quebec Bridge roadcut, north of the bridge, on the west side of the cut.

0–37	*Greywacke*	graded from medium-grained at the top to conglomeratic at the base. Pebbles mainly of quartz; up to 1 cm in diameter. Base sharp, welded on to beds below and showing megaripples or fluting, 4–5 ft in length.
37–45	*Greywacke*	coarse-grained and inhomogeneous. Lowest 2–3 ft appears to be a washout of the bed below, filled with finer-grained but very poorly sorted greywacke.
45–62	*Greywacke*	conglomeratic throughout, with shale pellets, especially in the top 3 ft. Pellets are fine-grained and greenish-grey.
62–63	*Greywacke*	medium to coarse-grained. Thickness varies from 1–3 ft as a result of very large scale fluting in the beds above. The flutes are up to 6 ft long.
63–66	*Greywacke*	concretion bed; sandy-brown weathering concretions and pieces of sandstone up to a foot in diameter (mostly 4–8 in.). Some of the sandstone fragments show undisturbed lamination. Some concretions contain a piece of black shale in the centre.

66–67	*Greywacke*	very coarse, conglomeratic. No sandstone balls.
67–70	*Greywacke*	concretion bed. Matrix of both concretion beds resembles the intervening bed. Quartz pebbles and pellets of greenish-grey and black shale. Section disturbed by thrusting below this point.

Quebec group section 2

Location: Roadcut on Highway No. 2, St. Romuald, Quebec. Measured beds cut by fault at the top of the section. Measured section begins at the first shale, at the top of the section. Above is massive greywacke.

0–1·0	*Shale*	greenish-grey, fissile.
1·0–2·0	*Greywacke*	quartzose, with cross-beds inclined to the south. Very coarse-grained.
2·0–8·5	*Greywacke*	graded with quartz pebbles at the base. Basal contact not very distinct, welded on to bed below.
8·5–10·5	*Greywacke*	conglomeratic, particularly at the base. Welded on to the bed below. At one point there is a washout cutting out about one half of the thickness of the bed, and filled with quartz pebble conglomerate.
10·5–13·2	*Greywacke*	as above, with quartz pebble conglomerate at the base. Base is sharp, irregular and welded on to the bed below.
13·2–14·5	*Greywacke*	very coarse-grained but very poorly sorted. Dark greenish-grey. Very few quartz pebbles.
14·5–15·5	*Quartzite*	cross-bedded at the top, conglomeratic at the base. Variable in thickness, showing cut and fill structures, almost cutting out the bed below.
15·5–16·5	*Greywacke*	very coarse-grained and very poorly sorted.
16·5–19·0	*Shale*	greenish-grey, silty, fissile.
19·0–19·5	*Greywacke*	varies in thickness to 1 ft, with a thin pebble zone at the base. Welded on to the bed below.
19·5–21·0	*Greywacke*	as above, with a pebble zone at the base, welded on to the bed below.
21·0–23·2	*Greywacke*	as above, very coarse-grained to conglomeratic at the base and grading upwards. Greenish-grey shale parting.
23·2–26·8	*Greywacke*	grades into shaly or silty parting near the top; only slightly graded in the remainder of the bed. Shows an internal bedding or lamination.
26·8–27·2	*Shale*	or silty shale, grading down to bed below. Reddish at top, greenish at base.
27·2–28·7	*Greywacke*	graded. Coarse to very coarse-grained at the top and conglomeratic at the base with pebbles up to 3 mm in diameter.
28·7–29·1	*Shale*	reddish at the top, greenish at the base. Grades down on to the bed below.
29·1–31·3	*Greywacke*	not obviously graded. Shale pellets in upper part.
31·3–33·2	*Siltstone*	greenish-grey, fissile, grades down on to fine-grained greywacke.
33·2–37·1	*Shale*	greenish-grey, with a little red near the top. 0·2–0·3 ft below the top there is a lens of cross-bedded quartzite, which reaches a thickness of 1 ft, but pinches out at the base of the cut. A bed of greywacke lies below the quartzite and grades up into shale. Below this bed is 0·5 ft of red and green shale.
37·1–38·5	*Greywacke*	grades up into shale above at top. Otherwise not markedly graded.
38·5–39·8	*Shale*	or siltstone, greenish-grey, grades down on to bed below.
39·8–41·4	*Greywacke*	
41·4–42·0	*Shale*	greenish-grey or red.
42·0–42·2	*Greywacke*	fine-grained.
42·2–46·9	*Greywacke*	very coarse-grained to conglomeratic. Light greenish-grey.
46·9–48·8	*Shale*	red with very thin green streaks.
48·8–50·4	*Greywacke*	red, coarse to very coarse-grained. Base irregular.

50·4–51·1	*Shale*	red.
51·1–52·1	*Greywacke*	argillaceous, red, graded. Weathers rubbly.
52·1–52·3	*Shale*	red.
52·3–54·6	*Greywacke*	red.
54·6–58·5	*Siltstone*	or shale, greenish-red with some red in the top 1 ft. The lower 1·5 ft of the interval is somewhat coarser.
58·5–66·0	*Greywacke*	greenish-grey, graded.
66·0–66·5	*Siltstone*	shaly.
66·5–78·0	*Greywacke*	greenish-grey, massive, slightly conglomeratic at the base. Welded on to the bed below.
78·0–82·5	*Greywacke*	as above.
82·5–94·5	*Greywacke*	greenish-grey, massive. Silty parting between this bed and the one above.
94·5–96·5	*Shale*	red and green.
96·5–97·2	*Greywacke*	greenish-grey, base irregular.
97·2–97·9	*Shale*	red.
97·9–98·7	*Shale*	or siltstone, greenish-grey.
98·7–99·8	*Shale*	red (0·5 ft) with fine-grained greywacke below, greenish-grey.
99·8–101·0	*Shale*	upper half red, lower half greenish-grey. Lowest 0·2 ft much coarser than the rest. Green shale parting.
101·0–102·3	*Greywacke*	upper two-thirds shows cross-bedding. Base irregular. Red shale parting.
102·3–105·2	*Greywacke*	greenish-grey, argillaceous.
105·2–107·0	*Greywacke*	very coarse, light greenish-grey, argillaceous.
107·0–108·6	*Greywacke*	reddish-brown, graded.
108·6–108·8	*Conglomerate*	with small quartz pebbles up to 0·5 cm in diameter. Not part of the bed above.
108·8–111·6	*Shale*	red, becoming sandy at 0·2 ft above the base.
111·6–112·0	*Quartzite*	variable in thickness from 0·2 to 0·6 ft; very coarse-grained to conglomeratic.
112·0–114·0	*Shale*	red, grading down in lower 0·7–0·8 ft to argillaceous red greywacke.
114·0–115·5	*Shale*	as above (0·2 ft) grading down into red argillaceous greywacke.
115·5–115·6	*Shale*	red.
115·6–117·5	*Greywacke*	greenish-grey in upper 0·8 ft, then light grey, grading down again to greenish-grey. Shale pellets. Conglomeratic at the base, with quartz pebbles up to 0·5 cm in diameter.
117·5–121·5	*Shale*	greenish-grey, fissile.
121·5–125·0	*Greywacke*	graded at the top.
125·0–125·9	*Shale*	red at the top, grading down to greenish-grey and grading on to the top of the bed below.
125·9–128·5	*Greywacke*	rather light greenish-grey, conglomeratic at the base.
128·5–132·7	*Shale*	red. One thin discontinuous bed of sandstone about 0·5 ft from the top.
132·7–133·0	*Sandstone*	greenish-grey, conglomeratic, discontinuous, with load casts on base.
133·0–133·8	*Shale*	red, grading down in lowest 0·3 ft to sandstone. Red above to grey at the base. Laminated.
133·8–140·0	*Shale*	red. Brownish-red sandstone (0·5 ft thick) 2·0 ft from base; below this, lowest 1·0 ft of shale is greenish-grey and grades down into the bed below.
140·0–147·0	*Greywacke*	or sandstone, greenish-grey. Abrupt change to conglomeratic zone in lowest 0·5 ft. Base irregular.
147·0–152·0	*Shale*	red. To base of section.

Table 1. Table of spectral lines

Line	Internal standard	Line	Internal standard
Ag 3280	Pd 3258	Mn 2801	Pd 3258
B 2497	Pd 2476	Mo 3193	Pd 3258
Ba 4554	Pd 3258	Ni 3414	Pd 3258
Be 3131	Pd 2476	Sc 4246	Pd 3258
Co 3453	Pd 3258	Sr 4607	Pd 3258
Cr 4254	Pd 3258	Ti 3321	Pd 3258
Cu 3273	Pd 3258	V 3102	Pd 2476
Ga 2943	Pd 3258	Y 3216	Pd 3258
La 4333	Pd 3258	Zr 3388	Pd 3258
Mg 2776	Pd 3258		

Table 2. Table of precision for several spectral lines

Element	This paper	Shaw	Standards this paper
Ba	12·8	12·6	W1
Co	8·7	9·0	W1
Cr	13·0	13·5	W1
Ni	8·4	8·4	W1
Sc	9·6	11·3	W1
Sr	10·7	13·2	G1

Table 3. Table of precision

Spectral line	Relative error for triplicate analysis (%)
Ag	11·6
B	19·4
Ba	12·6
Be	14·0
Co	9·0
Cr	13·5
Cu	14·6
Ga	12·4
Mg	8·9
Mn	11·1
Mo	11·6
Ni	8·4
Sc	11·3
Sr	13·2
Ti	7·5
V	11·8
Y	—
Zr	7·6

Table 4. Values (in p.p.m.) obtained for twenty-two samples of G1 and 10 samples of W1

	G1	W1
Silver	nd	nd
Boron	tr	28
Barium	s	127
Beryllium	tr	nd
Cobalt	tr	53
Chromium	tr	165
Copper	13	105
Gallium	14	12
Lanthanum	tr	nd
Magnesium	2600	s
Manganese	290	s
Molybdenum	nd	nd
Nickel	tr	88
Scandium	tr	25
Strontium	389	253
Titanium	2070	8640
Vanadium	16	127
Yttrium	nd	nd
Zirconium	233	tr

Table 5. Variation of elements within a bed

Bed† no.	Height above base (ft)	Analysis	B	Ba	Co	Cr	Cu	Ga	Mg	Mn	Ni	Sc	Sr	Sr*	Ti	V	Zr
1	0·0	1	120	410	24	100	26	2	1·7	490	45	11	240	170	9000	66	710
	2·7	2	120	410	19	19	24	10	1·8	480	41	9	290	200	7200	59	360
2	0·0	3	55	380	24	130	27	25	2·0	800	50	9	430	260	7600	90	480
	3·0	4	61	350	22	120	25	9	1·7	690	44	8	250	180	6600	86	550
	4·5	5	33	220	15	120	24	8	0·56	810	29	7	670	380	3700	59	480
3	0·0	6	56	240	14	93	25	9	1·2	440	32	6	140	120	4300	49	490
	5·0	7	74	280	15	95	22	9	1·3	520	32	6	140	120	4600	54	410
	10·0	8	73	320	17	100	25	11	1·6	560	35	8	230	170	5000	53	480
4	1·0	9	84	270	14	73	27	4	1·8	420	33	6	180	140	5700	45	430
	5·0	10	79	300	18	99	24	5	2·2	590	37	4	240	170	5400	40	310
5	0·0	11	42	430	23	210	52	15	0·96	740	50	12	300	200	6700	97	830
	3·1	12	38	380	16	140	31	14	1·0	560	39	9	300	200	4300	91	330
6	0·0	13	85	320	16	85	21	6	1·9	440	35	6	280	190	7000	51	530
	2·4	14	96	270	20	86	25	11	2·6	430	38	7	210	150	6600	48	430
7	0·0	15	98	330	20	100	25	tr	1·8	600	44	10	250	120	8600	56	640
	3·2	16	91	320	20	80	23	tr	1·5	410	43	9	200	150	6800	59	380
8	0·0	17	76	410	22	100	26	3	1·8	500	44	10	270	180	7700	61	560
	1·3	18	91	360	18	85	23	11	2·3	490	39	10	260	180	7700	49	370
9	0·0	19	83	390	20	98	26	3	1·7	500	44	10	320	210	8000	65	560
	4·3	20	99	400	16	82	23	3	1·6	420	38	10	240	170	7000	58	420
10	0·0	21	89	420	21	85	30	14	2·5	350	39	8	190	150	5400	61	330
	1·0	22	63	320	21	120	28	18	1·7	520	39	5	350	220	5200	62	470
	3·0	23	77	330	18	94	24	11	1·9	500	36	8	220	160	5300	57	320
	5·0	24	77	370	19	100	27	18	1·9	490	40	8	240	170	5300	58	270
11	0·0	25	89	150	9	87	30	tr	0·47	520	31	2	52	77	23000	56	1100
	1·3	26	110	350	18	56	2	5	0·83	500	28	5	110	110	13000	50	720
	4·7	27	74	280	24	57	8	6	1·8	—	29	6	180	140	7700	39	310

* Corrected values of strontium.
† Beds 1 to 10 are from the Normanskill formation; bed 11 is from the Charny formation.

Table 6. Statistical parameters distribution of elements in a turbidite bed

Element	t	F-test for common standard deviations		Order in which element tends to differentiate in a bed
B	0·000	Yes*	1% level	13
Ba	0·336	Yes	1% level	11
Co	0·602	Yes	1% level	9
Cr	0·949	Yes	1% level	6
Cu	2·010	Yes	1% level	2
Ga	0·712	Yes	1% level	8
Mg	0·417	Yes	1% level	10
Mn	0·053	Yes	1% level	12
Ni	1·600	Yes	1% level	3
Sc	0·000	Yes	1% level	14
Sr	0·900	Yes	1% level	7
Ti	1·540	No	1% level	4
V	1·090	Yes	1% level	5
Zr	3·320	No	1% level	1

* "Yes" indicates top and bottom populations have a common standard deviation.

Table 7. Table of t values

α	$t_{\frac{1}{2}\alpha}(20)$
0·01	−2·84
0·02	−2·53
0·05	−2·09
0·10	−1·72
0·20	−1·32
0·40	−0·86

Table 8. Variation within eleven beds

Means for 11 beds	B	Ba	Co	Cr	Cu	Ga	Mg	Mn	Ni	Sc	Sr	Sr*	Ti	V	Zr
Bed 1	120	407	22	91	25	6	1·78	482	43	10	267	184	8100	62	540
Bed 2	44	298	20	92	25	16	1·26	805	40	8	553	324	5600	74	480
Bed 3	65	280	16	90	25	10	1·40	498	34	7	211	144	4600	51	480
Bed 4	82	283	16	94	25	4	1·99	505	35	5	209	156	10,600	42	370
Bed 5	40	408	20	72	42	14	0·98	652	44	10	300	200	10,500	94	580
Bed 6	90	292	18	96	23	8	2·25	434	36	6	245	172	6800	50	480
Bed 7	95	327	20	125	24	—	1·65	505	44	10	224	162	7700	58	510
Bed 8	84	385	20	96	25	7	2·06	492	42	10	266	183	7700	55	460
Bed 9	91	392	18	86	25	3	1·64	463	41	10	279	190	7500	62	490
Bed 10	83	398	20	170	28	16	2·22	419	40	8	219	160	5400	60	300
Bed 11	82	216	16	86	19	—	1·14	—	30	4	114	108	15,200	48	720
Av. mean	80	335	19	100	26	9	1·67	526	39	8	262	180	8150	60	492
Standard deviations															
Bed 1	5	0	4	8	1	6	0·07	11	3	1	32	16	1300	5	250
Bed 2	16	118	6	11	2	12	1·0	10	15	1	178	84	2800	22	0
Bed 3	12	57	2	5	0	1	0·32	87	2	1	102	33	500	3	20
Bed 4	4	21	3	18	2	1	0·29	125	3	1	40	19	200	4	80
Bed 5	3	35	5	50	15	1	0·04	125	8	2	4	2	1700	4	350
Bed 6	8	35	3	1	3	3	0·49	6	2	1	52	26	300	15	70
Bed 7	5	3	0	16	1	—	0·17	139	1	1	43	20	1300	2	180
Bed 8	11	35	3	11	2	6	0·32	7	4	0	2	2	0	8	130
Bed 9	11	8	3	11	2	0	0·12	57	4	0	62	30	700	5	100
Bed 10	8	36	1	13	2	3	0·42	98	1	0	37	18	100	2	40
Bed 11	11	90	11	21	16	—	0·94	—	1	3	88	45	10,500	12	590
Av. s.d.	8	40	4	15	4	4	0·38	66	4	1	58	27	1760	7	164

Table 9. Section 1, Quebec group

Analysis	Height above base (ft)	B	Ba	Co	Cr	Cu	Ga	Mg	Mn	Ni	Sc	Sr	Sr*	Ti	V	Zr
49	6–7	94	48	tr	83	5	tr	0·55	130	42	7	92	98	5500	45	2000
50	27	100	120	10	66	5	14	0·68	76	22	5	95	99	3100	51	710
51	40	140	260	29	84	12	36	1·7	93	48	12	130	120	3800	52	810
52	43	80	92	8	61	5	10	0·61	92	33	6	72	87	3700	41	1500
53	62	43	99	tr	51	4	tr	0·30	89	19	4	63	83	2800	27	830
54	63	64	61	10	81	6	tr	0·40	87	47	6	73	88	3000	49	670
55	66	51	81	11	66	3	6	0·45	150	22	5	130	120	5600	30	890

* Corrected strontium values.

Table 10. Section 2, Quebec group

Analysis	Height above base (ft)	B	Ba	Co	Cr	Cu	Ga	Mg	Mn	Ni	Sc	Sr	Sr*	Ti	V	Zr
32	1·5	39	s	tr	120	4	4	0·19	480	9	nd	120	110	5300	34	650
33	8·5	62	110	14	93	tr	3	0·71	660	20	5	160	130	7600	40	670
34	14·5	68	86	4	170	7	tr	0·52	800	13	nd	59	81	8800	49	820
35	19·0	85	71	14	130	5	5	0·91	860	27	5	84	94	16,000	47	2000
36	33·2	63	180	17	110	13	4	0·70	940	28	nd	100	100	6100	45	510
37	38·0	73	210	32	110	32	18	1·5	830	40	8	120	110	11,000	43	530
38	44·5	76	290	22	110	7	13	1·2	900	27	5	110	110	13,000	47	790
39	63·0	57	400	16	110	9	14	1·3	1000	20	6	150	130	12,000	51	650
40	78·0	51	630	14	87	5	6	1·1	980	23	5	130	120	8700	38	530
41	93·5	49	200	18	100	4	10	1·3	s	31	5	110	110	14,000	49	790
42	102·0	49	s	16	77	6	tr	0·72	1000	20	tr	160	130	8000	33	450
43	112·0	69	s	8	54	19	3	0·40	370	14	3	100	100	7100	32	470
44	117·5	55	590	19	67	10	16	1·1	630	33	8	140	120	8600	49	410
45	126·1	60	s	7	79	14	3	0·42	350	14	1	84	93	7300	45	660
46	140·0	89	150	9	87	30	tr	0·47	520	31	3	52	77	23,000	56	1100
47	141·5	110	350	18	56	2	5	0·83	500	28	5	110	110	13,000	50	720
48	145·0	74	280	24	57	8	6	1·9	s	29	6	180	140	7700	39	310
	mean	66	270	16	95	11	8	0·89	720	24	5	110	110	10,400	44	710
	s.d.	17	180	7	29	9	5	0·45	230	8	2	35	17	4400	7	140

* Corrected strontium values.

Table 11. Variation between sections, Quebec group

	B	Ba	Co	Cr	Cu	Ga	Mg	Mn	Ni	Sc	Sr	Sr*	Ti	V	Zr
Section 1 7 samples	81	110	14	70	6	16	0·66	100	33	6	94	98	3900	42	1100
Section 2 17 samples	66	270	16	95	11	8	0·89	720	24	5	120	110	10,000	44	710
Mean	74	190	15	82	8	12	0·78	410	29	6	100	100	7200	43	880
s.d.	11	120	1	18	5	6	0·16	440	6	1	16	8	4600	1	250

* Corrected values of strontium.

Table 12. Variation between sections, Normanskill

	B	Ba	Co	Cr	Cu	Ga	Mg	Mn	Ni	Sc	Sr	Sr*	Ti	V	Zr
Section 1 composite 11 samples	21	450	27	180	43	18	1·0	640	53	7	610	350	5600	62	610
Section 2 composite 46 samples	24	230	18	120	32	14	0·97	590	34	7	240	170	3600	61	280
Section 3 composite 26 samples	33	400	20	140	26	14	1·1	550	39	9	470	280	4400	64	290
Section 4 composite 7 samples	61	440	21	120	30	11	1·7	650	47	10	330	210	6600	82	410
Mean	35	380	22	140	33	14	1·2	610	43	8	410	260	5100	67	400
s.d.	18	100	4	28	7	3	0·36	44	8	2	160	80	1300	10	160

* Corrected values of strontium.

Table 13. Comparison of greywackes analysed by Macpherson

		B	Ba	Co	Cr	Cu	Ga	Mg	Mn	Ni	Sc	Sr	Sr*	Ti	V	Zr
Arkosic greywacke	Weber no. 64	20	150	59	320	56	15	0·69	120	100	20	350	220	4800	96	230
	Macpherson no. 6	20	380	—	340	60	—	—	970	150	—	—	—	—	190	—
Feldspathic greywacke	Weber no. 65	30	120	27	180	46	13	0·58	110	84	9	230	170	3800	64	200
	Macpherson no. 14	60	180	—	180	60	—	—	410	80	—	—	—	—	90	—
Volcanic greywacke	Weber no. 66	30	170	33	230	35	14	0·61	120	110	11	510	300	3800	71	190
	Macpherson no. 21	40	360	—	180	60	—	—	830	120	—	—	—	—	130	—

* Corrected strontium values.

Table 14. Rensselaer formation

Analysis	B	Ba	Co	Cr	Cu	Ga	Mg	Mn	Ni	Sc	Sr	Sr*	Ti	V	Zr
56	23	800	20	140	24	13	1·9	950	30	7	330	220	7400	51	580
57	17	510	tr	130	5	tr	0·74	600	15	8	260	180	5600	41	460
58	32	840	13	110	11	8	1·2	630	21	5	340	220	5300	43	450
59	56	830	21	130	14	14	2·2	840	34	10	220	160	7000	59	360
Mean	32	750	14	130	14	9	1·5	750	25	8	290	190	6300	48	460
s.d.	17	160	4	12	8	3	0·60	170	9	2	58	29	1100	8	89

* Corrected values of strontium.

Table 15. Comparison of formations

	B	Ba	Co	Cr	Cu	Ga	Mg	Mn	Ni	Sc	Sr	Sr*	Ti	V	Zr
Normanskill Fm (4 sections)	35	380	22	140	33	14	1·2	600	43	8	410	260	5100	67	400
Quebec group (24 samples)	70	220	15	88	9	10	0·82	540	27	5	110	110	8500	43	810
Kiskatom red beds (4 samples)	120	530	28	250	—	6	1·9	850	77	11	140	120	11,000	88	440
Rensselaer Fm (4 samples)	32	750	14	130	14	9	1·5	750	25	8	290	190	6300	48	460
Pre-Cambrian volcanic greywackes (13 samples) MACPHERSON	59	—	—	240	51	—	—	—	130	—	—	—	—	—	—
Pre-Cambrian arkosic greywackes (11 samples) MACPHERSON	44	—	—	210	46	—	—	—	97	—	—	—	—	—	—
Pre-Cambrian feldspathic greywackes (5 samples) MACPHERSON	46	—	—	170	48	—	—	—	72	—	—	—	—	—	—
Mean	58	470	20	170	34	10	1·4	690	67	8	240	170	7700	62	530
s.d.	9	220	7	59	18	3	0·50	99	39	2	140	69	2500	21	190

* Corrected strontium values.

Table 16. Miscellaneous greywackes

	Analysis	B	Ba	Co	Cr	Cu	Ga	Mg	Mn	Ni	Sc	Sr	Sr*	Ti	V	Zr
Upper Mississippian "Kulm", Germany	67	69	270	16	130	4	8	3·3	670	32	8	140	120	5500	54	340
Upper Mississippian "Kulm", Germany	68	70	400	21	120	5	14	4·0	620	38	10	160	130	6400	66	250
Macigno, Italy	69	34	620	11	130	8	3	4·3	680	59	9	270	180	3700	48	200
Formazione "Marnoso-Arenacea", Italy	70	45	250	tr	92	5	tr	4·4	590	33	7	600	340	4500	42	340
Barmouth Grit, North Wales	71	63	570	29	87	7	6	2·1	s	37	10	110	110	8000	62	330
Gowganda, Ontario	72	26	500	31	170	150†	10	4·0	320	55	9	130	120	4700	77	200
Gowganda, Ontario	73	tr	290	tr	64	5	6	1·1	110	11	tr	92	98	1100	24	tr
Gowganda, Ontraio	74	15	470	18	190	2	16	3·8	510	52	7	170	140	4200	55	200
Gowganda, Ontario	75	13	470	15	150	tr	13	2·2	230	32	5	130	120	2500	42	210
Mean		42	430	20	120	5	9	3·2	470	39	8	200	150	4500	52	260
s.d.		20	300	7	40	2	4	1·2	220	15	1	160	77	2000	15	66

* Corrected strontium values.
† Mineralized. Ignored in average.

Table 17. Summary of variation
(Standard deviation as % of mean)

	B	Ba	Co	Cr	Cu	Ga	Mg	Mn	Ni	Sc	Sr	Sr*	Ti	V	Zr
Within bed (Normanskill) Average of 11 standard deviations	10	12	21	15	15	44	23	12	10	12	22	15	22	12	33
Between beds (Quebec section 2)	26	65	44	30	82	62	50	32	33	40	30	16	42	16	20
Between sections—Normanskill	51	27	18	20	21	21	30	7	19	25	39	32	39	15	39
—Quebec group	15	60	7	22	62	50	20	106	21	17	15	8	64	2	28
Between formations	16	47	35	34	53	30	37	14	58	25	59	41	32	34	37

* Corrected values of strontium.

Table 18. Order of elements showing variation

Within beds	Between beds	Between sections (Normanskill only)	Between formations
Gallium 44	Copper 82	Boron 51	Strontium 59
Zirconium 33	Barium 65	Strontium 39	Nickel 59
Magnesium 23	Gallium 62	Titanium 39	Copper 53
Strontium 22	Magnesium 50	Zirconium 39	Barium 47
Titanium 22	Cobalt 44	Magnesium 30	Magnesium 37
Cobalt 21	Titanium 42	Barium 27	Zirconium 37
Chromium 15	Scandium 40	Scandium 25	Cobalt 35
Copper 15	Nickel 33	Copper 21	Chromium 34
Barium 12	Manganese 32	Gallium 21	Vanadium 34
Manganese 12	Chromium 30	Chromium 20	Titanium 32
Scandium 12	Strontium 30	Nickel 19	Gallium 30
Vanadium 12	Boron 26	Cobalt 18	Scandium 25
Boron 10	Zirconium 20	Vanadium 15	Boron 16
Nickel 10	Vanadium 16	Manganese 7	Manganese 14

Figures are standard deviations as per cent of the mean.

Table 19. Effect of provenance on greywacke composition

	Rankama and Sahama (1950)		Nockolds and Allen (1953)		W1 and G1 standards		Greywackes	
	Acidic	Basic	Acidic	Basic	G1	W1	Quebec	Normanskill
Boron	uncertain	uncertain	uncertain	uncertain		high	high	
Barium	high		high		high			high
Cobalt		high		high		high		high
Chromium		high		high		high		high
Copper		high	—	—		high		high
Gallium	high		little difference		little difference			high
Magnesium		high		high		high		high
Manganese		high	—	—		high		high
Nickel		high		high		high		high
Scandium		high	uncertain	uncertain		high		high
Strontium	high		little difference		little difference			high
Titanium		high	—	—		high	high	
Vanadium		high		high		high		high
Zirconium	high		high		high		high	

Table 20. Estimates of crustal abundance

	1	2	3	4	5	6	7	8	9
Ba (p.p.m.)	250	250	240	400	250	500	400	400	500
B (p.p.m.)	3	3	6	10	3	100	10	10	10
Cr (p.p.m.)	200	200	190	330	200	300	380	330	370
Cc (p.p.m.)	23	23	4	12	40	20	12	12	10
Cu (p.p.m.)	70	70	10	10	10	10	10	10	10
Ga (p.p.m.)	15	15	15	—	15	10	—	—	—
Mg %	2·09	2·09	2·04	1·93	2·09	2·35	1·93	1·93	2·09
Mn (p.p.m.)	1000	1000	970	900	1000	1000	900	900	1000
Ni (p.p.m.)	80	80	100	180	100	200	180	180	200
Sc (p.p.m.)	5	5	5	6	5	6	6	—	—
Sr (p.p.m.)	300	300	150	170	150	350	200	200	190
Ti (p.p.m.)	4400	4400	43,000	5800	4400	6100	6300	5800	6300
V (p.p.m.)	150	150	1500	160	150	200	180	160	170
Zr (p.p.m.)	220	220	210	230	220	250	230	230	260

(1) Mason (1952), crust.
(2) Rankama and Sahama (1950), igneous rocks.
(3) Polanski (1948), crust.
(4) Anderson (1945), crust.
(5) Goldschmidt (1937), igneous rocks.
(6) Fersman (1933), crust.
(7) Schneiderhöhn (1934), crust.
(8) Berg (1929).
(9) Clarke and Washington (1924), igneous rocks.

Table 21. Reliable estimate of crustal abundance

	p.p.m.	Reference
B	—	
Ba	250	Green (1953)
Co	23	Rankama and Sahama (1950)
Cr	100	Shaw (1954)
Cu	70	Rankama and Sahama (1950)
Ga	20	Fleischer (1955)
Mg	2·09%	Green (1953)
Mn	1000	Green (1953)
Ni	80	Rankama and Sahama (1950)
Sc	15	Shaw (1954)
Sr	450	Turekian and Kulp (1956)
Ti	4400	Green (1953)
V	100	Shaw (1954)
Zr	156	Degenhardt (1957)

Table 22. Chemical composition of sandstones and shales

Element	Sandstones*	Shales*	Normanskill greywackes	Quebec sandstones
Boron	9–31	310	35	70
Barium	170	460	380	220
Cobalt	0	8	22	15
Chromium	68–200	410–680	140	88
Copper	—	190	33	9
Gallium	7	50	14	10
Magnesium	7100	14,800	12,000	8200
Manganese	tr	620	600	540
Nickel	2–8	24	43	27
Scandium	0·7	6·5	8	5
Strontium	26	170	260	110
Titanium	960	4300	5100	8500
Vanadium	20	120	67	43
Zirconium	—	120	400	810

* Rankama and Sahama (1950).

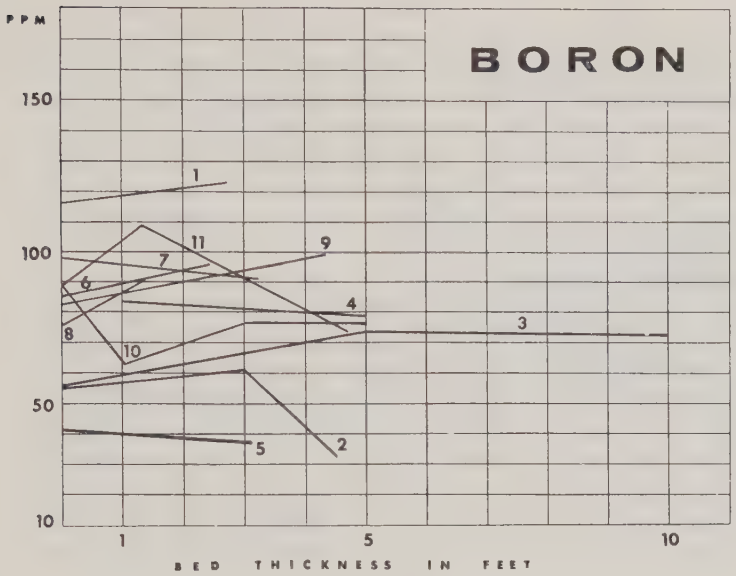

Fig. 1a

Fig. 1. Distribution of elements in eleven turbidite beds. Beds 1 to 10—Normanskill formation. Bed 11—Quebec Group. Corrected values of strontium. The uppermost readings on the abscissa indicate the top of the bed. Straight lines joint two, three or four analyses per bed.

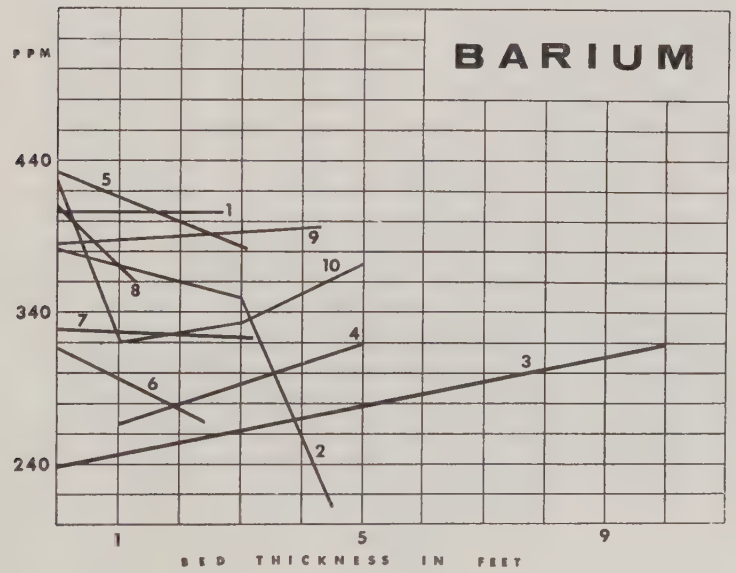

Fig. 1b

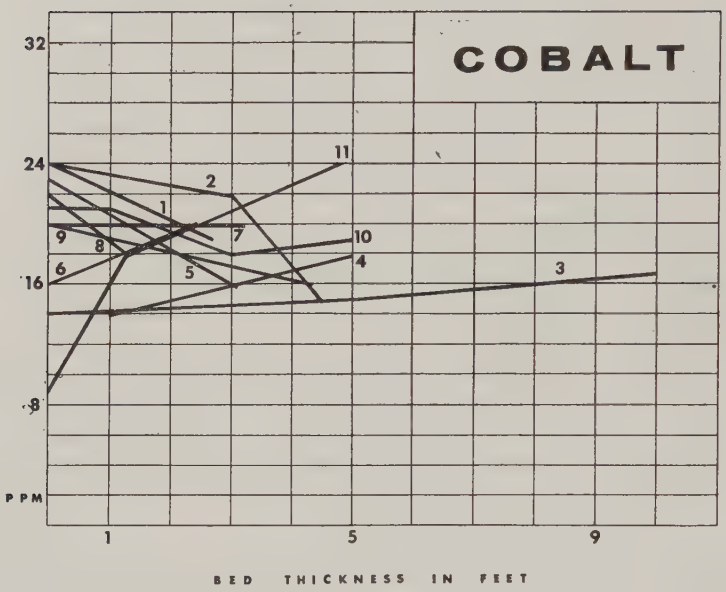
COBALT
32
24
16
8
PPM
1
5
9
BED THICKNESS IN FEET
11
2
1
7
9
8
10
6
5
4
3

Fig. 1c

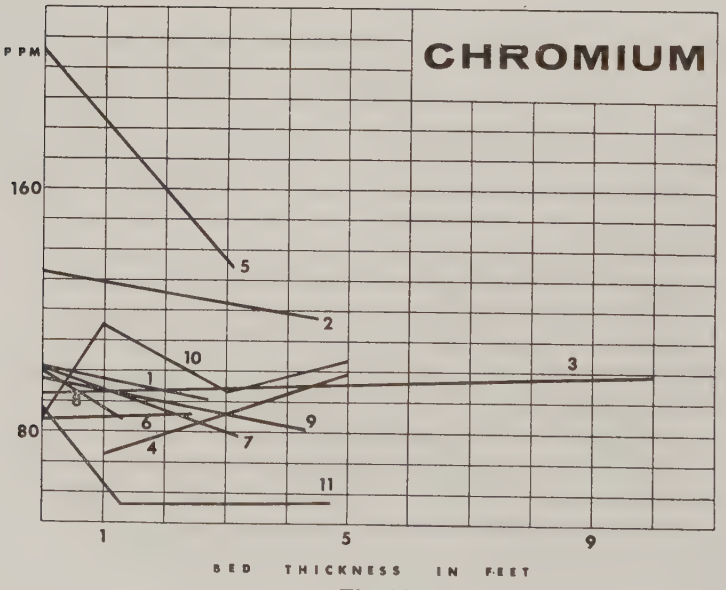
CHROMIUM
PPM
160
80
1
5
9
BED THICKNESS IN FEET
5
2
10
1
8
6
4
7
9
11
3

Fig. 1d

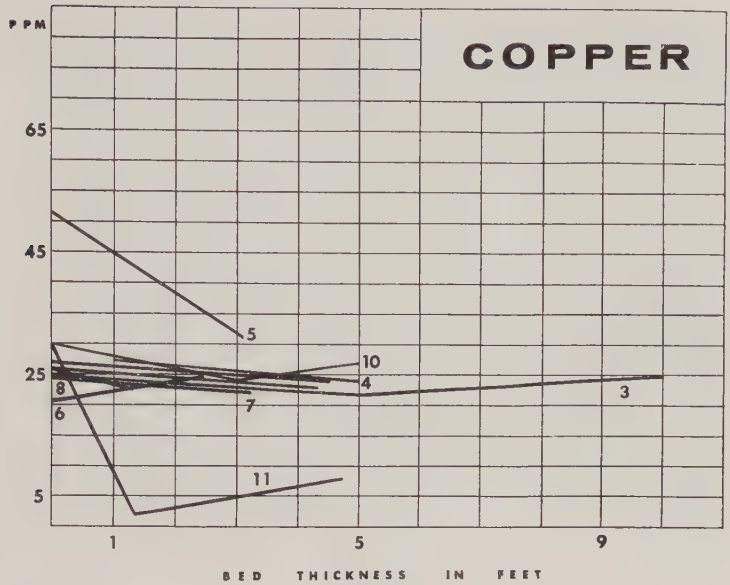
COPPER
PPM
65
45
25
5
1
5
9
BED THICKNESS IN FEET
5
10
4
3
8
7
6
11

Fig. 1e

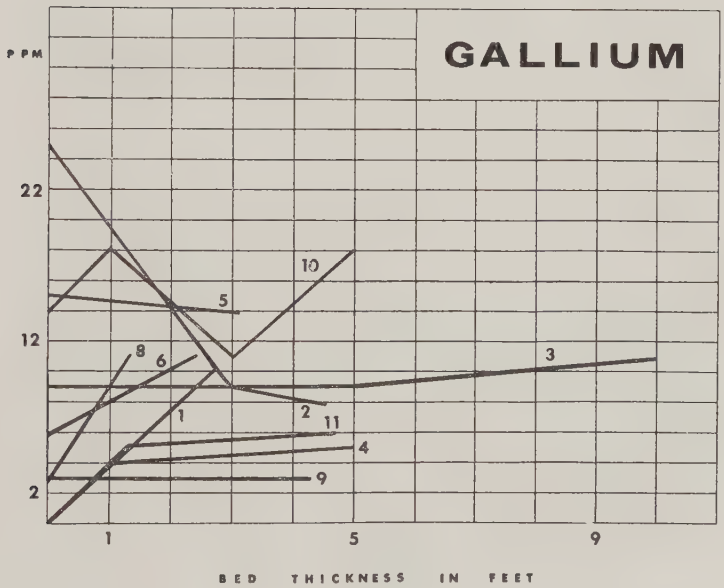
GALLIUM
PPM
22
12
2
1
5
9
BED THICKNESS IN FEET
10
5
8
6
3
1
2
11
4
9

Fig. 1f

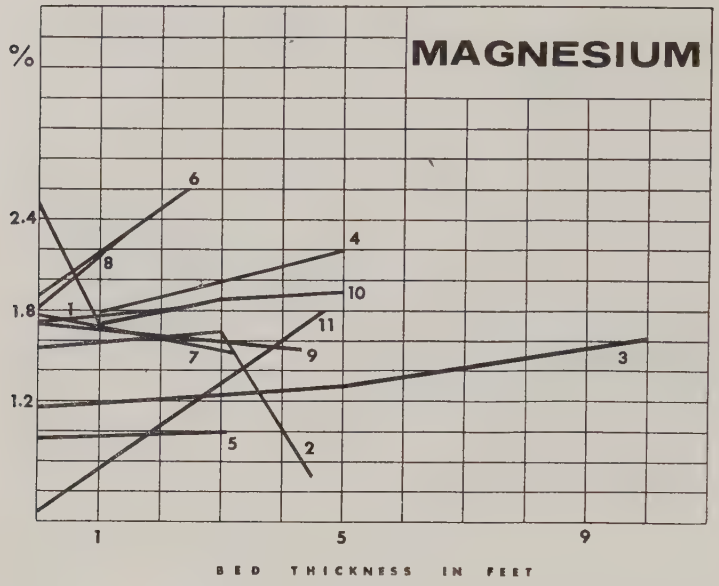
MAGNESIUM
%
2.4
1.8
1.2
1
5
9
BED THICKNESS IN FEET
1
2
3
4
5
6
7
8
9
10
11

Fig. 1g

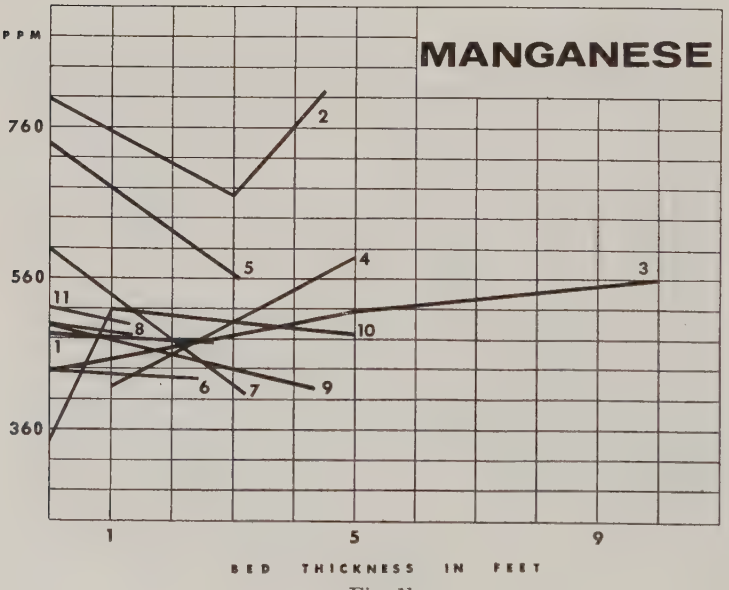
MANGANESE
PPM
760
560
360
1
5
9
BED THICKNESS IN FEET
1
2
3
4
5
6
7
8
9
10
11

Fig. 1h

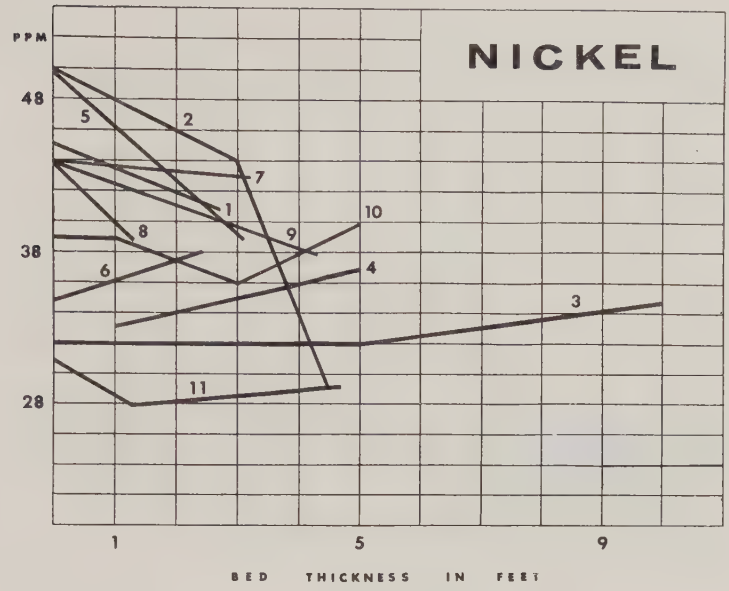
NICKEL
PPM
48
38
28
1
5
9
BED THICKNESS IN FEET
1
2
3
4
5
6
7
8
9
10
11

Fig. 1i

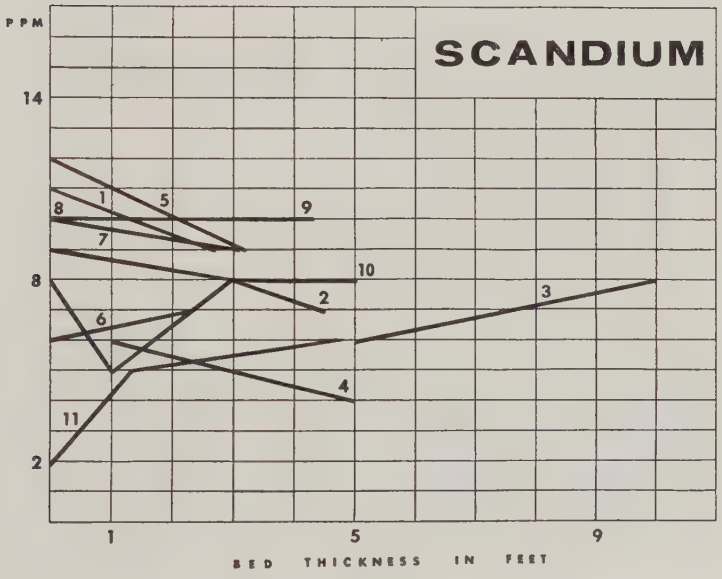
SCANDIUM
PPM
14
8
2
1
5
9
BED THICKNESS IN FEET
1
2
3
4
5
6
7
8
9
10
11

Fig 1j

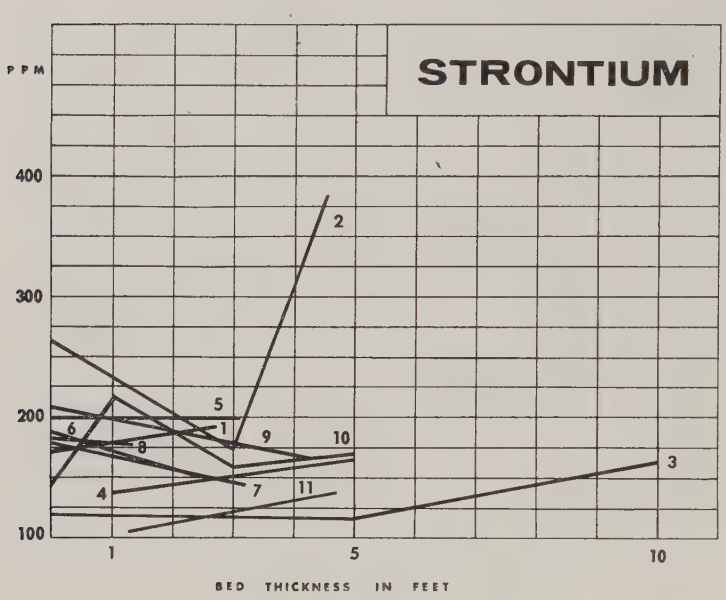
STRONTIUM
PPM
400
300
200
100
1
5
10
BED THICKNESS IN FEET
1
2
3
4
5
6
7
8
9
10
11

Fig. 1k

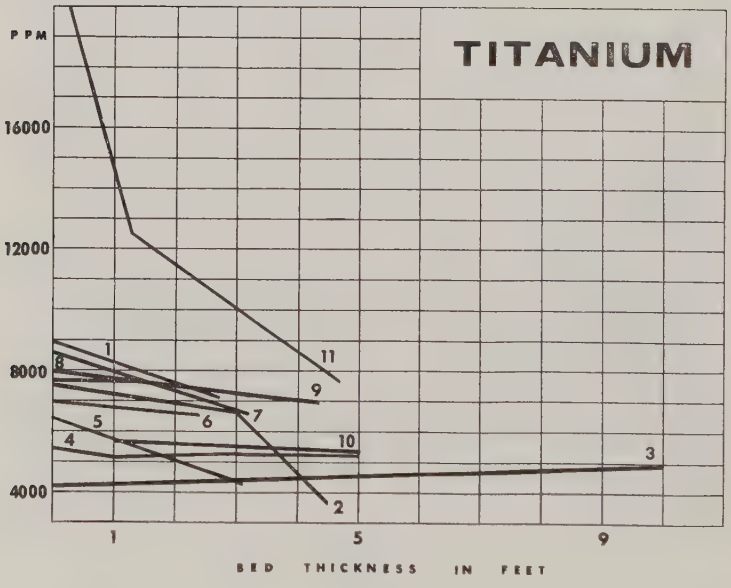
TITANIUM
PPM
16000
12000
8000
4000
1
5
9
BED THICKNESS IN FEET
1
2
3
4
5
6
7
8
9
10
11

Fig. 1l

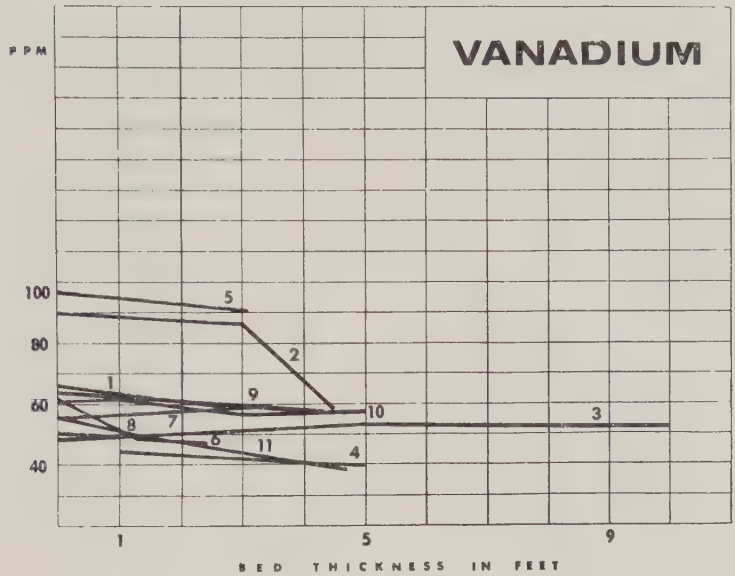
VANADIUM
PPM
100
80
60
40
1
5
9
BED THICKNESS IN FEET

Fig. 1m

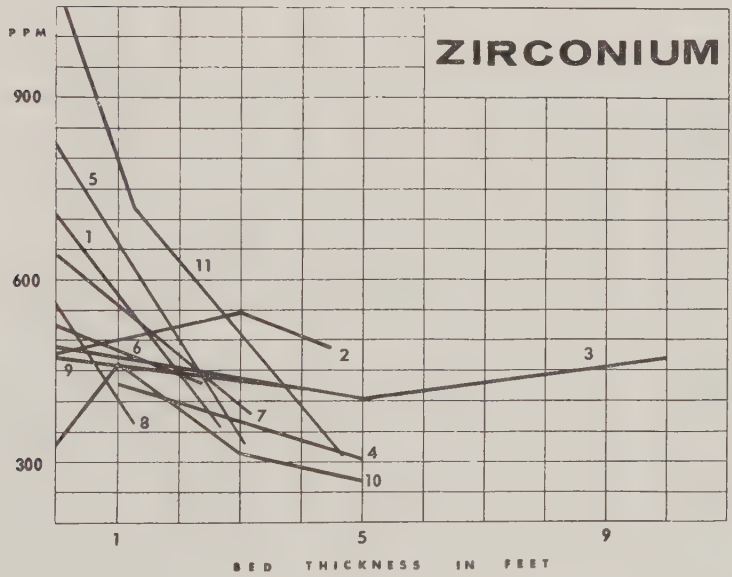
ZIRCONIUM
PPM
900
600
300
1
5
9
BED THICKNESS IN FEET

Fig. 1n

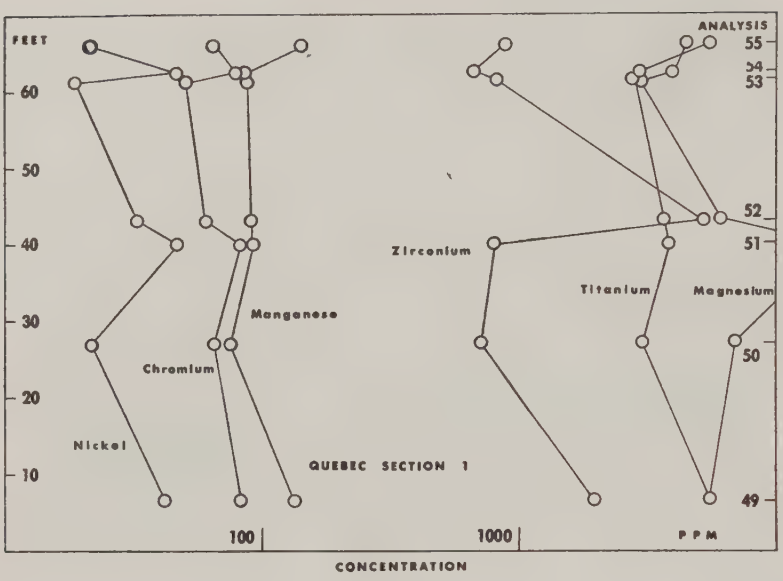

Fig. 2a

Fig. 2. Distribution of elements in a Quebec group stratigraphic section (a, b, and c, section 1).

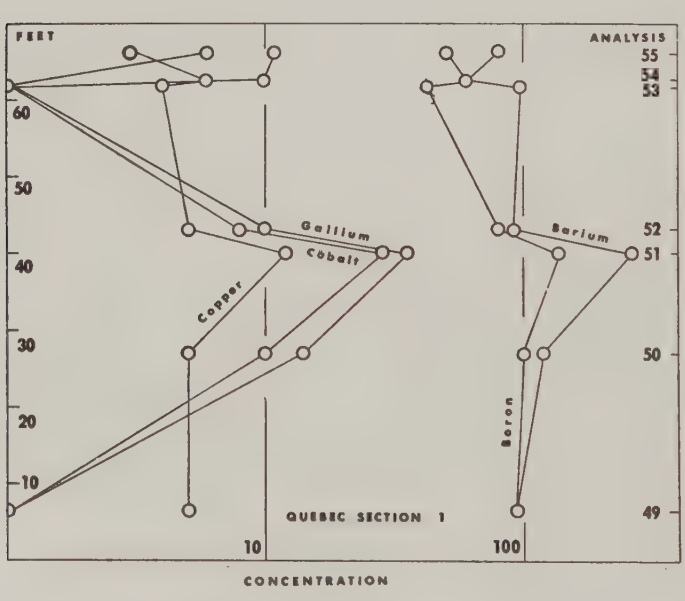

Fig. 2b

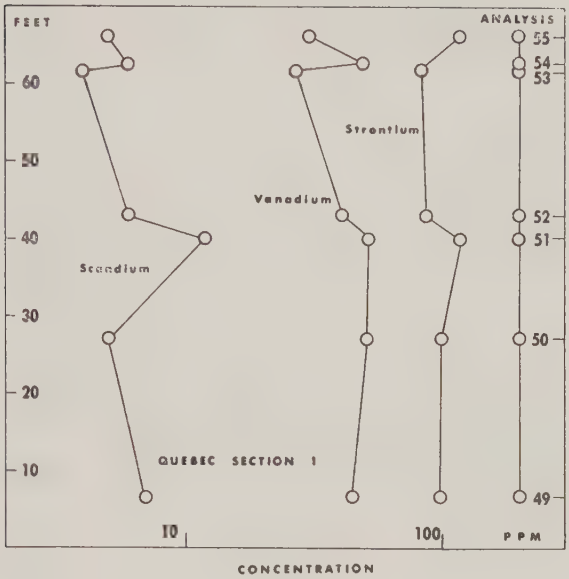

Fig. 2c

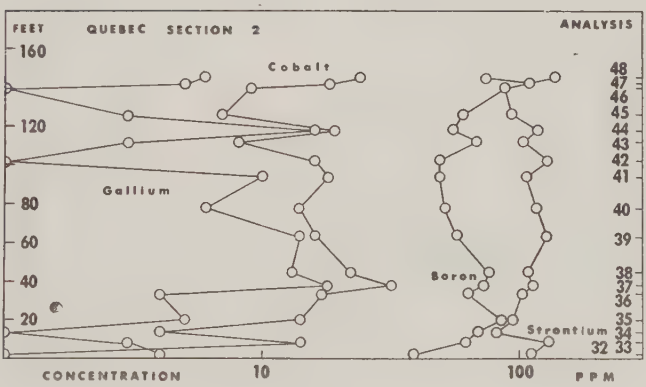

Fig. 3a

Fig. 3. Distribution of elements in a Quebec group stratigraphic section (Charny formation) (a, b and c, section 2; d and e, range of elements in section 2).

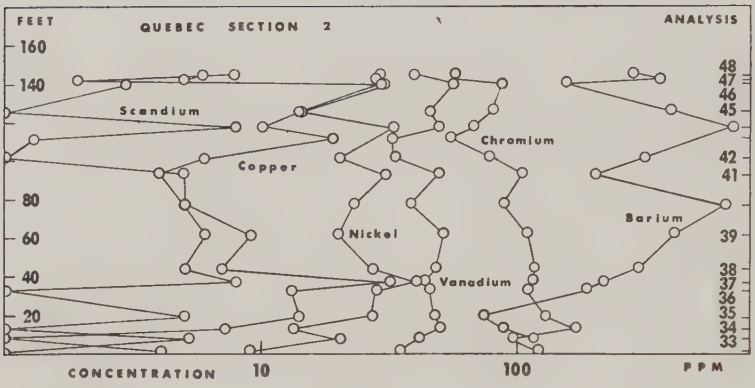
FEET
QUEBEC SECTION 2
ANALYSIS
160
140
80
60
40
20
Scandium
Copper
Nickel
Chromium
Vanadium
Barium
48
47
46
45
42
41
39
38
37
36
35
34
33
CONCENTRATION
10
100
PPM

Fig. 3b

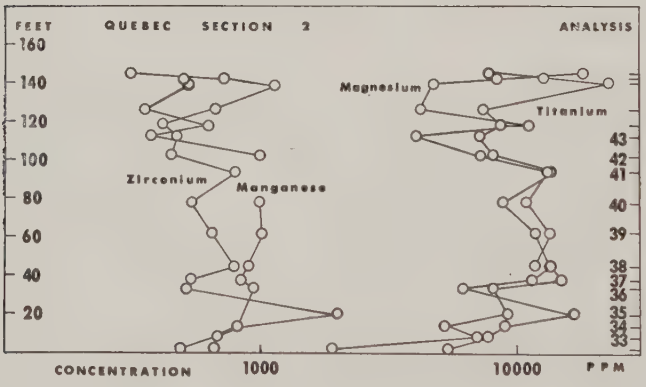
FEET
QUEBEC SECTION 2
ANALYSIS
160
140
120
100
80
60
40
20
Zirconium
Manganese
Magnesium
Titanium
43
42
41
40
39
38
37
36
35
34
33
CONCENTRATION
1000
10000
PPM

Fig. 3c

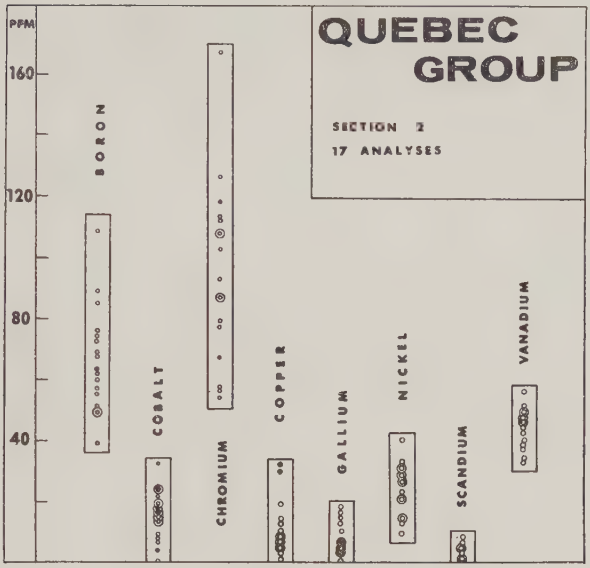
QUEBEC
GROUP
SECTION 2
17 ANALYSES
PPM
160
120
80
40
BORON
COBALT
CHROMIUM
COPPER
GALLIUM
NICKEL
SCANDIUM
VANADIUM

Fig. 3d

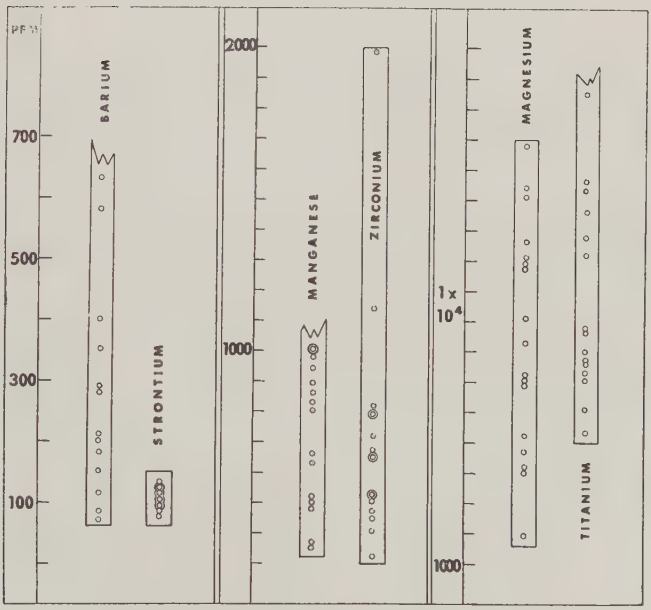
700
500
300
100
BARIUM
STRONTIUM
2000
1000
MANGANESE
ZIRCONIUM
1 x
10⁴
1000
MAGNESIUM
TITANIUM

Fig. 3e

Geochimica et Cosmochimica Acta, 1961, Vol. 22, pp. 244 to 288. Pergamon Press Ltd. Printed in Northern Ireland

Geochemistry of the turbidites of the Normanskill and Charny formations—II

Distribution of trace elements

J. N. Weber and G. V. Middleton
Department of Geology, McMaster University, Hamilton, Canada

(*Received in final form* 20 *May* 1960)

Abstract—Thirty-one Normanskill greywackes and twenty-four Quebec group (Charny formation) arkoses, of turbidite origin, have been analysed spectrographically to determine the concentrations of Ag, B, Ba, Be, Co, Cr, Cu, Ga, La, Mg, Mn, Mo, Ni, Sc, Sr, Ti, V, Y and Zr.

The distribution of the trace elements and of magnesium is shown by histograms. One greywacke was disaggregated into four major constituents, carbonate, clay, quartz–feldspar and heavy minerals, illustrating what each fraction contributes to the chemical composition of the rock. Correlation of chemical and mineral composition is attempted, statistical analysis was carried out showing correlations between all pairs of elements and the role of each element in the turbidites is discussed.

Introduction

Turbidites of the Normanskill formation of New York State and from the Charny formation (Quebec group) of Quebec, Canada, have been analysed by quantitative spectrographic methods for eighteen trace or minor elements and one major element. Ag, Be, La, Mo and Y were rarely or never detected. Details of the turbidite formations, sample localities and the analyses are presented in Part I of this paper.

Methods

The spectrographic techniques are described in Part I.

About 1900 g of one Normanskill greywacke sample were crushed to fine sand size between 100- and 200-mesh, and although much care was taken to reduce the fines fraction (less than 200-mesh) to as small a quantity as possible, 350 g of fine sand and 420 g of fines were produced.

The major constituents of the greywacke are: quartz and feldspar, carbonate, clay matrix and heavy minerals and each of the four fractions was separated and spectrographically analysed.

Quartz and feldspar were separated together from the fine sand fraction using the Franz isodynamic magnetic separator. Assuming that none of the elements determined are present in detectable quantities in the quartz, and using the ratio of the two minerals as determined in thin-section, the concentrations of the elements in feldspar may be determined, except for those of very low concentration, such as scandium, which might disappear by dilution.

Carbonate material was leached from both the fines and the fine sand fraction by dilute cold hydrochloric acid. About 50 g of carbonate residue was taken from 354 g of greywackes (i.e. 14 per cent by weight: for comparison it may be noted that 20 per cent carbonates was determined for this sample by modal analysis).

The clay matrix was separated, after hydrochloric acid had removed the carbonate, by forming a suspension of the fine material and separating the suspension after a length of time during which all but the very finest of particles had settled to the bottom. Filtration of the suspension yielded a clay-rich residue.

Heavy minerals were separated from the fine sand fraction by gravity settling using tetrabromethane (density 2·9). The grains with a density over 3·0 were washed with ethanol. Under the microscope, the grains were difficult to identify because of their very small size and over 50 per cent of the material was opaque. Among the transparent minerals, zircon comprised at least one-half.

Linear regression analysis was carried out using about 200 sets of data. The method detects correlation between two populations and determines parameters necessary to draw a straight line through the number of points produced when each X value from population X is plotted against each Y value from population Y.

The equation of this line is $\overline{Y}_x = \overline{Y} + b(X - \bar{X})$, where: $\overline{Y}_x$ is the statistical value of the ordinate Y for any given value of the abscissa X; b is the linear regression coefficient; $\bar{X}$ is the average of the X values and $\overline{Y}$ is the average of the Y values.

A value, t, is calculated from the equations given below and if a t-value falls outside the range $t_{\frac{1}{2}\alpha,(N-2)}$ to $t_{1-\frac{1}{2}\alpha,(N-2)}$, at the selected level of significance, α, Y values are considered to be dependent upon X-values, that is, a correlation between X and Y populations exists. The procedure in reality is determining whether or not the pattern of X–Y values is random or biased.

$$b = \frac{\Sigma XY - (\Sigma X \Sigma Y/N)}{\Sigma X^2 - (\Sigma X)^2/N}$$

$$s_x^2 = \frac{\Sigma X^2 - (\Sigma X)^2/N}{N-1} \qquad s_y^2 = \frac{\Sigma Y^2 - (\Sigma Y)^2/N}{N-1}$$

$$s_{y.x}^2 = \frac{N-1}{N-2}(s_y^2 - b^2 s_x^2)$$

$$t = \frac{b s_x \sqrt{(N-1)}}{s_{y.x}}$$

The analyses are given to two significant figures. All statistical manipulations, however, were carried out using three figures, and for this reason the means and standard deviations may differ slightly from those which might be obtained by using the stated concentrations.

In order to perform correlation tests, the minimum detection level of concentration was given to concentrations marked "tr" in the analyses. Thus the averages $\bar{X}$ and $\overline{Y}$ appearing in the tables listing correlation coefficients will not necessarily be identical with the averages used for the same set of analyses elsewhere. The procedure is valid for correlation analysis and these averages $\bar{X}$ and $\overline{Y}$ are used only in plotting correlation graphs.

Content of minor elements

The distribution patterns of thirteen minor elements and of magnesium in twenty-eight Normanskill greywackes are shown in Fig. 1. Boron, cobalt, nickel, scandium, titanium and magnesium appear to be distributed according to the Gaussian law. Chromium, copper, gallium, strontium, manganese and zirconium

are skewed toward smaller concentrations and vanadium shows very close grouping around a mode of from 50 to 60 p.p.m.

In the Quebec group arkoses, shown in Fig. 2, boron, nickel, scandium, strontium and vanadium are normally distributed while barium, cobalt, chromium, copper, gallium, magnesium and titanium are markedly skewed toward smaller concentrations. Manganese appears to be bimodal having one mode in the 0 to 200 p.p.m. concentration range, and another in the 800 to 1000 p.p.m. range. Zirconium shows an irregular distribution pattern.

Composition of constituents forming greywackes

About seven major constituents form a typical Normanskill greywacke: quartz, feldspar, clay matrix, "shale-like" rock fragments, carbonate cement, carbonate (limestone) rock fragments and heavy minerals. By the procedure described in the section discussing methods, one large sample of Normanskill greywacke was disaggregated into four fractions: carbonate, quartz–feldspar, clay and heavy minerals.

Because of the nature of the rock, separation is achieved with difficulty and a high degree of purity of the fractions is almost impossible to attain. Carbonate was leached from fine powder by the application of dilute cold hydrochloric acid. However, even though the hydrogen ion concentration was held to a low level, ions adsorbed on clays might be removed along with the various carbonates.

Quartz and feldspar were removed together by repeated use of a Franz isodynamic mineral separator. Despite the many runs and repeated examination of the grains under the microscope, a few grains of zircon appear to have remained in the mixture. Only one or two grains of zircon in a thousand of quartz are necessary to show the zirconium value obtained when analysing the quartz–feldspar mixture. Zirconium, because of its ionic size and electronic charge, is not taken into the quartz or feldspar structures in detectable quantities, if at all.

Clay minerals were separated by elutriation because of the very small size of the grains. It is unlikely but not impossible that minor amounts of other minerals were crushed fine enough to be included in the clay fraction.

Heavy minerals were separated by a liquid of high specific gravity so that any grain with a density exceeding 3·0 was included in this fraction.

It is important to note that values of precision which apply to the turbidite analyses cannot be used with analyses 76, 77 and 79. The spectrographic method has been developed assuming that the composition of the material analysed is not much different than that of the average igneous rock. The carbonate, quartz–feldspar and heavy minerals nowhere approach this composition and the concentration values given in Table 1 of Part I are valid, perhaps, only in the first figure.

Most of the carbonate material, which occurs as cement and as a replacement product of decaying minerals such as basic plagioclase feldspar, comprises calcite and dolomite. Barium, manganese and strontium are present either as their respective carbonates or else replacing small amounts of calcium in the dolomite and calcite. Copper, which is present in the analyses may have been leached from

the clays but this is unlikely as it is normally precipitated in the hydrolysates as a sulphide. Scandium is present also in the carbonate fraction, possibly contained in either calcium or ferrous carbonate with which it has occasionally been reported.

The quartz–feldspar fraction contains barium which occurs commonly in feldspars which contain varying amounts of the barium feldspar molecules such as hyalophane or celsian. Copper and zirconium are also indicated but probably occur as impurities in the mixture. It is important to note that even though such elements as strontium may frequently be present in feldspars, the content of feldspar in the Normanskill greywackes is generally so low that only barium in feldspars is shown by a rock analysis.

The clay or hydrolysate fraction, as would be expected, is rich in hydrolysate elements such as boron, barium, cobalt, chromium, copper, gallium, nickel, titanium and vanadium. Zirconium is only weakly associated with hydrolysates as is manganese, magnesium and strontium, and this is reflected in the analyses. All elements are to some degree contained in the clay-rich material.

The heavy mineral fraction is extremely rich in zirconium, showing an excess of 10,000 p.p.m. Barium, cobalt, chromium, copper, nickel, scandium, titanium and vanadium are all relatively enriched in the heavy mineral suite, contained in minerals such as ilmenite, zircon, chromite, pyrite, barite, monazite, rutile, tourmaline and others. Silver is present at a concentration of about 50 p.p.m. even though the element is undetected in the rock analyses.

Table 1 contains the concentrations of the various elements calculated on the basis of thin-section point counts for the four fractions, to show how much each fraction contributes to the entire rock. It can be seen that most of the boron, barium, chromium, copper, gallium, magnesium, nickel, titanium and vanadium is contained in the clays whereas the heavy minerals contribute much cobalt and zirconium. Carbonates add considerable quantities of barium, magnesium, manganese, scandium and strontium, and feldspar contributes much barium.

The amounts contributed by the various fractions are in fair agreement with the analysis of the entire rock considering the accuracy of the analyses and the point counts. For boron, barium, nickel, strontium and titanium, agreement is not as good as for the other elements.

Correlation of chemical composition with mineral composition

Mineralogical composition was determined by point-counting one to three thin-sections cut from each sample. Before this work was carried out, a programme to evaluate the degree of operator error was instituted. Four different operators counted two thin-sections of Normanskill greywacke in the same manner using a set of definitions to help distinguish between such minerals as clay matrix and carbonate cement.

Each slide was point counted for quartz, clay, feldspar, fine-grained rock fragments, carbonate rock fragments, other carbonates (including cement) and heavy minerals. It was evident that quartz could be accurately determined by 300 counts, with differences between operators of the order of ± 2 per cent. Both clay and rock fragments showed very large differences between estimates made by different operators (the differences being of the order of ± 12–25 per cent),

although each operator remained fairly consistent, even when the same slide was counted again after a period of several months. Moreover, different operators agreed in consistently estimating more or less of any constituent in a comparison between two slides, even when the actual estimates differed greatly.

In an attempt to minimize operator variation, the slides were counted only for quartz, feldspar, fine-grained rock fragments and clay (taken together), carbonates (undifferentiated) and accessories. Clay and rock fragments which were largely argillaceous in composition, were counted together because the operator error experiment indicated that it was unrealistic to attempt a distinction between them. All point counts were made by the junior writer, except those of analyses 72 to 75 inclusive which were measured by another operator, P. S. Simony, who was especially experienced in point-counting rocks of this formation.

Petrographic data are given in Table 2. Figs. 3 and 4 show the carbonate, rock fragments plus clay matrix, and quartz plus feldspar percentages of the turbidites plotted on triangular diagrams with the concentration of a particular element shown along side. Plots placing the maximum or average grain size against concentration showed scatter patterns.

The Normanskill formation shows no good correlation of any element with the corresponding petrographic data. There is, however, a weak tendency for boron, barium, nickel, scandium and titanium to be higher in concentration in the more clay-rich greywackes, and gallium to be lower. Cobalt shows high values in the centre of the diagram.

In the Quebec group, cobalt, gallium and magnesium appear to have higher values in turbidites which have a lower quartz–feldspar content but other correlations are decidedly indistinct.

Correlation could possibly be increased by a greater number of samples showing great ranges in clay, quartz–feldspar and carbonate contents. In this study, very little indication of the chemical composition of the greywackes may be inferred from thin-section point counts.

Correlation of elements

. The fourteen elements studied were taken two at a time in all possible combinations in both the Normanskill and Quebec turbidites. Statistics for each pair are listed in Tables 3 and 4. b is the regression coefficient affecting the slope of the line drawn through the points produced when one element is plotted against another. $\bar{X}$ is the average of one element plotted on the abscissa while $\bar{Y}$ is the average of the second plotted on the ordinate. The element of the pair to which $\bar{X}$ belongs will be determined by inspection of the tables. A correlation coefficient t was calculated by the laborious method listed in the chapter on methods. Values of t numerically greater than 2·779 in the Normanskill formation and numerically greater than 2·819 in the Quebec group indicate correlation between the pair of elements at the 1 per cent level of significance.

Pairs of elements which show a high degree of correlation are listed in Tables 5 and 6 in the order of decreasing significance.

Poor correlation is illustrated in Figs. 5 and 6 where the correlation coefficients are, respectively, 0·318 and 0·074. Good correlation is shown in Figs. 7, 8 and 9

where much higher correlation coefficients, 5·095, 9·975 and 4·458 obtain. All diagrams pertain to the Normanskill greywackes.

Compared with the Quebec turbidites, the Normanskill formation has a larger number of highly significant correlations, yet only three, barium–nickel, nickel–scandium and boron–gallium are common to both.

Correlations such as cobalt–nickel, chromium–copper, boron–chromium and chromium–vanadium reflect the varying presence of clay in the greywacke samples. A sample higher in clay would be expected to be higher in chromium and in copper although by no means will this always occur as the amounts supplied by the source area and the depositional characteristics also play a part. Similarly, because both manganese and strontium occur in the cementing substance, a sample higher in carbonate might show both higher strontium and higher manganese concentrations.

Because of the composite nature of turbidite deposits, some fractions being mechanically derived, others hydrolysed and deposited from marine water or precipitated by percolating intra-stratal fluids, it is not unexpected that a large number of correlations would exist.

Discussion

(a) Boron occurs largely in the clay fraction of the turbidites, although a minor amount may be shown by the heavy minerals if grains of tourmaline or other borosilicates are present. Normanskill greywackes which are high in boron, also tend to be low in chromium, manganese, strontium, gallium and copper and high in titanium. In the Quebec group, high boron values are correlative with high vanadium, nickel, scandium and gallium.

(b) Barium is derived from four fractions of the greywacke with clay material contributing the most. Carbonate cement and feldspars containing barium yield smaller but still significant amounts. A few parts per million may be added to the rock by the heavy mineral suite. Barium is associated with nickel and cobalt, both enriched in clays, in the Normanskill formation and to a lesser extent with scandium.

In the Quebec group, barium is correlative only with nickel. Both nickel and barium are elements of the hydrolysates, nickel-forming sulphides if very small amounts of hydrogen sulphide are present, and barium is removed by adsorption because of its ionic radius and potential. Much of the barium brought to the sea is removed in near-shore sediments. Because organic matter is carried down at delta mouths by flocculating agents, a supply of hydrogen sulphide would be generated which would precipitate elements such as nickel as sulphides.

(c) Cobalt. Although cobalt is another element typical of the hydrolysate environment where it is precipitated as a sulphide, much cobalt in the turbidites is supplied by the heavy mineral suite. One-third or less may be present in the clay. In the Normanskill formation, cobalt correlates with nickel, barium, chromium, copper and vanadium, all hydrolysate-loving elements which are precipitated near shore, especially in slightly sapropelic deltaic environments, the build up of which was largely responsible for the formation of the turbidity flows. In the Quebec group, cobalt is correlative with magnesium, gallium, strontium and scandium. Here, cobalt may occur almost exclusively in heavy minerals.

(d) Chromium is present both in the clay matrix and in heavy minerals such as chromite, magnetite and ilmenite. In the Normanskill formation, greywackes high in chromium are also high in copper, manganese, vanadium, nickel, strontium, cobalt and gallium and low in boron and magnesium. In the Quebec group, no correlative pairs are found to include chromium, possibly because chromium may be divided nearly equally between the heavy mineral and clay fractions.

(e) Copper is present in the analyses of all four fractions, undoubtedly as an impurity in some. Most likely, the bulk of the copper is found in the heavy minerals with considerable amounts added in the form of sulphides by clay particles. Copper is one of the first elements to precipitate from solution on the addition of slight amounts of hydrogen sulphide. For this reason, greywackes high in copper in the Normanskill are also high in chromium, nickel, vanadium and cobalt but are low in boron. Copper in the Quebec group of sandstones is unrelated to the concentration of other elements.

(f) Gallium is detected only in the clay fraction and the element is known to be typical of hydrolysates, although as one of the "dispersed elements" its concentration is unlikely to vary greatly. In the Quebec group, rocks with higher gallium content tend to have higher concentrations of scandium, cobalt, magnesium and boron. In the Normanskill formation, gallium follows boron and chromium.

(g) Magnesium appears in the clay matrix, possibly as chlorite, in the carbonate cementing material and to a smaller extent in some of the less-stable heavy minerals and in tourmaline. As interstitial cement, magnesium is present as dolomite. In clays, the magnesium has either been added from sea water by base exchange reactions with clay, or has been transported as magnesian clay from the weathering of basic rocks. The pH never attains a sufficient level in sea-water for the direct precipitation of magnesium hydroxide. Any addition of volcanic dust is liable to raise the concentration of magnesium.

In the Normanskill formation, magnesium correlates with chromium and titanium, and in the Quebec group with cobalt, gallium, scandium, strontium and manganese. The correlation of magnesium with elements of a diverse nature results from its appearance in three of the four fractions composing the greywackes.

(h) Manganese is largely contributed in the Normanskill greywackes by the carbonate cement where it occurs either as rhodochrosite, or as a replacement of Ca in the calcite or dolomite. Smaller amounts are present in the clays and heavy minerals. The manner in which manganese is incorporated into hydrolysate sediments is controversial. Correns (1941) claims manganese is biologically extracted while Kuenen (1941) claims manganese is a chemical precipitate from sea water. Pettersson (1945) has shown that manganese is largely adsorbed on volcanic dust, and it is interesting to note that of the three types of greywackes analysed by Macpherson (1958), volcanic greywackes show the highest manganese content.

In the Normanskill formation, manganese correlates well with chromiun, boron and vanadium which are in the clay fraction, and with strontium which occurs with manganese in the carbonate. In the Quebec group, manganese correlates with magnesium and titanium.

(i) Nickel is found mostly in the clay mineral fraction with a smaller amount contributed by heavy minerals. Rocks showing a high concentration of nickel in the Normanskill formation also show higher concentrations of cobalt, barium, titanium, scandium, vanadium, copper, chromium and zirconium and in the Quebec group show higher concentrations of scandium and boron and lower of barium.

(j) Scandium is contributed by the carbonate material and to a lesser extent by the clay and heavy minerals. Scandium is known to form scandium orthoborate, $ScBO_3$ (Goldschmidt and Hauptmann, 1932), with a structure of the calcite type and dimensions similar to those of ferrous carbonate with which it forms isomorphic mixtures. In heavy minerals, scandium is often found in considerable concentration in cassiterite, monazite, ferromagnesian minerals, biotite and to a lesser extent in garnet, allanite and tourmaline.

In the Normanskill greywackes, scandium is correlative with titanium, nickel, vanadium and barium and in the Quebec sandstones with nickel, gallium, magnesium, cobalt and boron. Correlation with a diverse group of elements is a result of its occurrence in several of the fractions constituting the rock.

(k) Strontium is found largely in the carbonate cement but smaller amounts are added by the heavy minerals. Unlike barium, strontium is not readily added to the hydrolysate sediments but remains largely in the sea where it is removed by organic processes and incorporated into the shells of radiolarians and organisms which have aragonite tests, as the compound strontium sulphate. The organic skeletal remains are included in turbidite beds but are soon dissolved by percolating intrastratal fluids and redistributed in the form of carbonate cement. In the Normanskill formation, much of the strontium is contributed by fragments of bioclastic limestone as well as primary remains. Normanskill greywackes high in strontium tend to be high in manganese also reflecting the amount of cementing material in the sample. Strontium is also correlative with boron and chromium which occur in the clay matrix. In the Quebec group, strontium correlates with magnesium and cobalt.

(l) Titanium is present both in the clay matrix and in the heavy mineral assortment. Because of the very small percentage of heavy minerals, however, the bulk of the titanium is contributed by the hydrolysate fraction where it has been extracted from solutions derived from the weathering of pyroxenes, amphiboles and micas. In the heavy mineral suite, titanium is bound up in the stable grains of rutile, ilmenite, brookite and anatase: in thin section an alteration product, leuxocene, is not uncommon. In the Normanskill greywackes, titanium is associated with boron and nickel, elements of the hydrolysates, with zirconium an element characteristic of the heavy minerals, and with scandium and magnesium. In the Quebec group, titanium is correlative only with manganese.

(m) Vanadium occurs largely in the clay matrix although smaller amounts are derived from heavy minerals. Vanadium is hydrolysed to some extent, especially in the presence of hydrogen sulphide in bituminous sediments where it forms insoluble V_2S_5. Because of this property, it occurs in the Normanskill formation along with chromium, nickel, manganese, copper, cobalt and scandium and in the Quebec group with boron. Jost (1932) has shown that vanadium occurs in higher concentrations in sandstones if argillaceous matter is included.

(n) Zirconium is present only in the heavy mineral fraction. Although zirconium is removed from solution by hydrolysis and added to the clays, very little of the element occurs in this medium because little goes into solution as a result of the mechanical and chemical stability of zircon.

In the Normanskill formation, greywackes rich in zirconium tend to be richer in titanium and nickel but no correlative pairs including zirconium are found in the Quebec group.

(o) Silver occurs in the heavy mineral fraction but is undetected in the rock analyses. Gold is undetected in both.

Summary

Elements typical of the hydrolysates are contributed to the turbidite by the clay matrix and elements such as magnesium, strontium, barium and manganese are abundant in the cementing carbonate material. Heavy minerals supply zirconium and smaller amounts of cobalt, nickel, silver and others.

Very little correlation between petrography and chemical composition is apparent. Highly significant correlations in the Normanskill greywackes are: Co–Ni, Cr–Cu, Cr–Mn, B–Cr, Cr–V and Ba–Ni. In the Quebec turbidites, significant correlations comprise: Co–Mg, Ni–Sc, Ga–Sc, Co–Ga, Ga–Mg.

References

Correns C. W. (1941) Beiträge zur Geochemie des Eisens und Mangans. *Nachr. Akad. Wiss Göttingen, Math.-Physik Klasse* 219.

Goldschmidt V. M. and Hauptmann H. (1932) Isomorphie von Boraten und Karbonaten. *Nachr. Ges. Wiss. Göttingen, Math.-Physik Klasse* III,, **28,** 402–407; *Ibid.* IV, **31,** 528–545.

Jost.K. (1932) Über den Vanadiumgehalt der Sedimentgesteine und sedimentären Legerstätten. *Chemie der Erde* **7,** 177–290.

Kuenen Ph. (1941) Geochemical calculations concerning the total amount of sediment in the earth. *Amer. J. Sci.* **239,** 161–190.

Macpherson H. G. (1958) A chemical and petrographic study of Pre-Cambrian sediments. *Geochim. et Cosmochim. Acta* **14,** 73–92.

Pettersson H. (1945) Iron and manganese on the ocean floor. A contribution to submarine geology. *Conseil Permanent Intern. Exploration Mer* **109,** No. 9, 66; *Göteborgs Kgl. Vetenskapsoch Vitterhets-Samhälles Handl.* 6F, Ser. B, **3,** No. 8, 1–37.

Table 1. Distribution of elements among four fractions of greywacke

Analysis	Fraction	Ag	B	Ba	Co	Cr	Cu	Ga	Mg	Mn	Ni	Sc	Sr	Sr*	Ti	V	Zr
76	Carbonate	nd	nd	240	nd	tr	35	nd	3·8	2400	tr	50	2800	—	nd	tr	nd
77	Quartz–feldspar	nd	tr	200	tr	tr	23	tr	tr	tr	tr	tr	tr	tr	tr	tr	1100†
78	Clay	tr	120	340	16	100	25	14	3·0	100	33	8	100	100	6400	68	310
79	Heavy minerals	50	26	410	700	900	75	tr	0·70	260	260	28	400	250	11000	320	s‡
1 and 2	Original rock	nd	120	410	22	91	25	6	1·8	480	43	10	270	180	8100	62	540
	Feldspar§	nd	nd	16	nd	nd	2	nd	nd	nd	nd	nd	nd	—	nd	nd	—
							Amounts Contributed to Greywacke by each Fraction										
Carbonate 22%		0	0	53	0	0	8	0	0·84	530	0	11	630	—	0	0	0
Quartz–feldspar 27%		0	0	53	0	0	6	0	0	0	0	0	0	—	0	0	—
Clay 46%		0	55	160	7	46	12	6	1·4	46	15	4	46	—	2900	31	140
Heavy minerals 2%		1	0·5	8	14	18	1·5	0	0·01	5	5	0·6	8	—	220	6·5	—
Total		1	55	270	21	64	27	6	2·2	580	20	16	680	—	3100	38	—
Original rock		nd	120	410	22	91	25	6	1·8	480	43	10	270	180	8100	62	540

* Corrected values of strontium.
† Present as an impurity.
‡ Over 10,000 p.p.m.
§ Assuming a thin-section ratio of 25/2 for Quartz/feldspar.

Statement of Analyses

Concentration of all elements except magnesium is given in parts per million (p.p.m.). Magnesium is stated in per cent (%). Sr* indicates corrected concentration values of strontium.)

Analysis	B	Ba	Co	Cr	Cu	Ga	Mg	Mn	Ni	Sc	Sr	Sr*	Ti	V	Zr
1	120	410	24	100	26	2	1·7	490	45	11	240	170	9000	66	710
2	120	410	19	91	24	10	1·8	480	41	9	290	200	7200	59	360
3	55	380	24	130	27	25	2·0	800	50	9	430	260	7600	90	480
4	61	350	22	120	25	9	1·7	670	44	8	250	180	6600	86	550
5	33	220	15	120	24	8	0·56	810	29	7	670	380	3700	59	480
6	56	240	14	93	25	9	1·2	440	32	6	140	120	4300	49	490
7	74	280	15	95	22	9	1·3	520	32	6	140	120	4600	54	410
8	73	320	17	100	25	11	1·6	560	35	8	230	170	5000	53	480
9	84	270	14	73	27	4	1·8	420	33	6	180	140	5700	45	430
10	79	300	18	99	24	5	2·2	590	37	4	240	170	5400	40	310
11	42	430	23	210	52	15	0·96	740	50	12	300	200	6700	97	830
12	38	380	16	140	31	14	1·0	560	39	9	300	200	4300	91	330
13	85	320	16	85	21	6	1·9	440	35	6	280	190	7000	51	530
14	96	270	20	86	25	11	2·6	430	38	7	210	150	6600	48	430
15	98	330	20	100	25	tr	1·8	600	44	10	250	180	8600	56	640
16	91	320	20	80	23	tr	1·5	410	43	9	200	150	6800	59	380
17	76	410	22	100	26	3	1·8	500	44	10	270	180	7700	61	560
18	91	360	18	85	23	11	2·3	490	39	10	260	180	7700	49	370
19	83	390	20	98	26	3	1·7	500	44	10	320	210	8000	65	560
20	99	400	16	82	23	3	1·6	420	38	10	240	170	7000	58	420
21	89	420	21	85	30	14	2·5	350	39	8	190	150	5400	61	330
22	63	320	21	120	28	18	1·7	520	39	5	350	220	5200	62	470
23	77	330	18	94	24	11	1·9	500	36	8	220	160	5300	57	320
24	77	370	19	100	27	18	1·9	490	40	8	240	170	5300	58	270
25	89	150	9	87	30	tr	0·47	520	31	2	52	77	23,000	56	1100
26	110	350	18	56	2	5	0·83	500	28	5	110	110	13,000	50	720
27	74	280	24	57	8	6	1·8	—	29	6	180	140	7700	39	310
28	21	450	27	180	43	18	1·0	640	53	7	610	350	5600	62	610
29	24	230	18	120	32	14	0·97	590	34	7	240	170	3600	61	280
30	33	400	20	140	26	14	1·1	550	39	9	470	280	4400	64	290
31	61	440	21	120	30	11	1·7	650	47	10	330	210	6600	82	410
32	39	s	tr	120	4	4	0·19	480	9	nd	120	110	5300	34	650
33	62	110	14	93	tr	3	0·71	660	20	5	160	130	7600	40	670
34	68	86	4	170	7	tr	0·52	800	13	nd	59	81	8800	49	820
35	85	71	14	130	5	5	0·91	860	27	5	84	94	16,000	47	2000
36	63	180	17	110	13	4	0·70	940	28	nd	100	100	6100	45	510
37	73	210	32	110	32	18	1·5	830	40	8	120	110	11,000	43	530
38	76	290	22	110	7	13	1·2	900	27	5	110	110	13,000	47	790
39	57	400	16	110	9	14	1·3	1000	20	6	150	130	12,000	51	650

Statement of Analysis (*contd*).

Analysis	B	Ba	Co	Cr	Cu	Ga	Mg	Mn	Ni	Sc	Sr	Sr*	Ti	V	Zr
40	51	630	14	87	5	6	1·1	980	23	5	130	120	8700	38	530
41	49	200	18	100	4	10	1·3	s	31	5	110	110	14,000	49	790
42	49	s	16	77	6	tr	0·72	1000	20	tr	160	130	8000	33	450
43	69	—	8	54	19	3	0·40	370	14	3	100	100	7100	32	470
44	55	580	19	67	10	16	1·1	630	33	8	140	120	8600	49	410
45	60	—	7	79	14	3	0·42	350	14	1	84	93	7300	45	660
46	89	150	9	87	30	tr	0·47	520	31	3	52	77	23,000	56	1100
47	110	350	18	56	2	5	0·83	500	28	5	110	110	13,000	50	720
48	74	280	24	57	8	6	1·8	—	29	6	180	140	7700	40	310
49	94	48	tr	83	5	tr	0·55	130	42	7	92	98	5500	45	2000
50	100	120	10	66	5	14	0·68	76	22	5	95	99	3100	51	710
51	140	260	29	84	12	36	1·7	93	48	12	130	120	3800	52	810
52	80	92	8	61	5	10	0·61	92	33	6	72	87	3700	41	1500
53	43	99	tr	51	4	tr	0·30	89	19	4	63	83	2800	27	830
54	64	61	10	81	6	tr	0·40	87	47	6	73	88	3000	49	670
55	51	81	11	66	3	6	0·45	150	22	5	130	120	5600	30	890
56	23	800	20	140	24	13	1·9	950	30	7	330	220	7400	51	580
57	17	510	tr	130	5	tr	0·74	600	15	8	260	180	5600	41	460
58	32	840	13	110	11	8	1·2	630	21	5	340	220	5300	43	450
59	56	830	21	130	14	14	2·2	840	34	10	220	160	7000	59	360
60	91	420	25	140	9	13	1·7	610	65	11	120	110	10,000	88	560
61	140	510	31	150	260	6	2·0	1200	70	15	150	130	13,000	100	520
62	74	s	19	110	12	tr	0·99	720	42	tr	110	110	5400	57	220
63	170	660	36	580	160	5	3·0	870	130	19	160	130	15,000	100	430
64	20	150	59	320	56	15	0·69	120	100	20	350	220	4800	96	230
65	30	120	27	180	46	13	0·58	110	84	9	230	170	3800	64	200
66	30	170	33	230	35	14	0·61	120	110	11	510	300	3800	71	190
67	69	270	16	130	4	8	3·3	670	32	8	140	120	5500	54	340
68	70	400	21	120	5	14	4·0	620	38	10	160	130	6400	66	250
69	34	620	11	130	8	3	4·3	680	59	9	270	180	3700	48	200
70	45	250	tr	92	5	tr	4·4	590	33	7	600	340	4500	42	340
71	63	570	29	87	7	6	2·1	s	37	10	110	110	8000	62	330
72	26	500	31	170	150	10	4·0	320	55	9	130	120	4700	77	200
73	tr	290	tr	64	5	6	1·1	110	11	tr	92	98	1100	24	tr
74	15	470	18	190	2	16	3·8	510	52	7	170	140	4200	55	200
75	13	470	15	150	tr	13	2·2	230	32	5	130	120	2500	42	210
76	nd	240	nd	tr	35	nd	3·8	2400	tr	50	2800	—	nd	tr	nd
77	tr	200	tr	tr	23	tr	tr	tr	tr	tr	tr	—	tr	tr	1100
78	120	340	16	100	25	14	3·0	100	33	8	100	100	6400	68	310
79	26	410	700	900	75	tr	0·70	260	260	28	400	250	11,000	320	s

Table 2. Petrographic data

Analysis	Quartz	Feldspar	Clay and rock fragments	Heavy minerals	Carbonate	Maximum grain size (mm)	Average grain size (mm)
1	32	2	42	2	22	0·9	0·25–0·5
2	18	2	53	0	27	0·3–0·35	0·1
3	34	3	42	3	19	0·8–1·0	0·1
4	35	1	49	2	13	1·0	0·15
5	27	2	34	1	35	0·6	0·35
6	47	4	32	1	14	1·35	0·35
7	42	2	37	1	18	1·3	0·3
8	39	3	28	1	28	1·15	0·15
9	39	1	42	0	18	1·35	0·5
10	32	1	50	0	17	0·85	0·35
11	40	2	44	2	13	1·50	0·20
12	22	1	60	—	17	0·3	0·1
13	16	1	46	1	37	1·15	0·2
14	30	2	52	1	14	0·8	0·1–0·2
15	18	1	63	—	18	0·8	0·08
16	27	2	60	—	11	0·67	0·15–0·25
17	27	0	58	0	15	1·2	0·3–0·5
18	15	2	57	0	25	0·65	0·15
19	23	1	55	2	19	2·0	0·25–0·5
20	20	3	59	0	17	0·9	0·15–0·20
21	30	1	44	1	23	1·05	0·2–0·3
23	30	1	48	2	18	0·7	0·15–0·3
24	29	3	51	1	16	0·55	0·1–0·15
32	76	12	8	3	0	1·7	1·0–0·4
33	39	12	9	1	37	—	—
34	77	5	15	2	0	12	2·5
35	61	17	17	4	1	2·88	0·5
36	58	13	26	2	1	1·68	0·6
37	29	10	58	2	1	0·95	0·10
38	47	20	31	2	—	2·3	0·3–0·4
39	46	13	38	2	1	2·84	0·3
40	52	20	22	1	4	1·65	0·3
41	46	16	30	4	3	1·5	0·3
42	52	17	21	2	7	1·0	0·35
43	54	11	27	4	4	1·4	0·3–0·4
44	49	13	21	16	—	1·25	0·3

Table 2—(*contd.*)

Analysis	Quartz	Feldspar	Clay and rock fragments	Heavy minerals	Carbonate	Maximum grain size (mm)	Average grain size (mm)
45	63	14	18	1	4	3·9	0·5
46	70	5	19	5	tr	6·0	0·7
47	47	11	39	2	1	0·7	0·15–0·25
48	20	11	39	—	30	0·6	0·10
56	57	19	20	3	1	12	0·3–0·5
57	73	9	13	0	5	2·5	—
58	51	17	29	2	1	2·8	0·5
59	48	12	38	4	—	1·5	0·35
60	28	1	60	8	—	0·3	0·15
61	19	0	76	1	1	0·4	0·15
62	32	1	67	—	—	1·15	0·45
63	19	0	68	10	—	0·5	0·15–0·10
69	39	10	17	1	28	0·90	0·15
71	40	7	51	—	—	—	—
72	16	6	76	2	tr	—	—
73	45	46	8	1	—	—	—
74	38	19	41	1	tr	—	—
75	30	30	38	2	—	—	—

Table 3. Correlation of elements in Normanskill Greywackes

	b	$\bar{X}$	$\bar{Y}$	t
1. *Boron*				
Chromium	−0·775	71	110	−5·034
Titanium	35·7	71	6100	4·321
Manganese	−2·64	71	540	−3·881
Strontium	−1·30	71	200	−3·467
Gallium	−0·123	71	10	−3·310
Copper	−0·127	71	27	−3·165
Vanadium	−0·218	71	62	−2·248
Barium	−0·538	71	340	−0·948
Scandium	0·012	71	8	0·905
Magnesium	0·013	71	1·6	0·500
Cobalt	−0·011	71	19	−0·466
Nickel	−0·006	71	40	−0·149
Zirconium	0·074	71	450	0·074

Table 3—(*contd.*)

	b	$\bar{X}$	$\bar{Y}$	t
2. *Barium*				
Nickel	0·048	340	40	4·458
Cobalt	0·024	340	19	3·648
Scandium	0·012	340	8	2·917
Vanadium	0·087	340	62	2·737
Copper	0·035	340	27	2·416
Chromium	0·159	340	110	2·385
Titanium	5·81	340	6100	1·661
Zirconium	0·534	340	450	1·644
Boron	−0·538	71	340	−0·948
Gallium	0·012	340	10	0·834
Strontium	0·126	340	200	0·832
Manganese	0·149	340	540	0·514
Magnesium	0·0003	340	1·6	0·318
3. *Cobalt*				
Nickel	1·57	19	40	9·975
Barium	0·024	340	19	3·648
Chromium	4·95	19	110	3·326
Copper	1·02	19	27	3·036
Vanadium	2·13	19	62	2·786
Titanium	212	19	6100	2·709
Zirconium	18·8	19	450	2·548
Scandium	0·242	19	8	2·288
Strontium	6·55	19	200	1·879
Gallium	0·593	19	10	1·718
Manganese	11·0	19	540	1·644
Magnesium	0·020	19	1·6	0·701
Boron	−0·011	71	19	−0·466
4. *Chromium*				
Copper	0·188	110	27	8·514
Manganese	2·80	110	540	5·095
Boron	−0·775	71	110	−5·034
Vanadium	0·340	110	62	4·913
Nickel	0·111	110	40	3·538
Strontium	1·17	110	200	3·433
Magnesium	−0·009	110	1·6	−3·411
Cobalt	4·95	19	110	3·326
Gallium	0·110	110	10	3·262

Table 3—(*contd.*)

	b	$\bar{X}$	$\bar{Y}$	t
Zirconium	2·10	110	450	2·583
Barium	0·159	340	110	2·385
Scandium	0·018	110	8	1·420
Tatanium	−6·79	110	6100	−0·6983
5. *Copper*				
Chromium	0·188	110	27	8·514
Nickel	0·510	27	40	3·580
Vanadium	1·22	27	62	3·324
Boron	−0·127	71	27	−3·165
Cobalt	1·02	19	27	3·036
Zirconium	9·63	27	450	2·599
Gallium	0·411	27	10	2·500
Barium	0·035	340	27	2·416
Manganese	7·17	27	540	2·206
Magnesium	−0·029	27	1·6	−2·115
Strontium	2·82	27	200	1·574
Scandium	0·084	27	8	1·492
Titanium	−19·8	27	6100	−0·443
6. *Gallium*				
Boron	−0·123	71	10	−3·310
Chromium	0·110	110	10	3·262
Copper	0·411	27	10	2·500
Vanadium	1·01	10	62	2·381
Manganese	7·55	10	540	2·167
Titanium	−92·6	10	6100	−2·088
Strontium	3·66	10	200	1·956
Cobalt	0·593	19	10	1·718
Zirconium	−4·49	10	450	−1·029
Nickel	0·166	10	40	0·904
Barium	0·012	340	10	0·834
Scandium	−0·038	10	8	−0·611
Magnesium	−0·006	10	1·6	−0·410
7. *Magnesium*				
Chromium	−0·009	110	1·6	−3·411
Titanium	1470	1·6	6100	2·861
Manganese	−113	1·6	540	−2·761

Table 3—(*contd.*)

	b	$\bar{X}$	$\bar{Y}$	t
Strontium	−59·4	1·6	200	−2·735
Copper	−0·029	27	1·6	−2·115
Vanadium	−9·44	1·6	62	−1·725
Zirconium	54·8	1·6	450	−1·021
Cobalt	0·020	19	1·6	0·701
Boron	0·013	71	1·6	0·500
Gallium	−0·006	10	1·6	−0·410
Nickel	0·830	1·6	40	0·363
Barium	0·0003	340	1·6	0·318
Scandium	−0·232	1·6	8	−0·303
8. *Manganese*				
Chromium	2·80	110	540	5·095
Strontium	0·343	540	200	4·353
Boron	−2·64	71	540	−3·881
Vanadium	0·072	540	62	3·608
Magnesium	−113	1·6	540	−2·761
Copper	7·17	27	540	2·206
Gallium	7·55	10	540	2·167
Zirconium	0·385	540	450	1·767
Cobalt	11·0	19	540	1·644
Nickel	0·014	540	40	1·457
Scandium	0·002	540	8	0·689
Titanium	−1·28	540	6100	−0·518
Barium	0·149	340	540	0·514
9. *Nickel*				
Cobalt	1·57	19	40	9·975
Barium	0·048	340	40	4·458
Titanium	153	40	6100	3·760
Scandium	0·198	40	8	3·730
Vanadium	1·46	40	62	3·634
Copper	0·510	27	40	3·580
Chromium	0·111	110	40	3·538
Zirconium	12·3	40	450	3·054
Manganese	0·014	540	40	1·457
Strontium	2·68	40	200	1·314
Gallium	0·166	10	40	0·904
Magnesium	0·830	1·6	40	0·363
Boron	−0·006	71	40	−0·149

Table 3—(*contd.*)

	b	$\bar{X}$	$\bar{Y}$	t
10. *Scandium*				
Titanium	456	8	6100	−3·763
Nickel	0·198	40	8	3·730
Vanadium	4·14	8	62	3·357
Barium	0·012	340	8	2·917
Cobalt	0·242	19	8	2·288
Zirconium	28·5	8	450	2·226
Copper	0·084	27	8	1·492
Chromium	0·018	110	8	1·420
Boron	0·012	71	8	0·905
Manganese	0·002	540	8	0·689
Gallium	−0·038	10	8	−0·611
Magnesium	−0·232	1·6	8	−0·303
Strontium	1·52	8	200	0·241
11. *Strontium*				
Manganese	0·343	540	200	4·353
Boron	−1·30	71	200	−3·467
Chromium	1·17	110	200	3·433
Magnesium	−59·4	1·6	200	−2·735
Gallium	3·66	10	200	1·956
Cobalt	6·55	19	200	1·879
Copper	2·82	27	200	1·574
Vanadium	0·064	200	62	1·455
Nickel	2·68	40	200	1·314
Zirconium	0·370	200	450	0·861
Barium	0·126	340	200	0·832
Titanium	3·45	200	6100	−0·742
Scandium	1·52	8	200	0·241
12. *Titanium*				
Boron	35·7	71	6100	4·321
Scandium	456	8	6100	−3·763
Nickel	153	40	6100	3·760
Zirconium	0·049	6100	450	3·149
Magnesium	1470	1·6	6100	2·861
Cobalt	213	19	6100	2·709

Table 3—(*contd.*)

	b	$\bar{X}$	$\bar{Y}$	t
Gallium	−92·6	10	6100	−2·088
Barium	5·81	340	6100	1·661
Strontium	3·45	200	6100	−0·742
Chromium	−6·79	110	6100	−0·698
Vanadium	0·001	6100	62	0·635
Manganese	−1·28	540	6100	−0·518
Copper	−19·8	27	6100	−0·443
13. *Vanadium*				
Chromium	0·340	110	62	4·913
Nickel	0·146	40	62	3·634
Manganese	0·072	540	62	3·608
Scandium	4·14	8	62	3·357
Copper	1·22	27	62	3·324
Cobalt	2·13	19	62	2·786
Barium	0·087	340	62	2·737
Gallium	1·01	10	62	2·381
Boron	−0·218	71	62	−2·248
Zirconium	0·035	450	62	1·821
Magnesium	−9·44	1·6	62	−1·725
Strontium	0·064	200	62	1·455
Titanium	0·001	6100	62	0·635
14. *Zirconium*				
Titanium	0·049	6100	450	3·149
Nickel	12·3	40	450	3·054
Copper	9·63	27	450	2·599
Chromium	2·10	110	450	2·583
Cobalt	18·8	19	450	2·548
Scandium	28·5	8	450	2·226
Vanadium	0·035	450	62	1·821
Manganese	0·385	540	450	1·767
Barium	0·534	340	450	1·644
Gallium	−4·49	10	450	−1·029
Magnesium	−54·8	1·6	450	−1·021
Strontium	0·370	200	450	0·861
Boron	0·074	71	450	0·074

Table 4. Correlation of elements in Quebec group sandstones

	b	$\bar{X}$	$\bar{Y}$	t
1. *Boron*				
Vanadium	0·192	71	43	3·251
Nickel	0·242	71	27	3·002
Scandium	0·065	71	5	2·930
Gallium	0·176	71	8	2·849
Barium	−6·59	71	400	−1·732
Zirconium	6·45	71	810	1·707
Manganese	−5·51	71	580	−1·640
Cobalt	0·110	71	14	1·594
Magnesium	0·006	71	0·83	1·507
Copper	0·056	71	9	0·780
Strontium	−0·093	71	110	−0·608
Chromium	−0·131	71	88	−0·514
Titanium	17·7	71	8500	0·404
2. *Barium*				
Nickel	−0·012	400	27	−2·912
Scandium	−0·003	400	5	−2·248
Zirconium	−0·419	400	810	−2·190
Vanadium	−0·006	400	43	−1·885
Boron	−6·59	71	400	−1·732
Strontium	0·010	400	110	1·221
Magnesium	−0·0002	400	0·83	−1·006
Gallium	−0·003	400	8	−0·737
Cobalt	−0·002	400	14	−0·664
Chromium	−0·008	400	88	−0·613
Manganese	0·096	400	580	0·516
Copper	−0·002	400	9	0·507
Titanium	−0·896	400	8500	−0·389
3. *Cobalt*				
Magnesium	0·050	14	0·83	8·606
Gallium	0·674	14	8	4·368
Strontium	1·23	14	110	3·376
Scandium	0·205	14	5	3·231
Nickel	0·642	14	27	2·624
Manganese	22·0	14	580	2·370
Zirconium	19·5	14	810	−1·771
Boron	0·110	71	14	1·594
Copper	0·307	14	9	1·511

Table 4—(*contd.*)

	b	$\bar{X}$	$\bar{Y}$	t
Vanadium	0·271	14	43	1·343
Titanium	141	14	8500	1·130
Barium	−0·002	400	14	−0·664
Chromium	0·085	14	88	0·114
4. *Chromium*				
Manganese	6·21	88	580	2·344
Titanium	58·6	88	8500	1·703
Vanadium	0·092	88	43	1·632
Scandium	0·030	88	5	−1·437
Zirconium	2·38	88	810	0·719
Nickel	−0·054	88	27	−0·686
Strontium	−0·086	88	110	−0·682
Barium	−0·008	400	88	−0·613
Boron	−0·131	71	88	−0·514
Copper	0·024	88	9	0·390
Magnesium	0·001	88	0·83	0·322
Cobalt	0·085	14	88	0·114
Gallium	0·001	88	8	0·018
5. *Copper*				
Titanium	250	9	8500	2·132
Cobalt	0·307	14	9	1·511
Vanadium	0·227	9	43	1·113
Nickel	0·266	9	27	0·971
Gallium	0·184	9	8	0·891
Strontium	−0·370	9	110	−0·834
Boron	0·056	71	9	0·780
Zirconium	−8·39	9	810	−0·722
Magnesium	0·008	9	0·83	0·682
Barium	0·002	400	9	0·507
Chromium	0·024	88	9	0·390
Manganese	3·64	9	580	0·351
Scandium	0·019	9	5	0·248
6. *Gallium*				
Scandium	0·269	8	5	5·116
Cobalt	0·674	14	8	4·368
Magnesium	0·039	8	0·83	4·309

Table 4—(*contd.*)

	b	$\bar{X}$	$\bar{Y}$	t
Boron	0·176	71	8	2·849
Nickel	0·638	8	27	2·570
Vanadium	0·369	8	43	1·873
Strontium	0·632	8	110	1·455
Copper	0·184	9	8	0·891
Barium	−0·003	400	8	−0·737
Zirconium	−6·64	8	810	−0·562
Titanium	−54·9	8	8500	−0·424
Manganese	−0·379	8	580	−0·361
Chromium	0·001	88	8	0·018
7. *Magnesium*				
Cobalt	0·050	14	0·83	8·606
Gallium	0·039	8	0·83	4·309
Scandium	4·00	0·83	5	3·775
Strontium	22·4	0·83	110	3·530
Manganese	471	0·83	580	3·051
Nickel	10·1	0·83	27	2·261
Vanadium	5·76	0·83	43	1·646
Boron	0·006	71	0·83	1·507
Titanium	2460	0·83	8500	1·113
Zirconium	−222	0·83	810	−1·097
Barium	−0·0002	400	0·83	−1·006
Copper	0·008	9	0·83	0·682
Chromium	0·001	88	0·83	0·322
8. *Manganese*				
Magnesium	471	0·83	580	3·051
Titanium	6·64	580	8500	2·993
Strontium	0·021	580	110	2·563
Cobalt	22·0	14	580	2·370
Chromium	6·21	88	580	2·344
Boron	−5·51	71	580	−1·640
Zirconium	−0·354	580	810	−1·547
Scandium	−0·002	580	5	−1·027
Nickel	−0·005	580	27	−0·905
Barium	0·096	400	580	0·516
Vanadium	0·002	580	43	0·447
Gallium	−3·79	8	580	−0·361
Copper	3·64	9	580	0·351

Table 4—(*contd.*)

	b	$\bar{X}$	$\bar{Y}$	t
9. *Nickel*				
Scandium	0·207	27	5	5·358
Boron	0·242	71	27	3·002
Barium	−0·012	400	27	−2·912
Cobalt	0·642	14	27	2·624
Gallium	0·638	8	27	2·570
Vanadium	0·342	27	43	2·402
Magnesium	10·1	0·83	27	2·261
Zirconium	11·0	27	810	1·271
Copper	0·266	9	27	0·971
Manganese	−0·005	580	27	−0·905
Chromium	−0·054	88	27	−0·686
Strontium	−0·052	27	110	−0·153
Titanium	−2·706	27	8500	−0·028
10. *Scandium*				
Nickel	0·207	27	5	5·358
Gallium	0·269	8	5	5·116
Magnesium	4·00	0·83	5	3·775
Cobalt	0·205	14	5	3·231
Boron	0·065	71	5	2·930
Barium	−0·003	400	5	−2·248
Chromium	−0·030	88	5	−1·437
Vanadium	0·777	5	43	1·396
Strontium	1·59	5	110	1·323
Manganese	−0·002	580	5	−1·027
Zirconium	23·8	5	810	0·739
Titanium	−127	5	8500	−0·358
Copper	0·019	9	5	0·248
11. *Strontium*				
Magnesium	22·4	0·83	110	3·530
Cobalt	1·23	14	110	3·376
Zirconium	−12·9	110	810	−2·654
Manganese	0·021	580	110	2·563
Gallium	0·632	8	110	1·455
Scandium	1·59	5	110	1·323
Barium	0·010	400	110	1·221
Vanadium	−0·102	9	43	−1·048
Copper	−0·370	110	110	−0·834

Table 4—(*contd.*)

	b	$\bar{X}$	$\bar{Y}$	t
Chromium	−0·086	88	110	−0·682
Titanium	−22·2	110	8500	−0·365
Boron	−0·093	71	110	−0·608
Nickel	−0·052	27	110	−0·153
12. *Titanium*				
Manganese	6·64	580	8500	2·993
Vanadium	0·001	8500	43	2·357
Copper	250	9	8500	2·132
Chromium	58·6	88	8500	1·703
Cobalt	141	14	8500	1·129
Magnesium	2460	0·83	8500	1·113
Zirconium	0·017	8500	810	0·874
Gallium	−54·9	8	8500	−0·424
Boron	17·7	71	8500	0·404
Barium	−0·896	400	8500	−0·389
Strontium	−22·2	110	8500	−0·365
Scandium	−127	5	8500	−0·358
Nickel	−2·71	27	8500	−0·028
13. *Vanadium*				
Boron	0·192	71	43	3·251
Nickel	0·342	27	43	2·402
Titanium	0·001	8500	43	2·357
Barium	−0·006	400	43	−1·885
Gallium	0·369	8	43	1·873
Magnesium	5·76	0·83	43	1·646
Chromium	0·092	88	43	1·632
Scandium	0·777	5	43	1·396
Cobalt	0·271	14	43	1·343
Copper	0·227	9	43	1·113
Strontium	−0·102	110	43	−1·048
Zirconium	0·003	810	43	0·856
Manganese	0·002	580	43	0·447
14. *Zirconium*				
Strontium	−12·9	110	810	−2·654
Barium	−0·419	400	810	−2·190
Cobalt	−19·5	14	810	−1·771
Boron	6·45	71	810	1·707
Manganese	−0·354	580	810	−1·547
Nickel	11·0	27	810	1·271

Table 4—(*contd.*)

	b	$\bar{X}$	$\bar{Y}$	t
Magnesium	−222	0·83	810	−1·097
Titanium	0·017	8500	810	0·874
Vanadium	0·003	810	43	0·856
Scandium	23·8	5	810	0·739
Copper	−8·39	9	810	−0·722
Chromium	2·38	88	810	0·719
Gallium	−6·64	8	810	−0·562

Table 5. Highly significant correlations in Normanskill Greywackes

	t		t
Cobalt–nickel	9·975	Copper–nickel	3·580
Chromium–copper	8·514	Chromium–nickel	3·538
Chromium–manganese	5·095	Boron–strontium	3·467
Boron–chromium	5·034	Chromium–strontium	3·433
Chromium–vanadium	4·913	Chromium–magnesium	3·411
Barium–nickel*	4·458	Scandium–vanadium	3·357
Manganese–strontium	4·353	Copper–chromium	3·326
Boron–titanium	4·321	Copper–vanadium	3·324
Boron–manganese	3·881	Boron–gallium*	
Scandium–titanium	3·763	Chromium–gallium	3·262
Nickel–titanium	3·760	Boron–copper	3·165
Nickel–scandium*	3·730	Titanium–zirconium	3·149
Barium–cobalt	3·648	Nickel–zirconium	3·054
Nickel–vanadium	3·634	Cobalt–copper	3·036
Manganese–vanadium	3·608	Barium–scandium	2·917
		Magnesium–titanium	2·861
		Cobalt–vanadium	2·786

* Occur also in Quebec Group sandstones.

Table 6. Highly significant correlations in Quebec group sandstones

	t		t
Cobalt–magnesium	8·606	Cobalt–scandium	3·231
Nickel–scandium	5·358	Magnesium–manganese	3·051
Gallium–scandium	5·116	Boron–nickel	3·002
Cobalt–gallium	4·368		
Gallium–magnesium	4·309	Magnesium–titanium	2·993
Magnesium–scandium	3·775	Boron–scandium	2·930
Magnesium–strontium	3·530	Boron–nickel	2·912
Cobalt–strontium	3·376		
Boron–vanadium	3·251	Boron–gallium	2·849

Fig. 1. Distribution of elements in twenty-eight Normanskill greywackes. Corrected values of strontium.

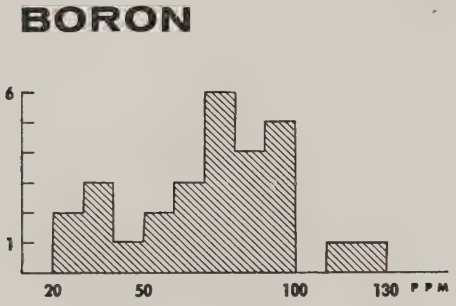

Fig. 1a.

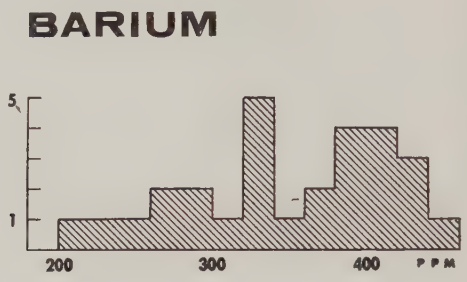

Fig. 1b.

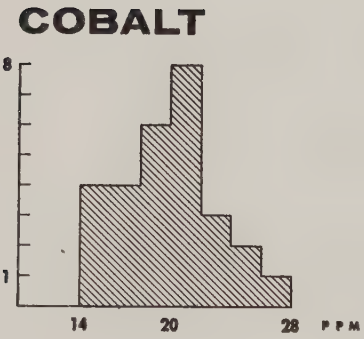

Fig. 1c.

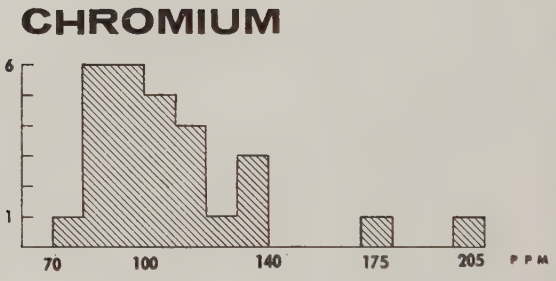

Fig. 1d.

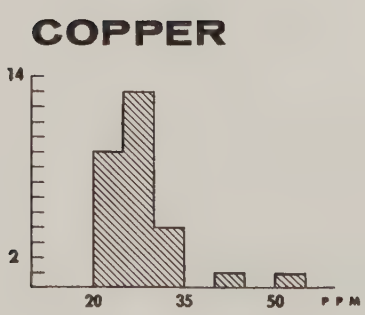

Fig. 1e.

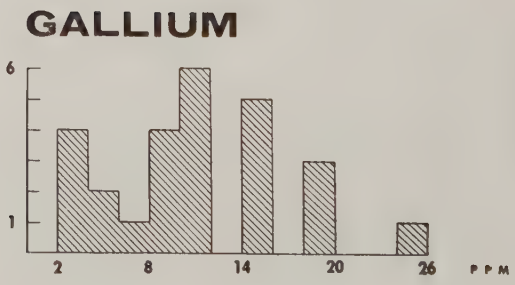

Fig. 1f.

MAGNESIUM

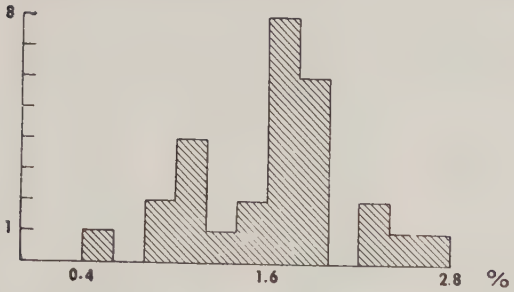

Fig. 1g.

MANGANESE

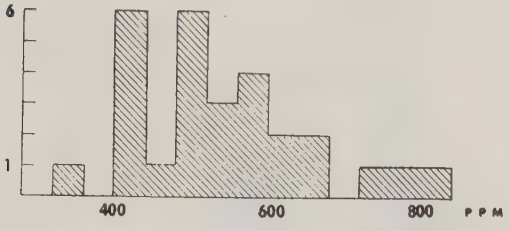

Fig. 1h.

NICKEL

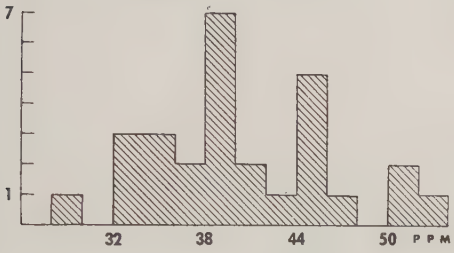

Fig. 1i.

SCANDIUM

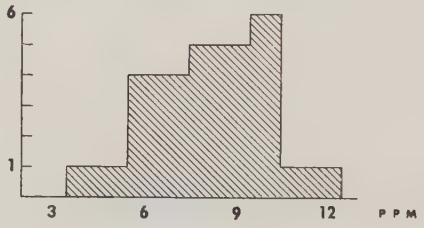

Fig. 1j.

STRONTIUM *

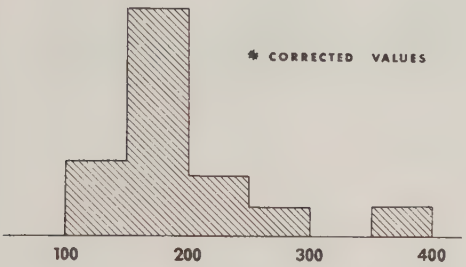

Fig. 1k.

TITANIUM

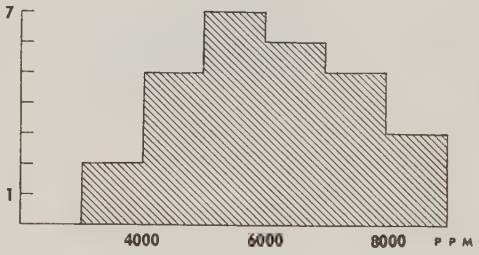

Fig. 1l.

VANADIUM

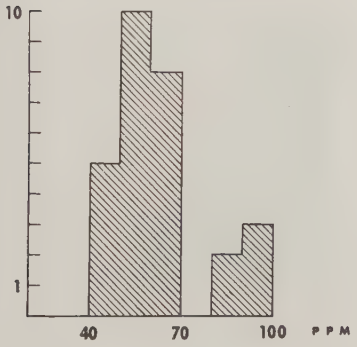

Fig. 1m.

ZIRCONIUM

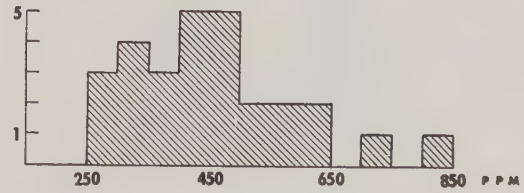

Fig. 1n.

Fig. 2. Distribution of elements in twenty-four Quebec group sandstones. Corrected values of strontium.

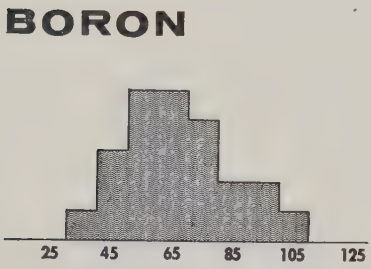

Fig. 2a.

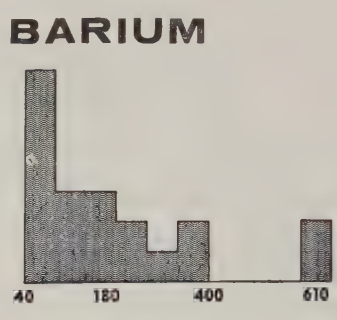

Fig. 2b.

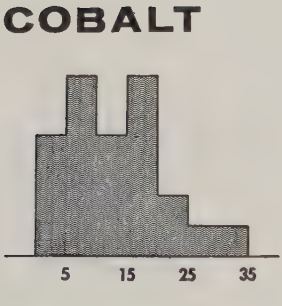

Fig. 2c.

Fig. 2d.

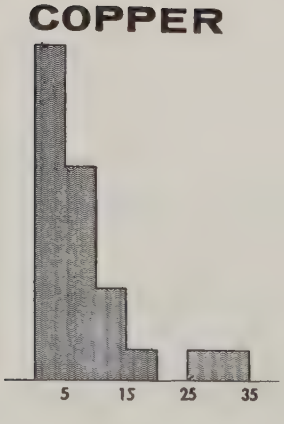

Fig. 2e.

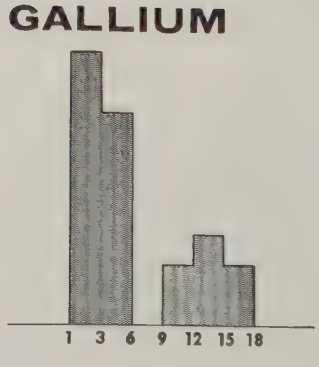

Fig. 2f.

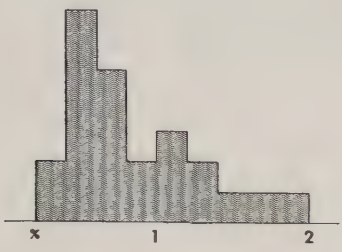

Fig. 2g.

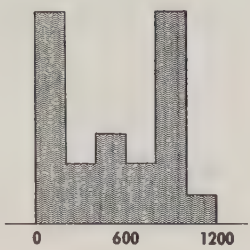

Fig. 2h.

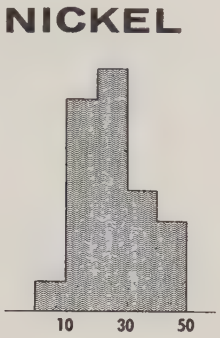

Fig. 2i.

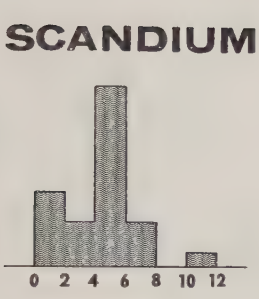

Fig. 2j.

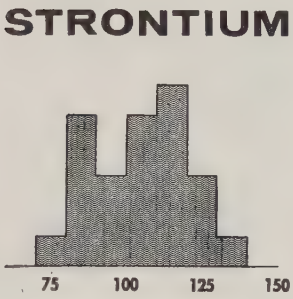

Fig. 2k.

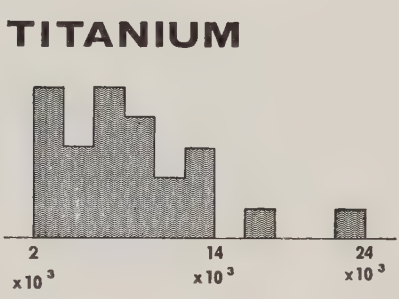

Fig. 2l.

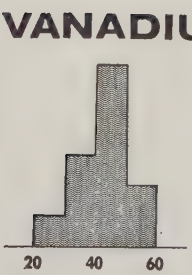

Fig. 2m.

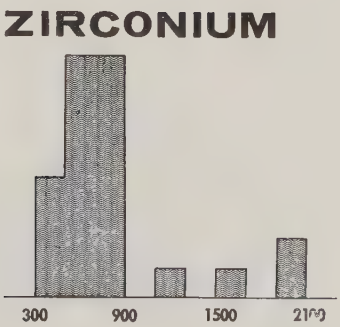

Fig. 2n.

Fig. 3. Correlation of petrography and geochemistry. Normanskill greywackes. Carbonate plus carbonate rock fragments (C), clay and rock fragments (R), and quartz–feldspar (Q) plotted on triangular diagrams with the concentration of the elements corresponding to the respective thin-sections added. All elements are in parts per million (p.p.m.) except magnesium which is in per cent (%). Figures for titanium represent hundreds of parts per million. Corrected values of strontium.

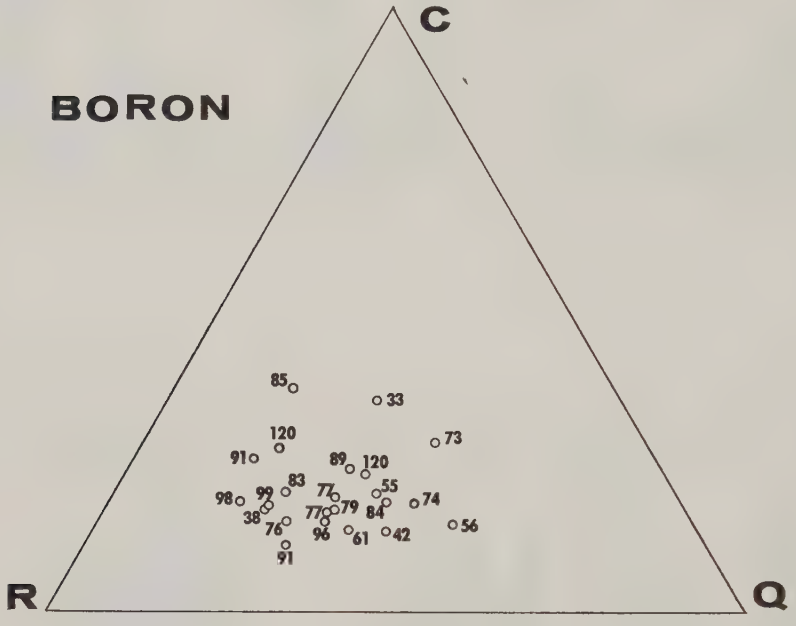

Fig. 3a

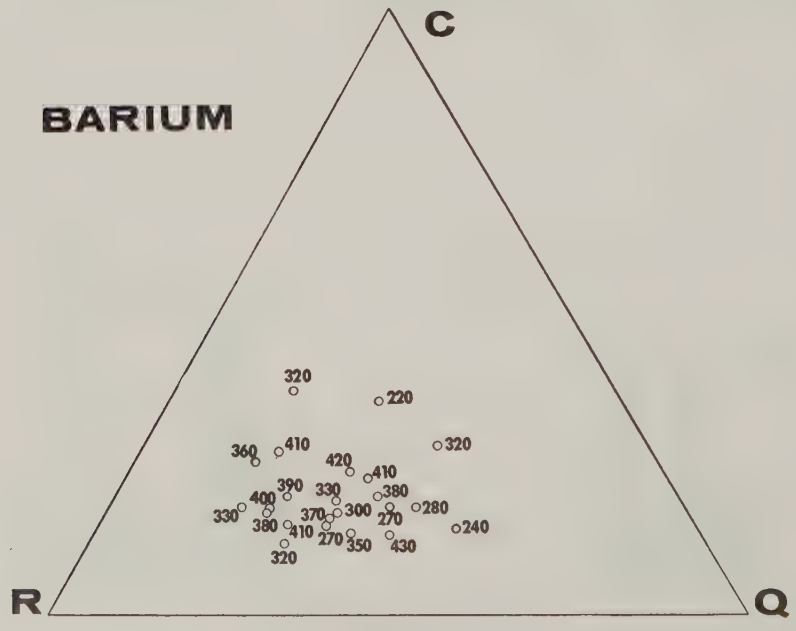

Fig. 3b

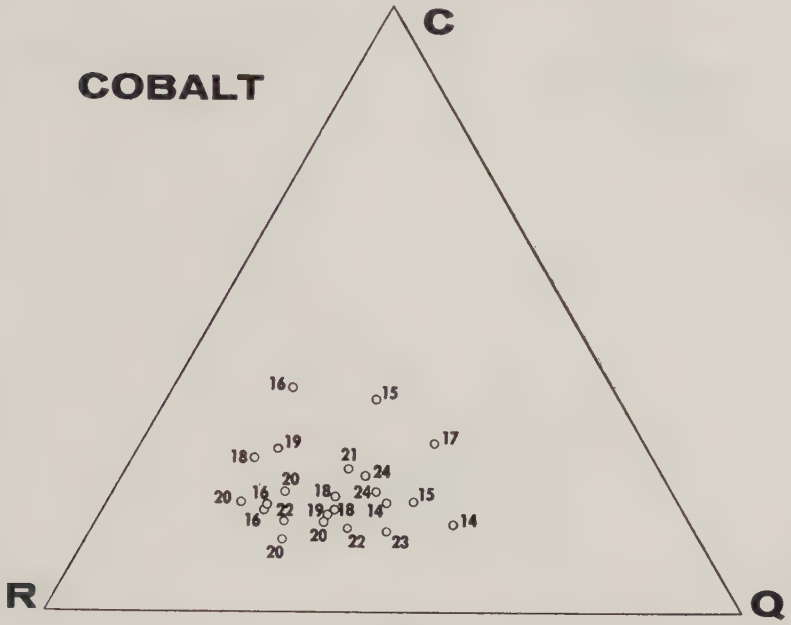
COBALT
C
R
Q
16
15
18
19
21
17
24
20
20
16
18
24
15
16
22
19
18
14
14
20
20
22
23

Fig. 3c

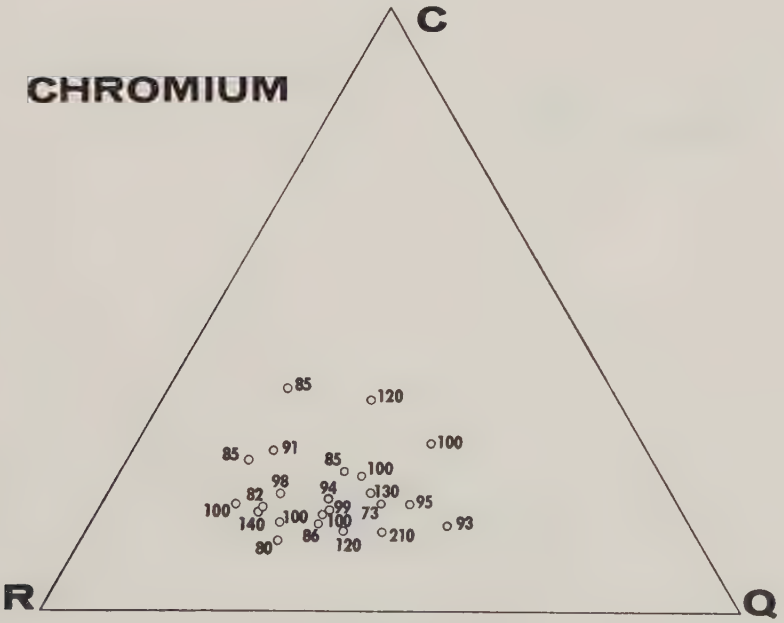
CHROMIUM
C
R
Q
85
120
100
85
91
85
100
98
94
130
82
95
100
99
73
140
100
100
93
86
210
80
120

Fig. 3d

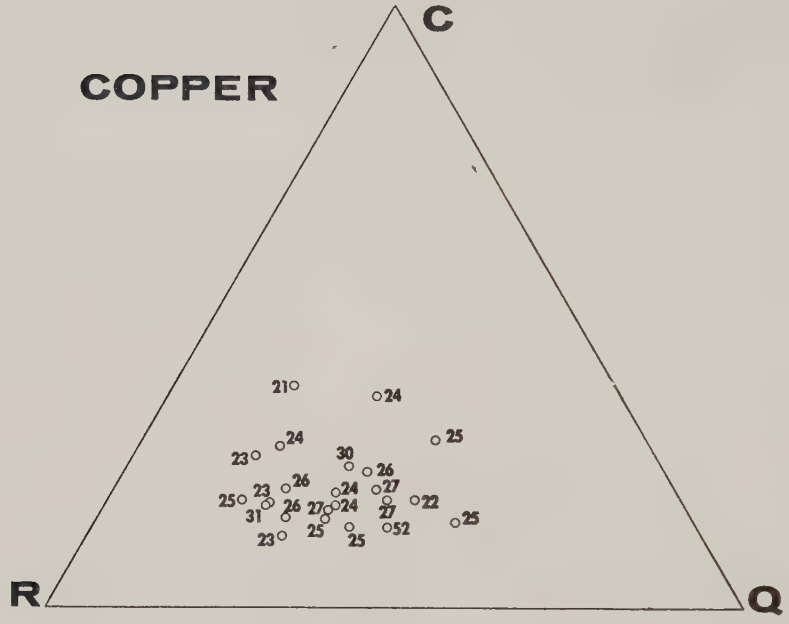
C
COPPER
R
Q
21
24
24
25
23
30
26
25
23
26
24
27
22
31
26
27
24
27
25
23
25
25
52

Fig. 3e

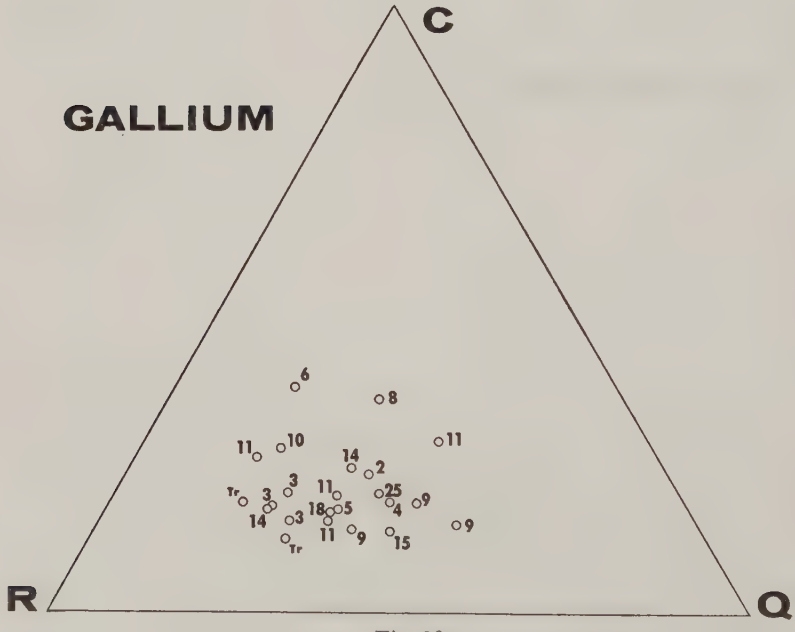
C
GALLIUM
R
Q
6
8
11
10
14
11
2
3
11
25
9
Tr
3
18
5
4
14
3
11
9
15
9
Tr

Fig. 3f

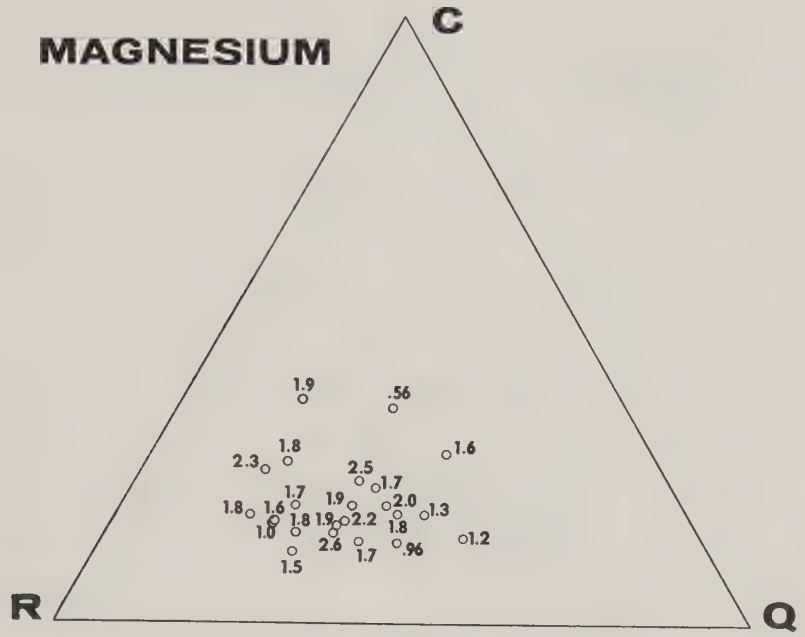
MAGNESIUM
C
R
Q
1.9
.56
1.8
2.3
1.6
2.5
1.7
1.7
1.9
2.0
1.8
1.6
1.3
1.8
1.9
2.2
1.0
1.8
2.6
1.7
.96
1.2
1.5

Fig. 3g

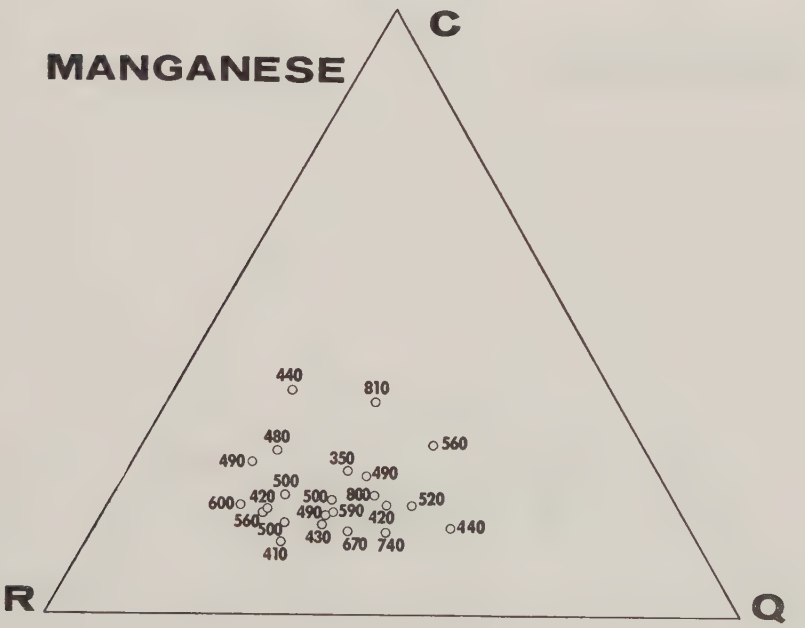
MANGANESE
C
R
Q
440
810
480
560
490
350
490
500
600
420
500
800
520
560
490
590
420
440
500
430
670
740
410

Fig. 3h

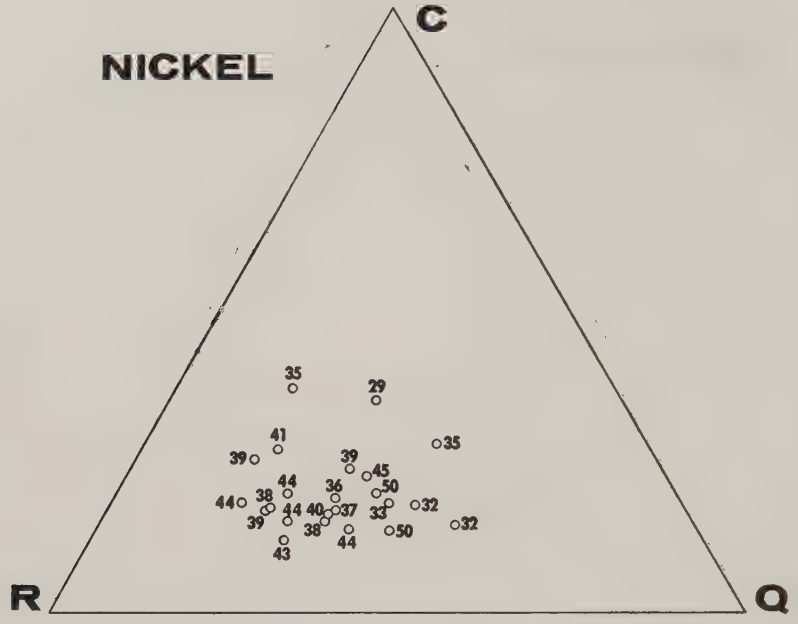
NICKEL
C
R
Q
35
29
41
39
39
35
45
44
36
50
44
38
40
37
33
32
32
39
44
38
50
44
43

Fig. 3i

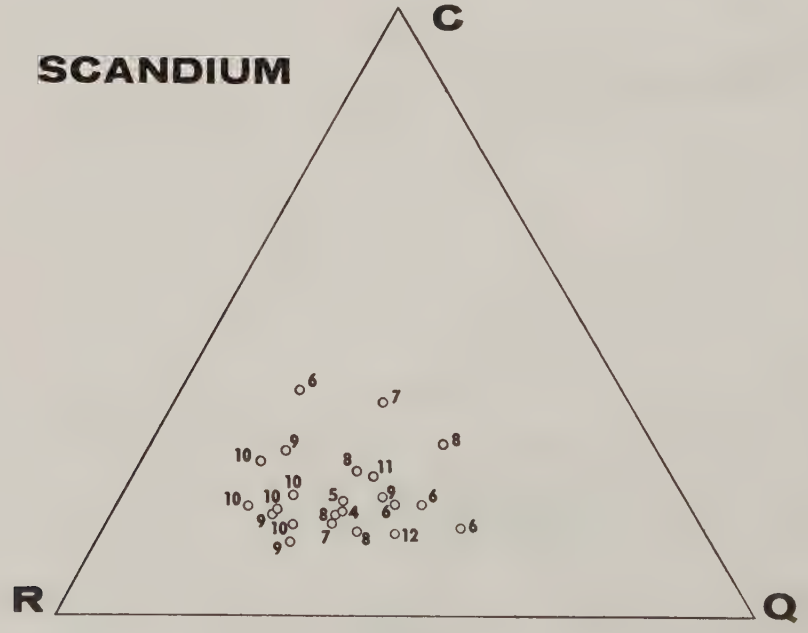
SCANDIUM
C
R
Q
6
7
10
9
8
8
11
10
10
5
9
6
6
9
4
8
10
9
7
8
12
6

Fig. 3j

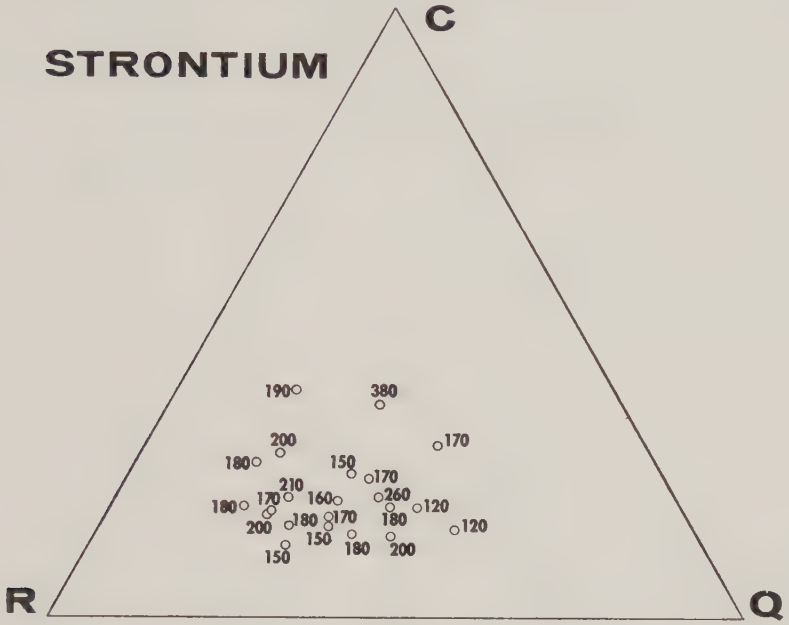
STRONTIUM
C
R
Q
190
380
200
170
180
150
170
210
180
170
160
260
120
200
180
170
180
120
150
150
180
200

Fig. 3k

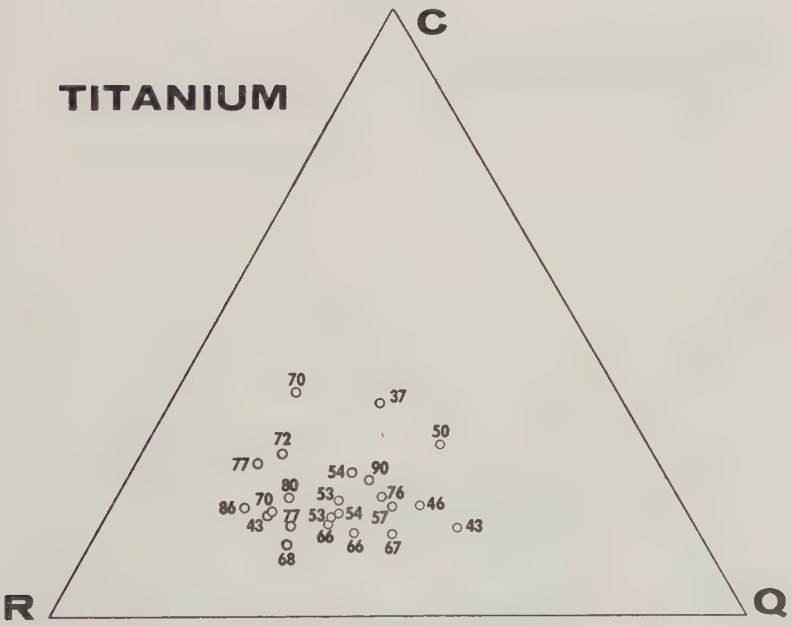
TITANIUM
C
R
Q
70
37
72
50
77
54
90
80
53
76
86
70
46
77
53
54
57
43
43
66
66
67
68

Fig. 3l

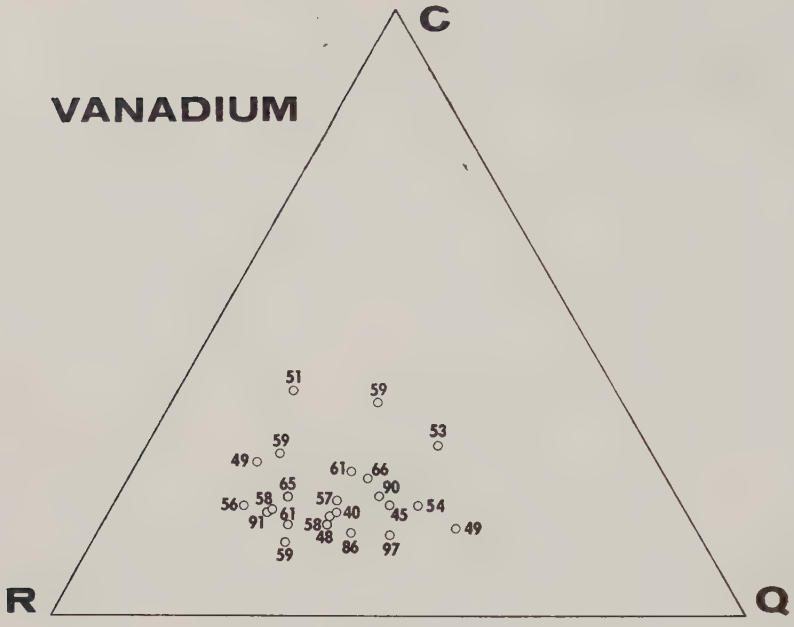
C
VANADIUM
R
Q
51
59
53
59
49
61
66
65
90
56
58
57
54
91
61
40
45
58
48
49
86
97
59

Fig. 3m

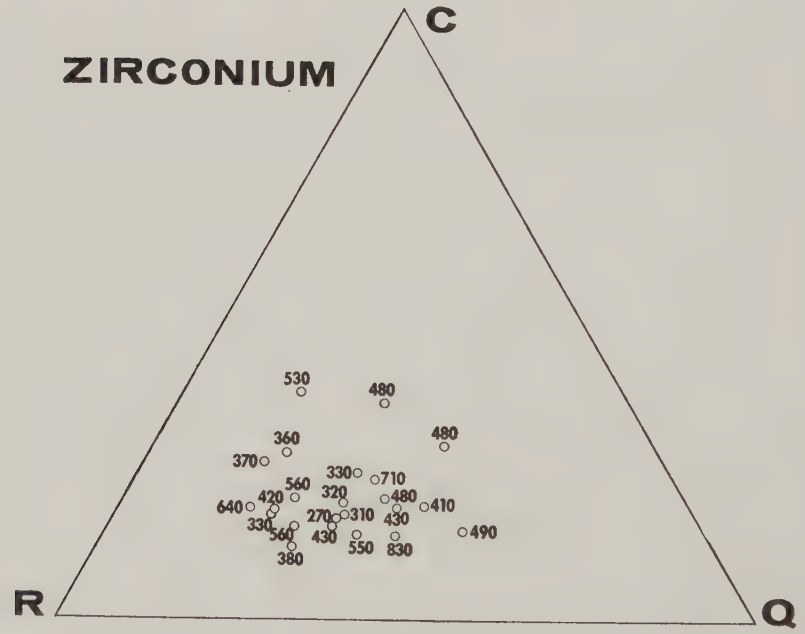
C
ZIRCONIUM
R
Q
530
480
360
480
370
330
710
560
320
480
640
420
410
270
310
430
330
560
430
490
550
830
380

Fig. 3n

Fig. 4. Correlation of petrography and geochemistry. Quebec Group sandstones. *C*, carbonate; *R*, clay and rock fragments; *Q*, quartz and feldspar. Magnesium in per cent, titanium in hundreds of parts per million, other elements in parts per million. Corrected values of strontium.

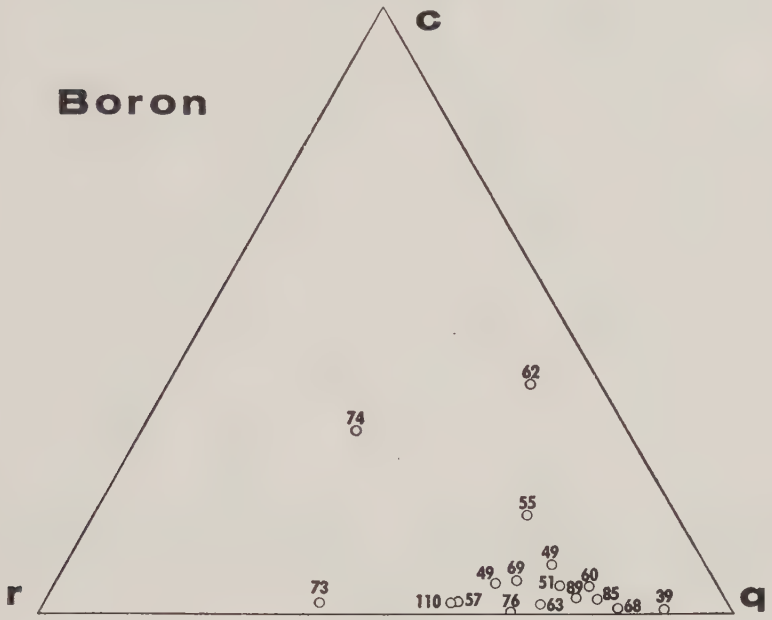

Fig. 4a

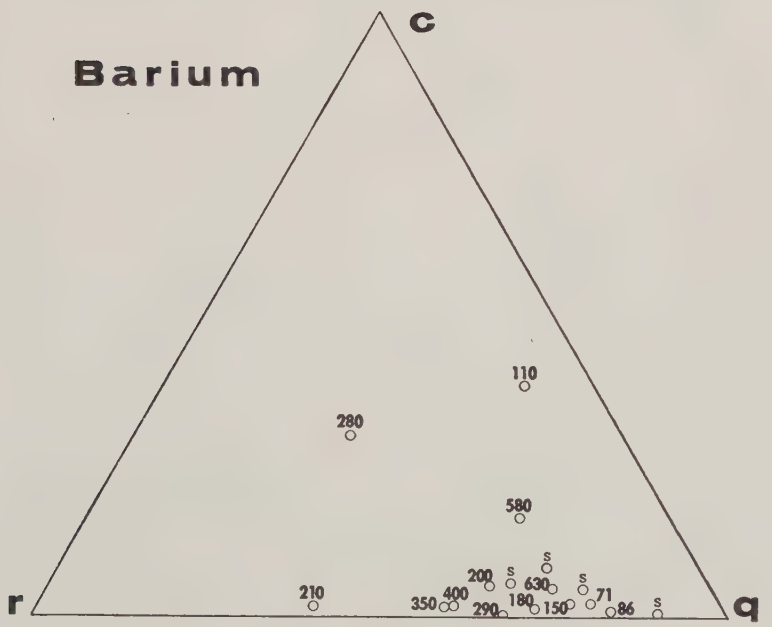

Fig. 4b

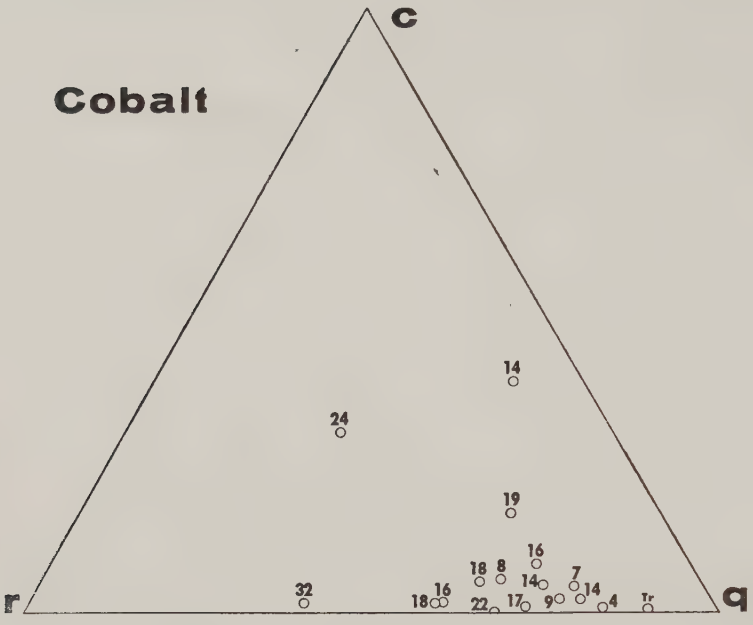
c
Cobalt
r
q
14
24
19
16
18
8
7
14
32
16
18
22
17
9
14
4
Tr

Fig. 4c

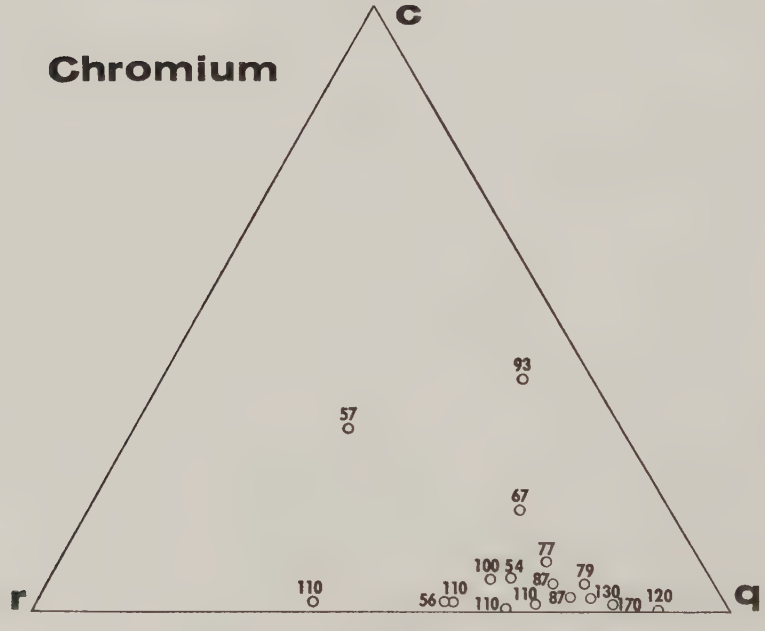
c
Chromium
r
q
93
57
67
77
100
54
87
79
110
110
56
110
110
87
130
170
120

Fig. 4d

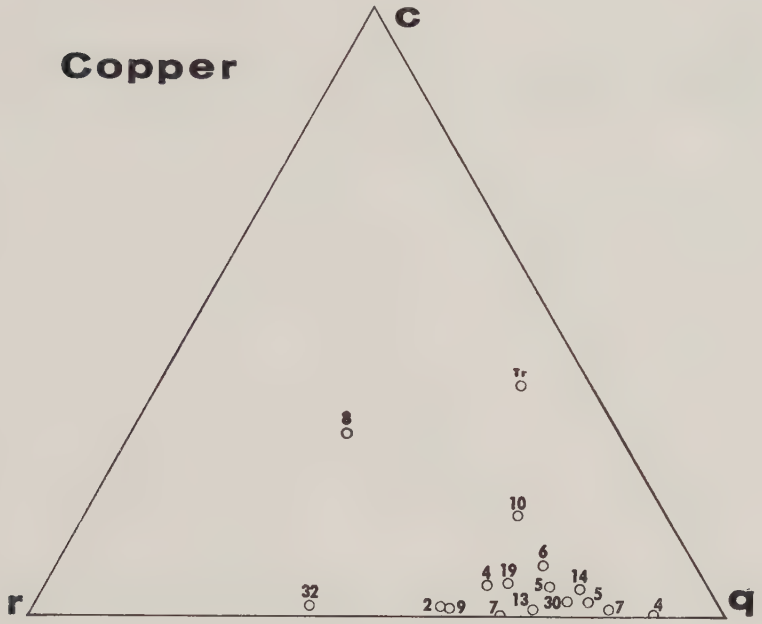
Copper
c
r
q
Tr
8
10
6
4
19
5
14
32
2
9
7
13
30
5
7
4

Fig. 4e

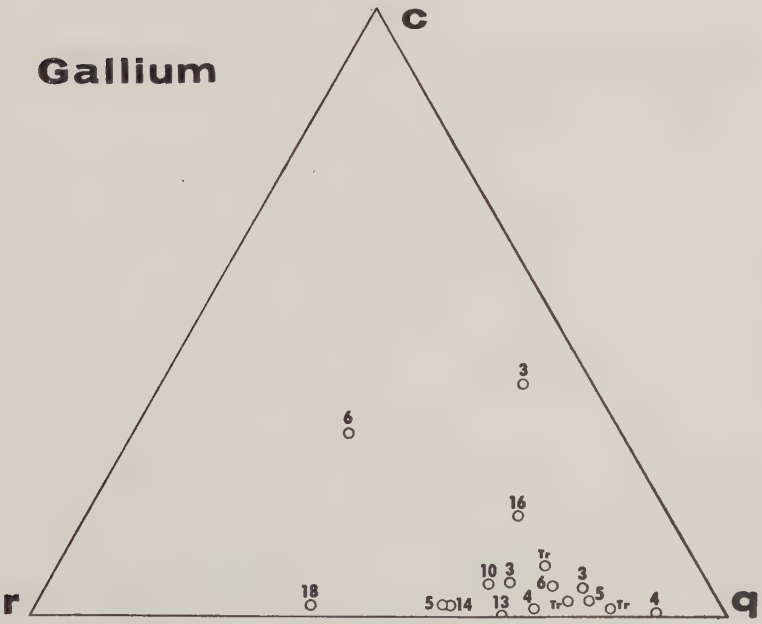
Gallium
c
r
q
3
6
16
Tr
10
3
6
3
18
5
14
13
4
Tr
5
Tr
4

Fig. 4f

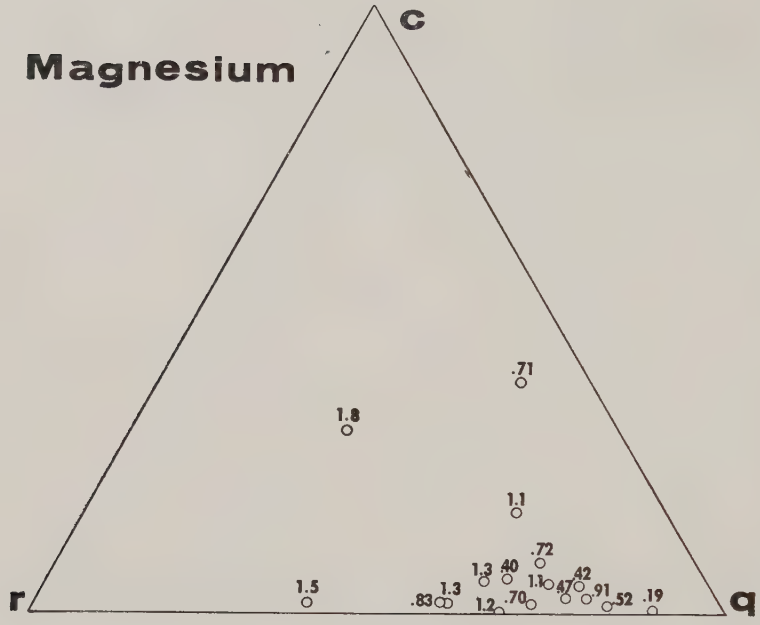
Magnesium
c
r
q
.71
1.8
1.1
.72
1.3
40
1.1
47
42
1.5
1.3
.83
1.2
.70
91
52
.19

Fig. 4g

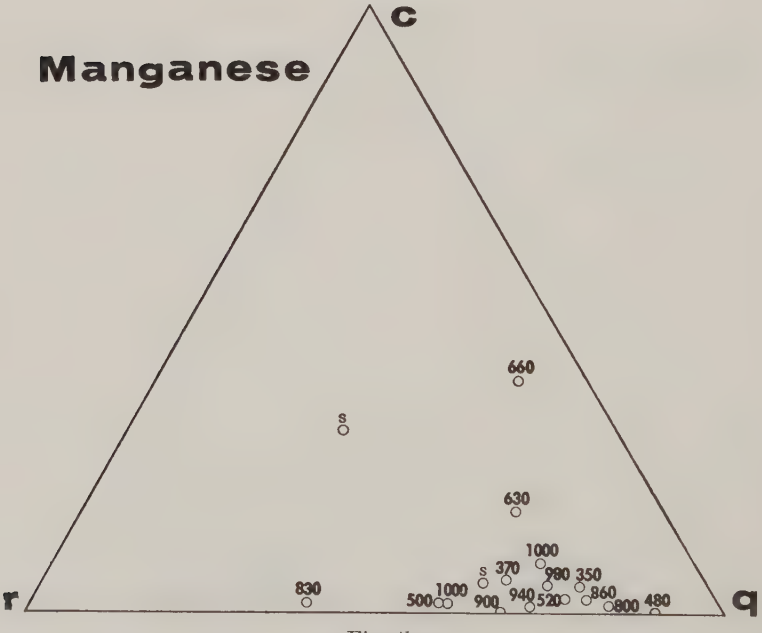
Manganese
c
r
q
660
s
630
1000
s
370
980
350
830
1000
500
900
940
520
860
800
480

Fig. 4h

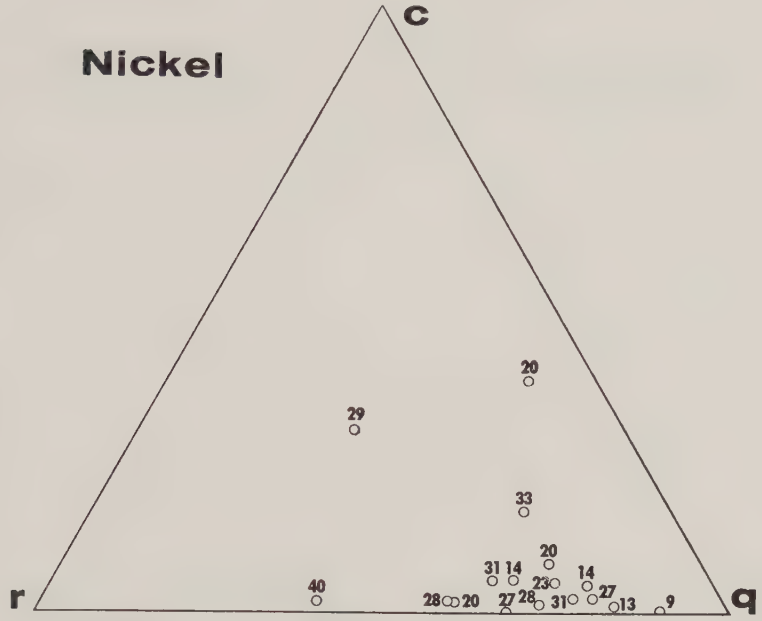
Nickel
c
r
q
20
29
33
20
31 14
14
40
23
27
28 20 27 28 31 27
13
9

Fig. 4i

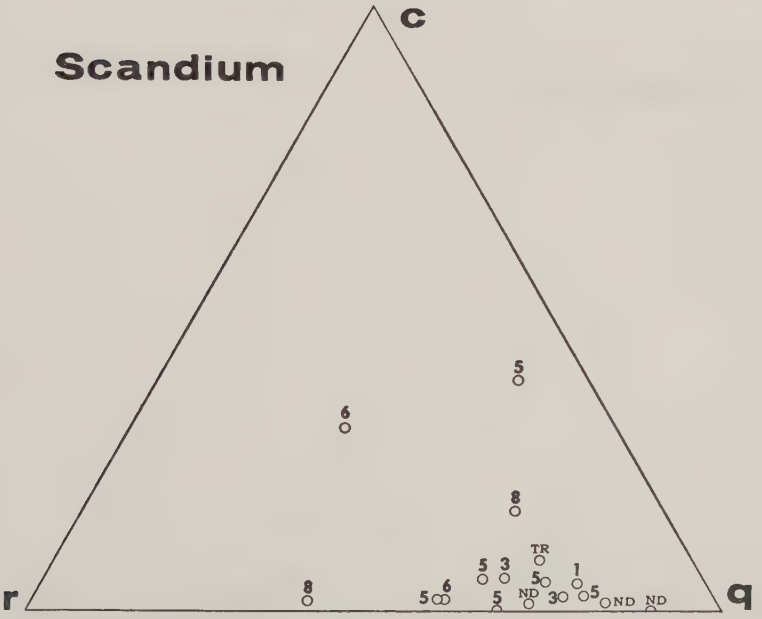
Scandium
c
r
q
5
6
8
TR
5 3
1
8
5 6
5
ND
3
5
ND ND

Fig. 4j

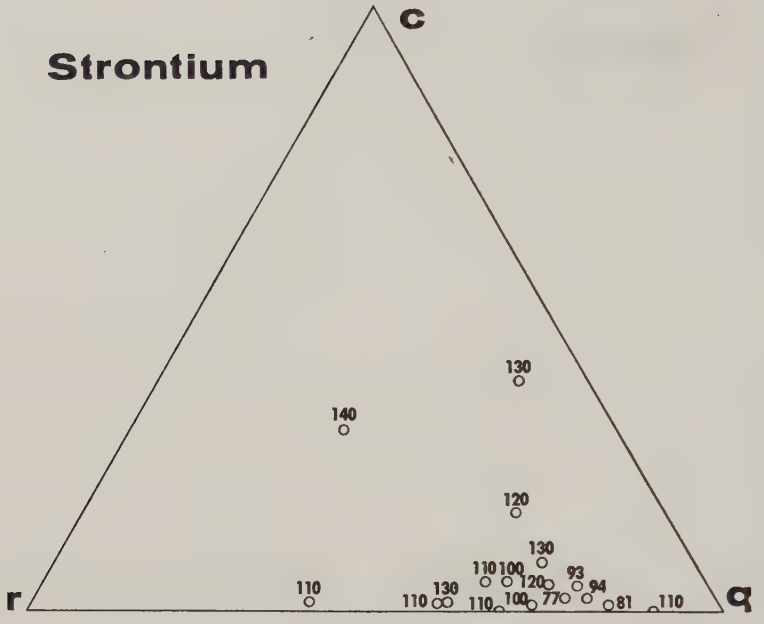
Strontium
c
r
q
130
140
120
130
110
100
120
93
94
110
130
110
100
77
81
110

Fig. 4k

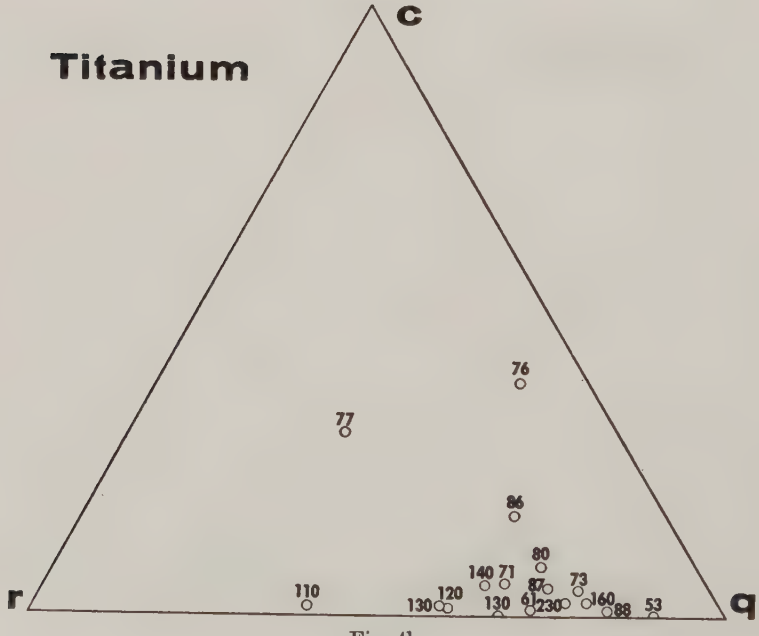
Titanium
c
r
q
76
77
86
80
140
71
87
73
110
120
130
130
61
230
160
88
53

Fig. 4l

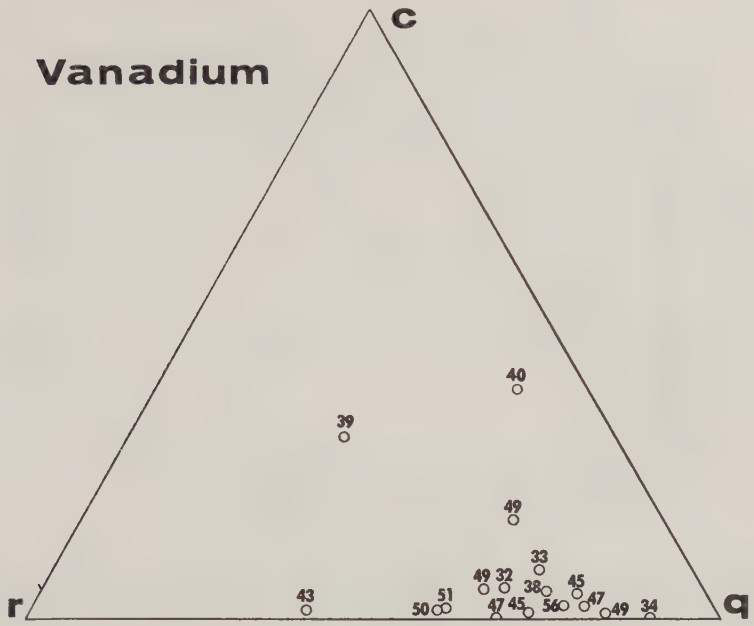
Vanadium
c
r
q
40
39
49
33
49
32
38
45
43
51
50
47
45
56
47
49
34

Fig. 4m

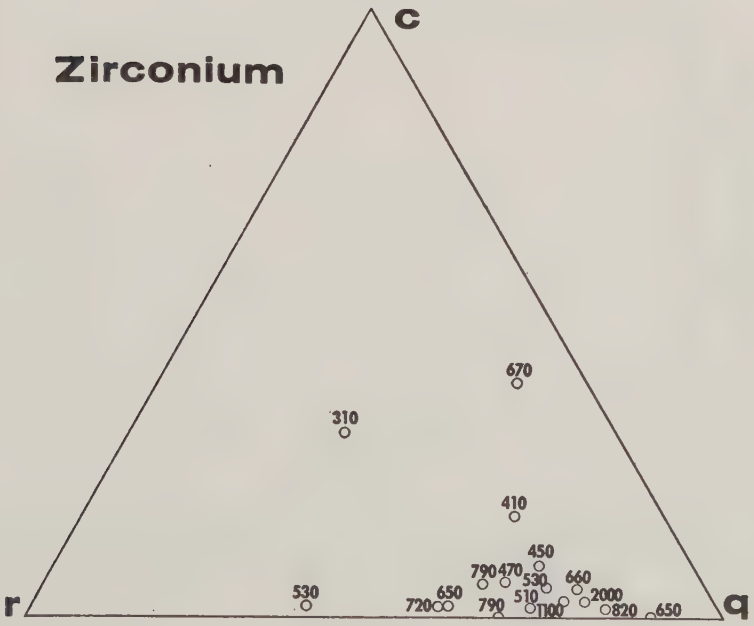
Zirconium
c
r
q
670
310
410
450
790
470
530
660
530
650
720
650
790
510
2000
1100
820
650

Fig. 4n

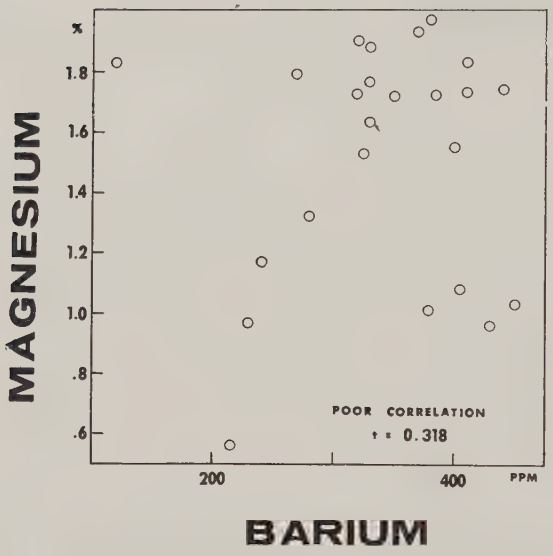

Fig. 5.

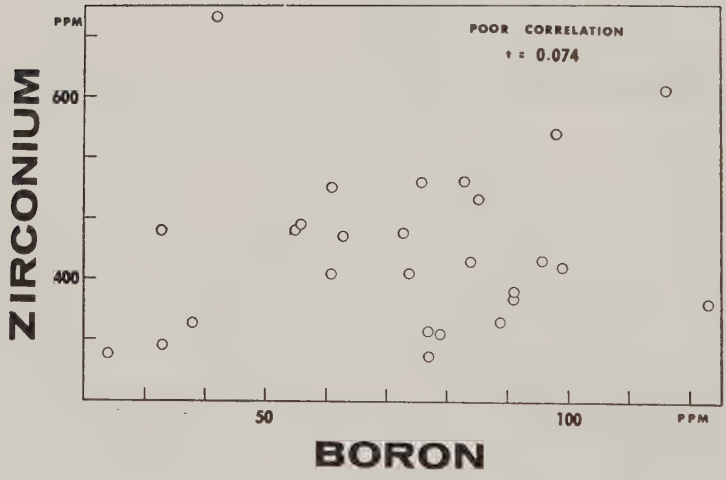

Fig. 6.

Figs. 5 and 6. Examples of poor correlation. Very low values of the correlation coefficient t suggest very poor correlation between magnesium and barium, and between zirconium and boron. Normanskill greywackes.

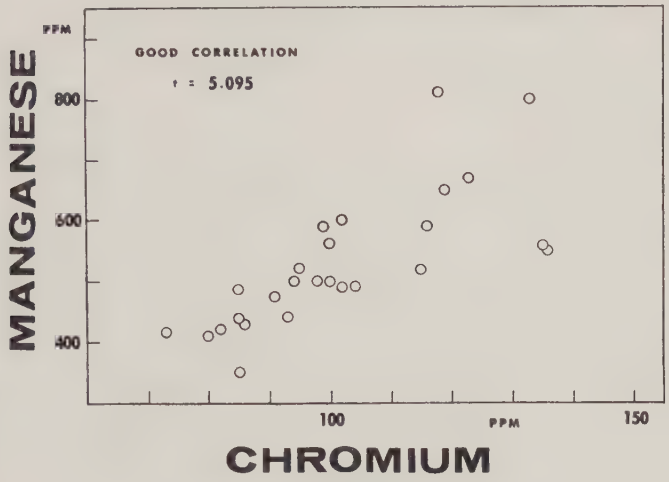

Fig. 7.

Fig. 7. Example of good correlation. Good correlation between manganese and chromium in Normanskill greywackes is indicated by a high numerical value of the correlation coefficient t. Normanskill greywackes more concentrated in manganese tend to show higher chromium values.

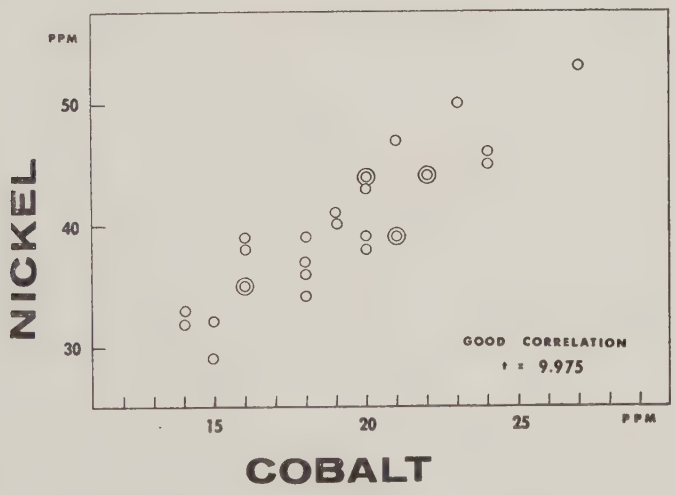

Fig. 8.

Fig. 8. Example of good correlation. A high numerical value of the correlation coefficient t indicates good correlation between nickel and cobalt in Normanskill greywackes. Samples with a higher concentration of nickel tend to have a higher value for cobalt.

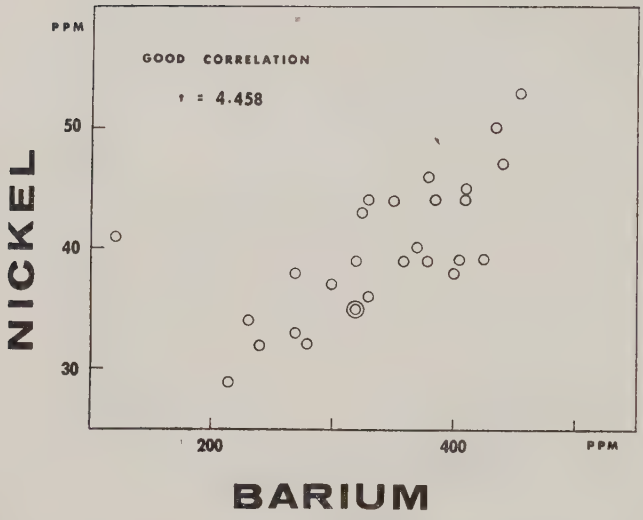

Fig. 9.

Fig. 9. Example of good correlation. Normanskill greywackes high in nickel tend to be highly concentrated in barium as well. The correlation coefficient t has a relatively high numerical value.

Geochimica et Cosmochimica Acta, 1961, Vol. 22, pp. 289 to 290. Pergamon Press Ltd. Printed in Northern Ireland

GEOCHEMICAL NOTE

The carbon isotopic compositions of certain marine invertebrates and coals from the Australian Permian

In a recent paper Compston (1960) presented interesting data on the carbon isotopic compositions of some Australian coals, which, he concluded, showed no correlation of the rank or the chemical composition of the coal with the carbon isotopic composition. However, in view of the nature of the samples used, Compston's conclusions do not seem fully justified.

Although in the text reference is made to "pure component macerals", in Table 5a figures are given for the lithotypes vitrain, clarain, durain and duroclarain. The macerals (Stopes, 1935; International Committee for Coal Petrology, 1957) are the fundamental microscopic components of coals and combined in varying proportions they make up the lithotypes. Thus the macerals are essentially homogeneous, whereas the lithotypes are heterogeneous. As the macerals of a coal sample may have different isotopic compositions the value of the data for the lithotypes is restricted unless the maceral composition of the samples is known. It may also be observed that the Bulli and Wongawilli seams, referred to in Table 5a, belong to the Illawarra Coal Measures, which cannot be correlated exactly with the Newcastle Coal Measures.

Many of the seams in the Greta Coal Measures have a canneloid appearance in hand specimen, but microscopic examination has shown that true cannel texture and composition are rare or absent. Small amounts of alginite are sometimes present in the Greta seam, and this maceral is the main constituent of torbanite. Thus the slightly more positive values of the Greta coals may be due to the presence of alginite. However, as different plants evidently have different isotopic compositions it would be desirable to distinguish torbanites of algal origin from cannels, which are largely derived from higher plants.

In considering the possibility of differences in isotopic fractionation during biochemical and rank changes, the rank of the coals must be clearly distinguished from the type. The rank is usually defined in terms of the total carbon content, or the volatile-matter content, of the vitrinite of the seam, expressed on a dry ash-free basis. The hydrogen content of a seam is related to the type of the coal, but coal types are most accurately expressed in terms of the maceral or microlithotype analyses.

Compston infers that the variations in the fixed-carbon content of Artie's seam are due to differences in rank. However, this is not borne out by data on the seam which were obtained by the Division of Coal Research, CSIRO, in the course of its systematic assessment of Australian coal resources. For example, from the table below, showing analyses of two samples of coal from Artie's seam which are identical in rank, it would appear that, in the absence of further information, the variations in the fixed-carbon content of Compston's samples could be due to differences in the proportions of macerals present. Therefore it is not possible, on the basis of the information provided, to conclude that isotopic fractionation does not take place during rank changes.

In order to disentangle the effects of rank and of maceral composition it would be necessary to test samples of individual macerals from one occurrence of a seam and also to test samples of the individual macerals at other localities where, on the evidence of its

Table 1. Simplified maceral analyses and fixed-carbon contents of two sub-sections of Artie's seam, Pikes Gully Trial Shaft, No. 7

Sample no.	Vitrinite	Exinite	Micrinite	Semifusinite	Fusinite	Fixed carbon (d.a.f.)
783 M	59	5	8	27	1	61·1
784 N	79	3	3	13	2	57·0

carbon content or volatile-matter content, the vitrinite is known to be of different rank. The first procedure would show what differences in isotopic composition there were in the original plant material, and how fractionation had occurred during the early peat stage. The second procedure would show the nature of the fractionation (if any) which had occurred in the macerals over the range of rank covered by the samples. In this manner it would be possible to eliminate some of the variables mentioned by Compston.

A. C. Cook.

Division of Coal Research
Commonwealth Scientific and
Industrial Research Organization
P.O. Box 3, Chatswood, New South Wales, Australia

References

Compston W. (1960) The carbon isotopic compositions of certain marine invertebrates and coals from the Australian Permian. *Geochim. et Cosmochim. Acta* **18,** 1.

International Committee for Coal Petrology, Nomenclature Sub-Committee (1957 Ed.)

Stopes M. C. (1935) On the petrology of banded bituminous coal. *Fuel, Lond.* **14,** 4.

Geochimica et Cosmochimica Acta, 1961, Vol. 22, pp. 291 to 294. Pergamon Press Ltd. Printed in Northern Ireland

BOOK REVIEWS

CONRAD BURRI: **Petrochemische Berechungsmethoden auf Äquivalenter Grundlage.** Birkhäuser Verlag, Basel, 1959. 334 pp., 38 Swiss francs.

Geochemists, particularly petrochemists, have been anxiously awaiting this first systematic and comprehensive documentation of the Niggli system of petrochemical calculation methods. They have wanted to know whether significant advances or changes have been made in recent years, but more particularly they have been interested in having a treatment of all of the methods and their uses in a single volume. This is in part because many of the older works in which certain aspects of the subject are discussed in detail are out of print and not widely available, and in part because many examples and discussions were to be found only in dissertations of NIGGLI's students; no less than eleven such dissertations are cited in the five page bibliography.

Mechanics of the calculations has changed not at all; other details of the methods only slightly. For example, the method of adding oxides of minor elements to those of the major elements before calculating the equivalent molecular numbers has been modified. The allotments were formerly made on the basis of chemical similarity, i.e. valence and position in the periodic table. Modern crystal chemical studies, however, have demonstrated that ionic radius and charge are the dominant factors controlling substitution in the crystal lattice. Thus, Cr_2O_3 and V_2O_3, which formerly were added to the Al_2O_3 on the basis of their trivalency, are now allotted to Fe_2O_3, since their ionic radii, Cr^{3+}, 0·64 and V^{3+}, 0·65 are much closer to Fe^{3+}, 0·67 than to Al^{3+}, 0·57.

BURRI has recalculated tables of molecular numbers for the twenty-one most important rock-forming oxides, and for chlorine, fluorine, and sulphur, based on the most recent values for the respective atomic weights. These are given in an appendix in considerably more detail than the corresponding tables in JOHANNSEN's *Descriptive Petrography of the Igneous Rocks* (1931), but in much less detail, of course, than in VON PHILIPSBORN's *Tabellen zur Berechnung von Mineral und Gesteinsanalysen* (1933).

The book starts off with a thirty-two page introduction in which the meaning and representation of chemical relations in rocks are discussed and the methods of graphic presentation outlined.

The great bulk of the text (213 pages), as would be expected from the title, is devoted to NIGGLI's methods of calculation. The first section of this chapter (fifty-three pages) discusses Niggli-numbers under the following headings:

(1) The calculation of Niggli-numbers.
(2) Demonstration of fundamental petrochemical relations by means of Niggli-numbers.
(3) Limits of use of Niggli-numbers
(4) Further applications of Niggli-numbers.
(5) Types of magmas.

The balance of the chapter is devoted to the equivalent norm. A general section on calculation of normative mineral composition is followed by a special discussion of the Niggli equivalent norm and its relation to a variety of problems in igneous and metamorphic petrology, with discussions of the concepts of kata-norm, compositions expressed as cation per cents, etc.

The whole lengthy chapter on methods is copiously illustrated with sets of examples for each method described. For example, after a three and a half page discussion of Niggli-numbers and their calculation from weight per cents (of oxides in a rock) there are two pages of examples showing exactly how the calculations are made. Then, after a discussion of the reverse process, there are the same number of examples showing just how to go from Niggli-numbers back to the

component oxides. This very detailed treatment is continued throughout; for Niggli-numbers and cation per cents, Niggli-numbers and molecular per cents, etc., and for no less than twelve methods and manipulations involving the equivalent norm.

This amount of detail is perhaps unnecessary for petrologists who have done some petrochemical calculations, even though they are unfamiliar with Niggli's methods, but it is certainly a very attractive feature for students and even for teachers who are trying to convey to students some of the finer points of systems of rock classifications and methods of petrochemical calculations. A large proportion of the examples of calculations revolve around three rocks: a calc-alkali quartz diorite ("normal") from Spanish Peak, California; a garnet-bearing cordierite andesite (high alumina) from Hoyazo, Spain; and an alkalic syenite (arfvedsonite lujavrite; high alkali) from Lille Elv, Greenland. Repeated use of these same analyses gives one a familiarity with their characteristics and makes it much easier to follow the calculations, transformations, and the reasoning concerning them than it would have been if different sets of rocks and their analyses had been used for each example.

The last chapter of the book is a short discussion (twelve pages) of the proposals of Barth and Eskola for the use of anions in petrochemical calculations and their relation to the Niggli equivalent norm. There are general examples of calculations with respect to anions and detailed ones to illustrate the concept and use of Barth's "standard cell'.

No other system, either of calculation or classification, is mentioned in either the table of contents or the index. The CIPW norm is discussed briefly in two places in the book. On pages 100–103 it is used as an example in a demonstration of the superiority of the Niggli system in fulfilling the three essential requirements of a method of petrographic calculations. This depends of course, on what the objectives of the calculations are. The other mention (pp. 175–176) appears to be principally to illustrate the deviation of the Niggli equivalent norm from the CIPW norm.

It is a little surprising that for a system so widely used and useful that there is no discussion or example of the calculation of the CIPW norm. It is even more surprising that the name of Osann does not appear in the book, considering that the "Niggli system" was derived from the "Osann system", which antedated it by a good 20 years. The Niggli system is a simplification, improvement and extension of the earlier one, and was based directly on it, even though the methods differ considerably.

Burri, student and long-time co-worker of Niggli's, was certainly the logical individual to prepare a work of this kind. Indeed, Niggli had in mind preparation of a book like the one under review, and had selected Burri to be its co-author, before his untimely death in 1953. Burri dedicated the volume to his great teacher and colleague and, inspired by his memory, has prepared a remarkably comprehensive, clear and useable treatise that will undoubtedly serve as the text and reference work on Niggli's methods for many, many years to come.

He points out that the system has wide usefulness because it can be applied to metamorphic and sedimentary rocks as well as to igneous; also, because among the 121 mineral "molecules" used in the system (as opposed to thirty-two in the CIPW system) a large proportion closely approximate compositions of natural minerals, many of which occur only in metamorphic rocks.

Another advantage is the rapidity with which transformations from one heteromorphic facies to another, and other calculations, can be made. In an appendix 187 equations for such transformations, involving thirteen important mineral groups, are given. Most of the equations needed will be found here, but others can be patterned after them, as needed. The coefficients of the formulae are chosen so that the sum of the electropositive elements (except for H_2O and CO_2) is equal to one. Thus, in the equations, the sum of the coefficients of the reacting compounds is equal to the sum of the coefficients of the products. This not only speeds the writing and balancing of the equations, but renders recalculation of the amounts of products to 100 per cent unnecessary.

Burri points out that this matter of speed is particularly advantageous just now when rapid methods of analysis are giving data more rapidly than ever before and when for certain types of problems large numbers of calculations are required for statistical treatment.

It must be clear from the above that the Niggli system does not involve a mineralogical classification of igneous rocks. The Niggli-numbers, however, allow the classification of the

analyses into three series of "magma types", calc-alkali, soda, and potash—each of which can be divided into many subtypes ranging from granitic to peridotitic.

BURRI takes exception to the use of the terms "petrochemistry" and "petrochemical" in connexion with products derived from petroleum and natural gas, and states emphatically that these words have undoubted priority in the sense of "rock chemistry". The reviewer is wholeheartedly in sympathy with this point of view, but after spending a great deal of time over a period of 5 years or so in trying to get those responsible for the misuse to change to "petrolochemistry" or some other suitable compromise, he is convinced that the second meaning, at least for "petrochemical(s)" as a noun, is here to stay.

The book is very nicely printed on high quality paper. With very few exceptions the figures are clear and easily readable. The reviewer did not have time to read the volume word for word, but in studying the subject matter carefully very few typographical or other errors were noted. In the footnote on page 51, where the three rocks most used as examples in the calculations are described briefly, the one from Spanish Peak, California, is referred to as a "Hornblende–Quarzdiorit" whereas in the original description it is called a "mica quartz diorite" and the photomicrograph does not show hornblende. On the same line the analyst's name, given as "Stockes" should be "Stokes".

On page 175, paragraph 2, the date of WASHINGTON's *Professional Paper* **99** (1917) is given as 1915 and in the Bibliography, page 322, in the reference by Tilley "Pettshire" should be "Perthshire".

One other thing that should probably be changed in a new printing is the use throughout the book of "CPIW-Klassification", "CPIW-norm", etc., instead of the commonly used "CIPW", although the names in the article from which the letters derive are given in the proper order, both in the text and the bibliography.

I am sure that I can properly express gratitude and appreciation to Professor BURRI on behalf of petrologists the world over for the great amount of time, effort and care expended in this superb account of a most useful and important system of petrographic calculations. He and the publisher are due the congratulations and thanks of everyone interested in any aspect of the chemistry of rocks.

EARL INGERSON

Clays and Clay Minerals: Proceedings of the Seventh National Conference on Clays and Clay Minerals. Edited by ADA SWINEFORD. Monograph No. 5, Earth Science Series. Pergamon Press, London, 1960. 369 pp., 60s.

THE Seventh National Conference on Clays and Clay Minerals was held in Washington, in October 1958 and the Proceedings contain twenty-four papers, the work of thirty-eight authors. The majority of these papers may be grouped under one or other of four headings—studies of ancient sediments, studies of modern sediments and sedimentation, experimental studies and descriptions of techniques.

In New Jersey, Delaware and Maryland, non-marine Cretaceous sediments are characterized by kaolinite, marine deposits by illite and montmorillonite, and it is concluded that this is a consequence of the existence of two separate source areas. A similar distribution occurs in the Cretaceous of North and South Carolina and in this case it is suggested that both formation of montmorillonite by marine diagenesis and prolonged weathering of a varied clay mineral assemblage to produce kaolinite may have been operative. A study of Pennsylvanian fireclay from the Eastern Kentucky Coalfield shows a wide range in the degree of crystallinity of the kaolinite present. Clay partings in gypsum deposits from south-west Indiana offer an opportunity for the investigation of the clay minerals associated with an evaporite sequence. Studies of the clay minerals in certain Jurassic rocks of the Colorado Plateau formed part of the investigation of this uranium province by the U.S. Geological Survey but, so far, gross clay mineral content has not proved satisfactory as a guide to ore.

Recent sediments studied include the bottom deposits of the Rappahannock River in Virginia where a progressive change in the mineralogy occurs between the fresh-water and saline-water parts of the river system. The dominant factor controlling the nature of the clay

minerals in the Recent sediments of the Gulf of Mexico is believed to be source with environment exerting a subsidiary influence.

Experimental studies indicate that both differential transport and differential settling of clay minerals occur in estuarine and marine environments, that Mg^{2+} ions from sea water move into the exchange positions in the minerals in preference to Ca^{2+} and Na^{+} ions and that appreciable amounts of SiO_2 Al_2O_3 and Fe_2O_3 are added to the sea water. Another experimental investigation shows that chlorite-like complexes form from montmorillonite so readily in the laboratory that a similar process may be expected in sediments and soils.

Among the many useful techniques described are various developments in X-ray diffractometry, in the removal of coatings of free iron oxides on clay particles by a dithionite–citrate system buffered with sodium bicarbonate and in the pre-treatment of soils and clays for measurement of external surface area by glycerol retention.

Many of the subjects discussed have some economic relevance to civil engineering, petroleum technology, mineral exploration, the ceramic industry or soil science. The book should therefore commend itself to a wide circle of readers. Although it is appreciably smaller than the previous year's Proceedings, the price remains the same.

J. H. Taylor

Department of Geology
King's College, University of London

Researches in Geochemistry. Edited by P. H. Abelson. John Wiley, New York, 1959. 511 pp. $11.00.

From the title of this book it might be inferred that it is a general summary of geochemical research, or at least of current researches in geochemistry. This is not the case however; it is a collection of more or less unrelated essays ranging from fairly broad surveys such as the ones on the "Geochemistry of Organic Substances" and on "Geochronology" to very localized studies such as the one on "Mineral Assemblages of the Green River Formation".

Nevertheless, as can be seen from a summary of fields covered, a remarkably broad spectrum of types of geochemical problems is treated: There are three papers dealing with the geochemistry of sediments, two with organic geochemistry, three with radioactive and two with stable isotopes, four with high temperature and pressure phenomena, four with thermodynamic applications, two with metamorphic processes, and one each with X-ray studies, meteorites and geochemical prospecting. Several of the papers could have been listed under two or more of the topics mentioned.

In a volume of this size there is no room for comprehensive or detailed surveys of broad fields; hydrothermal studies, for example, are discussed for amphiboles only, and of the geochemistry of stable isotopes only oxygen and sulphur are treated. These and the other essays give clear pictures of current methods and theoretical developments in their respective fields, however, so that they serve admirably the purpose for which they were chosen—to provide a cross-section of current research activity in numerous areas of inquiry.

Many other areas are touched only lightly, or not at all, and there are no articles primarily concerned with igneous petrology, volcanology, hydrogeochemistry, chemical oceanography, atmogeochemistry, distribution of the elements, crystal chemistry, etc.

Of the contributors eight were at the Geophysical Laboratory at the time the volume was published; twelve, at a like number of distinguished university departments; three with the U.S. Geological Survey; and two with the Atomic Energy Commission. With this array of talent Abelson's editorship, and publication by Wiley, it is hardly necessary to state that the work is outstanding in content, accurate and consistent in detail, and pleasing in format. It is a book that any library, department, or individual interested in the current status of geochemistry must have.

It is also a book that will further the science of geochemistry indirectly for a long time to come. The editor and contributors have very generously assigned their royalties to the Geochemical Society where they will accumulate in a special fund that will be used to help make the results of future geochemical research available in published form.

Earl Ingerson

INFORMATION FOR CONTRIBUTORS

I. GENERAL

1. Papers on *geochemistry* should be submitted to the appropriate Executive Editor—Prof. L. R. WAGER for papers from the United Kingdom and British Commonwealth and for papers in English from Europe; PROF. C. W. CORRENS for papers in German or French; Prof. E. INGERSON for papers from the American continents. Papers submitted for publication will naturally be judged from the standpoint of scientific originality and novelty. Technical details of apparatus used in scientific investigation can, however, be presented in brief notes. Critical comments or preliminary results requiring early publication should be submitted as letters to the editors. Where possible, letters should be confined to 500 words. The preparation of progress reports and review articles will be invited by the editors from time to time. The journal appears as independent and complete numbers, which are combined into volumes of about 300 pages.

2. Only papers which have not been previously published can be accepted. Authors must agree not to publish elsewhere a paper submitted to and accepted by *Geochimica et Cosmochimica Acta*.

3. Fifty reprints of each paper are provided free. Additional copies can be purchased if ordered at the time the first proofs are returned. A reprint order form will accompany first proofs.

II. SCRIPT REQUIREMENTS

1. Scripts must be written in one of the three official languages—English, French or German.

2. The script should be typed (not a carbon copy). The text must be ready for printing and should be carefully checked for errors. Authors will receive proofs for correction.

3. Illustrations should accompany the script mounted on separate sheets. Line diagrams that require to be redrawn should include all relevant details. Half-tone illustrations should be restricted to the minimum necessary. Photographs should be enlarged sufficiently to permit their clear reproduction and if words or numbers appear on them, two copies should be sent, one clearly printed and the other without inscription. All illustrations should be provided with descriptive legends, which should be given on a separate sheet. Any lettering on diagrams—other than Greek letters, symbols, etc.—should be stencilled and should be sufficiently large and bold to permit reproduction when the diagram has been reduced to a size suitable for inclusion in the journal.

4. References in the text should be given by quoting the authors name and year of publication, i.e. AHRENS (1952). *Full references should be listed at the end of each paper, in alphabetical order, in the following manner*

AHRENS, L. H. (1952). The use of ionization potentials—I. Ionic radii of the elements. *Geochim. et Cosmochim. Acta* **2**, 155–169.

and should include the full title of the article, standard abbreviated title of the journal, year, volume number and inclusive page numbers.

5. The text of articles submitted should be concise and in a readily understandable style. The technical description of the methods used should only be given in detail when such methods are new. The essential contents of each paper should be briefly recapitulated in an abstract in English. Such an abstract, may however, be submitted by the author in the language of the original typescript for translation into English by the editorial staff.

6. To conserve space, authors are requested to mark less important portions of the paper (such as description of methods, record of experimental results, etc.) for printing in smaller type.

7. Indices of refraction should be denoted by the symbols α, β, γ, ω, ε, n, and vibration directions by X, Y, Z, O and E.

Pergamon Press are also publishers of the following Journals.

JOURNAL OF NUCLEAR ENERGY (*including* THE SOVIET JOURNAL OF ATOMIC ENERGY*). PART A: REACTOR SCIENCE; PART B: REACTOR TECHNOLOGY; PART C: PLASMA PHYSICS — ACCELERATORS — THERMONUCLEAR REACTORS
HEALTH PHYSICS (*The Official Journal of the Health Physics Society*)
JOURNAL OF INORGANIC AND NUCLEAR CHEMISTRY
TETRAHEDRON (*The International Journal of Organic Chemistry*)
TALANTA (*An International Journal of Analytical Chemistry*)
INTERNATIONAL JOURNAL OF APPLIED RADIATION AND ISOTOPES
BIOCHEMICAL PHARMACOLOGY
ARCHIVES OF ORAL BIOLOGY
* BIOPHYSICS
* JOURNAL OF MICROBIOLOGY, EPIDEMIOLOGY AND IMMUNO-BIOLOGY.
* PROBLEMS OF HEMATOLOGY AND BLOOD TRANSFUSION
* PROBLEMS OF VIROLOGY
* PROBLEMS OF ONCOLOGY
* SECHENOV PHYSIOLOGICAL JOURNAL OF THE U.S.S.R.
* PAVLOV JOURNAL OF HIGHER NERVOUS ACTIVITY
* ELECTRIC TECHNOLOGY, U.S.S.R.
* RADIO ENGINEERING
* RADIO ENGINEERING AND ELECTRONICS
* TELECOMMUNICATIONS
* PHYSICS OF METALS AND METALLOGRAPHY
* THE ABSTRACTS JOURNAL OF METALLURGY
* APPLIED MATHEMATICS AND MECHANICS
CHEMICAL ENGINEERING SCIENCE
JOURNAL OF ATMOSPHERIC AND TERRESTRIAL PHYSICS
PLANETARY AND SPACE SCIENCE
ANNALS OF THE INTERNATIONAL GEOPHYSICAL YEAR
SPECTROCHIMICA ACTA
JOURNAL OF THE MECHANICS AND PHYSICS OF SOLIDS
ACTA METALLURGICA (*for the Board of Governors of Acta Metallurgica*)
INTERNATIONAL JOURNAL OF THE PHYSICS AND CHEMISTRY OF SOLIDS
DEEP-SEA RESEARCH
JOURNAL OF NEUROCHEMISTRY
JOURNAL OF PSYCHOSOMATIC RESEARCH
JOURNAL OF INSECT PHYSIOLOGY
INTERNATIONAL JOURNAL OF AIR POLLUTION
INTERNATIONAL ABSTRACTS OF BIOLOGICAL SCIENCES (*for Biological and Medical Abstracts Ltd.*)
RHEOLOGY ABSTRACTS
VACUUM
OPERATIONAL RESEARCH QUARTERLY
ANNALS OF OCCUPATIONAL HYGIENE
ELECTROCHIMICA ACTA
JOURNAL OF CHILD PSYCHOLOGY AND PSYCHIATRY
JOURNAL OF SMALL ANIMAL PRACTICE
SOLID-STATE ELECTRONICS
INTERNATIONAL JOURNAL OF MECHANICAL SCIENCES

* *Translations of Russian journals published on behalf of the Pergamon Institute, a division of Pergamon International Corporation*

Leaflets giving further details and subscription rates of each of these journals are available on request

22 May 61
ED IN STACKS

THE GEOCHEMICAL SOCIETY

OFFICERS

TOM F. W. BARTH, President
HAROLD C. UREY, Vice-President
KONRAD B. KRAUSKOPF, Secretary
GEORGE T. FAUST, Treasurer

COUNCILLORS

E. F. OSBORN, 1958–1960
H. G. THODE, 1958–1960
ALBERT E. J. ENGEL, 1959–1961
FRIEDRICH G. HOUTERMANS, 1959–1961
RALPH CANNON, 1960–1962
TH. G. SAHAMA, 1960–1962

REGIONAL VICE-PRESIDENTS

LOUIS H. AHRENS
RUI RIBEIRO FRANCO
ING. GEORGES ORDOÑEZ
C. W. CORRENS
J. F. LOVERING
KEN SUGAWARA

COMMITTEES

Auditing Committee:
JOSEPH J. TREGONING, Chairman
WILLIAM L. HILL
C. R. NASSER

Constitution and By-Laws Committee:
MICHAEL FLEISCHER, Chairman
JULIAN R. GOLDSMITH
DENIS M. SHAW

Education Committee:
H. D. HOLLAND, Chairman
J. A. S. ADAMS
D. M. HENDERSON
KURT E. LOWE
G. D. NICHOLLS
HANS P. EUGSTER

Membership Committee:
R. M. GARRELS, Chairman
HARVEY C. DIEHL
CHESTER B. SLAWSON
JAMES E. SLOSSON
IRVING BREGER

Nominating Committee:
WM. PECORA, Chariman
TH. G. SAHAMA
C. E. TILLEY
G. TUNELL

Programme Committee:
H. T. EVANS, Chairman
GORDON J. F. MACDONALD
H. E. LOWENSTAM

Publications Committee:
E. W. HEINRICH, Chairman
JULIAN R. GOLDSMITH
JOHN C. MAXWELL
N. W. RAKESTRAW
S. C. ROBINSON
L. R. WAGER
EARL INGERSON

Research Committee:
C. G. DODD, Chairman
W. F. BRADLEY
R. A. ROWLAND
T. G. THOMPSON

Russian Translations Committee:
EARL INGERSON

Standards Committee:
ALVIN VAN VALKENVERG, Chairman
MICHAEL FLEISCHER
LOREN STIEFF
GEORGE SWITZER
GEORGE TILTON

Tellers Committee:
CHARLES MEYER, Chairman
HENRY R. CORNWALL
COLIN O. HUTTON